INSIGHTS INTO AMINOFLUORINATION STRATEGIES AND SPHINGOSINE ANALOGUE SYNTHESIS TOWARDS THE DEVELOPMENT OF SELECTIVE SPHK2 INHIBITORS

Albert Granell Fort

UNIVERSITAT ROVIRA i VIRGILI

Insights into Aminofluorination Strategies and Sphingosine Analogue Synthesis towards the Development of Selective SphK2 Inhibitors

ALBERT GRANELL FORT

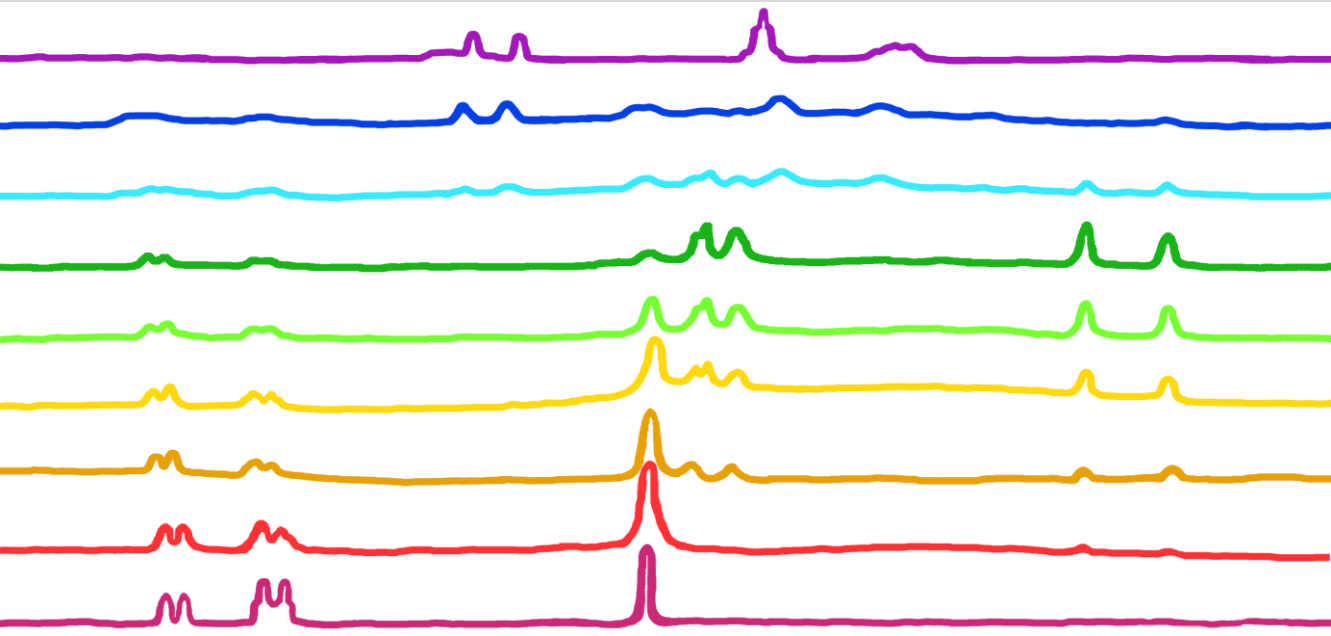

TESI DOCTORAL
2024

UNIVERSITAT ROVIRA I VIRGILI
INSIGHTS INTO AMINOFLUORINATION STRATEGIES AND SPHINGOSINE ANALOGUE SYNTHESIS TOWARDS THE DEVELOPMENT OF SELECTIVE SPHK2 INHIBITORS
Albert Granell Fort

Albert Granell Fort

Insights into Aminofluorination Strategies and Sphingosine Analogue Synthesis towards the Development of Selective SphK2 Inhibitors

DOCTORAL THESIS

Supervised by

Dr. Yolanda Díaz Giménez
Prof. Maria Isabel Matheu Malpartida

UNIVERSITAT ROVIRA I VIRGILI

Department of Analytical Chemistry and Organic Chemistry

Tarragona 2024

UNIVERSITAT ROVIRA I VIRGILI
INSIGHTS INTO AMINOFLUORINATION STRATEGIES AND SPHINGOSINE ANALOGUE SYNTHESIS TOWARDS THE DEVELOPMENT OF SELECTIVE SPHK2 INHIBITORS
Albert Granell Fort

UNIVERSITAT ROVIRA I VIRGILI

Departament de Química Analítica i Química Orgànica

C/ Marcel·lí Domingo, 1

Campus Sescelades

43007, Tarragona

Dr. Yolanda Díaz Giménez and Prof. Maria Isabel Matheu Malpartida from the Department of Analytical Chemistry and Organic Chemistry at the University Rovira i Virgili,

We STATE that the present study, entitled "Insights into Aminofluorination Strategies and Sphingosine Analogue Synthesis towards the Development of Selective SphK2 Inhibitors", presented by Albert Granell Fort for the award of the degree of Doctor, has been carried out under our supervision at the Department of Analytical Chemistry and Organic Chemistry of this University.

Tarragona, 4th April 2024

Thesis supervisors

DIAZ GIMENEZ MARIA YOLANDA - 39687039X

Firmado digitalmente por DIAZ GIMENEZ MARIA YOLANDA - 39687039X
Fecha: 2024.04.03 12:31:45 +02'00'

Dr. Yolanda Díaz Giménez

María Isabel Matheu Malpartida - DNI 39682609L (TCAT)

Firmado digitalmente por María Isabel Matheu Malpartida - DNI 39682609L (TCAT)
Fecha: 2024.04.03 13:01:50 +02'00'

Prof. Maria Isabel Matheu Malpartida

UNIVERSITAT ROVIRA I VIRGILI
INSIGHTS INTO AMINOFLUORINATION STRATEGIES AND SPHINGOSINE ANALOGUE SYNTHESIS TOWARDS THE DEVELOPMENT OF SELECTIVE SPHK2 INHIBITORS
Albert Granell Fort

The work performed in the present Doctoral Thesis has been possible thanks to the Martí i Franquès Research Fellowship Program (2018PMF-PIPF-26). This thesis has been carried out thanks to the funding of the research projects: CTQ2017-89750-R and PID2021-125923OB-I00 funded by MCIN/AEI/10.13039/501100011033/ and by FEDER Una manera de hacer Europa.

UNIVERSITAT ROVIRA I VIRGILI
INSIGHTS INTO AMINOFLUORINATION STRATEGIES AND SPHINGOSINE ANALOGUE SYNTHESIS TOWARDS THE DEVELOPMENT OF SELECTIVE SPHK2 INHIBITORS
Albert Granell Fort

Acknowledgements

I would like to express my heartfelt gratitude to all those who have supported me throughout this journey of pursuing my Ph.D. I am indebted to all individuals who have contributed to the successful completion of this thesis.

My gratitude to the URV for the Martí Franquès grant that allowed me to pursue this thesis in full commitment. In the same direction, I would like to thank all the organisms that have funded this project.

I extend my appreciation to my supervisors Yolanda and Maribel for giving me the opportunity to grow as a scientist in his lab. I also must thank Sergio and Omar for their invaluable contributions in making our research group a collaborative and productive environment.

I would like to also express my gratitude to all my labmates from SintCarb Jordi, Isa, Paula, Miguel, Pablo, Jorge, Javi, Eric and many more.

Finally, I extend my deepest acknowledgements to my family for their unwavering support throughout this journey. I am incredibly fortunate to have you all by my side.

UNIVERSITAT ROVIRA I VIRGILI
INSIGHTS INTO AMINOFLUORINATION STRATEGIES AND SPHINGOSINE ANALOGUE SYNTHESIS TOWARDS THE DEVELOPMENT OF SELECTIVE SPHK2 INHIBITORS
Albert Granell Fort

Table of contents

Chapter IV: I(III)-Mediated Aminofluorination of Allylic Carbamates

Chapter V: General conclusions

UNIVERSITAT ROVIRA I VIRGILI
INSIGHTS INTO AMINOFLUORINATION STRATEGIES AND SPHINGOSINE ANALOGUE SYNTHESIS TOWARDS THE DEVELOPMENT OF SELECTIVE SPHK2 INHIBITORS
Albert Granell Fort

UNIVERSITAT ROVIRA I VIRGILI
INSIGHTS INTO AMINOFLUORINATION STRATEGIES AND SPHINGOSINE ANALOGUE SYNTHESIS TOWARDS THE DEVELOPMENT OF SELECTIVE SPHK2 INHIBITORS
Albert Granell Fort

Abbreviations and Acronyms

A	
Ac	Acetyl
ACN	Acetonitrile
ADP	Adenosine Diphosphate
AHF	Anhydrous hydrogen fluoride
Ar	Aryl
ATP	Adenosine Triphosphate
B	
brs	Broad singlet
BHT	*tert*-Butyl hydroxytoluene
Bn	Benzyl
Boc	*tert*-Butyl carbamate
b.p.	Boiling point
BTM	2-Phenyl-2,3-dihydroimidazo[2,1-b][1,3]benzothiazole
Bu	Butyl
Bz	Benzoyl
C	
Calc.	Calculated
CAN	Cerium (IV) ammonium nitrate
Conv.	Conversion
COSY	Proton homonuclear correlation
D	
d	Doublet
2D	Two dimensional
DBU	1,8-Diazabicyclo[5,4,0]undec-7-ene
DCE	Dichloroethane
DCM	Dichloromethane
dd	Doublet of doublets
ddd	Double doublet of doublets
DIAD	Diisopropyl azodicarboxylate
DMAP	4-Dimethylaminopyridine

DMF	*N,N*-Dimethylformamide
DMPU	*N,N'*-Dimethylpropyleneurea
DMSO	Dimethyl sulfoxide
dr	Diastereomeric Ratio
E	
EDG	Electron Donating Group
eq	Equivalent(s)
ESI-TOF	Electrospray ionization-time of flight
Et	Ethyl
EtONa	Sodium ethoxide
EWG	Electron Withdrawing Group
F	
FTIR	Fourier transform infrared spectroscopy
G	
gCOSY	Gradient correlation spectroscopy
gHMBC	Gradient Heteronuclear multiple bond correlation
gHSQC	Gradient heteronuclear single quantum coherence
H	
HIR	Hypervalent Iodine Reagent
h	Hour(s)
HRMS	High-resolution Mass Spectrometry
HUVECs	Human Umbilical Vein Endothelial Cells
Hz	Hertz
I	
i-Pr	Isopropyl
IR	Infrared
J	
J	Coupling constant
L	
L	Ligand
M	
m	Multiplet

mCPBA	meta-Chloroperbenzoic Acid
Me	Methyl
MOE	Molecular Operating Environment
m.p.	Melting Point
Ms	Mesyl
MS	Molecular Sieves
MTT	3-(4,5-Dimethylthiazol-2-yl)-2,5-diphenyltetrazolium Bromide
m/z	Mass Under Charge
N	
NHC	*N*-heterocyclic Carbene
NMR	Nuclear Magnetic Resonance
Nu	Nucleophile
P	
PDB	Protein Database
Ph	Phenyl
PhIO	Iodosylbenzene
PIDA	(Diacetoxyiodo)benzene
Piv	Pivaloyl
pKa	$-\text{Log}_{10}\ K\text{a}$
PP	Polypropylene
ppm	Parts per million
PTSA	*p*-Toluenesulfonic Acid
Py	Pyridine
Q	
q	Quartet
quint	Quintet
R	
RDS	Rate-determining Step
R_f	Retention Factor
rt	Room temperature
S	
s	Singlet
Sph	Sphingosine

SphK1	Sphingosine Kinase 1
SphK2	Sphingosine Kinase 2
T	
t	Triplet
TAI	Trichloroacetyl Isocyanate
TBAF	Tetrabutylammonium Fluoride
tBuOH	tert-Butanol
TEMPO	(2,2,6,6-Tetramethylpiperidin-1-yl)oxyl
THF	Tetrahydrofuran
TLC	Thin layer chromatography
TMAF	Tetramethylammonium Fluoride
Tol	4-methylphenyl
TR-FRET	Time Resolved Fluorescence Energy Transfer
TS	Transition state
Ts	Tosyl
U	
UV/Vis	Ultraviolet/visible

UNIVERSITAT ROVIRA I VIRGILI
INSIGHTS INTO AMINOFLUORINATION STRATEGIES AND SPHINGOSINE ANALOGUE SYNTHESIS TOWARDS THE DEVELOPMENT OF SELECTIVE SPHK2 INHIBITORS
Albert Granell Fort

UNIVERSITAT ROVIRA I VIRGILI
INSIGHTS INTO AMINOFLUORINATION STRATEGIES AND SPHINGOSINE ANALOGUE SYNTHESIS TOWARDS THE DEVELOPMENT OF SELECTIVE SPHK2 INHIBITORS
Albert Granell Fort

Summary

In the last years our research group has been interested in the synthesis of sphingosine analogues as potential inhibitors of Sphingosine Kinase (SphK), an enzyme that is closely associated with cancerous processes. In this context, the work presented in this PhD thesis is conducted towards the obtention of new inhibitors. The thesis is divided in two main topics: 1) synthesis of sphingosine analogues for cancer therapy and 2) study of the aminofluorination of allyl carbamates using hypervalent iodine reagents.

- Chapter 3 contains attempts at the enantioselective preparation of two sphingosine analogues bearing a quaternary centre in C-3, a polynitrogenated dimethylhydrazino group and an alkynyl moiety as a linker between the polar head and the lipidic tail of the molecule. These analogues show good inhibition towards Sphingosine Kinase isoform SphK2. The main idea of the synthesis is based on the aziridination of a conjugated alkene, followed by the opening of the aziridine with water to obtain the aminodiol scaffold.

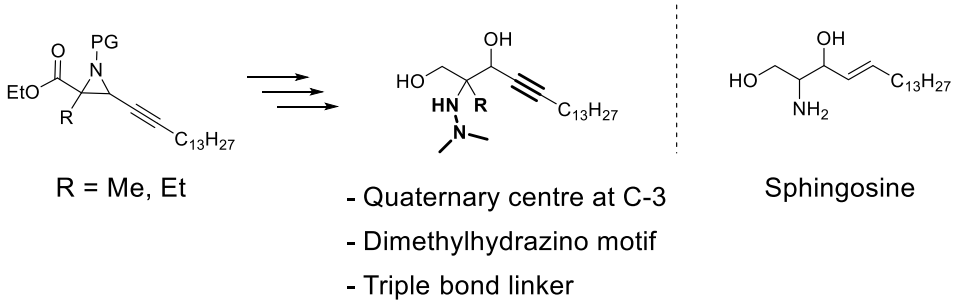

Scheme 1

Based on previous inhibition assays, molecular dockings are performed in collaboration with Prof. Xavier Barril (UB, Barcelona) to understand the possible interactions between the analogues and the active site of SphK. The alkynyl linker shows that the shape of the hydrophobic pocket of SphK2 may have a big impact in the fit of the inhibitor, leading to major changes in the conformation of the guest that

can affect the guest-host interactions in a major way. Finally, cell viability assays, carried out in collaboration with Prof. Mª Jesús Sanz (UV, València), showed negligible cytotoxicity of the methyl analogue.

- Chapter 4 contains a study of the aminofluorination reaction with hypervalent iodine reagents, applied to allyl carbamates. The development of an easy methodology for the obtention of β-fluoroamines from allyl carbamates is a first step towards the preparation of C-3 fluorinated sphingosine analogues. Two main approaches are stablished for the aminofluorination: 1) use of $TolIF_2$, a well-known HIR that acts both as the oxidant agent and the fluorine source, and 2) a two-step methodology consisting of the aziridination of the allyl carbamate followed by the ring-opening of the aziridine with an external F^- reagent.

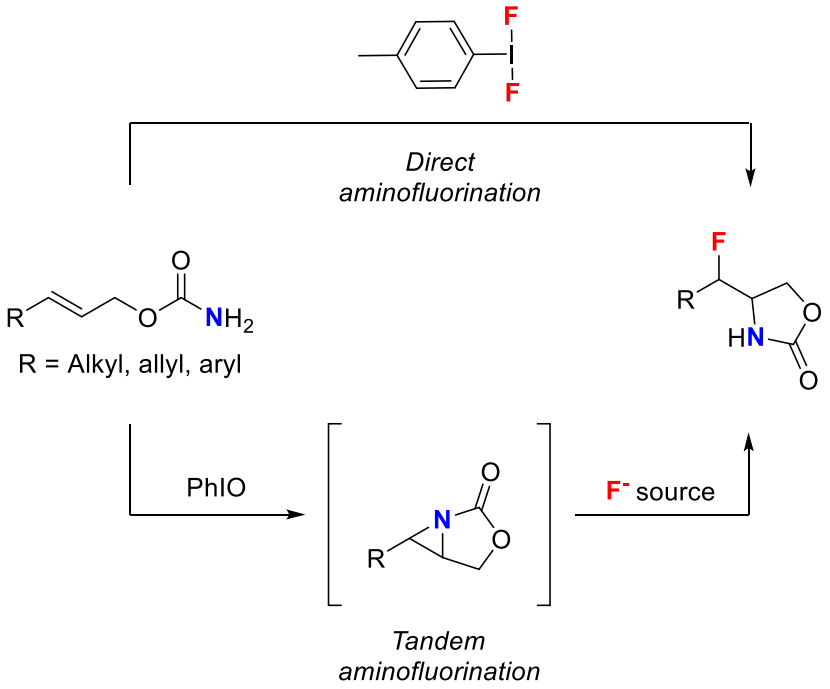

Scheme 2

Summary

An emphasis is made in the effect of the substitution and acidity of the carbamate and the configuration of the double bond on the efficiency and the stereoselectivity of the process. The mechanism and the scope of the reaction are studied using mainly cinnamyl carbamates, which serve as simple allyl carbamates. *p*-Substituted cinnamyl carbamates are a useful tool to gain knowledge about the electronics of the transformation.

Experimental and computational evidence of the mechanism is showcased, including kinetic studies and Hammett competition plots. Computational calculations have been carried out in collaboration with Prof. Feliu Maseras' group (ICIQ, Tarragona). The aminofluorination with $TolIF_2$ goes through the formation of an aziridine intermediate that is afterwards opened with fluorine via H-bond assisted *syn* delivery to a pseudo-carbocation transition state, stabilised by the secondary electronic unit of the substrate. In the ring-opening phase of the tandem strategy a similar behaviour is observed, although selectivity varies depending on the fluorinating agent. The protonation of the aziridine is described as the decisive event for the selectivity of the transformation.

UNIVERSITAT ROVIRA I VIRGILI
INSIGHTS INTO AMINOFLUORINATION STRATEGIES AND SPHINGOSINE ANALOGUE SYNTHESIS TOWARDS THE DEVELOPMENT OF SELECTIVE SPHK2 INHIBITORS
Albert Granell Fort

CHAPTER I

General Introduction

UNIVERSITAT ROVIRA I VIRGILI
INSIGHTS INTO AMINOFLUORINATION STRATEGIES AND SPHINGOSINE ANALOGUE SYNTHESIS TOWARDS THE DEVELOPMENT OF SELECTIVE SPHK2 INHIBITORS
Albert Granell Fort

1.1. Sphingosine Kinase (SphK) as a Target for Cancer Therapy

Bioactive sphingolipids play a central role in multiple biological and physiological processes including lymphocyte trafficking, cell growth, apoptosis, mitogenesis, radio and chemo-sensitization, angiogenesis, inflammation and cancer.[1] There are three well-studied bioactive sphingolipids: ceramide (Cer), sphingosine (Sph) and sphingosine-1-phosphate (S1P), which are interconvertible in a complex biosynthetic pathway regulated by specific enzymes, usually referred to as *Ceramide-Sphingosine-1-Phosphate Rheostat* (Figure **1.1**). This equilibrium determines cell fate and triggers a cascade of biochemical processes. that as a whole, may be related to apoptosis or survival processes, depending on the state of this *rheostat.* In this regard, increased levels of Cer and Sph have been associated with pro-apoptotic processes whereas increased levels of S1P have been related to cell survival.[2] This dynamic equilibrium has attracted the interest of the scientific community towards the development of pharmacological tools against cancer, since favouring apoptosis may ultimately lead to cancer regression or, in the other way, cell survival may result in cancer progression.

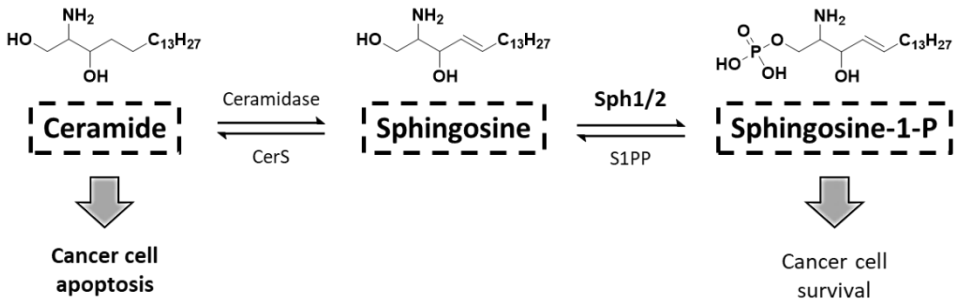

Figure 1.1. Ceramide-Sphingosine-1-phosphate rheostat.

One of the most relevant enzymes involved in sphingolipid metabolism is Sphingosine Kinase (SphK), which catalyzes the fosforylation

[1] Swinson, J. *Manuf. Chemist*. **2005**, 35–36.
[2] Cuvillier, O.; Pirianov, G.; Kleuser, B.; Vanek, P. G.; Coso, O. A.; Gutkind, J. S.; Spiegel, S. *Nature*, **1996**, *381*, 800-803.

of sphingosine (Sph) into sphingosine-1-phosphate (S1P) (Figure **1.1**). This enzyme exists in two isoforms, SphK1 and SphK2.[3] These two kinases are located in dissimilar sites in the cell, and this difference seems to induce different functions.[4] In fact, reported data describing action of SphK2 in cancer development may sometimes appear contradictory.[5,6,7] SphK1 is found in cytoplasm, and can be transported to the plasma membrane after stimulation of numerous growth factors, cytokines and oncogenes.[8] On the other hand, SphK2 is located in the mitochondria, endoplasmic reticulum and nucleus.[7,9]

Overexpression of SphK1 has a pro-inflammatory effect in leukemia[10] and solid tumors, including breast, colon, lung, ovary, stomach, uteri, kidney, rectum and prostate.[11] Furthermore, increased levels of

---

[3] Plano, D.; Amin, S.; Sharma, A. K. *J. Med. Chem.* **2014**, *57*, 5509-5524.

[4] a) Chan, H.; Pitson, S. M. *Biochim. Biophys. Acta* **2013**, *1831*, 147–156; b) Neubauer, H. A.; Pitson, S. M. *FEBS J.* **2013**, *280*, 5317–5336.

[5] Kharel, Y.; Raje, M.; Gao, M.; Gellett, A. M.; Tomsig, J. L.; Lynch, K. R.; Santos, W. L. *Biochem. J.* **2012**, *447*, 149–157.

[6] a) Okada, T.; Ding, G.; Sonoda, H.; Kajimoto, T.; Haga, Y.; Khosrowbeygi, A.; Gao, S.; Miwa, N.; Jahangeer, S.; Nakamura, S. *J. Biol. Chem.* **2005**, *280*, 36318−36125; b) French, K. J.; Zhuang, Y.; Maines, L. W.; Gao, P.; Wang, W.; Beljanski, V.; Upson, J. J.; Green, C. L.; Keller, S. N.; Smith, C. D. *J. Pharmacol. Exp Ther.* **2010**, *333*, 129-139; c) Venkata, J. K.; An, N.; Sturat, R.; Costa, L. J.; Cai, H.; Coker, W.; Song, J. H.; Gibbs, K.; Matson, T.; Garrett-Mayer, E.; Wan, Z.; Ogretmen, B.; Smith, C.; Yang, Y. *Blood* **2014**, *124*, 1945-1925.

[7] Maceyka, M.; Sankala, H.; Hait, N. C.; Le Stunff, H.; Liu, H.; Toman, R.; Collier, C.; Zhang, M.; Satin, L. S.; Merrill, A. H.; Milstien, S.; Spiegel, S. *J. Biol. Chem.* **2005**, *280*, 37118-37129.

[8] a) Spiegel S.; Milstien S. *J. Biol. Chem.* **2002**, *277*, 25851-25854; b) Pilson, S. M.; Moretti, P. A.; Zebol, J. R.; Lynn, H. E.; Xia, P.; Vadas, M. A.; Wattenberg, B. W. *EMBO J.* **2003**, *22*, 5491-5500; c) Pitson, S. M.; Xia, P.; Leclercq, T. M.; Moretti, P. A.; Zebol, J. R.; Lynn, H. E.; Xia, P.; Wattenberg, B. W.; Vadas, M. A. *J. Exp. Med.* **2005**, *201*, 49-54; d) Spiegel, S.; Milstein, S. *Nat. Rev. Mol. Cell. Biol.* **2003**, *4*, 397-407; e) Wattemberg, B. W.; Pitson, S. M.; Raben, D. M. *J. Lipid Res.* **2006**, *47*, 1128-1139; f) Spiegel, S.; Milstein, S. *Nat. Rev. Immunol.* **2011**, *6*, 403-415.

[9] Chipuk, J. E.; McStay, G. P.; Bharti, A.; Kuwana, T.; Clarke, C. J.; Siskind, L. J.; Obeid, L. M.; Green, D. R. *Cell* **2012**, *148*, 988–1000.

[10] a) Wallington-Beddoe, C. T.; Powell, J. A.; Tong, D.; Pitson, S. M.; Bradstock, K. F.; Bendall, L. J. *Cancer Res.* **2014**, *74*, 2803–2815; b) Paugh, S. W.; Paugh, B. S.; Rahmani, M.; Kapitonov, D.; Almenara, J. A.; Kordula, T.; Milstien, S.; Adams, J. K.; Zipkin, R. E.; Grant, S.; Spiegel, S. *Blood* **2008**, *112*, 1382−1391; c) Bonhoure, E.; Lauret, A.; Barnes, D. J.; Martin, C.; Malavaud, B.; Kohama, T.; Melo, J. V.; Cuvillier, O. *Leukemia* **2008**, *22*, 971−979.

[11] a) Shirai, K.; Kaneshiro, T.; Wada, M.; Furuya, H.; Bielawski, J.; Hannun, Y. A.; Obeid, L. M.; Ogretmen, B.; Kawamori, T. *Cancer Prev. Res.* **2011**, *4*, 454–462; b) Li, W.; Yu, C. P.; Xia, J. T.; Zhang, L.; Weng, G. X.; Zheng, H. Q.; Kong, Q. L.; Hu, L. J.; Zeng, M. S.; Zeng, Y. X.; Li, M.; Li, J.; Song, L. B. *Clin. Cancer Res.* **2009**, *15*, 1393−1399; c) Johnson, K. R.; Johnson, K.

SphK1 are also associated with drug resistance and reduced patient survival.[12] Despite the fact that SphK1 is apparently more related to cancer processes, some studies have indicated that anti-cancer effects derived from loss of SphK2 are stronger than those derived from loss of SphK1.[13]

All these findings suggest that the modulation of the *rheostat* might produce changes in cell fate just shifting its position. It is therefore not surprising that the inhibition of SphK has become a target therapy.

Y.; Crellin, H. G.; Ogretmen, B.; Boylan, A. M.; Harley, R. A.; Obeid, L. M. *J. Histochem. Cytochem.* **2005**, *53*, 1159–1166; d) Erez-Roman, R.; Pienik, R.; Futerman, A. H. *Biochem. Biophys. Res. Commun.* **2010**, *391*, 219–223; e) Ruckhaberle, E.; Rody, A.; Engels, K.; Gaetje, R.; von Minckwitz, G.; Schiffmann, S.; Grosch, S.; Geisslinger, G.; Holtrich, U.; Karn, T.; Kaufmann, M. *Breast Cancer Res. Treat.* **2008**, *112*, 41–52; f) Kawamori, T.; Kaneshiro, T.; Okumura, M.; Maalouf, S.; Uflacker, A.; Bielawski, J.; Hannun, Y. A.; Obeid, L. M. *FASEB J.* **2009**, *23*, 405–414.

[12] Gustin, D. J.; Li, Y.; Brown, M. L.; Min, X.; Schmitt, M. J.; Wanska, M.; Wang, X.; Connors, R.; Johnstone, S.; Cardozo, M.; Cheng, A. C.; Jeffries, S.; Franks, B.; Li, S.; Shen, S.; Wong, M.; Wesche, H.; Xu, G.; Carlson, T. J.; Plant, M.; Morgenstern, K.; Rex, K.; Schmittf, J.; Coxon, A.; Walker, N.; Kayser, F.; Wang, Z. *Bioorg. Med. Chem. Lett.* **2013**, *23*, 4608-4616.

[13] Gao, P.; Smith, C. D. *Mol. Cancer Res.* **2011**, *9*, 1509-1519.

1.2. Structure of Sphingosine Kinase 1 (SphK1)

In 2013, Wang and co-workers first reported the crystal structure of human SphK1 in the apo form and in complexes with sphingosine and with other inhibitors and adenosine diphosphate (ADP).[14] Similarly, the isolation of the crystal structure of SphK1 with inhibitor PF-543 was published by Pyne one year later.[15]

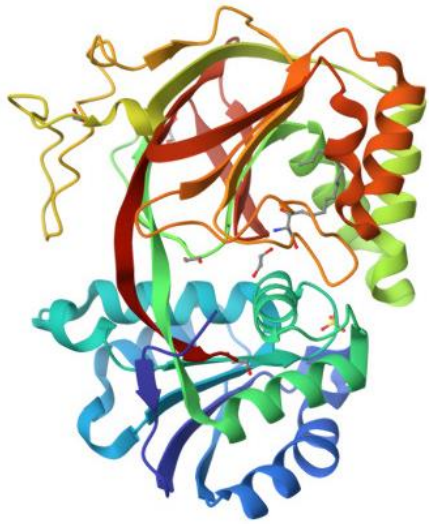

Figure 1.2. X-Ray structure of Sphingosine Kinase 1. PDB DOI: https://doi.org/10.2210/pdb3VZB/pdb.

The crystal structure of this kinase has been deeply analysed and discussed by both authors. Features of note regarding the active site are listed below:

- The structure has a two-domain architecture.
- The polar head of sphingosine is located between both domains and interacts with polar amino acids through hydrogen bonds.

[14] Wang, Z.; Min, X.; Xiao, S.-H.; Johnstone, S.; Romanow, W.; Meininger, D.; Xu, H.; Liu, J.; Dai, J.; An, S.; Thibault, S.; Walker, N. *Structure* **2013**, *21*, 798–809.
[15] Wang, J.; Knapp, S.; Pyne, N. J.; Pyne, S.; Elkins, J. *ACS Med. Chem. Lett.* **2014**, *5*, 1329-1333.

- Sphingosine long alkyl chain is buried in a hydrophobic pocket, also called the "J-channel", stablishing Van der Vaals interactions with non-polar residues.

- The lipid-binding cavity is small. For this matter, bulky substituents in the lipid scaffold might not fit.

1.2.1. Structure of SphK2

SphK2 has not been yet crystallised and therefore its structure remains unknown. However, Pyne et al.[16] identified key structural differences in the J-channel of the active site between SphK1 and SphK2 by mapping SphK2 sequence differences onto an SphK1/PF-543 (a selective SphK1 inhibitor) cocrystal structure. By tuning the structure of PF-543 and observing the host-guest interactions, a good picture of the SphK2 surface structure was drawn.

The key residue differences in the binding pocket of the two SphK isoforms are basically Phe288, Ile174, Met272 in SphK1, corresponding to Cys569, Val340 and Leu553 in SphK2.[17] In addition, Leu553 in SphK2 induces distinct orientational changes in residues Phe358 (Phe192 in SphK1) and Arg357 (Arg191 in SphK1). These structural changes lead to a longer and slightly wider J-shaped pocket in SphK2 (Figure **1.3**). It has also been reported that enhancing the contacts with the Leu549, the Ser334 and Asp344 of SphK2 around the polar region might lead to a stronger selective inhibition against this isoform.[18]

[16] Adams, D. R.; Tawati, S.; Berreta, G.; Lopez Rivas, P.; Baiget, J.; Jiang, Z.; Alsfouk, J.; Mackay, S. P.; Pyne, N. J.; Pyne, S. *J. Med. Chem.* **2019**, *62*, 3658–3676.

[17] Note that both SphK1 and SphK2 have several isoforms and some authors refer to different isoforms. For clarity, the residue numbering correspond to the canonical isoform 1 for both proteins. SphK1: https://www.uniprot.org/uniprot/Q9NYA1#sequences. SphK2: https://www.uniprot.org/uniprot/Q9NRA0#sequences.

[18] Sibley, C. D.; Morris, E. A.; Kharel, Y.; Brown, A. M.; Huang, T.; Bevan, D. R.; Lynch, K. R.; Santos, W. L. *J. Med. Chem.* **2020**, *63*, 1178–1198.

The study concludes that SphK2 presents two main differences in the J-channel, where the apolar part of the inhibitor fits to interact with the enzyme: widening of the heel of the aliphatic pocket and shortening of the toe of the toe-end (Figure **1.3**). These findings allow for better SphK2 inhibitor design.

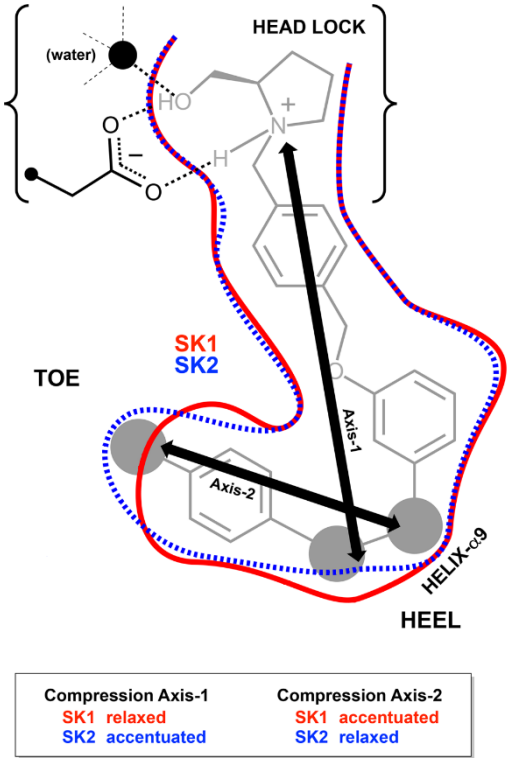

Figure 1.3. Structural difference of the "J-pocket" between SphK1 and 2 isoforms from a SphK1/PF-543 cocrystal structure model.

1.3. Sphingosine Kinase inhibitors (SphKIs)

As discussed before, the cell fate depends on the position of the *ceramide-sphingosine-1-phosphate rheostat*. The inhibition of either of the two kinases, SphK1 or SphK2, shifts the equilibrium to the accumulation of sphingosine (or biosynthesis of ceramide) favouring cell apoptosis. Conversely, no inhibitory effect over this enzyme would promote the formation of S1P leading to cell proliferation. In this sense, several research groups and pharmaceutical companies have worked in the development of inhibitors of this kinase with the aim of shifting the equilibrium towards the formation of apoptosis cell signalling molecules.

The elucidation of the crystal structure of SphK1 has brought about a great breakthrough in the inhibition of this enzyme. However, many SphKIs were described before its isolation. Considering these premises, here we will highlight some of the most relevant advancements in the development of SphKIs. These inhibitors will be classified according to their selectivity.

1.3.1. Dual SphK1/SphK2 inhibitors

Some SphK inhibitors are considered as non-selective as they do not demonstrate preference for any isomorph of SphK, and work on both enzymes within the same range of concentration.

Safingol (DHS) and *N,N*-dimethylsphingosine (DMS) were reported as some of the first inhibitors of SphK. They were prepared by minor modifications of the sphingosine structure, consisting of the removal of the *trans* double bond and methylation of amine group, respectively.[19]

Enigmol is another sphingosine derivative prepared by formal transposition of a hydroxyl group from the position 1 to carbon 5, thus avoiding the phosphorylation by SphK to form S1P. *In vitro,* this compound

[19] Orr Gandy, K. A.; Obeid, L. *Biochim. Biophys. Acta* **2013**, *1*, 157–166.

has shown potent anticancer activity in cells present in multiple types of cancer as well as inhibition of ceramide synthase.[20]

SKI-I and SKI-II were found in the same study,[21] and although both decrease the cellular S1P, they also play different roles in several diseases. *In vitro*, SKI-I reduces cell growth of some kinds of cancer cells, and SKI-II intensifies the effects of other anti-cancer agents on cell lines. *In vivo*, SKI-I exerts anti-tumour activity in melanoma and breast cancer, and SKI-II is effective at reducing growth of lung cancer xenografts, myeloid leukaemia, pulmonary fibrosis, inflammation and hyperalgesia as well as favouring the sensitivity of an inhibitor against breast cancer.[22]

On the other hand, computational tools have also contributed to develop new SphKIs. In this regard, RB-042,[23] MP-A08,[24] and ABC294735[25] were screened after modelling studies revealing moderate to good inhibition for both enzymes (Figure **1.4**).

[20] Esteve, J.; Larente, A.; Romea, P.; Urpí, F.; Ríos-Luci, C.; Padrón, J. M. *Eur. J. Org. Chem.* **2011**, 960-967.
[21] French, J. K.; Schrecengost, R. S.; Lee, B. D.; Zhuang, Y.; Smith, S. N.; Eberly, J. L.; Yun, J. K.; Smith, C. D.; *Cancer Res.* **2003**, *63*, 5962–5969.
[22] Pitman, M. R.; Costabile, M.; Pitson, S. M. *Cell. Signal.* **2016**, *28*, 1349-1363.
[23] Baek, D. J.; MacRitchie, N.; Anthony, N. G.; Mackay, S. P.; Pyne, S.; Pyne, N. J.; Bittman, R. *J. Med. Chem.* **2013**, *56*, 9310–9327.
[24] Pitman, M. R.; Powell, J. A.; Coolen, C.; Moretti, P. A.; Zebol, J. R.; Pham, D. H.; Finnie, J. W.; Don, A. S.; Ebert, L. M.; Bonder, C. S.; Gliddon, B. L.; Pitson, S. M. *Oncotarget* **2015**, *6*, 7065–7083.
[25] Gao, P.; Peterson, Y. K.; Smith, R. A.; Smith, C. D. *PLoS One* **2012**, *7*, e44543.

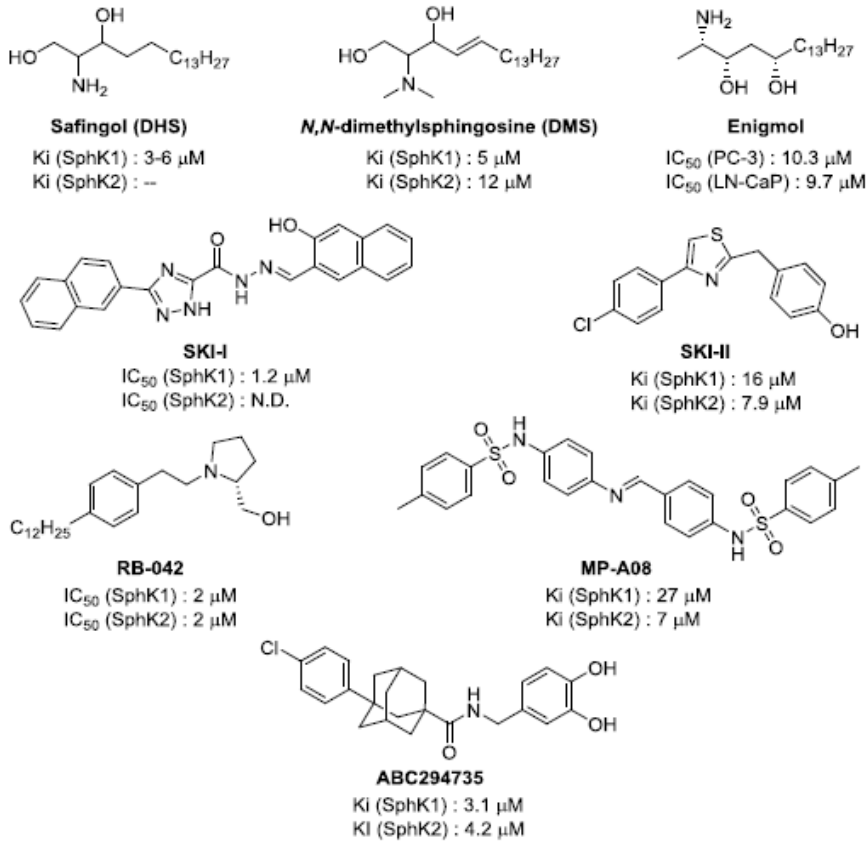

Figure 1.4. Non-selective inhibitors of Sphingosine Kinase 1 and Sphingosine Kinase 2

1.3.2. Selective SphK1 inhibitors

Relative to the syntheses of SphKIs, SphK1 has been more deeply studied than SphK2 due to the availability of a crystal structure and to its greater association with cancer progress.

Modifications in sphingosine structure have led to the formation of promising inhibitors. FTY720 is a sphingosine derivative bearing an aryl group and a tetrasubstituted centre, which is reported to act as an agonist

of S1P receptors after phosphorylation by SphK2.[26] It is also used in the treatment of several autoimmune diseases.[27]

A structurally related derivative of FTY720 is the (*S*)-FTY720-vinylphosphonate, in which one of the prochiral alcohols has been replaced by a vinylphosphonate group to block the phosphorylation by SphK2.[28]

Other compounds including SKI-1, LCL 351 and SK1-5c can be also considered sphingosine derivatives. They are implicated in reducing tumour volumes in xenografts[29] and migration rate of some cells involved in prostate human cancer[30] and sensitizing chemotherapeutic agents in breast cancer, [31] respectively (Figure **1.5**).

[26] a) Brinkmann, V.; Davis, M. D.; Heise, C. E.; Albert, R.; Cottens, S.; Hof, R.; Bruns, C.; Prieschl, E.; Baumruker, T.; Hiestand, P.; Foster, C. A.; Zollinger, M.; Lynch, K. R. *J. Biol. Chem.* **2002**, *277*, 21453−21457; b) Mandala, S.; Hajdu, R.; Bergstrom, J.; Quackenbush, E.; Xie, J.; Milligan, J.; Thornton, R.; Shei, G. J.; Card, D.; Keohane, C.; Rosenbach, M.; Hale, J.; Lynch, C. L.; Rupprecht, K.; Parsons, W.; Rosen, H. *Science* **2002**, *296*, 346−349.

[27] a) Ubai, T.; Azuma, H.; Kotake, Y.; Inamoto, T.; Takahara, K.; Ito, Y.; Kiyama, S.; Sakamoto, T.; Horie, S.; Muto, S.; Takahara, S.; Otsuki, Y.; Katsuoka, Y. *Anticancer Res.* **2007**, *27*, 75−88; b) Zheng, T.; Meng, X.; Wang, J.; Chen, X.; Yin, D.; Liang, Y.; Song, X.; Pan, S.; Jiang, H.; Liu, L. *J. Cell. Biochem.* **2010**, *111*, 218−228.

[28] Lim, K. G.; Tonelli, F.; Berdyshev, E.; Gorshkova, I.; Leclercq, T.; Pitson, S. M.; Bittman, R.; Pyne, S.; Pyne, N. J. *Int. J. Biochem. Cell Biol.* **2012**, *44*, 1457−1464.

[29] a) Paugh, S. W.; Paugh, B. S.; Rahmani, M.; Kapitonov, D.; Almenara, J. A.; Kordula, T.; Milstien, S.; Adams, J. K.; Zipkin, R. E.; Grant, S.; Spiegel, S. *Blood* **2008**, *112*, 1382−1391; b) Kapitonov, D.; Allegood, J. C.; Mitchell, C.; Hait, N. C.; Almenara, J. A.; Adams, J. K.; Zipkin, R. E.; Dent, P.; Kordula, T.; Milstien, S.; Spiegel, S. *Cancer Res.* **2009**, *69*, 6915−6923.

[30] Sharma, A. K. *Expert Opin. Ther. Patents* **2011**, *21*, 807-811.

[31] Datta, A.; Loo, S. Y.; Huang, B.; Wong, L.; Tan, S. S.; Tan, T. Z.; Lee, S. C.; Thiery, J. P.; Lim, Y. C.; Yong, W. P.; Lam, Y.; Kumar, A. P.; Yap, T. C. *Oncotarget* **2014**, *5*, 5920-5933.

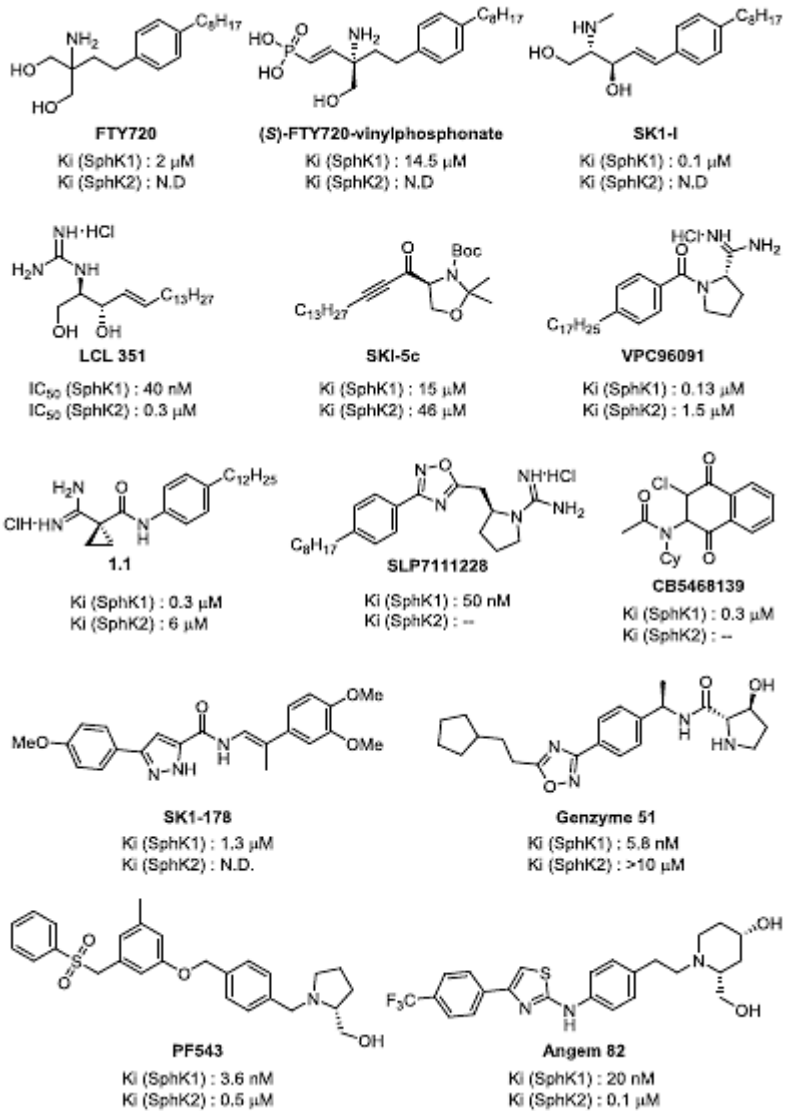

Figure 1.5. Selective inhibitors for Sphingosine Kinase 1

1.3.3. Selective SphK2 inhibitors

The absence of crystal structure of human SphK2 has slowed down the development of SphKIs for this isoform. Despite this, some SphK2-specific inhibitors have emerged to be effective in numerous diseases acting in micromolar scale.

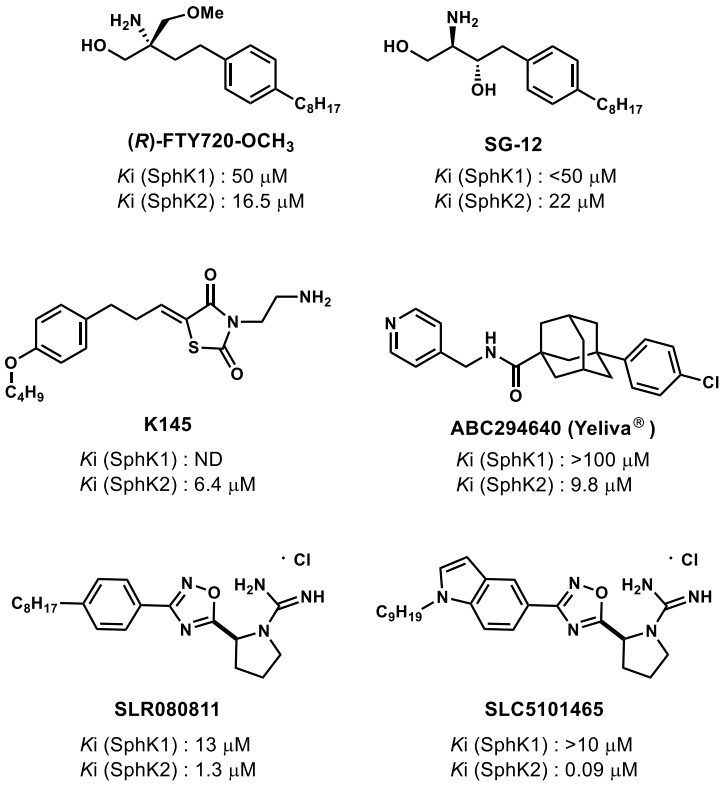

Figure 1.6. Selective inhibitors for Sphingosine Kinase 2.

(*R*)-FTY720-OMe and SG-12 are sphingosine analogues which induced apoptosis of cells involved in leukaemia[32] as well as inhibiting DNA synthesis of breast cancer cells[33] and promote death cells of murine B-lymphoma after phosphorylation,[34] respectively. *In* vitro, SLR080811 decreases levels of S1P in leukaemia and ovarian cancer cells although increases blood S1P levels *in vivo*.[5] On the other hand, K145 is implicated in dwindling S1P levels, hindering growth and suppressing ERK/AKT signalling in U937 cells and inhibiting tumour growth *in vivo*.[35] Docking

[32] Evangelisti, C.; Evangelisti, C.; Teti, G.; Chiarini, F.; Falconi, M.; Melchionda, F.; Pession, A.; Bertaina, A.; Locatelli, F.; McCubrey, J. A.; Beak, D. J.; Bittman, R.; Pyne, S.; Pyne, N. J.; Martelli, A. M. *Oncotarget* **2014**, *5*, 7886-7901.
[33] Lim, K. G.; Sun, C.; Bittman, R.; Pyne, N. J.; Pyne, S. *Cell. Signal.* **2011**, *23*, 1590-1595.
[34] Hara-Yokoyama, M.; Terasawa, K.; Ichinose, S.; Watanabe, A.; Podyma-Inoue, K. A.; Akiyoshi, K.; Igarashi, Y.; Yanagishita, M. *Bioorg. Med. Chem. Lett.* **2013**, *23*, 2220–2224.
[35] Liu, K.; Guo, T. L.; Hait, N. C.; Allegood, J.; Parikh, H. I.; Xu, W.; Kellogg, G. E.; Grant, S.; Spiegel, S.; Zhang, S. *PLoS One* **2013**, *8*, e56471.

studies have led to synthesis of aryladamantane ABC294640 which suppresses the cell proliferation *in vitro*[36] and has been used in the treatment of numerous diseases *in vivo*.[3,37] Recently, SLC5101465,[38] the most selective SphK2-selective inhibitor to date, resulted from an optimization process from SLR080811 (Figure **1.6**).[39]

1.3.4. Fluorinated Sphingosine Analogues as SphK2 inhibitors

The incorporation of fluorine to an organic molecule leads to important changes in its physical, chemical and biological properties. These changes are often produced by the formal replacement of hydrogen by fluorine, although exchanges of hydroxyl groups also have been described. The van der Waals radius of C-F bond (1.41 Å) falls between that of C-O bond (1.43 Å) and the C-H bond (1.09 Å), making fluorine a versatile element for bioisosteric replacement.[40] Thus, it is no wonder that fluorinated compounds have great relevance in pharmaceutical, agrochemical or medicinal research.[41]

The β-fluoroamine motif is a remarkable fragment for medicinal chemistry. The electron-withdrawing character of the fluorine atom in β position is able to decrease the pK_a of the amine, improving the

[36] French, K. J.; Zhuang, Y.; Maines, L. W.; Gao, P.; Wang, W.; Beljanski, V.; Upson, J. J.; Green, C. L.; Keller, S. N.; Smith, C. D. *J. Pharmacol. Exp. Ther.* **2010**, *333*, 129–139.
[37] Pyne, S.; Adams, D. R.; Pyne, N. J. *Prog. Lipid Res.* **2016**, *62*, 93-106.
[38] Congdon, M.; Fritzemeier, R.G.; Kharel, Y.; Brown, A. M.; Serbulea, V.; Bevan, D.R.; Lynch, K.R.; Santos, W.L. *Eur. J. Med. Chem.* **2021**, *212*, 113121.
[39] Kharel, Y.; Raje, M.; Gao, M.; Gellet, A.; Tomsig, J.L.; Lynch, K.R.; Santos, W.L. *Biochem. J.* **2012**, *447*, 149-457.
[40] a) Olah, G. A.; Chambers, R. D.; Prakash, G. K. S. *Synthetic Fluorine Chemistry*; John Wiley: New York, **1992**; b) Hudlicky, M.; Pavlath, A. E. *Chemistry of Organic Fluorine Compounds II*; American Chemical Society: Washington, DC, **1995**; c) Chambers, R. D. *Fluorine in Organic Chemistry*; Blackwell Publishing: Oxford, **2004**; d) Durnitz, J. D.; Scheweizer, W. B. *Chem. Eur. J.* **2006**, *12*, 6804-6815.
[41] a) Müller, K.; Faeh, C.; Diederich, F. *Science* **2007**, *317*, 1881-1886; b) Purser, S.; Moore, P. R.; Swallow, S.; Gouverneur, V. *Chem. Soc. Rev.* **2008**, *37*, 320-330; c) Tredwell, M.; Preshlock, S. M.; Taylor, N. J.; Gruber, S.; Huiban, M.; Passchier, J.; Mercier, J.; Génicot, C.; Gouverneur, V. *Angew. Chem. Int. Ed.* **2014**, *53*, 7751-7755; *Angew. Chem.* **2014**, *126*, 7885-7889; d) Jeschke, P. *ChemBioChem* **2004**, *5*, 570-589; e) Wang, J.; Sánchez-Roselló, M.; Aceña, J. L.; del Pozo, C.; Sorochinsky, A. E.; Fustero, S.; Soloshonok, V. A.; Liu, H. *Chem. Rev.* **2014**, *114*, 2432-2506; f) Liu, S.; Lu, K.; Zhang, Y.; Li, X. *Chin. J. Org. Chem.* **2022**, *42*, 2124–2133.

bioavailability of the compound containing the β-fluoroamine motif and increasing its blood-brain barrier penetration.[42] Furthermore, the β-fluoroamine moiety is also involved in improvements in metabolic stability and binding affinity, thereby constituting an important building block in drugs with anticancer, anticholinergic and anti-inflammatory properties.[43]

In this sense, the interest in preparing new compounds featuring this scaffold in their structures has increased during the last years.[44] This unit is easily accessible through different methods that rely on the α-fluorination of carbonyl compounds through their enol form, one-pot α-fluorination/reductive amination protocols (Scheme **1.1**, **a**),[45] intramolecular cyclization of indoles and amides (Scheme **1.1**, **b**), and others.[46] Among them, the ring-opening of aziridines with nucleophilic fluorine sources (Scheme **1.1**, **c**) is one of the preferred methods due to low cost of reagents, mild reaction conditions, and general accessibility of substrates.[47]

---

[42] O'Hagan, D. *Chem. Soc. Rev.* **2008**, *37*, 308-319.

[43] a) Cox, C. D.; Coleman, P. J.; Breslin, M. J.; Whitman, D. B.; Garbaccio, R. M.; Fraley, M. E.; Buser, C. A.; Walsh, E. S.; Hamilton, K.; Schaber, M. D.; Lobell, R. B.; Tao, W.; Davide, J. P.; Diehl, R. E.; Abrams, M.T.; South, V. J.; Huber, H. E.; Torrent, M.; Prueksaritanont, T.; Li, C.; Slaughter, D. E.; Mahan, E.; Fernandez-Metzler, C.; Yan, Y.; Kuo, L. C.; Kohl, N. E.; Hartman, G. D. *J. Med. Chem.* **2008**, *51*, 4239-4252; b) Welsch, J. T.; Eswarakrishamn, S. *Fluorine in Bioorganic Chemistry*, Wiley, New York, **1991**.

[44] a) Yadav, J. S.; Reddy, B. V. S.; Chaya, D. N.; Kumar, G. G. K. S. N.; Naresh, P.; Jagadeesh, B. *Tetrahedron Lett.* **2009**, *50*, 1799-1802; b) Liu, F.; Martin-Mingot, A.; Jouannetaud, M. P.; Zunino, F.; Thibaudeau, S. *Org. Lett.* **2010**, *12*, 868-871; c) Al-Maharik, N.; O'Hagan, D. *Aldrichimica Acta* **2011**, *44*, 3, 65-75; d) Andrews, P. C.; Bhaskar, V.; Bromfield, K. M.; Dodd, A. M.; Duggan, P. J.; Duggan, S. A. M.; McCarthy, T. D. *Synlett* **2004**, *2004*, 5, 0791-0794; e) Malamakal, R. M.; Hess, W. R.; Davis, T. A. *Org. Lett.* **2010**, *12*, 2186-2189; f) Chen, P.; Liu, G. *Eur. J. Org. Chem.* **2015**, 4295–4309.

[45] a) Ishimaru, T.; Shibata, N.; Horikawa, T.; Yasuda, N.; Nakamura, S.; Toru, T.; Shiro, M. *Angew. Chem.* **2008**, *120*, 4225-4229; *Angew. Chem. Int. Ed.* **2008**, *47*, 4157-4161. b) Beeson, T. D.; MacMillan, D. W. C. *J. Am. Chem. Soc.* **2005**, *127*, 8826–8828. c) Fadeyi, O. O.; Lindsley, C. W. *Org. Lett.* **2009**, *11*, 943-946.

[46] Lozano, O.; Blessley, G.; Martínez del Campo, T.; Thompson, A. L.; Giuffredi, G. T.; Bettati, M.; Walker, M.; Borman, R.; Governeur, V. *Angew. Chem.* **2011**, *123*, 8255-8259; b) *Angew. Chem. Int. Ed.* **2011**, *50*, 8105-8109.

[47] a) Jensen, K. L.; Standley, E. A.; Jamison, T. F. *J. Am. Chem. Soc.* **2014**, *136*, 11145–11152. b) Hu, X. E. *Tetrahedron* **2004**, *60*, 12, 2701-274. c) McNally, A.; Haffemayer, B.; Collins, B. S. L.; Gaunt, M. J. *Nature* **2014**, *510*, 7503, 129-133. d) Wade, T. N.; Guedj, R. *Tetrahedron Lett.* **1978**, 3247. e) Alvernhe, G. M.; Ennakoua, C. M.; Lacombe, S. M.; Laurent, A. *J. Org. Chem.* **1981**, *46*, 4938-4948. f) Fan, R.; Zhou, Y.; Zhang, W.; Hou, X.; Dai, L. *J. Org. Chem.*

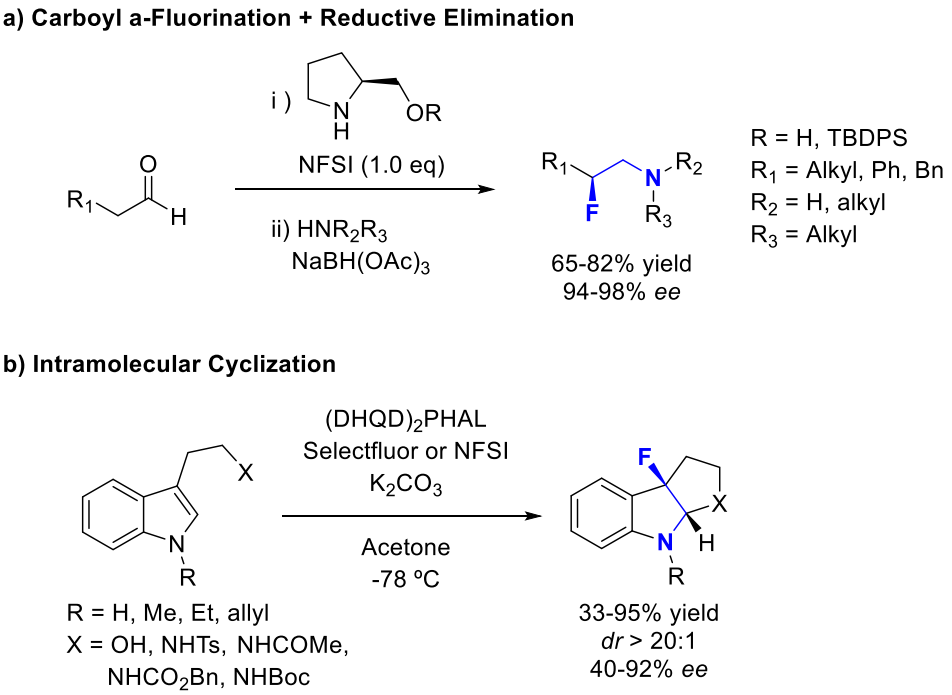

Scheme 1.1 Examples of different methodologies for the preparation of β-fluoroamines

In 1990, Wu et al. reported the synthesis of sphingosine analogues **1** and **2** (Figure **1.7**) replacing one of the hydroxyl groups of sphingosine by fluorine.[48] These analogues presented higher inhibition of SphK than DMS, usually used as a reference as a good inhibitor of SphK.[49] Unfortunately,

2004, *69*, 335-338. g) Zhang, W. X.; Su, L.; Hu, W. G.; Zhou, J. *Synlett* **2012**, *23*, 16, 2413-2415.

[48] Kozikowski, A. P.; Wu, J. *Tetrahedron Lett.* **1990**, *31*, 30, 4309-4312.

[49] De Jonghe, S.; Van Overmeire, I.; Poulton, S.; Hendrix, C.; Busson, R.; Van Calenbergh, S.; De Keukeleire, D.; Spiegel, S; Herdewijn, P. *Bioorg. Med. Chem. Lett.* **1999**, *9*, 3175-3180.

IC50 are not given for the inhibitors and instead a percentage of sphingosine kinase activity is portrayed in the article.

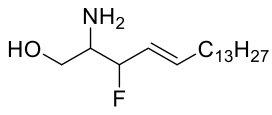

1

% inhibition = 82

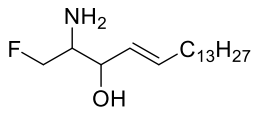

2

% inhibition = 80

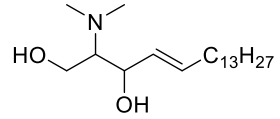

DMS

% inhibition = 48

Figure 1.7. Inhibition of Sphingosine Kinase Activity (%) of inhibitors 1, 2 and DMS.

Nonetheless, this promising result points to fluorine as a good replacement for the hydroxyl groups in the polar head of sphingosine for SphK inhibition (the article does not specify the isoform). In this regard, a methodology to easily access the β-fluoroamine scaffold present in the fluorinated analogues could be interesting to explore this family of sphingosine analogues further.

UNIVERSITAT ROVIRA I VIRGILI
INSIGHTS INTO AMINOFLUORINATION STRATEGIES AND SPHINGOSINE ANALOGUE SYNTHESIS TOWARDS THE DEVELOPMENT OF SELECTIVE SPHK2 INHIBITORS
Albert Granell Fort

UNIVERSITAT ROVIRA I VIRGILI
INSIGHTS INTO AMINOFLUORINATION STRATEGIES AND SPHINGOSINE ANALOGUE SYNTHESIS TOWARDS THE DEVELOPMENT OF SELECTIVE SPHK2 INHIBITORS
Albert Granell Fort

CHAPTER II

General Objectives

UNIVERSITAT ROVIRA I VIRGILI
INSIGHTS INTO AMINOFLUORINATION STRATEGIES AND SPHINGOSINE ANALOGUE SYNTHESIS TOWARDS THE DEVELOPMENT OF SELECTIVE SPHK2 INHIBITORS
Albert Granell Fort

2.1. General objectives

This PhD work revolves around the synthesis of new sphingosine analogues as potential inhibitors of the enzymes SphK1 and SphK2 for cancer therapy, which is one of the main research lines of our group. The thesis is structured in two chapters with very distinct topics: Chapter 3 contains the enantioselective synthesis of two sphingosine analogues based on the previous work of Dr. Macarena Corro and subsequent experiments to understand the inhibition results.[1] Chapter 4 is a preliminary study with the idea to develop a methodology to prepare a new family of sphingosine analogues with fluorine replacing the secondary alcohol in the polar head of sphingosine. Below are listed the specific aims of each chapter of the thesis:

Chapter 3: Previous research in the group discovered a number of structural features that are beneficial for the inhibition of enzyme SphK: A tetrasubstituted C-2 carbon, a polynitrogenated group in the amine functionality and a triple bond between C-4 and C-5.

- The preparation of sphingosine analogues with the mentioned features, with methyl and ethyl groups in the tetrasubstituted carbon.
- The separation of the respective enantiomers for the assessment of the inhibition activity of each isomer separately.
- The modelling of the poses of the inhibitors with SphK1 and SphK2 through molecular docking.
- The performance of cell viability assays.

[1] Corro-Morón, M.; Granell, A.; Ivanova, V.; Domingo, C.; Beltrán-Debón, R.; Barril, X.; Sanz, M.; Matheu, M. I.; Castillón, S; Díaz, Y. *Bioorg. Chem.* **2022**, *121*, 105668.

Chapter 4: The development of a methodology for the obtention of β-fluoroamines with the ultimate aim to synthetize sphingosine analogues containing fluorine in the C-3 position, since fluorine is a known bioisostere of the hydroxyl group. The aminofluorination of dienyl carbamates using hypervalent iodine reagents can be a facile way to access this fragment. In this regard, the aminofluorination of the simpler allyl carbamates is studied.

- The research of the best route for the aminofluorination of alkenes with HIR based on the current bibliography.
- The optimization of the reaction conditions to find the most suitable procedure.
- The study of the mechanism of the transformation via experimental and computational methods.
- The study of the scope and the selectivity of the reaction.
- The application of the optime procedure to dienyl carbamates as a first approach to the synthesis of C-3 fluorinated sphingosine analogues.

UNIVERSITAT ROVIRA I VIRGILI
INSIGHTS INTO AMINOFLUORINATION STRATEGIES AND SPHINGOSINE ANALOGUE SYNTHESIS TOWARDS THE DEVELOPMENT OF SELECTIVE SPHK2 INHIBITORS
Albert Granell Fort

UNIVERSITAT ROVIRA I VIRGILI
INSIGHTS INTO AMINOFLUORINATION STRATEGIES AND SPHINGOSINE ANALOGUE SYNTHESIS TOWARDS THE DEVELOPMENT OF SELECTIVE SPHK2 INHIBITORS
Albert Granell Fort

CHAPTER III

Dimethylhydrazino Sphingosine Analogues as Potential SphK2 Inhibitors for Cancer Therapy

UNIVERSITAT ROVIRA I VIRGILI
INSIGHTS INTO AMINOFLUORINATION STRATEGIES AND SPHINGOSINE ANALOGUE SYNTHESIS TOWARDS THE DEVELOPMENT OF SELECTIVE SPHK2 INHIBITORS
Albert Granell Fort

3.1. Introduction

3.1.1. Synthesis of Sphingosine Analogues as Potential SphK1/2 inhibitors

As discussed in the general introduction about SphK inhibitors, the inclusion of poli-nitrogenated groups, like guanidine or amidine, to the sphingosine scaffold seemed to improve the interaction with the binding pocket of the enzyme providing potent inhibitors.[1] In regard to these breakthroughs, our group investigated the preparation of a library of sphingosine-based analogues bearing triazoles as spacers between the polar headgroup and the hydrophobic tail, acting as poly-nitrogenated surrogates of the alkene moiety in the natural sphingosine.[2] It was observed that just like DMS, the *N,N*-dimethylamino analogues presented selective inhibition of SphK2. The increase in inhibition activity with the fluorination of the lipidic tail was also observed.

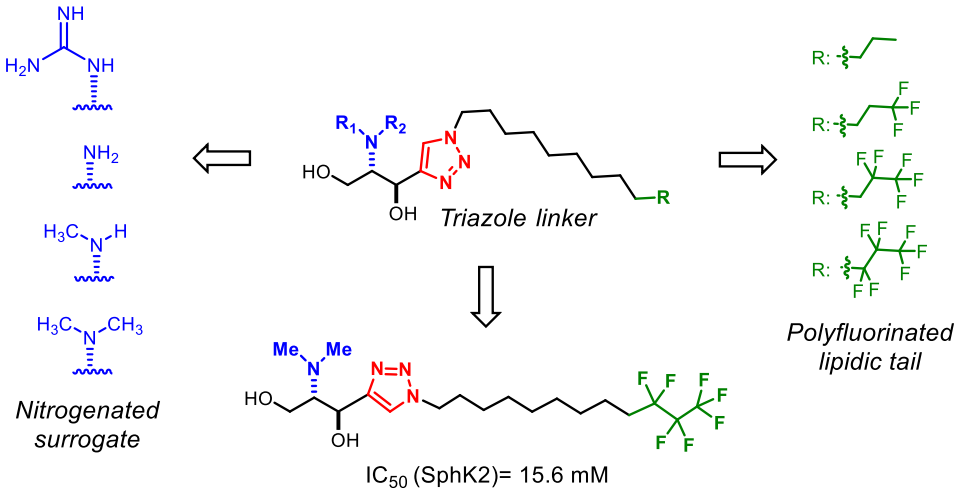

Figure 3.1. Site-diversity modifications undertaken by Escudero-Casao *et al* and structure of the most SphK2 selective inhibitor.

[1] Kharel, Y.; Raje, M.; Gao, M.; Gellett, A. M.; Tomsig, J. L.; Lynch, K. R.; Santos, W. L. *Biochem. J.* **2012**, *447*, 149–157.

[2] Escudero-Casao, M.; Cardona, A.; Beltrán-Debón, R.; Díaz, Y.; Matheu, M. I. and Castillón S. *Org. Biomol. Chem.* **2018**, *16*, 7230.

More recent studies in our group performed by Corro-Morón *et al.* envisioned the synthesis of a family of sphingosine analogues based on similar principals.

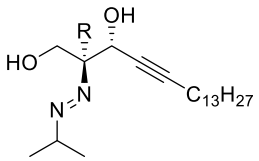

3.1 R = Me
3.2 R = Et

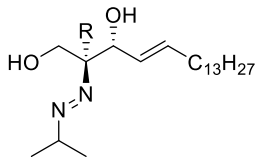

3.3 R = Me
3.4 R = Et

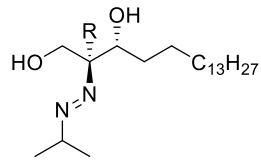

3.5 R = Me
3.6 R = Et

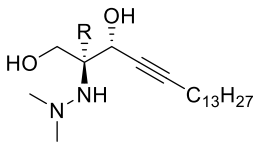

3.7 R = Me
3.8 R = Et

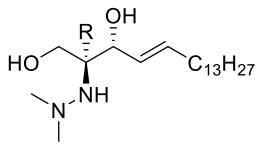

3.9 R = Me
3.10 R = Et

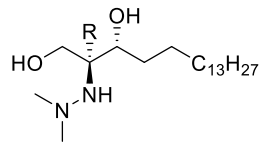

3.11 R = Me
3.12 R = Et

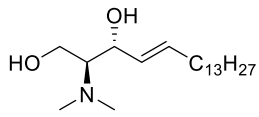

DMS

Inhibitor	SphK1	SphK2	Inhibitor	SphK1	SphK2
3.1	50.4	19.5	**3.7**	>200	17.5
3.2	43.0	9.8	**3.8**	>200	32.5
3.3	>70	15.5	**3.9**	-	-
3.4	-	-	**3.10**	33.3	29.9
3.5	>200	>200	**3.11**	72.1	>200
3.6	>200	>200	**3.12**	>200	>200
DMS	31.5	9.1			

Figure 3.2. Sphingosine analogues prepared in the group and the respective IC_{50} values for each SphK, also DMS for reference. IC_{50} values expressed as concentrations (μM). Analogues without value were not tested due to purification issues.

The presence of different nitrogenated functional groups, the role of a tetrasubstituted C2 carbon in sphingosine polar head, and the influence of different rigid spaces connected to the aliphatic chain such as a triple bond in the C4-C5 space were explored.[3] Inhibitors **3.7** and **3.8** (Figure **3.2**) resulted especially attractive, as they showed selective inhibition of SphK2.

The designed retrosynthetic pathway towards **3.7** and **3.8** can be seen in Scheme **3.1**. Based on the experience of the group on alkene aziridination,[4] the synthesis was envisioned by construction of the *anti*-amino alcohol moiety in **A** through the ring-opening reaction of an alkynyl aziridine intermediate **B**.[5,6] The corresponding amino-aziridine intermediate, in turn, can be obtained from the corresponding *trans*-α,β-unsaturated ester **C**, easily available by a Horner-Wadsworth-Emmons olefination (HWE) starting from the formylation product of 1-pentadecyne. 1-pentadecyne is commercially available and possesses the aliphatic carbon chain that conforms the apolar tail of sphingosine.

The analogues were obtained as racemic mixtures. Therefore, the interesting selective SphK2 inhibitory evaluation of these analogues must have provided underrated IC_{50} values, which should be expected to be far superior for the corresponding single enantiomers. Thus, to this end, the preparation of single enantiomers of the most promising SphK2 inhibitors **3.7** and **3.8** was intended.

Additionally, we aimed at delving into the ligand-enzyme interactions that might explain the SphK2-selectivity activity shown by some of the analogues. The absence of a crystal structure of SphK2 is an obstacle for the use of computational tools. To this purpose, docking studies of a selection of the synthesized analogues based on SphK1-SphK2

[3] Corro-Morón, M.; Granell, A.; Ivanova, V.; Domingo, C.; Beltrán-Debón, R.; Barril, X.; Sanz, M.; Matheu, M. I.; Castillón, S; Díaz, Y. *Bioorg. Chem.* **2022**, *121*, 105668.
[4] Giménez-Nueno, I.; Guasch, J.; Funes-Ardoiz, I.; Maseras, F.; Matheu, M. I.; Castillón, S.; Díaz, Y. *Chem. Eur. J.* **2019**, *25*, 12628 –12635.
[5] a) Degennaro, L.; Trinchera, P.; Luisi, R. *Chem. Rev.* **2014**, *114*, 7881-7929; b) Ohno, H. *Chem. Rev.* **2014**, *114*, 7784-7814.
[6] a) Llaveria, J.; Díaz, Y.; Matheu, M. I.; Castillón, S. *Eur. J. Org. Chem.* **2011**, 1514–1519; b) Gao, Y.; He, X.; Ding, F.; Zhang, Y. *Synthesis* **2016**, *48*, 4017–4037.

homology structures would enable us to unveil some the topological insights of the latter enzyme.

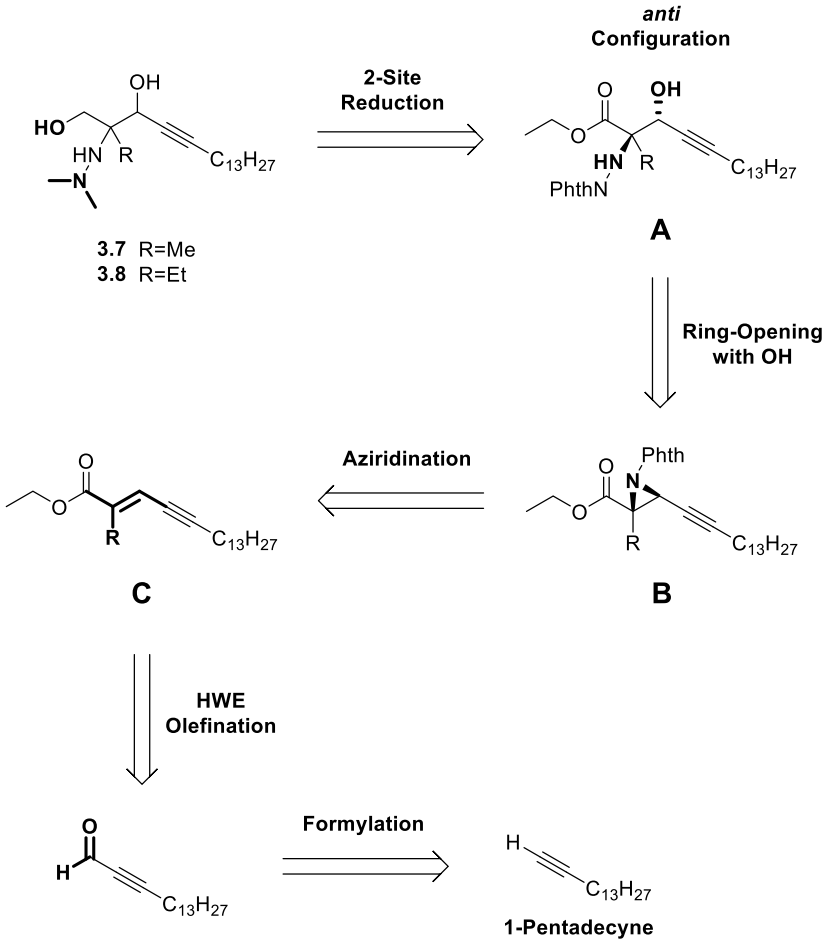

Scheme 3.1 Retrosynthetic analysis of the target sphingosine analogues racemic synthesis.

3.2. Objectives

Inhibitors bearing a triple bond and a dimethyhydrazino moiety resulted most interesting in the inhibition tests with SphK2 and are therefore further explored in this chapter. Most importantly, the enantiomeric separation of **3.7** and **3.8**.

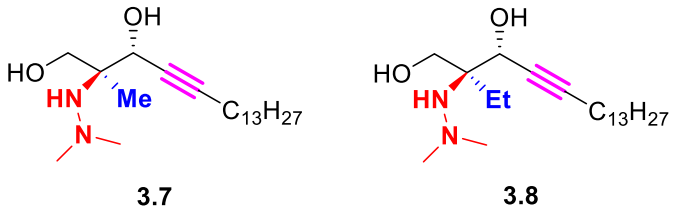

3.7 **3.8**

Figure 3.3. Structures of the inhibitors with the different variables contemplated for the family of sphingosine analogues.

In order to understand the role of the features of these inhibitors, several tests will be performed. So, the main objectives of this chapter are:

- The obtention of the enantiomeric pairs of **3.7** and **3.8** by means of enantioselective preparation or racemic synthesis + enantiomer separation. Along the synthetic plan, some of the steps needed some optimization with the respect the initial results obtained.

- The use of computational tools such as molecular docking and homology studies towards gaining insight in the interactions between the active site of SphK2 and the inhibitors. This will help understand the effect of the modifications in the IC_{50}.

- The performance of cell viability assays to assess whether the modifications have cytotoxic effects on cells.

3.3. Results and Discussion

3.3.1. Approaches to the enantioselective synthesis of analogues 3.7 and 3.8

Initial attempts towards the separation of final compounds **3.7** and **3.8** into single enantiomers involved semi-preparative chiral HPLC techniques, which proved unsuccessful due to the UV-inactivity of these compounds. Selective protection of 1-OH as a tert-butyldiphenylsilyl ether was also ineffective.

Given the availability of hydroxyl groups in the late steps of the synthesis (Scheme **3.1**), the derivatisation of the racemic analogues into diastereomeric mixtures was considered as a ready method for the preparation of single enantiomeric forms **3.7** and **3.8**. This would allow for standard separation without the need for chiral columns.

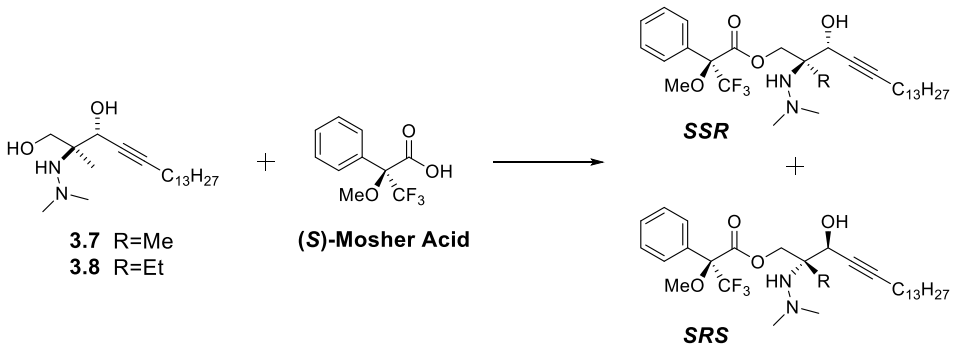

Scheme 3.2 Enantiomeric resolution of **3.7** and **3.8** using chiral agent (S)-Mosher Acid.

The derivatisation of the racemic mixture with a chiral agent was attempted. Esterification with chiral Mosher acid is a common technique for the derivatisation of enantiomers.[7] Mosher acid is a carboxylic acid engineered for the separation of enantiomers. The methoxy and trifluoromethyl fragments make it easy to detect and distinguish by ^{1}H and

[7] a) Dale, J. A.; Dull, D. L.; Mosher, H. S. *J. Org. Chem.* **1969**, *34*, 2543; b) Hoye, T. R.; Jeffrey, C. S.; Shao, F. *Nat. Protoc.* **2007**, *2*, 10, 2451.

^{19}F NMR, and the phenyl ring makes it detectable in the UV light. The suitability of Mosher esters also stems from the absence of a H alpha to the carbonyl functionality, which makes it very robust towards racemization. Also, the crowded chiral centre would be expected to provide enough differentiation between diastereomers, increasing the R_f difference and the possibilities of chromatographic separation. Esterification of the racemate with (*S*)-Mosher's acid would result in pairs of *SSR* and *SRS* diastereomers that should be separated without the need of chiral columns. Hydrolysis of the resulting isolated esters would render the single enantiomers.

3.3.1.1. Resolution Screening with Model Substrate 1,3-butanediol and Mosher Acid

Despite esterification being a trivial reaction, the substrates are quite populated and there are potential sub-products deriving from their high degree of functionalization, with a secondary alcohol or the secondary nitrogen in the hydrazine group, arguably the most nucleophilic site, although quite impeded. For that reason, 1,3-butanediol was used as a simple model substrate for esterification assays to explore the chemoselectivity of the conditions.

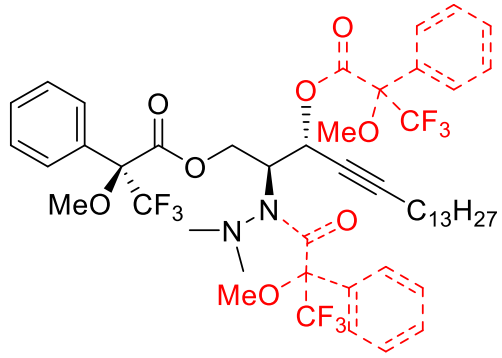

Figure 3.4. Possible selectivity issues for the esterification of **3.7** or **3.8**.

Two methods were tested for the asymmetric esterification of 1,3-butanediol: the Steglich esterification, using different urea-based coupling agents and 4-dimethylaminopyridine (DMAP) as a basic catalyst, and the

Mitsunobu reaction, using a triphenylphosphine/diisopropyl azodicarboxylate (DIAD) couple that generates a phosphonium intermediate that acts as the coupling agent.[8] Steglich esterification would conserve the configuration of the carbinol in the substrate. Instead, when secondary alcohols are used as a substrate in the Mitsunobu reaction, there is inversion of configuration. There is an S_N2 substitution in the final step of the mechanism (Scheme **3.3**). Although the inversion of configuration is not an issue for a primary alcohol, Mitsunobu reaction has been applied for the esterification of such alcohols due to its mild conditions. In this regard, we should guarantee the chemoselective derivatisation of the primary alcohol in substrates **3.7** and **3.8** without affecting the rest of functionalities and especially the secondary alcohol, since that would invert its configuration, thus rendering *syn* diastereoisomeric products, different from those desired, with an *anti* configuration.

[8] a) Neises, B.; Steglich, W. *Angew. Chem. Int. Ed. Engl.* **1978**, *17*, 7; b) Hughes, D. L. *Org. Prep. and Proc. Int.*, **1996**, *2*, 28, 127-164.

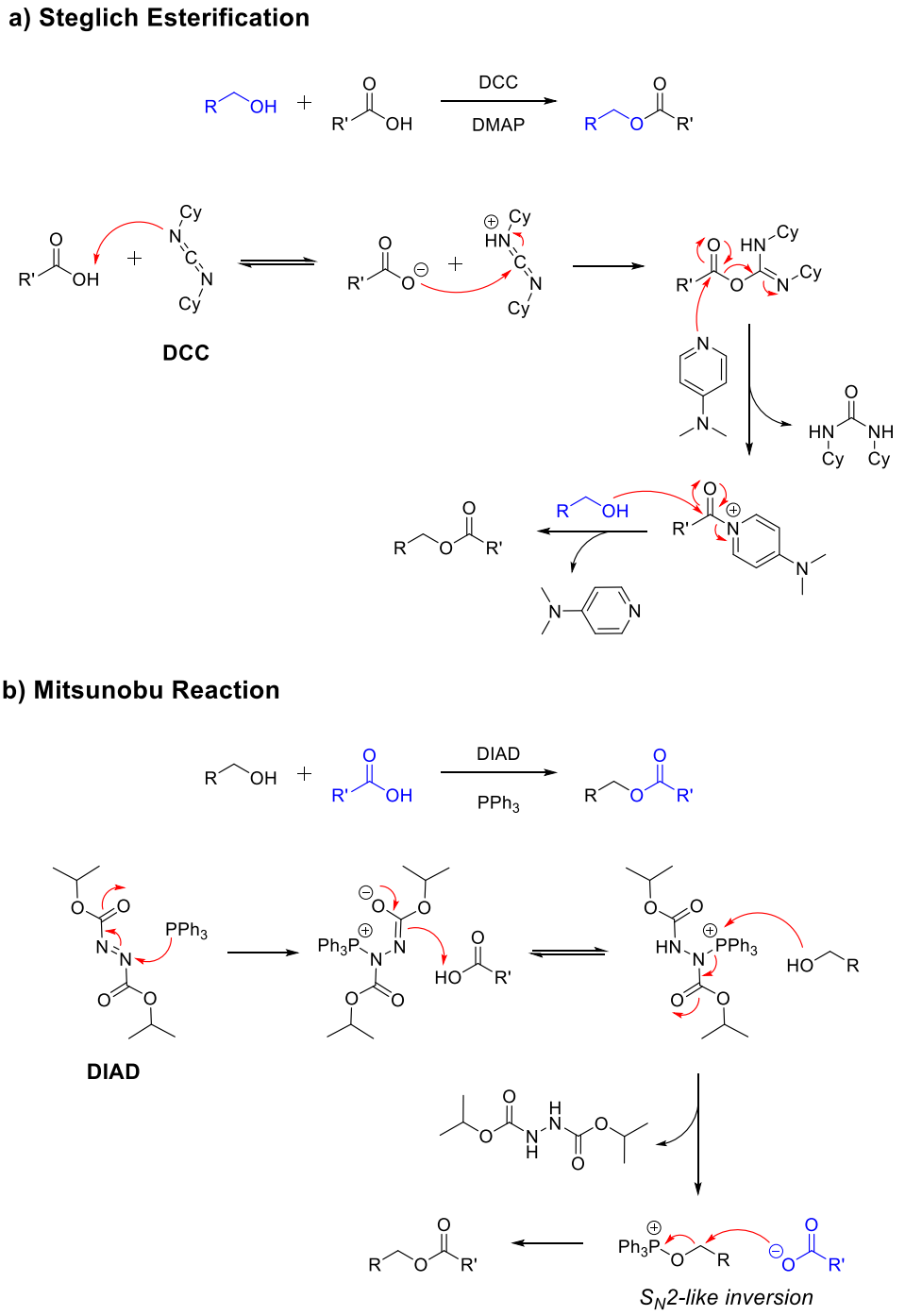

Scheme 3.3 General scheme and mechanism of the chosen derivatisation methods: the Steglich Esterification (a) and the Mitsunobu Reaction (b).

The optimization of the esterification of butane-1,3-diol with (*S*)-Mosher acid using both techniques is shown in Table **3.1**. *N,N'*-Dicyclohexylcarbodiimide (DCC), 1-ethyl-3-(3-dimethylaminopropyl) carbodiimide (EDC) and carbonyldiimidazole (CDI), coupled with DMAP, were used as coupling agents for the Steglich esterification.

Table 3.1. Esterification assays with butane-1.3-diol and optimisation.

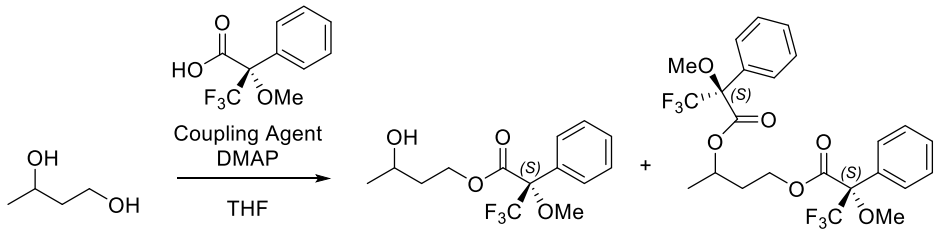

3.13 **3.14**

Entry	Coupling Agent	Equiv[a]	T (ºC)	Time	Conv[b]	Ratio 3.13/3.14[b]
1	-	1.5	rt	4d	-	-
2	CDI	1.5	rt	4d	30	?
3	EDC	1.5	rt	4d	-	-
4	EDC	1.5	Reflux	24h	52	Mono
5	DCC	1.5	rt	4d	100	67:33
6	DCC	1.5	Reflux	4d	100	57:43
7	DCC	1.1	rt	+1 week	60	91:9
8[c]	DCC	1.5	Reflux	+1 week	90	75:25
9	DIAD/Ph_3P	1.2	rt	24h	100	57:43
10	DIAD/Ph_3P	1.05	rt	24h	100	83:17

[a]Steglich: Equiv CA = equiv DMAP = equiv Mosher acid. Mitsunobu: Equiv Ph_3P = Equiv Mosher, equiv DIAD = 1. [b]Calculated by ^1H NMR. [c]Not under inert conditions.

The reaction between butane-1.3-diol and Mosher acid was first tested without any coupling reagent (Table **3.1**, entry **1**) and as expected, no conversion was observed after four days. Afterwards, DCC, EDC and CDI were tested at room temperature (Table **3.1**, entries **2**, **3**, **5**). DCC yielded a 67:33 mixture of the mono- and disubstituted products **3.13** and **3.14** in substantial amount. EDC showed no butane-1,3-diol conversion and CDI yielded low conversion to a complex mixture in the ^{1}H-NMR spectrum. EDC and DCC were tested in refluxing THF to try to reduce reaction rates and increase the conversion (Table **3.1**, entries **4**, **6**). In the case of EDC, increasing temperature produced a noticeable improvement in the reaction rate. Still, the reaction plateaued at 24h affording only the monosubstituted product. DCC showed no improvement in the rate, but the ratio of **3.14** increased significantly. Since DCC was the only reagent to show complete conversion, further optimisation was carried out with it. In order to avoid difunctionalisation, the reaction was tested using 1.1 equiv of Mosher acid instead of 1.5 (Table **3.1**, entry **7**). Equivalent control of Mosher's acid granted good selectivity towards the primary alcohol, although the conversion was lowered to 60%. Finally, the reaction was tested open to air, for simplicity's sake (Table **3.1**, entry **8**). The reaction proceeded in good conversion, although the reaction time was elongated.

Butane-1,3-diol and Mosher acid were also submitted to standard Mitsunobu conditions with 1.5 and 1.1 equiv of Mosher acid (Table **3.1**, entries **9**, **10**). Full conversion was observed after one day in both cases. As expected, lower amount of acid resulted in the increase towards **3.13**.

After the screening of reaction conditions, the Mitsunobu reactions was considered a better method for the derivatisation of analogues **3.7** and **3.8**.

3.3.1.2. Derivatization of Analogues 3.7 and 3.8

With the good conditions in hand, the esterification of the sphingosine analogues was explored. The resolution was considered at two different stages of the synthesis of the analogues. One option is the derivatisation of the final product, carrying the whole synthesis as the

racemate and separating the diastereomers at the end. A second option was to perform the esterification in the secondary alcohol generated after the ring-opening of the aziridine (**A**, Scheme **3.1**).

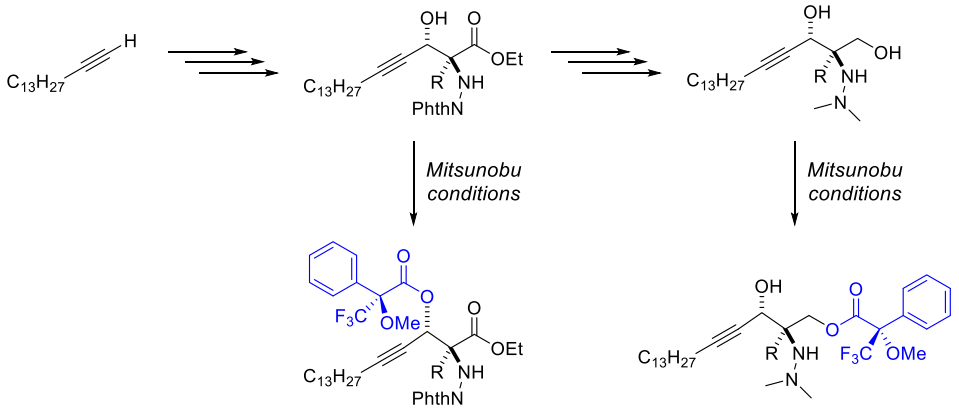

Scheme 3.4 Preferred positions for the derivatization of **3.7** and **3.8**, after the formation of the 2,3-aminol and in the final product.

Since the esterification in the assays with butane-1,3-diol was not completely selective towards the primary alcohol, esterification of the secondary alcohol with Mosher's acid at an early stage, while the other oxygenated functionality was in the form of a ethyl ester, was envisaged as a good alternative for the derivatisation. After the separation of the diastereomers and removal of the Mosher moiety, the synthesis could be resumed with each separated enantiomer separately.

With that, the racemic synthesis of **3.7** and **3.8** was carried out as starting materials for the derivatization with Mosher acid. The synthetic process is shown following the retrosynthesis in Scheme **3.1**.

The two-step synthesis of **3.15** and **3.16** was carried out in a one-pot formylation + HWE.[9] Deprotonation of 1-pentadecyne with nBuLi followed by slow addition of N-formylpipiridine rendered 1-pentadecynal, which was directly submitted to Horner-Wadsworth-Emmons (HWE) olefination conditions with the phosphonate bearing the corresponding

[9] He, L.; Byun, H. S.; Bittman, R. *J. Org. Chem.* **2000**, *22*, 65, 7627–7633.

methyl or ethyl group in basic conditions. The esters were obtained in good yield and excellent *trans*/*cis* stereoselectivity after two steps.

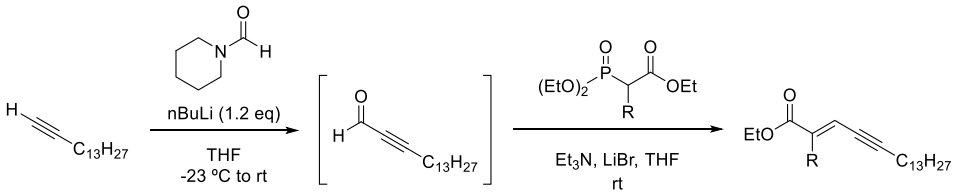

3.15 R = Me dr *trans*/*cis* = 93:7 67%
3.16 R = Et dr *trans*/*cis* = 90:10 69%

Scheme 3.5 Synthesis of the *trans*-α,β-unsaturated esters.

The *trans* configuration of the major compound was assigned based on NOE experiments. The presence of NOE correlations between the vinylic proton and the protons in the R group in the *cis* isomer contrasted with the absence of the corresponding NOE correlations in **3.15**, thus confirming the *trans* configuration of the latter. The configuration of **3.16** was assumed by analogy.

The first step towards the construction of the *anti*-α-amino alcohol scaffold of the analogues was the aziridination of the olefin in **3.15** and **3.16**. Aziridines **3.17** and **3.18** were obtained from the corresponding esters in excellent yields and diastereo- and chemoselectivities by reaction with N-aminophthalimide as a nitrene precursor and phenyliodide(III) diacetate (PIDA), a hypervalent iodine reagent, as oxidant.[10]

[10] Li, J.; Liang, J. L.; Chan, P. W. H.; Che, C. M. *Tetrahedron Lett.* **2004**, *12*, 45, 2685–2688; b) Krasnova, L. B.; Hili, R. B.; Chernoloz, O. V.; Yudin, A. K.; Stevens, C. V. *ARKIVOC IV* **2005**, 4, 26–38.

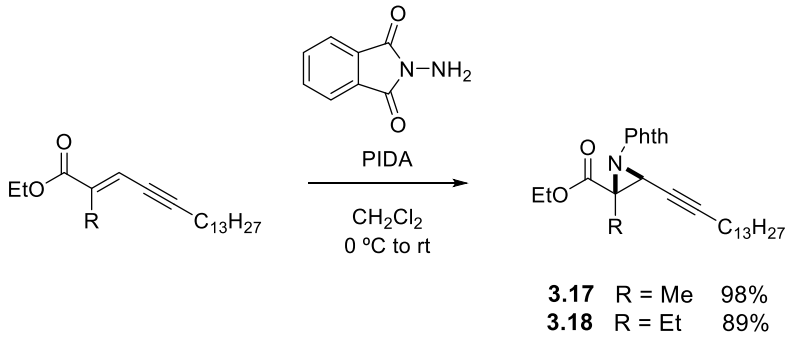

Scheme 3.6 Aziridination of the conjugated esters via HIR-mediated nitrene addition.

It is well-known that conventional alkene aziridination involving sources of nitrogen and aryliodinanes proceeds *via* nitrene precursors. However, a different mechanism[11] has been proposed in this case based on the mechanism previously reported by Atkinson.[12] PIDA and *N*-aminophthalimide react to form aminoiodane **A**, releasing acetic acid in the medium. Then, the reduction of iodine (III) to iodine (I) favours the formation of the acetoxy nitrenium **B** as the aziridinating agent, which acts as a nitrene equivalent. Finally, the generated species is attacked by the olefin to undergo aziridination.

[11] Krasnova, L. B.; Hili, R. M.; Chernoloz, O. V.; Yudin, A. K. *ARKIVOC* **2005**, *IV*, 26-38.
[12] a) Atkinson, R. S.; Grimshire, M. J.; Kelly, B. J. *Tetrahedron* **1989**, *45*, 2875-2886; b) Atkinson, R. S.; Jones, D. W.; Kelly, B. J. *J. Chem. Soc., Perkin Trans. 1* **1991**, 1344-1346.

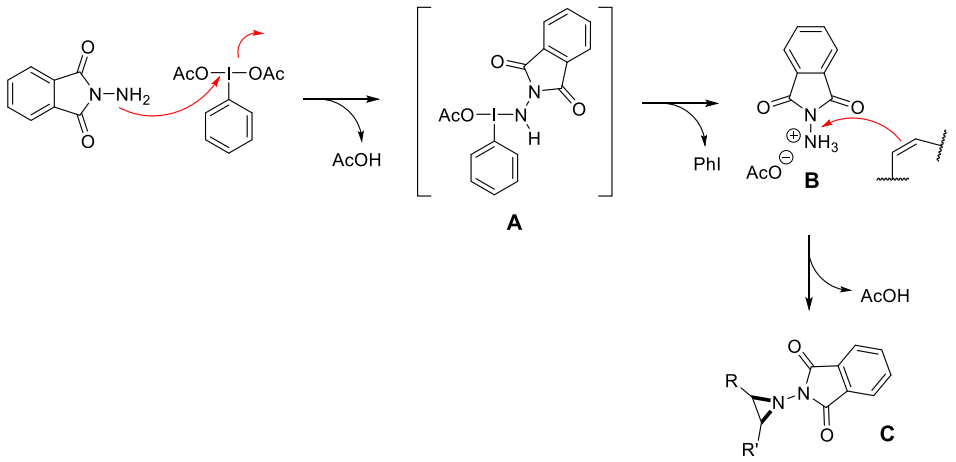

Scheme 3.7 Proposed mechanism for the aziridination with PhthN-NH_2 and PIDA.

The desired *anti*-α-amino alcohol was achieved by opening the aziridine with a nucleophilic source of water. Ring-opening of activated aziridines bearing electron-withdrawing moieties such as Ts or phosphoryl groups directly attached to nitrogen relies on the formation of a good leaving group during the ring-opening process and is fully documented. Conversely, the ring-opening of non-activated aziridines has been much less exploited and is more challenging, as acidic conditions required for that purpose should be compatible with the rest of present functionalities in the compounds.

Ring-opening reaction of non-activated aziridines **3.17** and **3.18** had been initially achieved by treatment with 1.1 equiv of *p*-toluenesulfonic acid (PTSA) in a refluxing 1:1 dioxane-water mixture to afford anti-amino-alcohols in good and modest yield, respectively (Table **3.2**, entry **5**).[13] In order to optimize the efficiency of the ring-opening process, especially towards **3.20**, alternative reaction conditions were explored.

[13] a) Akhtar, R.; Naqvi, S. A. R.; Zahoor, A. F.; Saleem, S. *Mol. Div.* **2018**, *22*, 447-501; b) Hu, X. E. *Tetrahedron* **2004**, *60*, 2701-2743; c) Watson, I. D. G.; Yudin, A. K. *J. Org. Chem.* **2003**, *68*, 5160-5167.

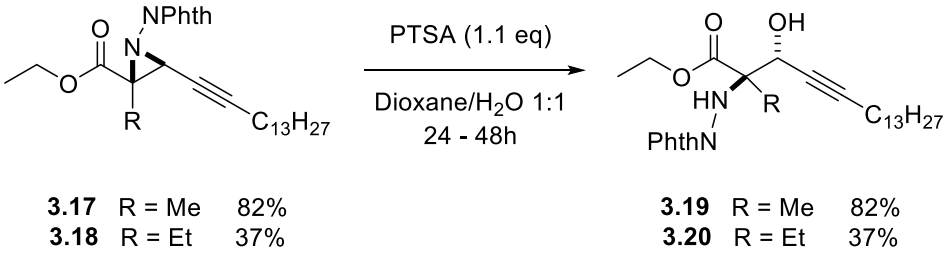

3.17 R = Me 82%
3.18 R = Et 37%

3.19 R = Me 82%
3.20 R = Et 37%

Scheme 3.8 Ring-opening of aziridines with water using PTSA as the promoter.

Reaction of aziridine **3.17** with KOH in refluxing dichloromethane led to hydrolysis of the ester moiety without detecting any traces of the ring-opened product **3.19** (Table **3.2**, entry **1**).

Cerium(IV) ammonium nitrate (CAN) is a popular reagent for the ring-opening of unactivated aziridines with water under mild conditions.[14] Use of 10 mol% CAN in ACN/H_2O did not show conversion at room temperature (Table **3.2**, entry **2**). Heating to reflux led to **3.19** in very low yield (Table **3.2**, entry **3**).

$HClO_4$ and PTSA were also tested as promoters, and both yielded better yields than CAN, with PTSA giving the best results (Table **3.2**, entries **4** and **5**). After a small scope of water-soluble solvents to try to avoid the two-phase reaction conditions, dioxane resulted in an 82% yield (Table **3.2**, entry **6**). The desired *anti* configuration was obtained exclusively in all experiments, as expected.

[14] a) Chandrasekhar, S.; Narsihmulu, C. H.; Shameem, S. *Tetrahedron Lett.* **2002**, *41*, 7361–7363; b) Chakraborty, T.K.; Ghosh, A.; Raju, T.V. *Chem. Lett.* **2003**, *32*, 82–83.

Table 3.2. Optimization for the ring opening of aziridines with water.

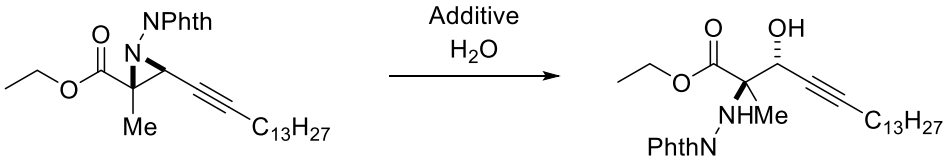

3.17 **3.19**

Entry	Additive	OH^- Source	Solvent	T (ºC)	Time (h)	Yield (%)[a]
1	18-Crown-6	KOH[b]	CH_2Cl_2	reflux	72	-
2	CAN	H_2O	ACN	rt	48	-
3	CAN	H_2O	ACN	reflux	24	19
4	$HClO_4$	H_2O	THF	reflux	24	32
5	PTSA	H_2O	THF	reflux	72	49
6	PTSA	H_2O	DMF	reflux	24	-
7	PTSA	H_2O	Dioxane	reflux	24	82

Typical conditions: aziridine (0.02 mmol), additive (1.1 equiv), solvent/H_2O 1:1. [a]Isolated yield. [b]KOH (0.15 mmol, 7 equiv).

With the *anti*-amino alcohol scaffold in hand, the next step is the construction of the dimethylhydrazino moiety. The deprotection of phthalhydrazines is reported with methylhydrazine or other similar basic hydrazines.[15] The mechanism is a standard double substitution mechanism. The hydrazine displaces both carbonyl groups in the phthalimide, to furnish phthalhydrazine derivative with release of a hydrazine directly attached to C-3 of the sphingosine analogue. Methylhydrazine is usually the reagent of choice due to the formed by-product, methyl-phthalhydrazide , being less acidic than other hydrazine-

[15] a) Sammis, G. M.; Flamme, E. M.; Xie, H.; Ho, D. M.; Sorensen, E. J. *J. Am. Chem. Soc.* **2005**, *127*, 8612–8613; b) Brosse N.; Pinto M.; Jamart-Gregoire, B. *Tetrahedron. Lett.* **2000**, *41*, 205-207.

derived by-products. This avoids the formation of complexes with the free amine resulting in a cleaner reaction.[16]

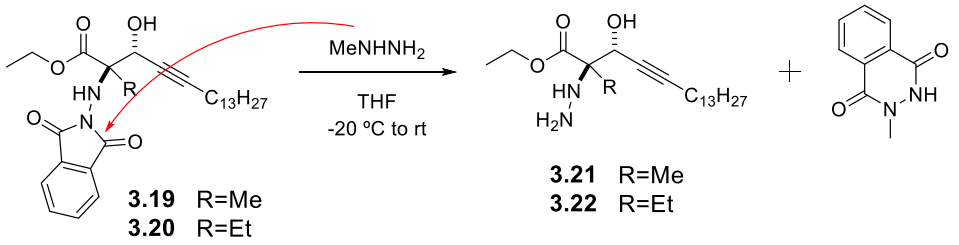

Scheme 3.9 Scheme of the deprotection of the phthalhydrazine with methylhydrazine.

Initial assays revealed that **3.21** and **3.22** are not stable and must be submitted to the next step directly after the deprotection. The free hydrazine derivatives were directly submitted to reductive amination with excess *p*-formaldehyde and $NaBH_3CN$ to afford the corresponding dimethylhydrazino derivatives (Scheme **3.10**).

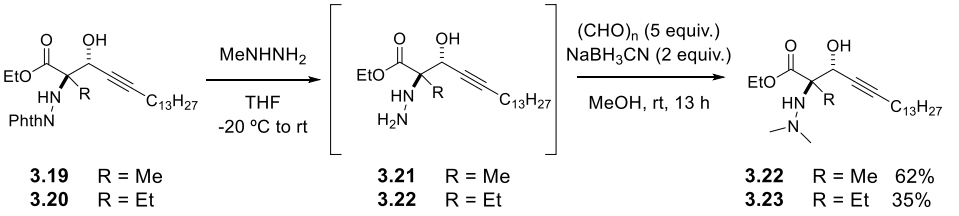

Scheme 3.10 Scheme of the construction of the dimethylhydrazine moiety. Yield given for the two steps.

Initial reaction led to a complex mixture of monomethyl, dimethyl and trimethylderivatives, difficult to separate but with good time control, the *N,N*-dimethylated product was obtained in satisfactory yield minimizing the mono- and trimethylated by-products. The dimethylhydrazine compounds were obtained in moderate yields.

[16] Kukolja, S.; Lammert, S. R. *J. Am. Chem. Soc.* **1975**, *97*, 5582-5583.

The final step for the completion of the synthesis of the sphingosine analogues is the reduction of the terminal ester group to a primary alcohol. Compounds **3.21** and **3.22** were reacted with 2.5 equiv. of DIBAL to obtain the final products **3.7** and **3.8**.

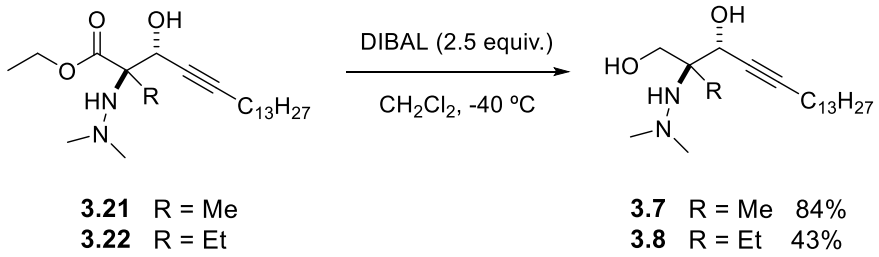

Scheme 3.11 Scheme of the reduction of the ester group to primary alcohol with DIBAL.

With the final product in hand, we were in disposition to undertake the resolution of enantiomers by conversion to dastereoisomeric pairs by reaction with Mosher's acid.

Mitsunobu conditions were applied to analogues **3.7** and **3.8** (Scheme **3.12**). Reactions proceeded to full conversion and lasted about 4h, and only mono-ester products were observed in the ^{19}F NMR spectra.

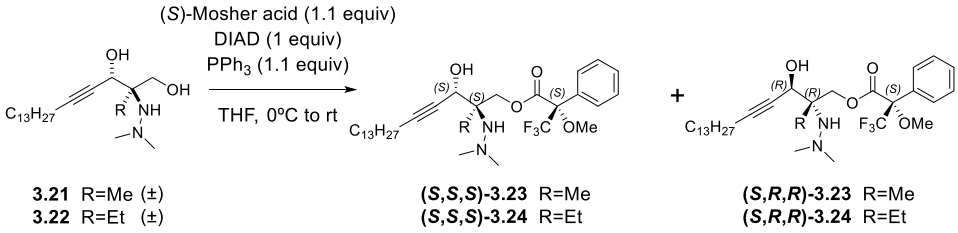

Scheme 3.12 Derivatisation of analogues **3.21** and **3.22** with (*S*)-Mosher acid to obtain separable diastereomers.

However, the diastereomeric mixtures proved inseparable by flash column chromatography either in silica gel or alumina. Attempts to separate them either by radial chromatography, preparative TLC or even semi-preparative HPLC also resulted fruitless.

After the unfortunate separation issues, the derivatization in an earlier stage of the synthesis was attempted (Scheme **3.13**). As commented before, the derivatization of a secondary alcohol might provide higher steric hindrance and therefore, more chances of diastereomer separation. Moreover, esterification at this stage posed no chemoselectivity issues, since only one hydroxyl function was present. Since Mitsunobu conditions would produce inversion of the configuration in C2, thus resulting in the *syn* disposition between C2-amine and C3-hydroxyl group instead of the desired *anti* configuration, precursor **3.17** was submitted to Steglich esterification with DCC (Scheme **3.13**). Without chemoselectivity restrictions, 2.4 equiv of Mosher acid were used to ensure full conversion of **3.17**.

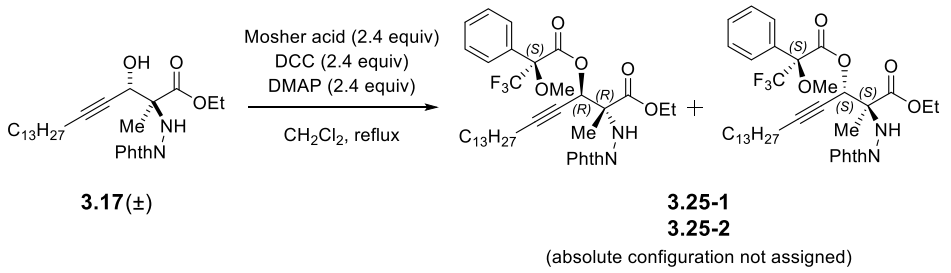

Scheme 3.13 Derivatization of **3.17** into **3.25** diastereomeric mixture.

The reaction was left stirring overnight and full conversion was obtained. The reaction crude was submitted to flash column chromatography to remove byproducts, obtaining a quite pure mixture of (S,R,R) and (S,S,S) diastereomers. A second more accurate purification enabled to separate the two diastereomers in moderate success. The obtained products were named **3.25-1** and **3.25-2** (Scheme **3.13**), but the absolute configuration of each diastereomer was not identified. Small samples of pure diastereomers were obtained in 40% (158 mg) of **3.25-1** and 7% (25 mg) of **3.25-2**.

The synthesis was continued separately with each diastereomer, **3.25-1** and **3.25-2**, which were submitted to deprotection/demethylation conditions to obtain the *N,N*-dimethylhydrazine moiety products (Scheme

3.14). Phthalimide was removed from both diastereomers successfully, but the reductive amination step yielded undesired products.

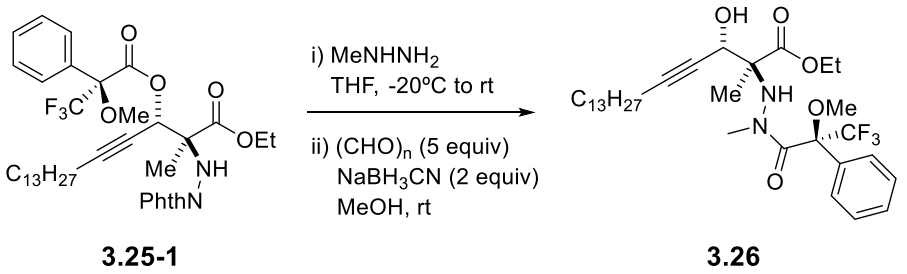

3.25-1 **3.26**

Scheme 3.14 Transacylation of **3.25-1** under deprotection/demethylation conditions. Only relative configuration for C2 and C3 is shown.

Reaction from diastereomer **3.25-1** proceeded for one week and, after column purification, the only product observed was temptatively assigned to **3.26**, arising from the transacylation to the terminal nitrogen of the free hydrazine. The ^{1}H NMR spectrum reveals that the terminal nitrogen of the free hydrazine is functionalized with one methyl and the Mosher acid moiety, indicating equilibrated competition between the acylation and the methylation of the free hydrazine. The dimethylhydrazino derivative was not observed.

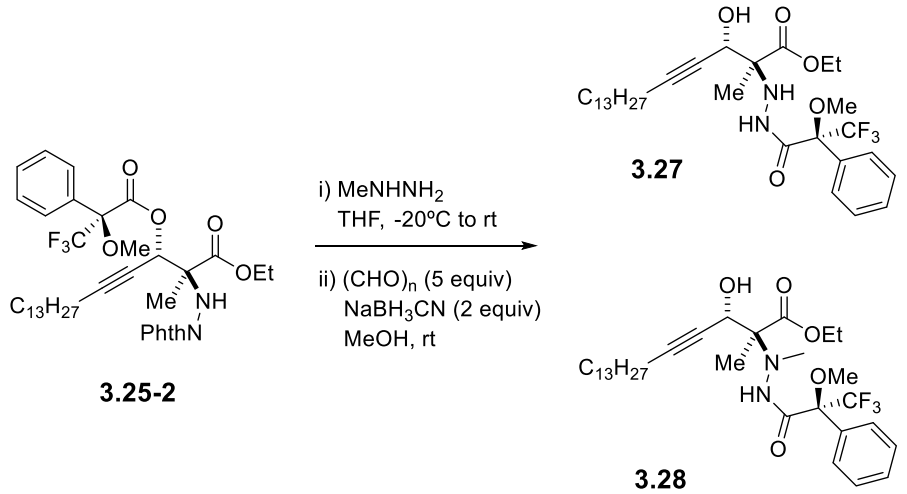

3.25-2

Scheme 3.15 Transacylation of **3.25-2** under deprotection/demethylation conditions. Only relative configuration at the sphingosine scaffold is shown.

Diastereomer **3.25-2** did not yield the desired compound either (Scheme **3.15**). Instead, two major products were identified: the product of direct transacylation of the Mosher moiety to the terminal nitrogen **3.27**, and the product of the methylation of the internal nitrogen after the transacylation **3.28**. Allegedly, the formation of the amide renders the terminal nitrogen less nucleophilic for the reductive amination and hence the internal nitrogen is methylated despite the stearic impediment.

The difference in reactivity of the two diastereomers is surprising. It looks as if with **3.25-1** the monomethylation takes place before the transacylation, as the formation of the amide seem to trigger methylation of the internal nitrogen. Instead, with **3.25-2** the transacylation happens first. Because there is no difference in the reaction conditions between the two reactions, the difference in reactivity must be given by the relative position of the C2-hydrazine and the Mosher ester. It can be speculated that the stabilization of the 6-membered transacylation intermediate via H-bonding with the MeO group in the reductive amination of **3.25-2** favours the reaction (Scheme **3.16**).

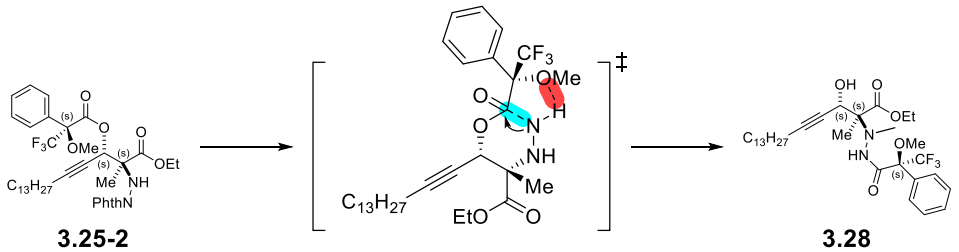

Scheme 3.16 Proposed intermediate for the rapid transacylation of **3.25-2**.

If the assumption is correct, the absolute configuration of **3.25-2** should be (*S*,*S*,*S*) for the hydrazine and the methoxy group to be in the same face of the molecule. Therefore, **3.25-1** would be assigned the (*S*,*R*,*R*) configuration.

To avoid transacylation, the hydrolysis of the Mosher ester was proposed prior to reductive amination. With this procedure, the separated enantiomers of **3.17** and **3.18** would be obtained and the normal synthesis could be carried out normally with either enantiomer.

Removal of Mosher acid was tested with sodium ethoxide (EtONa) to avoid saponification or transesterification of the terminal ester group.[17] An unseparated mixture of **3.25-1** and **3.25-2** was reacted with a solution of EtONa in dry ethanol. Unfortunately, no conversion was observed with EtONa/EtOH neither at 0ºC nor at room temperature (Scheme **3.17**). Heating the reaction was disregarded because of the fear of decomposition due to the complexity of the molecule.

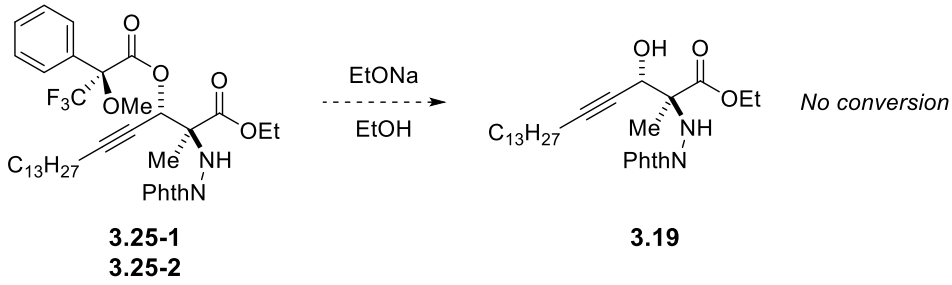

3.25-1
3.25-2

3.19

Scheme 3.17 Hydrolysis of the Mosher ester in **3.25-1** and **3.25-2** mixture with EtONa/EtOH.

Finally, the simultaneous reduction of the methyl ester and the Mosher's ester to unmask hydroxyl groups in C1 and C3, respectively, was tested with DIBAL. In the racemic synthesis, the ester reduction is performed after the dimethylation step to avoid possible methylation of the primary alcohol. Nonetheless, hydrazine is substantially more prone to methylation, so the dual reduction was tested.

[17] Asada, M.; Obitsu, T.; Nagase, T.; Sugimoto, I.; Yamaura, Y.; Sato, K.; Narita, M.; Ohuchida, S.; Nakai, H.; Toda M. *Bioorg. Med. Chem.* **2009**, *17*, 6567–6582.

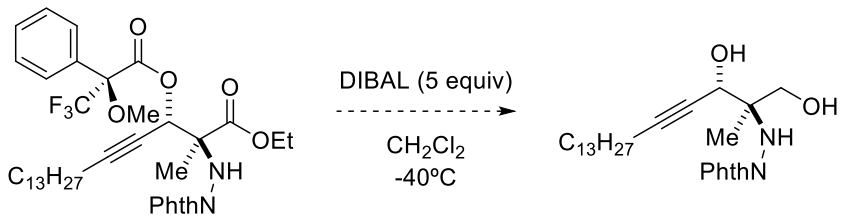

3.25-1
3.25-2

3.29

Scheme 3.18 Deprotection of the primary and secondary hydroxyl groups with DIBAL.

The reaction was set up using the same conditions as those in the standard reduction in the racemic synthesis, with two-fold equivalents of DIBAL (Scheme **3.18**). A very complex mixture was observed in the ^{1}H-NMR spectrum, with no signs of the phthalimide or the triple bond, compatible with extensive decomposition. No major product was detected, so the route was also discarded.

Tests were performed with the methyl analogue **3.7** since it yielded sensibly higher yields in most steps of the synthesis. It is safe to assume that outcomes of the final derivatization experiments with the ethyl analogue **3.8** would have proceeded in a similar manner.

Due to time constraints, and with the disappointing results, the enantioselective synthesis of **3.7** and **3.8** was abandoned. Chemoselective transformations in these densely functionalised compounds proved very challenging and unfortunately did not enable enantiomer resolution.

With the impossibility to test the enantiomers separately in biological assays, we recurred to computational methods to understand the possible difference in activity between the two enantiomers of each analogue.

3.3.2. Molecular Dockings of the Interactions with SphK1/2

Molecular Docking (MD) is an essential tool in the search for an enzyme inhibitor. The complexity of the structure of the enzymes and, more often than not, the laborious and time-consuming preparation of inhibitors make computational resources a valuable alternative to assess the potential of a molecule as a specific inhibitor. MD can predict the guest-host interactions between the active site of an enzyme and a proposed inhibitor in a three-dimensional space with high confidence, and thus help with the rational design of inhibitors.[18]

In order to better understand the results obtained in the inhibition activity assays, and to have insight in the interactions that the inhibitors stablish with the enzymes, molecular docking was employed to assess the potential binding modes of **3.7**, **3.8** and **3.10** (Figure **3.2**). **3.10** acts as a dual inhibitor of SphK1 and Sphk2, which can help understand the different interactions in the active site of the two SphK isoforms. Additionally, compounds featuring a trisubstituted carbon atom at C2 were also modelled to understand the role of the tetrasubstituted centre. The two enantiomers of these ligands were independently docked to compare and identify their preferred conformations.

The analogues are modelled with SphK1 and a homology model of SphK2. Structural biology has provided a plethora of knowledge on protein structure enabling prediction for the translation of a protein's primary sequence, through secondary structure (alpha helices, beta sheets, etc), to common motifs, domains, folds, tertiary and quaternary arrangement of subunits.[18] Homology modelling builds a 3D structure from a protein sequence of interest based on the 3D structure of a similar protein. A homology model can provide an alternative for subsequent receptor-ligand analysis such as molecular docking or dynamics as long as a three-dimensional structure exists for a similar protein.

[18] Lohning, A. E.; Levonis, S. M.; Williams-Noonan, B.; Schweiker, S. S. *Current Topics in Medicinal Chemistry* **2017**, *17*, 18, 2023-2040.

As explained in this chapter introduction, SPhK2 crystal structure in not available and therefore the exact sequence of the isoform remains unknown. To salvage this inconvenience, the known relevant sequence differences between SphK1 and SphK2 were introduced to an already existing SphK1 model to generate a homology SphK2 model.

Computational work was carried out in collaboration with Xavier Barril's group in ICREA, Barcelona. Calculations were performed using MOE-Dock based on the cocrystal structure of SphK1 with Sph (3VZB, chain A, resolution 2 Å), which was also used as a template for the SphK2 homology model after sequence alignment.[19]

The best scored binding mode for the **(2*S*,3*R*)-3.10** enantiomer shows a J-shaped binding conformation of the hydrophobic tail, while the polar dimethylhydrazino group interacts with the carboxyl group of residue Asp178 (Figure **3.5**, left). Moreover, the same Asp178 participated in a H-bond with the 3-hydroxyl group making a bidentate interaction between the Aspartic acid and the inhibitor. Additionally, the 3-hydroxyl group was found to form a second hydrogen bond with the structural water molecule next to Ser168. On the other side of the polar region, a H-bond was established between Leu268 and the 1-hydroxyl group. The ethyl group at C2 occupied a hydrophobic region made up by Leu167 and Leu268. This arrangement around the polar region of the J-channel was found optimal for binding in SphK1 since it led to a maximum number of reasonable interactions between the ligand and SphK1 key residues.

Docking poses of the **(2*R*,3*S*)-3.10** enantiomer show a switch at both chiral centres, resulting in a rearrangement of the polar head groups to an unfavourable positioning for plausible key interactions (Figure **3.5**, right). This docking pose trend was observed in all enantiomers and might imply that the (2*S*,3*R*) configuration is preferable for SphK1 inhibition.

[19] Molecular Operating Environment (MOE), 2019.01; Chemical Computing Group ULC, 1010 Sherbooke St. West, Suite #910, Montreal, QC, Canada, H3A 2R7, 2021.

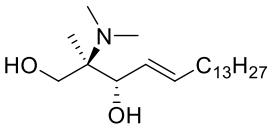

(2*S*,3*R*)-3.10

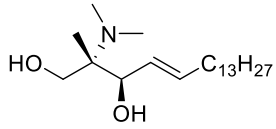

(2*R*,3*S*)-3.10

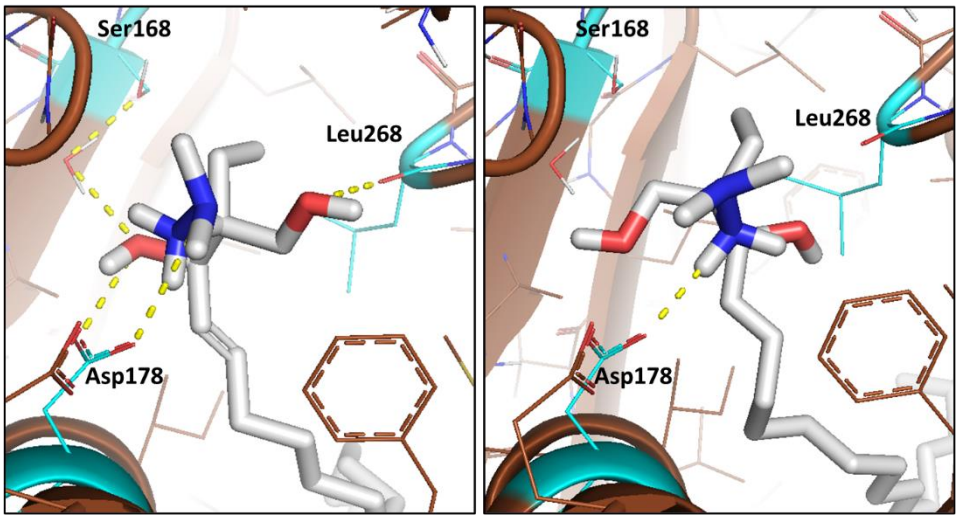

Figure 3.5. Binding mode of (2*S*,3*R*)-3.10 enantiomer (left) and (2*R*,3*S*)-3.10 enantiomer (right) in SphK1.

In comparison to **(2*S*,3*R*)-3.10**, the docking poses of **(2*S*,3*R*)-3.7** and **(2*S*,3*R*)-3.8** in SphK1 showed that their lipophilic tail becomes stiffer and longer due to the presence of a linear triple bond as linker. The tail's elongation apparently leads to a conflict between the ligands and Phe288 at the toe of the binding pocket of SphK1, causing them to enter deeper into the polar region and, thus, losing key interactions with the protein. This kind of ligand position was observed in many docking poses (Figure **3.6**, left). In the case of poses with more binding sites in the polar head, the tail was unable to fit into the cavity and folded, causing a loss of contact surface area with the protein (i.e. loss of hydrophobic interactions) (Figure **3.6**, right). This explains the lack of inhibition for SphK1.

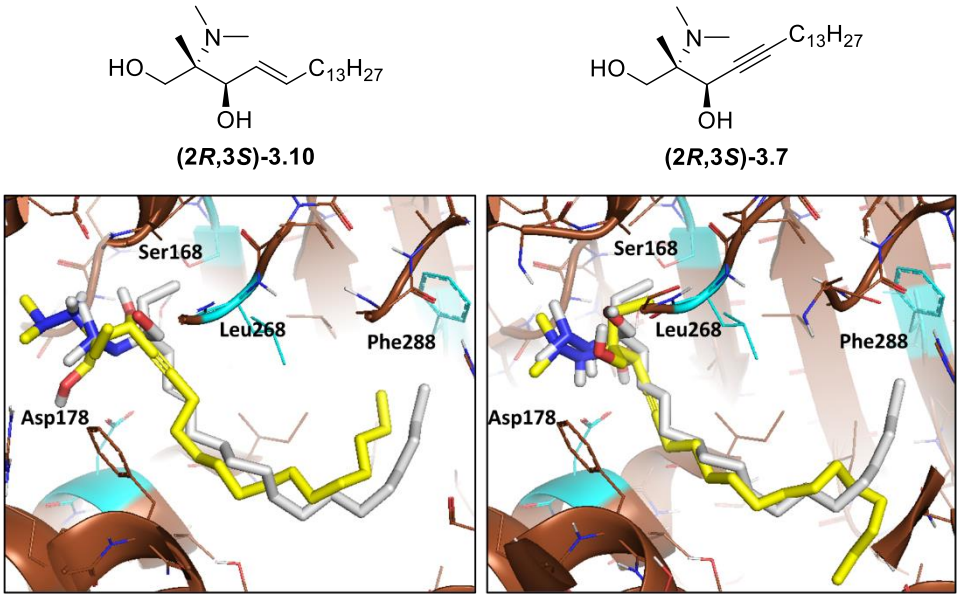

Figure 3.6. Docking poses of (2*S*,3*R*) enantiomers of ligands 3.10 (white) and 3.7 (yellow) in SphK1. Left: Pose with good lipidic tail fit. Right: Pose with good polar head fit.

The effect of the chiral quaternary centre at C2 was studied by docking the trisubstituted C2 analogue. The docking poses show a wide variety of possible binding modes, which may be indicative of a heterogeneous binding mode, while the tetrasubstituted C2 analogues show preference for a particular binding mode with a more extensive network of interactions. It seems like the alkyl group, with its tendency to occupy the only hydrophobic region around the head and its bulk, helps fixing the inhibitor position and orient the polar groups maximizing the number of interactions with the enzyme.

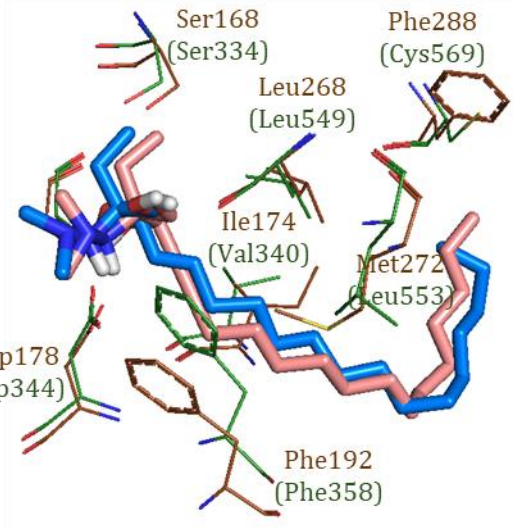

Figure 3.7. Docking poses of (2*S*,2*R*)-3.10 (blue) and (2*S*,3*R*)-3.8 (pink) in the SphK2 homology model.

Molecular dockings were performed also in the SphK2 homology model. The model was docked with **3.7** and **3.8,** together with **3.9** and **3.10** (for comparison). The better fit of **3.8** in the longer lipophilic pocket of SphK2 makes the analogue preserve all the interactions in the polar head while producing full contact of the fatty tail with the enzyme pocket (Figure **3.7**). The triple bond that elongates the hydrophobic tail grants worse fit with SphK1 but, in the contrary, a better fit in SphK2. This is in agreement with the biological tests, which show selective inhibition of SphK2.

3.3.3. Cell Viability Assays

Cell viability assays are cell detection experiments aimed to ensure that the drug is not harmful for the organism. They are quantitative methods that calculate the percentage of living cells in a sample. Measuring the amount of living cells before and after incubation of the sample with a desired drug is a direct indicator of the cytotoxicity of that drug. Regardless of the inhibitor performance of an analogue, low cytotoxicity is a requirement for any drug-aspiring compound.

Cell viability assays were performed in collaboration with Dr. Elena Domingo from the Faculty of Medicine and Odontology of the University of Valencia. The assays were performed on primary cell cultures of human umbilical vein endothelial cells (HUVECs) using two techniques: flow cytometry and MTT colorimetric assay.

Flow cytometry is a technique that allows for rapid counting and differentiation of cells. A suspension of cells is injected into the flow cytometer, focused to ideally flow one cell at a time through a laser beam, where the light scattered is characteristic to the cells and their components. Light is converted to electronic signals and analysed by a computer. Cell apoptosis can be quantified by flow cytometry by measuring DNA destruction, mitochondrial membrane potential, permeability alterations, and caspase activity.[20]

MTT test is the most commonly used colorimetric assay. It relies on the reduction of MTT (3-(4,5-dimethylthiazol-2-yl)-2,5-diphenyltetrazolium bromide), a popular tetrazolium-based dye, into formazan crystals (Figure **3.8**). This reaction is catalysed by specific dehydrogenases in the mitochondria of viable cells. The reduction of MTT causes colour change, which can be detected by spectroscopy. This method is an indirect indicator of the mitochondrial function in the cell

[20] McKinnon, K. M.; *Curr. Protoc. Im.* **2018**, *120*, 5.1.1-5.1.11.

and, therefore, its life-death status.[21] Cell suspensions are incubated with MTT at 37ºC for 3-4h, and the obtained formazan crystals are measured.

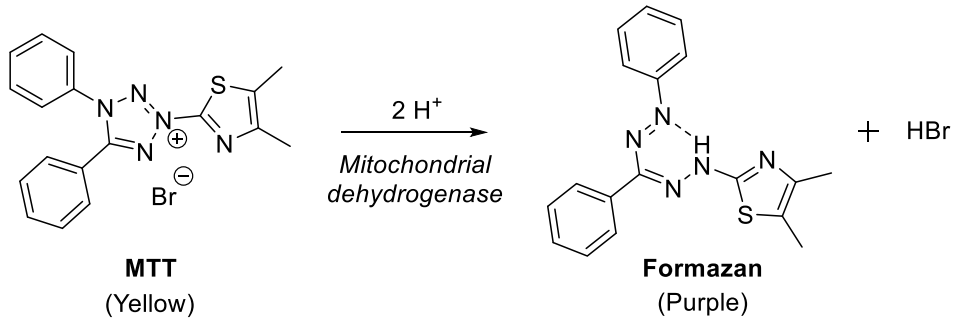

Figure 3.8. Reduction of MTT to Formazan. MTT colorimetry is based on the reduction of this indicator.

The assays were performed with the two prepared analogues **3.7** and **3.8** because they gave promising inhibitor activity towards SphK2 selectively. They both were primarily tested at 10, 30 and 100 μM of inhibitor for potential cytotoxic effects on primary cell cultures of HUVECs after 24h incubation with the analogues.

The studies showed that compound **3.7** was not cytotoxic to human endothelial cells at 30 μM either by a cytofluorimetric assay to determine apoptosis and survival or by the MTT (3[4,5-dimethylthiazol-2-yl]-2,5-diphenyltetrazolium bromide) nor by colorimetric assay (Figure **3.9**, graphs **A**, **B** and **C**). However, at 100 μM, compound **3.7** resulted completely cytotoxic, with a calculated EC50 toxicity value (63.1 μM) that is over 3 times higher than its IC50 value (17 μM). On the other hand, compound **3.8** caused cell damage at at 30 μM in both assays (Figure **3.9**, graphs **D, E** and **F**).

[21] Gavanji, S.; Bakhtari, A.; Famurewa, A. C.; Othman, E. M. *Chem. Biodiversity* **2023**, *20*, e202201098.

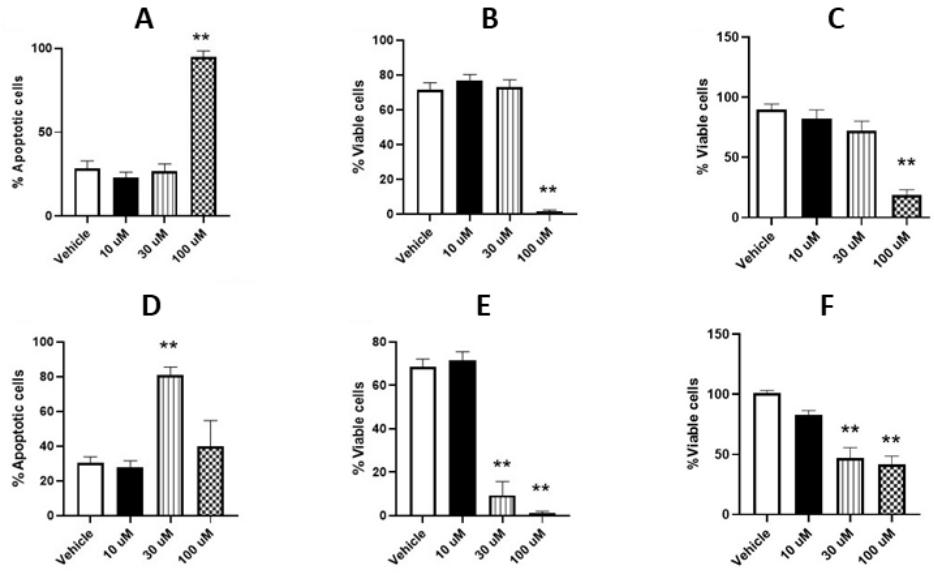

Figure 3.9. Effect in percentage of Compound **3.7** and **3.8** on HUVEC viability and apoptosis. (A) Percentage of apoptotic HUVECs. (B) Survival HUVEC after 24 h incubation with compound **3.7**. (C) Results of the MTT assay for compound **3.7**. (D) Percentage of apoptotic HUVECs (E) Survival HUVEC after 24 h incubation with compound **3.8**. (F) Results of the MTT assay for compound **3.8**. Apoptotic cells were quantified as the percentage of total population of annexin V+, PI− cells, late apoptotic, and/or necrotic cells as annexin V+, PI+, and viable nonapoptotic cells as annexin V− and PI−. The columns are the mean ± SEM of n=5-6 independent experiments. **p< 0.01 relative vehicle group.

3.4. Conclusions

Sphingosine-based SphK2 inhibitors **3.7** and **3.8** have been prepared featuring a polar head bearing a tetrasubstituted carbon at C-2, a dimethylhydrazine as a polynitrogenated scaffold and a triple bond as a linker with the lipidic tail. Separation of the enantiomers was attempted for inhibition testing of the separate isomers. Derivatization of the hydroxyl groups with Mosher acid was attempted, although the high complexity of the analogues was too challenging. Separation via chiral chromatography was also unsuccessful.

Docking studies of these compounds into the binding pocket of SphK1 and a homology model of SphK2 have revealed some key interactions that may account for the SphK2-selective inhibition activity. The study revealed a network of polar and unprecedented hydrophobic interactions of the head group of the ligand with the head of the binding pocket.

The presence of a triple bond as a linker between the polar and the hydrophobic parts showed a better fit of the tail into the extended hydrophobic pocket of SphK2. This accounts for the selectivity of the prepared inhibitors towards SphK2.

Cytofluorimetric assays and MTT colorimetric assays showed that **3.7** is not cytotoxic to human endothelial cells below 30 μM, which is a higher concentration than its IC_{50} (17.5 μM).

3.5. Experimental Part

3.5.1. General Considerations

All solvents were dried with activated 3Å molecular sieves (3Å MS). Proton (^{1}H NMR), carbon (^{13}C NMR) and fluorine (^{19}F NMR) nuclear magnetic resonance spectra were recorded on a 400 MHz Varian VNMR-S400 NMR instrument at 25°C in $CDCl_3$. All chemical shifts are quoted on the δ scale in ppm using the residual solvent as internal standard (^{1}H NMR: $CDCl_3$ = 7.26 ppm) and ^{13}C NMR: $CDCl_3$ = 77.16 ppm). Coupling constant (J) are reported in Hz with the following splitting abbreviations: s = singlet, d = doublet, t = triplet, q = quartet, m = multiplet, bs = broad singlet. Infrared (IR) spectra were recorded on a JASCO FTIR-680 plus Fourier Transform Infrared Spectrophotometer, wavenumbers in cm-1. ESI MS were run on an Agilent®1200 Series HPLC-TOF instrument. Thin layer chromatography (TLC) was carried out on 0.25 mm E. Merck® aluminum backed sheets coated with 60 F254 silica gel. Visualization of the silica plates was achieved using a UV lamp (λmax = 254 nm) and *p*-anisaldehyde stain. Flash column chromatography was carried out using silica gel 60 A CC (230–400 mesh). Mobile phases are reported in relative composition (e.g., 1:1 hexane/EtOAc v/v). All reactions using anhydrous conditions were performed using dry apparatus under argon atmosphere. Activation of molecular sieves was performed in a flame-dried apparatus under high vacuum (<5 mbar) with a heat gun. Brine refers to a saturated solution of sodium chloride. Anhydrous sodium sulphate (Na_2SO_4) and anhydrous magnesium sulphate ($MgSO_4$) were indifferently used as drying agents after reaction work-up.

3.5.2. General Procedures

3.5.2.1. ***General Procedure for the Preparation of α,β-unsaturated esters[9]***

A 2.5 M solution of *n*-BuLi in hexanes (5.3 mmol) was slowly added to a solution of 1-pentadecyne (4.8 mmol) in THF (19 mL) at –23 ºC. After 2 h the reaction was allowed to warm to rt, and it was stirred for another 2 h before cooling to 0 ºC. Then, 1-formylpiperidine (5.38 mmol) was added to the pentadecynyllithium suspension at 0 ºC and it was stirred at rt for 2 h. The reaction was quenched with 20 mL of 10 % aqueous $NaHSO_4$ and the product was extracted with Et_2O (4×20 mL). The organic layer was washed with 10 % aqueous $NaHSO_4$, dried over anhydrous $MgSO_4$, filtered and concentrated under reduced pressure. The crude alkynal was directly submitted to a Horner-Wadsworth-Emmons olefination without further purification.

To a solution of LiBr (20.9 mmol) in THF (100 mL), the corresponding phosphonate (4.9 mmol) was added at rt. After 10 min, Et_3N (6.3 mmol) was added to the reaction mixture and it was stirred for 15 min. Then, the freshly synthesized alkynal was dissolved in 20 mL of THF and added to the solution. Once the reaction was completed, the reaction mixture was filtered through silica gel to remove the precipitate formed during the reaction. The pad was washed with 200 mL of hexane/AcOEt 60:40 and the solvent were then removed under reduced pressure. The resulting crude was purified by flash chromatography using hexane/Et_2O mixtures.

3.5.2.2. ***General Procedure for the Aziridination of α,β-unsaturated esters[10b]***

A solution of PIDA (1.5 mmol) in CH_2Cl_2 (2.5 mL) was added to a suspension of *N*-aminophthalimide (2.0 mmol) and the corresponding alkene (1.0 mmol) in CH_2Cl_2 (2.5 mL) at 0 ºC. The reaction mixture was stirred at rt until completion, monitored by TLC. It was then quenched by using a saturated $NaHCO_3$ solution and filtered through celite. The mixture was extracted with CH_2Cl_2 (3×25 mL), and the combined organic layers

were dried over anhydrous $MgSO_4$, filtered and concentrated under reduced pressure. The resulting crude was purified by flash chromatography on silica gel using hexane/AcOEt mixtures.

3.5.2.3. ***General Procedure for the Ring-Opening of Aziridines with Water***

To a solution of aziridine (0.5 mmol) in dioxane/water 1:1 (7 mL), PTSA (0.6 mmol) was added at rt and the reaction mixture was heated under reflux until completion observed by TLC. Then, the mixture was extracted with Et_2O (3x20 mL) and the combined organic layers were dried over anhydrous $MgSO_4$, filtered and concentrated under reduced pressure. The resulting crude was purified by flash chromatography using hexane/AcOEt mixtures.

3.5.2.4. ***General Procedure for the Hydrazine Deprotection and Dimethylation***

Methylhydrazine (0.8 mmol) was added to a solution of the ring-opened product (0.5 mmol) in THF (3.3 mL) at -20 °C. The solution was stirred for 30 min and it was allowed to warm to rt until completion, monitored by TLC. The solvent was removed under vacuum and the crude was redissolved in AcOEt and filtered through cotton. The filtrate was evaporated and the residue was redissolved in MeOH (13.8 mL). $NaBH_3CN$ (1.0 mmol) and paraformaldehyde (2.0 mmol) were added to the reaction mixture at 0 ºC, and the mixture was stirred at rt for 24 or 48 h. The solvent was removed under reduced pressure and the crude was redissolved in AcOEt and filtered through celite. The filtrate was then evaporated and the resulting crude was purified by silica gel chromatography using hexane/AcOEt mixtures.

3.5.2.5. ***General Procedure for the Reduction of the Ester Group***

A 1 M solution of DIBAL in CH_2CL_2 (0.3 mmol) was added dropwise to a solution of *N,N*-dimethylhydrazino compound (0.1 mmol) in CH_2Cl_2 (0.3 mL) at -40 °C. Once the reaction was completed, the mixture was quenched with a 1M solution of NaOH, filtered through celite using $CHCl_3$

and extracted with $CHCl_3$ (3x5 mL). The combined organic layers were dried over anhydrous $MgSO_4$, filtered and concentrated under reduced pressure. The resulting crude was purified by silica gel chromatography using hexane/AcOEt mixtures.

3.5.2.6. ***General Procedure for the Asymmetric Mitsunobu Esterification***

A solution of aminodiol (0.08 mmol, 1 eq), (*S*)-Mosher acid (0.09 mmol, 1.05 eq) and Ph_3P (0.09 mmol, 1.05 eq) in THF (0.5 mL) was cooled to 0ºC. DIAD was added dropwise and the reaction was stirred at rt until completion, monitored by TLC. The mixture was washed with water, and the aqueous phase was extracted with CH_2Cl_2. The organic phases were dried over anhydrous $MgSO_4$, filtered and evaporated under reduced pressure.

3.5.2.7. ***General Procedure for the Asymmetric Stemlich Esterification***

A mixture of alcohol (0.1 mmol), (*S*)-Mosher acid (0.24 mmol), DCC (0.24 mmol) and DMAP (0.24 mmol) in CH_2Cl_2 (5 mL) was refluxed until completion, monitored by TLC. The reaction mixture was filtered off with celite and the filtrate was evaporated under reduced pressure.

3.5.3. Compound Characterization Data

Rac-(2*R*,2*S*)-2-(2,2-dimethylhydrazinyl)-2-methyloctadec-4-yne-1,3-diol (3.7)

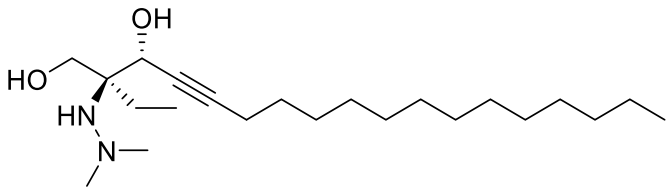

The title compound was prepared following the general procedure for the reduction of esters to alcohols starting from **3.22** (69 mg, 0.17 mmol) and DIBAL (0.43 mL, 1 M in CH_2Cl_2, 0.42 mmol). The crude was purified by column chromatography using a mobile phase of Hexane/AcOEt (90:10 to 80:20) to give **3.7** as a white solid (52 mg, 0.15 mmol, 84%).

M. p. 34-35 °C. **IR (neat):** 3735, 3381, 2953, 2853, 2366, 2354, 2340, 1467, 1042, 749 cm^{-1}. **^{1}H NMR** (400 MHz, $CDCl_3$, δ in ppm): 4.61 (t, J=2.0 Hz, 1H, H_3), 3.82 (d, J=11.1 Hz, 1H, H_1), 3.69 (m, 2H, H1, H_{NH}), 2.50 (s, 6H, $N(CH_3)_2$), 2.23 (td, J=7.1, 2.0 Hz, 2H, H_6), 1.56 – 1.42 (m, 2H, H_7), 1.42 – 1.17 (m, 20H), 1.05 (s, 3H, CH_3), 0.87 (t, J=6.8 Hz, 3H, H_{18}). **^{13}C NMR** (100 MHz, $CDCl_3$, δ in ppm): 87.9 (C_5), 78.6 (C_4), 67.0 (C_3), 66.6 (C_1), 61.3 (C_2), 50.7 ($N(CH_3)_2$), 32.0, 29.8, 29.7, 29.5, 29.3, 29.1, 28.8 (C_8), 22.8 (C_7), 18.9 (C_6), 18.4 (CH_3), 14.3 (C_{18}). **HR ESI-TOF MS** for $[M+H^+]$ $C_{21}H_{43}N_2O_2^+$ (m/z): 355.3319; found: 355.331.

Rac-(2*R*,2*S*)-2-(2,2-dimethylhydrazinyl)-2-ethyloctadec-4-yne-1,3-diol (3.8)

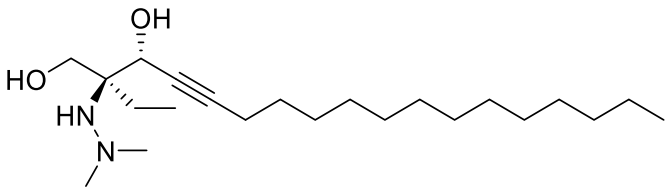

The title compound was prepared following the general procedure for the reduction of esters to alcohols starting from **3.23** (46 mg, 0.11 mmol) and DIBAL (0.28 mL, 1 M in CH_2Cl_2, 0.28 mmol). The crude was purified by column chromatography using a mobile phase of $CHCl_3$/MeOH/NH_4OH (99.5:0.5:0.1) to give **3.8** as a yellow oil (18 mg, 0.05 mmol, 43%).

IR (neat): 3305, 2923, 2853, 2775, 2358, 2320, 1464, 1045 cm^{-1}. **^{1}H NMR** (400 MHz, MeOD, δ in ppm): 4.54 (t, J=2.1 Hz, 1H, H_3), 3.80 (d, J=11.0 Hz, 1H, H_1), 3.65 (d, J=11.0 Hz, 1H, $H_{1'}$), 2.51 (s, 6H, $N(CH_3)_2$), 2.26 (td, J=6.8, 2.1 Hz, 2H, H_6), 1.68 – 1.38 (m, 6H), 1.31 (bs, 19H), 0.97 – 0.88 (m, 6H). **^{13}C NMR** (100 MHz, $CDCl_3$, δ in ppm): 87.9 (C_5), 80.1 (C_4), 67.6 (C_2), 64.7 (C_3), 63.7 (C_1), 50.5 ($N(CH_3)_2$), 33.1, 30.8, 30.7, 30.5, 30.3, 29.9 (C_8), 29.8 (C_7), 25.1, 23.8 (CH_3CH_2), 19.4 (C_6), 14.5 (C_{18}), 7.8 (CH_3CH_2). **HR ESI-TOF MS** for $[M+H^+]$ $C_{22}H_{45}N_2O_2^+$ (m/z): 369.3476; found: 369.3475.

Ethyl (*E*)-2-methyloctadec-2-en-4-ynoate (3.15)

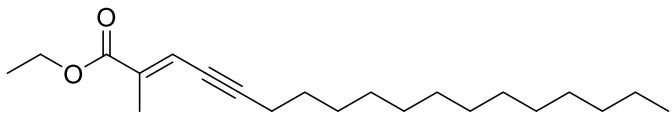

The title compound was prepared following the general procedure for the preparation of *α*,*β*-unsaturated esters starting from 1-pentadecyne (1.3 mL, 4.8 mmol) and triethyl phosphonopropionate (1.2 mL, 4.8 mmol) to afford a mixture of *cis/trans* stereoisomers (7:93). The crude was purified by column chromatography using a mobile phase of Hexane/Et_2O (99:1) to give the *trans* product **3.15** as a yellowish oil (877 mg, 2.74 mmol, 67% yield over two steps).

IR (neat): 2924, 2854, 2213, 1713, 1465, 1344, 1258, 1119, 631 cm^{-1}. **^{1}H NMR** (400 MHz, $CDCl_3$, δ in ppm): 6.61 (m, 1H, H_3), 4.19 (q, J=7.1 Hz, 2H, CH_3CH_2O), 2.40 (td, J=7.0, 2.2 Hz, 2H, H_6), 2.02 (d, J=1.3 Hz, 3H, CH_3), 1.55 (m, 2H, H_7), 1.40 (m, 2H, H_8), 1.28 – 1.20 (m, 21H), 0.87 (t, J=6.9 Hz, 3H, H_{18}). **^{13}C NMR** (100 MHz, $CDCl_3$, δ in ppm): 167.5 (C_1), 137.9 (C_3), 120.5 (C_2), 103.9 (C_5), 77.7 (C_4), 60.9 (CH_3CH_2O), 32.0, 29.9, 29.8, 29.7, 29.6, 29.5, 29.2, 29.0, 28.7, 22.8, 20.0, 15.2 (CH_3), 14.3 (C_{18}), 14.2 (CH_3CH_2O). **HR ESI-TOF MS** for [M+Na_+] $C_{21}H_{36}NaO_2^+$ (m/z): 343.2608; found: 343.2613.

Ethyl (*E*)-2-ethyloctadec-2-en-4-ynoate (3.16)

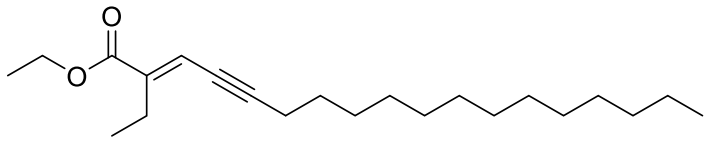

The title compound was prepared following the general procedure for the preparation of *α,β*-unsaturated esters starting from 1-pentadecyne (1.3 mL, 4.8 mmol) and triethyl phosphonopropionate (1.2 mL, 4.8 mmol) to afford a mixture of *cis/trans* stereoisomers (12:88). The crude was purified by column chromatography using a mobile phase of Hexane/Et_2O (95:5) to give the *trans* product **3.16** as a yellowish oil (1141 mg, 3.31 mmol, 69% yield over two steps).

IR (neat): 2923, 2853, 5357, 2212, 1712, 1609, 1463, 1309, 1238, 1129 cm^{-1}. **^{1}H NMR** (400 MHz, $CDCl_3$, δ in ppm): 6.59 (t, J=2.3 Hz, 1H, H_3), 4.20 (q, J=7.1 Hz, 2H, CH_3CH_2O), 2.50 (q, J=7.5 Hz, 2H, CH_3CH_2), 2.41 (td, J=7.0, 2.3 Hz, 2H, H_6), 1.62 – 1.49 (m, 2H, H_7), 1.49 – 1.35 (m, 2H, H_8), 1.35 – 1.17 (m, 21H), 1.06 (t, J=7.5 Hz, 3H, CH_3CH_2), 0.88 (t, J=6.9 Hz, 3H, H_{18}). **^{13}C NMR** (100 MHz, $CDCl_3$, δ in ppm): 167.2 (C1), 144.0 (C2), 120.0 (C3), 103.5 (C5), 77.4 (C4), 60.8 (CH_3CH_2O), 32.0, 29.8, 29.7, 29.5, 29.3, 29.0, 28.7, 22.9, 22.8 (CH_3CH_2), 20.1, 14.4 (CH_3CH_2O), 14.3 (C18), 13.5 (CH_3CH_2). **HR ESI-TOF MS** for [M+H$^+$] $C_{22}H_{39}O_2^+$ (m/z): 335.2945; found: 335.2950.

Ethyl rac-(2*R*,2*S*)-[1-(1,3-dioxo-1,3-dihydro-2*H*-isoindol-2-yl)-2-methyl-3-(pentadec-1-yn-1-yl)aziridine]-2-carboxylate (3.17)

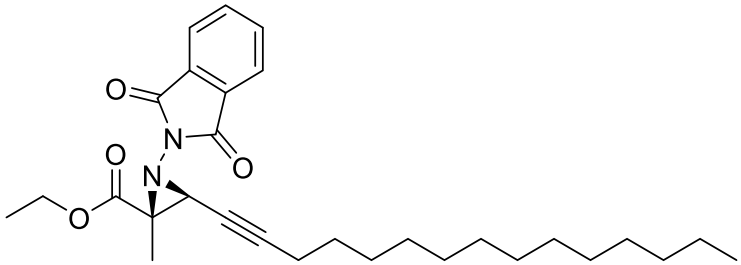

The title compound was prepared following the general procedure for the aziridination of *α*,*β*-unsaturated esters starting from **3.15** (880 mg, 2.74 mmol), *N*-aminophthalimide (589 mg, 5.48 mmol) and PIDA (1324 mg, 4.11 mmol). The crude was purified by column chromatography using a mobile phase of Hexane/AcOEt (95:5) to give **3.17** as a yellowish oil in quantitative yield.

IR (neat): 2927, 2855, 2220, 1715, 1261, 1121, 746, 631 cm^{-1}. **^{1}H NMR** (400 MHz, $CDCl_3$, δ in ppm): 7.74 (dd, J= 5.5, 3.0 Hz, 2H, H_{ar}), 7.66 (dd, J=5.5, 3.0 Hz, 2H, H_{ar}), 4.14 – 4.04 (m, 2H, CH_3CH_2O), 4.02 (t, J=1.8 Hz, 1H, H_3), 2.27 (td, J=7.1, 1.8 Hz, 2H, H_6), 1.74 (s, 3H, CH_3), 1.59 – 1.48 (m, 2H, H_7), 1.44 – 1.33 (m, 2H, H_8), 1.33 – 1.22 (bs, 18H), 1.19 (t, J=7.1 Hz, 3H, CH_3CH_2O), 0.87 (t, J=6.9 Hz, 3H, H_{18}). **^{13}C NMR** (100 MHz, $CDCl_3$, δ in ppm): 167.2 (C_1), 164.5 (C_{ar}), 134.1 (C_{ar}), 130.4 (C_{ar}), 123.2 (C_{ar}), 87.0 (C_5), 72.8 (C_4), 62.4 (CH_3CH_2O), 49.9 (C_2), 43.9 (C_3), 32.0, 29.8, 29.6, 29.5, 29.2, 29.0 (C_7), 28.5 (C_8), 22.8, 19.0 (C_6), 15.5 (CH_3), 14.3 (C_{18}), 14.0 (CH_3CH_2O). **HR ESI-TOF MS** for [2M+Na^+] $C_{58}H_{80}N_4NaO_8^+$ (m/z): 983.5868; found: 983.5875.

Ethyl rac-(2*R*,2*S*)-[1-(1,3-dioxo-1,3-dihydro-2*H*-isoindol-2-yl)-2-ethyl-3-(pentadec-1-yn-1-yl)aziridine]-2-carboxylate (3.18)

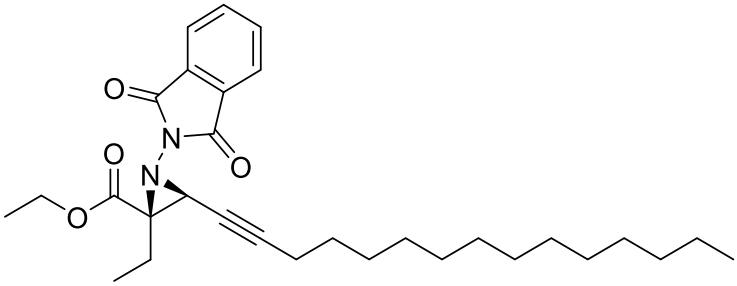

The title compound was prepared following the general procedure for the aziridination of *α*,*β*-unsaturated esters starting from **3.16** (1000 mg, 2.90 mmol), *N*-aminophthalimide (940 mg, 5.80 mmol) and PIDA (1400 mg, 4.35 mmol). The crude was purified by column chromatography using a mobile phase of Hexane/AcOEt (95:5) to give **3.18** as a yellowish (1277 mg, 2.58 mmol, 89% yield).

IR (neat): 3337, 2923, 2853, 2360, 1718, 1466, 1377, 1301, 1237, 1153, 705 cm^{-1}. **^{1}H NMR** (400 MHz, $CDCl_3$, δ in ppm): 7.73 (dd, J=5.5, 3.0 Hz, 2H, H_{ar}), 7.65 (dd, J=5.5, 3.0 Hz, 2H, H_{ar}), 4.15 – 4.05 (m, 2H, CH_3CH_2O), 4.01 (t, J=1.8 Hz, 1H, H_3), 2.32 – 2.19 (m, 2H, H_6), 1.92 (dq, J=14.6, 7.2 Hz, 2H, CH_3CH_2), 1.59 – 1.47 (m, 2H, H_7), 1.44 – 1.33 (m, 2H, H_8), 1.33 – 1.22 (m, 21H), 1.19 (t, J=7.2 Hz, 3H, CH_3CH_2), 0.87 (t, J=6.9 Hz, 3H, H_{18}). **^{13}C NMR** (100 MHz, $CDCl_3$, δ in ppm): 166.8 (C_1), 164.5 (C_{ar}), 134.1 (C_{ar}), 130.3 (C_{ar}), 123.1 (C_{ar}), 86.7 (C_5), 72.9 (C_4), 62.3 (CH_3CH_2O), 54.1 (C_2), 43.7 (C_3), 32.1, 29.8, 29.7, 29.5, 29.2, 29.0 (C_8), 28.5 (C_7), 23.6 (CH_3CH_2), 22.8, 19.0 (C_6), 14.3 (C_{18}), 14.0 (CH_3CH_2O), 9.8 (CH_3CH_2). **HR ESI-TOF MS** for [M+H$^+$] $C_{30}H_{43}N_2O_4^+$ (m/z): 495.3217; found: 495.3218.

Ethyl rac-(2*R*,2*S*)-2-((1,3-dioxo-1,3-dihydro-2*H*-isoindol-2-yl)amino)-3- hydroxy-2-methyloctadec-4-ynoate (3.19)

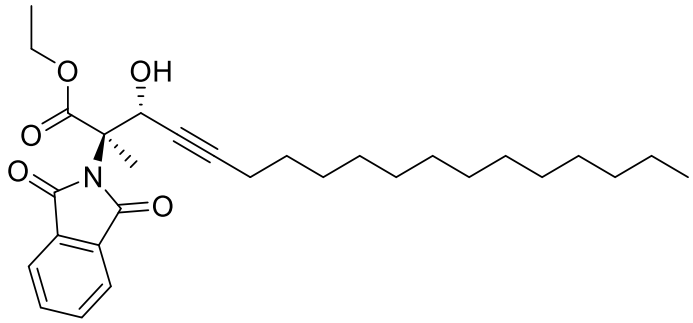

The title compound was prepared following the general procedure for the ring-opening of aziridines starting from **3.17** (1300 mg, 2.70 mmol), and PTSA (511 mg, 2.97 mmol). The crude was purified by column chromatography using a mobile phase of Hexane/AcOEt (90:10 to 80:20) to give **3.19** as a yellowish oil (1102 mg, 2.21 mmol, 82%).

IR (neat): 3448, 3230, 2924, 2853, 2223, 1788, 1725, 1466, 1378, 1259, 713, 631 cm^{-1}. **^{1}H NMR** (400 MHz, $CDCl_3$, δ in ppm): 7.86 (dd, J=5.4, 3.1 Hz, 2H, H_{ar}), 7.76 (dd, J=5.4, 3.1 Hz, 2H, H_{ar}), 5.77 (s, 1H, H_{NH}), 4.42 (dt, J=10.9, 2.0 Hz, 1H, H_3), 4.38 – 4.18 (m, 2H, CH_3CH_2O), 4.19 (d, J=10.9 Hz, 1H, H_{OH}), 2.17 (td, J=7.1, 2.0 Hz, 2H, H_6), 1.52 – 1.40 (m, 2H, H_7), 1.39 – 1.17 (m, 26H), 0.87 (t, J=6.8 Hz, 3H, H_{18}). **^{13}C NMR** (100 MHz, $CDCl_3$, δ in ppm): 172.2 (C_1), 167.8 (C_{ar}), 134.7 (C_{ar}), 129.9 (C_{ar}), 123.9 (C_{ar}), 87.4 (C_5), 77.5 (C_4) 68.2 (C_3), 67.8 (C_2), 62.2 (CH_3CH_2O), 32.0, 29.8, 29.7, 29.6, 29.5, 29.2, 28.9, 28.6 (C_8), 22.8, 18.8 (C_6), 17.4 (CH_3), 14.3 (C_{18}), 14.2 (CH_3CH_2O). **HR ESI-TOF MS** for [M+Na^+] $C_{29}H_{42}N_2NaO_5^+$ (m/z): 521.2986; found: 521.2982.

Ethyl rac-(2*R*,2*S*)-2-((1,3-dioxo-1,3-dihydro-2*H*-isoindol-2-yl)amino)-3- hydroxy-2-ethyloctadec-4-ynoate (3.20)

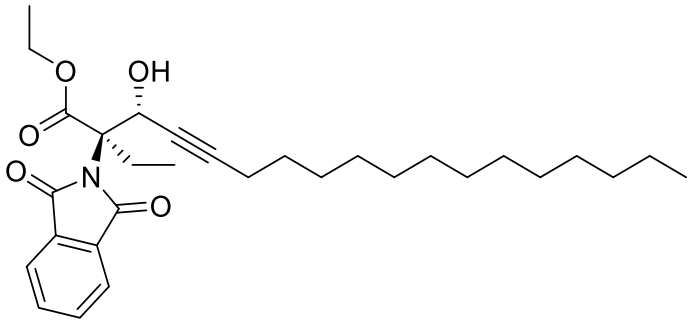

The title compound was prepared following the general procedure for the ring-opening of aziridines starting from **3.18** (311 mg, 0.63 mmol), and PTSA (131 mg, 0.69 mmol). The crude was purified by column chromatography using a mobile phase of Hexane/AcOEt (90:10 to 80:20) to give **3.20** as a yellowish oil (122 mg, 0.23 mmol, 37%).

IR (neat): 3446, 3312, 2924, 2853, 2363, 1725, 1450, 1378, 1237 cm^{-1}. **^{1}H NMR** (400 MHz, $CDCl_3$, δ in ppm): 7.85 (dd, J=5.5, 3.1 Hz, 2H, H_{ar}), 7.76 (dd, J=5.5, 3.1 Hz, 2H, H_{ar}), 5.66 (s, 1H, H_{NH}), 4.53 (s, 2H, H_3), 4.35 – 4.17 (m, 2H, CH_3CH_2O), 2.09 (t, J=7.0 Hz, 2H, H_6), 1.96 (dq, J=14.8, 7.4 Hz, 1H, CH_3CH_2), 1.63 (dq, J=14.8, 7.4 Hz, 1H, CH_3CH_2), 1.46 – 1.34 (m, 2H, H_7), 1.34 – 1.17 (m, 23H), 1.02 (t, J=7.4 Hz, 3H, CH_3CH_2), 0.86 (t, J=6.6 Hz, 3H, H_{18}). **^{13}C NMR** (100 MHz, $CDCl_3$, δ in ppm): 171.5 (C_1), 168.1 (C_{ar}), 134.7 (C_{ar}), 130.0 (C_{ar}), 123.8 (C_{ar}), 87.2 (C_5), 77.6 (C_4), 71.5 (C_2), 65.5 (C_3), 61.9 (CH_3CH_2O), 32.0, 29.8, 29.7, 29.5, 29.2, 28.9, 28.6 (C_7), 24.7 (CH_3CH_2), 22.8, 18.8 (C_6), 14.3 (C_{18}), 14.2 (CH_3CH_2O), 8.3 (CH_3CH_2). **HR ESI-TOF MS** for [M+H$^+$] $C_{30}H_{45}N_2O_5^+$ (m/z): 513.3323; found: 513.3324.

Ethyl rac-(2*R*,2*S*)-2-(2,2-dimethylhydrazinyl)-3-hydroxy-2-methyloctadec-4- ynoate (3.21)

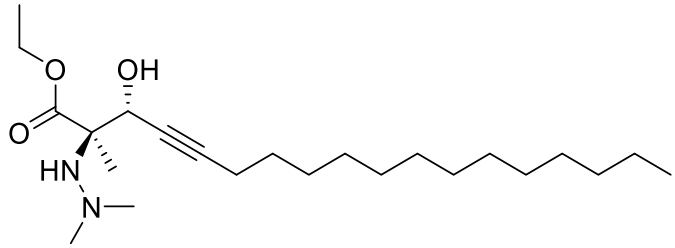

The title compound was prepared following the general procedure for the deprotection + dimethylation starting from **3.19** (139 mg, 0.28 mmol) and methylhydrazine (22 µL, 0.42 mmol). Then, paraformaldehyde (42 mg, 1.40 mmol) and $NaBH_3CN$ (106 mg, 1.68 mmol). The crude was purified by column chromatography using a mobile phase of Hexane/AcOEt (95:5 to 90:10) to give **3.21** as a yellow oil (69 mg, 0.17 mmol, 62%).

IR (neat): 3615, 3420, 2926, 2855, 2360, 1715, 1456, 1264, 1122, 888, 740, 631 cm^{-1}. **^{1}H NMR** (400 MHz, $CDCl_3$, δ in ppm): 4.52 (dd, J=2.5, 1.5 Hz, 1H, H_3), 4.29 – 4.09 (m, 2H, CH_3CH_2O), 2.47 (s, 6H, $N(CH_3)_2$), 2.26 – 2.10 (m, 2H, H_6), 1.54 – 1.39 (m, 5H, H7, CH_3), 1.39 – 1.12 (m, 23H, CH_3CH_2O), 0.86 (t, J=6.9 Hz, 3H, H_{18}). **^{13}C NMR** (100 MHz, $CDCl_3$, δ in ppm): 174.3 (C_1), 87.4 (C_5), 78.1 (C_4), 68.0 (C_3), 66.8 (C_2), 61.4 (CH_3CH_2O), 50.1 ($N(CH_3)_2$), 32.0, 29.8, 29.7, 29.5, 29.2, 29.0, 28.7 (C_8), 22.8 (C_7), 19.4 (CH_3), 18.8 (C_6), 14.3 (C_{18}), 14.2 (CH_3CH_2O). **HR ESI-TOF MS** for $[M+H^+]$ $C_{23}H_{45}N_2O_3^+$ (m/z): 397.3425; found: 397.3431.

Ethyl rac-(2*R*,2*S*)-2-(2,2-dimethylhydrazinyl)-3-hydroxy-2-ethyloctadec-4- ynoate (3.22)

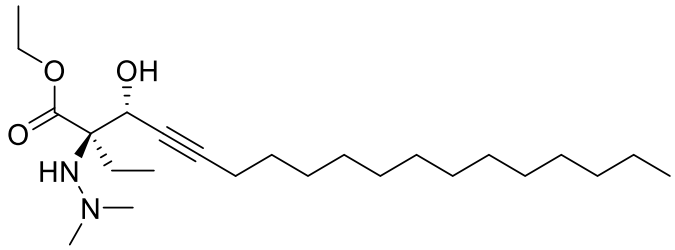

The title compound was prepared following the general procedure for the deprotection + dimethylation starting from **3.20** (145 mg, 0.28 mmol) and methylhydrazine (22 µL, 0.42 mmol). Then, paraformaldehyde (34 mg, 1.13 mmol) and $NaBH_3CN$ (36 mg, 0.57 mmol). The crude was purified by column chromatography using a mobile phase of Hexane/AcOEt (95:5) to give **3.22** as a colorless oil (44 mg, 0.11 mmol, 35%).

IR (neat): 3437, 2923, 2853, 2360, 1735, 1457, 1374, 1231, 1025cm^{-1}. **^{1}H NMR** (400 MHz, $CDCl_3$, δ in ppm): 4.57 (s, 1H, H_3), 4.24 – 4.10 (m, 2H, CH_3CH_2O), 2.49 (s, 6H, $N(CH_3)_2$), 2.30 – 2.14 (m, 2H, H_6), 1.99 – 1.90 (m, 2H, CH_3CH_2), 1.57 – 1.20 (m, 25H), 0.97 – 0.84 (m, 6H). **^{13}C NMR** (100 MHz, $CDCl_3$, δ in ppm): 173.5 (C_1), 87.9 (C_5), 79.8 (C_4), 71.2 (C_2), 68.1 (C_3), 62.0 (CH_3CH_2O), 50.2 ($N(CH_3)_2$), 33.1, 30.8, 30.5, 30.3, 29.9 (C_8), 29.7 (C_7), 26.2, 23.8 (CH_3CH_2), 19.4 (C_6), 14.6 (CH_3CH_2O), 14.5 (C_{18}), 8.7 (CH_3CH_2). **HR ESI-TOF MS** for $[M+H^+]$ $C_{24}H_{47}N_2O_3^+$ (m/z): 411.3581; found: 411.3588.

Ethyl (2*S*,3*S*)-2-(1,3-dioxoisoindolin-2-yl)-2-methyl-3-(((*S*)-3,3,3-trifluoro-2-methoxy-2-phenylpropanoyl)oxy)octadec-4-ynoate (3.25-1)

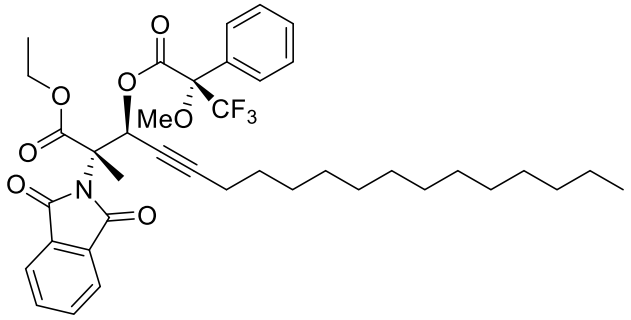

The title compound was prepared following the general procedure for derivatization of secondary alcohols with Mosher's reagent, starting from **3.17** (274 mg, 0.55 mmol), (S)-Mosher's acid (335 mg, 1.42 mmol), DMAP (175 mg, 1.42 mmol) and DCC (295 mg, 1.42 mmol) in CH_2Cl_2 (19 mL). The crude was first purified by flash chromatography using a mobile phase of hexane/AcOEt (80:20) and then the mixture of diastereomers was re-purified 3 times by radial chromatography using a mobile phase of CH_2Cl_2/hexane/MeOH (60:40:0.075). The desired product **3.25-1** was obtained as a yellowish oil (158 mg, 0.22 mmol, 40%).

$[\alpha]D_20$ = -36.84 (c 0.72, $CHCl_3$). **IR (neat):** 3492, 3285, 2924, 2853, 2359, 2237, 1790, 1759, 1730, 1378, 1169, 711. **1H NMR** (400 MHz, $CDCl_3$, δ in ppm): 7.88 – 7.80 (m, 2H), 7.78 – 7.72 (m, 2H), 7.57 – 7.49 (m, 2H), 7.40 – 7.28 (m, 3H), 5.92 (t, J = 1.9 Hz, 1H), 5.13 (s, 1H), 4.15 – 3.97 (m, 2H), 3.57 (s, 3H), 2.29 (td, J = 7.1, 1.9 Hz, 2H), 1.64 – 1.49 (m, 2H), 1.46 (s, 3H), 1.43 – 1.15 (m, 23H), 0.87 (t, J = 6.9 Hz, 3H). **19F NMR** (377 MHz, $CDCl_3$, δ in ppm): -71.54. **13C NMR** (100 MHz, $CDCl_3$, δ in ppm): 170.1, 166.8, 164.9 (x2), 134.6 (x2), 132.4, 130.1 (x2), 129.7, 128.4 (x2), 127.6 (x2), 123.8 (x2), 123.4 (q, J = 288.8 Hz), 119.1, 90.7, 84.4 (q, J = 27.7 Hz), 77.4, 73.1, 69.5, 66.8, 62.3, 55.6, 32.1, 29.8 (x2), 29.7, 29.5, 29.3, 29.0, 28.5, 22.8, 18.9, 16.1, 14.3, 13.9. **HR ESI-TOF MS** for [M+Na^+] $C_{39}H_{49}F_3N_2NaO_7^+$ (m/z): 737.3384; found: 737.3391.

Ethyl (2*R*,3*R*)-2-(1,3-dioxoisoindolin-2-yl)-2-methyl-3-(((*S*)-3,3,3-trifluoro-2-methoxy-2-phenylpropanoyl)oxy)octadec-4-ynoate (3.25-2)

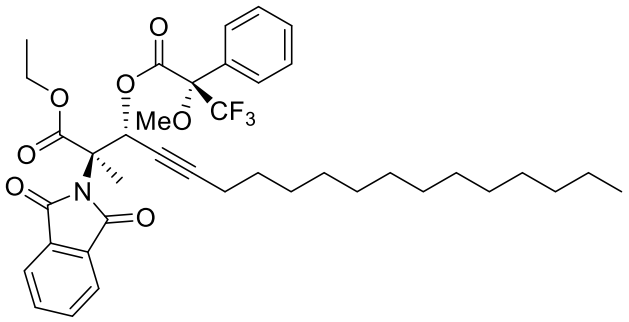

The title compound was prepared following the general procedure for derivatization of secondary alcohols with Mosher's reagent, starting from **3.17** (274 mg, 0.55 mmol), (S)-Mosher's acid (335 mg, 1.42 mmol), DMAP (175 mg, 1.42 mmol) and DCC (295 mg, 1.42 mmol) in CH_2Cl_2 (19 mL). The crude was first purified by flash chromatography using a mobile phase of hexane/AcOEt (80:20) and then the mixture of diastereomers was re-purified 3 times by radial chromatography using a mobile phase of CH_2Cl_2/hexane/MeOH (60:40:0.075). The desired product **3.25-2** was obtained as a colorless oil (26 mg, 0.04 mmol, 7%).

$[\alpha]D_20$ = 5.33 (c 0.15, $CHCl_3$). **IR (neat):** 3505, 3294, 2924, 2853, 2359, 2339, 1791, 1757, 1729, 1467, 1242, 1170, 999, 711. **1H NMR** (400 MHz, $CDCl_3$, δ in ppm): 7.89 – 7.82 (m, 2H), 7.79 – 7.72 (m, 2H), 7.52 (m, 2H), 7.43 – 7.33 (m, 3H), 5.90 (t, J = 2.0 Hz, 1H), 5.20 (s, 1H), 4.24 – 4.05 (m, 2H), 3.52 (s, 3H), 2.25 (td, J = 7.1, 2.0 Hz, 2H), 1.63 – 1.43 (m, 6H), 1.43 – 1.14 (m, 22H), 0.88 (t, J = 6.9 Hz, 3H). **19F NMR** (377 MHz, $CDCl_3$, δ in ppm): -71.99. **13C NMR** (100 MHz, $CDCl_3$, δ in ppm): 170.4, 166.8, 164.9 (x2), 134.6 (x2), 132.0, 130.1 (x2), 129.7, 128.4 (x2), 127.9 (x2), 123.8 (x2), 123.4 (q, J = 288.2 Hz), 90.4, 84.9 (q, J = 27.8 Hz), 77.4, 73.0, 69.8, 66.8, 62.4, 55.6, 32.1, 29.8 (x2), 29.7, 29.5, 29.3, 29.0, 28.4, 22.8, 18.9, 16.1, 14.3, 13.9. **HR ESI-TOF MS** for $[M+NH_4^+]$ $C_{39}H_{53}F_3N_3O_7^+$ (m/z): 732.3830; found: 732.3836.

3.5.4. Molecular Modelling

The co-crystal structure of SphK1 with its substrate sphingosine (3VZB, chain A, resolution 2 Å) was used as a template to build a SphK2 homology model with MOE 2019 software after sequence alignment.[22] The latter revealed additional residues 1–170 and 394–513 in SphK2, from which residues 1 to 170 were deleted due to the absence of a suitable template. Additional residues 394–513 were also excluded from the model since they did not directly affect the sphingolipid binding regions and lacked a suitable template. Subsequently, the homology model was verified by Ramachandran plots, which showed only 4 outliners far from the binding site, not connecting with it. The three distinctively different residues in the binding pocket were reproduced by the homology model and led to essential changes in the J-channel. In this regard, the replacement of Met272 with Leu553 at the pocket throat also led to a change in the position of identical residue Phe192, altering the shape of the J-channel. Further residue difference Ala339 in SphK1, corresponding to a Thr620 in SphK2, might also be relevant for the selectivity of potential ligands targeting the J-channel. This residue lies in the polar region and its variation affects a network of polar interactions that engage with the inhibitors.

3.5.5. Molecular Docking

The crystal structure of SphK1 (3vzb) and the SphK2 homology model were prepared for docking with the MOE software using the Protein preparation protocol. One water molecule was kept in the SphK1 protein preparation process since it was found in all available X-ray crystal structures, forming H-bonds with Ser168, Gly342 and the respective ligand. For the homology model of SphK2, the water molecule was omitted, considering a difference with respect to SphK1 residue Ala339 (Thr620 in SphK2), which was found by the homology model to displace the water molecule from its interactions with Ser334 and the Gly623. Both

[22] Molecular Operating Environment (MOE), 2019.01; Chemical Computing Group ULC, 1010 Sherbooke St. West, Suite #910, Montreal, QC, Canada, H3A 2R7, 2021.

enantiomers (2*R*,3*S*) and (2*S*,3*R*) of the designed compounds were drawn in MOE and underwent ligand preparation using Corina version 4.3.0 software[23], openbabel 3 version 3.0.0[24] and ChemAxon software[25]. Additionally, the corresponding unsynthesized compounds with a trisubstituted center at C-2 were also prepared for docking. After the preparation steps, the rDock software[26] was used for cavity generation, using the co-crystal sphingosine substrate as a reference ligand. Subsequently, the designed molecules were docked in the generated binding pocket with rDock, using permissive pharmacophoric restraints to ensure that the polar heads of the ligands remain in the polar region.

3.5.6. Toxicological Studies

3.5.6.1. ***Cell Culture***

Human umbilical vein endothelial cells (HUVEC) were isolated by collagenase treatment[27] and maintained in human endothelial cell specific medium (EBM-2, Lonza, Barcelona, Spain), supplemented with endothelial growth media (EGM-2, Lonza) and containing 10% fetal bovine serum (FBS, Biowest, Nuaill´e, France). Cells were grown to confluence up to passage 1 to preserve endothelial features. Prior to every experiment, cells were incubated for 24 h in medium containing 1% FBS for apoptosis and 0.1% for MTT assays.

3.5.6.2. ***Colorimetric Cytotoxicity Assay***

A 100 µL suspension of HUVECs in supplemented RPMI medium ($2x10^{5n}$ cells/mL) was added to each well of a 96-well microtiter plate. Cells

[23] Chemoinformatics ProgramPackage CORINA Classic, developed and distributed by Molecular Networks GmbH, Nuremberg, Germany and Altamira LLC, Columbus, OH, USA. www.mn-am.com.
[24] N.M. O'Boyle, M. Bank, C.A. James, C. Morley, T. Vandermeersch, G.R. Hutchison, Open Babel: An open chemical toolbox, *J. Cheminformatics* **2011**, *3*, 33.
[25] ChemAxon software was used for drawing, displaying and characterizing chemical structures, ChemAxon (https://www.chemaxon.com).
[26] S. Ruiz-Carmona, D. Alvarez-Garcia, N. Foloppe, A.B. Garmendia-Doval, S. Juhos, P. Schmidtke, X. Barril, R. Hubbard, S.D. Morley *PLoS Comput. Biol.* **2014**, *10*, 4, e1003571.
[27] E.A. Jaffe, R.L. Nachman, C.G. Becker, C.R. Minick *J. Clin. Invest.* **1973**, *52*, 2745–2756.

in 0.1% FBS supplemented EBM-2 medium (Lonza, Verviers, Belgium) were incubated in the absence or presence of compounds **3.1** and **3.2** (10, 30 and 100 μM) at 37ºC for 24 h. 3-(4,5-Dimethylthiazol-2-yl)-2,5-diphenyltetrazolium bromide (MTT, Sigma-Aldrich, Saint Louis, MO) was freshly prepared at 3 mg/mL in PBS, and 100 μL of MTT solution was added to each well followed by incubation at 37ºC for 3 h. The supernatants were discarded and 200 μL of DMSO was added to each well to dissolve the formazan product. The optical density at dual wavelengths (560 and 630 nm) was determined in a spectrophotometer (Infinite M200, Tecan, Mannedorf, Switzerland).

3.5.6.3. ***Cell Apoptosis and Survival Assay***

HUVEC cells were cultured on a 12-well plate and incubated in the absence or presence of compounds **3.1** and **3.2** (10, 30 and 100 μM) for 24 h in 1% FBS supplemented EBM-2 medium (Lonza) as described previously.[28] Then, cells were detached with StemPro Accutase cell dissociation reagent (5 min at 37ºC, Gibco, Thermo Fisher Scientific, Waltham, MA) and recovered by centrifugation (1400 rpm, for 10 min at 4ºC). Cells were resuspended in Annexin V Binding Buffer to obtain $1x10^5$ cells in a final volume of 100 μL. Samples were incubated with 5 μL of FITC-Annexin V and 5 μL of propidium iodide (PI) from FITC Annexin V Detection Kit I (BD Biosciences, Franklin Lakes, NJ) for 15 min at room temperature in the dark following the manufacturer instructions and as previously described.[29] Cells were analyzed in a flow cytometer (BD Fortessax20, BD Biosciences, San Jose, CA) and differentiated as early apoptotic (annexin V+ and PI-), late apoptotic and/or necrotic (annexin V+ and PI+), and viable nonapoptotic (annexin V- and PI-) cells. Results are presented as percentage of apoptotic and viable cells.

[28] M.T. Garcia, M.A. Blazquez, M.J. Ferrandiz, M.J. Sanz, N. Silva-Martin, J. A. Hermoso, A.G. de la Campa *J. Biol. Chem.* **2011**, *286*, 6402–6413.
[29] M.C. Martin, I. Dransfield, C. Haslett, A.G. Rossi *J. Biol. Chem.* **2001**, *276*, 45041–45050.

3.5.6.4. ***Statistical Analysis***

Differences between two groups were determined using an unpaired Student's *t* test. Values were expressed as mean ±SEM. Data were considered statistically significant when p values were <0.05.

UNIVERSITAT ROVIRA I VIRGILI
INSIGHTS INTO AMINOFLUORINATION STRATEGIES AND SPHINGOSINE ANALOGUE SYNTHESIS TOWARDS THE DEVELOPMENT OF SELECTIVE SPHK2 INHIBITORS
Albert Granell Fort

CHAPTER IV

I(III)-Mediated Aminofluorination of Allylic Carbamates

UNIVERSITAT ROVIRA I VIRGILI
INSIGHTS INTO AMINOFLUORINATION STRATEGIES AND SPHINGOSINE ANALOGUE SYNTHESIS TOWARDS THE DEVELOPMENT OF SELECTIVE SPHK2 INHIBITORS
Albert Granell Fort

4.1. Introduction

4.1.1. β-Fluoroamines

The incorporation of fluorine to an organic molecule leads to important changes in its physical, chemical and biological properties. These changes are often produced by the formal replacement of hydrogen by fluorine, although exchanges of hydroxyl groups also have been described. The van der Waals radius of C-F bond (1.41 Å) falls between that of C-O bond (1.43 Å) and the C-H bond (1.09 Å), making fluorine a versatile element for bioisosteric replacement.[1] Thus, it is no wonder that fluorinated compounds have great relevance in pharmaceutical, agrochemical or medicinal research.[2]

The β-fluoroamine motif is a remarkable fragment for medicinal chemistry. The electron-withdrawing character of the fluorine atom in β position is able to decrease the pK_a of the amine, improving the bioavailability of the compound containing the β-fluoroamine motif and increasing its blood-brain barrier penetration.[3] Furthermore, the β-fluoroamine moiety is also involved in improvements in metabolic stability and binding affinity, thereby constituting an important building block in drugs with anticancer, anticholinergic and anti-inflammatory properties.[4]

---

[1] a) Olah, G. A.; Chambers, R. D.; Prakash, G. K. S. *Synthetic Fluorine Chemistry*, John Wiley: New York, **1992**; b) Hudlicky, M.; Pavlath, A. E. *Chemistry of Organic Fluorine Compounds II*, American Chemical Society: Washington, DC, **1995**; c) Chambers, R. D. *Fluorine in Organic Chemistry*, Blackwell Publishing: Oxford, **2004**; d) Durnitz, J. D.; Scheweizer, W. B. *Chem. Eur. J.* **2006**, *12*, 6804-6815.

[2] a) Müller, K.; Faeh, C.; Diederich, F. *Science* **2007**, *317*, 1881-1886; b) Purser, S.; Moore, P. R.; Swallow, S.; Gouverneur, V. *Chem. Soc. Rev.* **2008**, *37*, 320-330; c) Tredwell, M.; Preshlock, S. M.; Taylor, N. J.; Gruber, S.; Huiban, M.; Passchier, J.; Mercier, J.; Génicot, C.; Gouverneur, V. *Angew. Chem. Int. Ed.* **2014**, *53*, 7751-7755; *Angew. Chem.* **2014**, *126*, 7885-7889; d) Jeschke, P. *ChemBioChem* **2004**, *5*, 570-589; e) Wang, J.; Sánchez-Roselló, M.; Aceña, J. L.; del Pozo, C.; Sorochinsky, A. E.; Fustero, S.; Soloshonok, V. A.; Liu, H. *Chem. Rev.* **2014**, *114*, 2432-2506; f) Liu, S.; Lu, K.; Zhang, Y.; Li, X. *Chin. J. Org. Chem.* **2022**, *42*, 2124−2133.

[3] O'Hagan, D. *Chem. Soc. Rev.* **2008**, *37*, 308-319.

[4] a) Cox, C. D.; Coleman, P. J.; Breslin, M. J.; Whitman, D. B.; Garbaccio, R. M.; Fraley, M. E.; Buser, C. A.; Walsh, E. S.; Hamilton, K.; Schaber, M. D.; Lobell, R. B.; Tao, W.; Davide, J. P.;

In this sense, the interest in preparing new compounds featuring this scaffold in their structures has increased during the last years.[5] Some of the most popular strategies for the synthesis of β-fluoroamines are the deoxyfluorination of a β-hydroxylated amine with (diethylamino)sulfur trifluoride (DAST),[6] the fluorination of unsaturated amines (imines, enamines, allylic amines),[7] amination of allyl fluorides,[8] α-fluorination of a carbonyl compound and subsequent reductive amination,[9] or ring-opening of aziridines with nucleophilic fluorine (Scheme **4.1**).[10]

Among the different methodologies towards β-fluoroamines, the ring-opening of aziridines with nucleophilic fluorine sources is one of the preferred methods due to low cost of reagents, mild reaction conditions,

Diehl, R. E.; Abrams, M.T.; South, V. J.; Huber, H. E.; Torrent, M.; Prueksaritanont, T.; Li, C.; Slaughter, D. E.; Mahan, E.; Fernandez-Metzler, C.; Yan, Y.; Kuo, L. C.; Kohl, N. E.; Hartman, G. D. *J. Med. Chem.* **2008**, *51*, 4239-4252; b) Welsch, J. T.; Eswarakrishamn, S. *Fluorine in Bioorganic Chemistry*, Wiley, New York, **1991**.

[5] a) Yadav, J. S.; Reddy, B. V. S.; Chaya, D. N.; Kumar, G. G. K. S. N.; Naresh, P.; Jagadeesh, B. *Tetrahedron Lett.* **2009**, *50*, 1799-1802; b) Liu, F.; Martin-Mingot, A.; Jouannetaud, M. P.; Zunino, F.; Thibaudeau, S. *Org. Lett.* **2010**, *12*, 868-871; c) Al-Maharik, N.; O'Hagan, D. *Aldrichimica Acta* **2011**, *44*, 3, 65-75; d) Andrews, P. C.; Bhaskar, V.; Bromfield, K. M.; Dodd, A. M.; Duggan, P. J.; Duggan, S. A. M.; McCarthy, T. D. *Synlett* **2004**, *2004*, 5, 0791-0794; e) Malamakal, R. M.; Hess, W. R.; Davis, T. A. *Org. Lett.* **2010**, *12*, 2186-2189; f) Chen, P.; Liu, G. *Eur. J. Org. Chem.* **2015**, 4295–4309.

[6] Singh, R. P.; Shreeve, J. M. *Synthesis* **2002**, *17*, 2561–2578.

[7] a) Han, X.; Kwiatkowski, J.; Xue, F.; Huang, K. W.; Lu, Y. *Angew. Chem. Int. Ed.* **2009**, *48*, 7604– 7607; b) Pan, Y.; Zhao, Y.; Ma, T.; Yang, Y.; Liu, H.; Jiang, Z.; Tan, C. H. *Chem. Eur. J.* **2010**, *16*, 779–782; c) Dilman, A. D.; Belyakov, P. A.; Struchkova, M. I.; Arkhipov, D. E.; Korlyukov, A. A.; Tartakovsky, V. A. *J. Org. Chem.* **2010**, *75*, 5367–5370; d) Thibaudeau, S.; Martin-Mingot, A.; Jouannetaud, M. P.; Karam, O.; Zunino, F. *Chem. Commun.* **2007**, 3198–3200.

[8] Combettes, L. E.; Schuler, M.; Patel, R.; Bonillo, B.; Odell, B.; Thompson, A. L.; Claridge, T. D. W.; Gouverneur, V. *Chem. Eur. J.* **2012**, *18*, 13126–13132.

[9] a) Ishimaru, T.; Shibata, N.; Horikawa, T.; Yasuda, N.; Nakamura, S.; Toru, T.; Shiro, M. *Angew. Chem.* **2008**, *120*, 4225-4229; *Angew. Chem. Int. Ed.* **2008**, *47*, 4157-4161. b) Beeson, T. D.; MacMillan, D. W. C. *J. Am. Chem. Soc.* **2005**, *127*, 8826–8828. c) Fadeyi, O. O.; Lindsley, C. W. *Org. Lett.* **2009**, *11*, 943-946.

[10] a) Jensen, K. L.; Standley, E. A.; Jamison, T. F. *J. Am. Chem. Soc.* **2014**, *136*, 11145–11152. b) Hu, X. E. *Tetrahedron* **2004**, *60*, 2701-274. c) McNally, A.; Haffemayer, B.; Collins, B. S. L.; Gaunt, M. J. *Nature* **2014**, *510*, 7503, 129-133. d) Wade, T. N.; Guedj, R. *Tetrahedron Lett.* **1978**, 3247. e) Alvernhe, G. M.; Ennakoua, C. M.; Lacombe, S. M.; Laurent, A. *J. Org. Chem.* **1981**, *46*, 4938-4948. f) Fan, R.; Zhou, Y.; Zhang, W.; Hou, X.; Dai, L. *J. Org. Chem.* **2004**, *69*, 335-338. g) Zhang, W. X.; Su, L.; Hu, W. G.; Zhou, J. *Synlett* **2012**, *23*, 2413-2415.

and general accessibility of substrates. Given the context of our group research history, this methodology resulted very attractive.

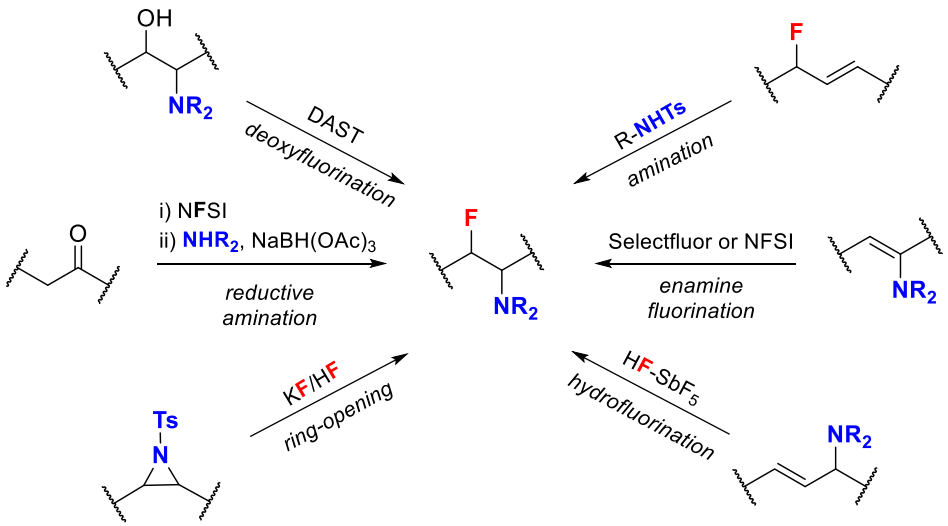

Scheme 4.1 Examples of different methodologies for the preparation of β-fluoroamines.

Our group has recently studied the metal-free amination of alkenes using hypervalent iodine reagents (HIR), a two-step procedure to obtain *anti*-β-heteroatomic oxazolidinones starting from dienyl carbamates (Scheme **4.2**).[11] The first step is the intramolecular aziridination of the carbamate mediated by PhIO, a popular HIR, to obtain a vinyl aziridine that is stable in the reaction media. Intramolecular reaction ensures complete regioselectivity to the proximal alkene to the carbamate group. Then, an O, N or S-based nucleophile is added to the reaction mixture and the aziridine is opened yielding the corresponding *anti*-α-substituted oxazolidinone with complete stereoselectivity. This procedure, together with kinetic resolution with chiral agent (*R*)-2-phenyl-2,3-dihydroimidazo[2,1-*b*][1,3]benzothiazole (BTM), granted facile access to enantiopure sphingolipid scaffolds.

[11] Giménez-Nueno, I.; Guasch, J.; Funes-Ardoiz, I.; Maseras, F.; Matheu, M. I.; Castillón, S.; Díaz, Y. *Chem. Eur. J.* **2019**, *25*, 12628 –12635.

(III)-Mediated Aminofluorination of Allyl Carbamates

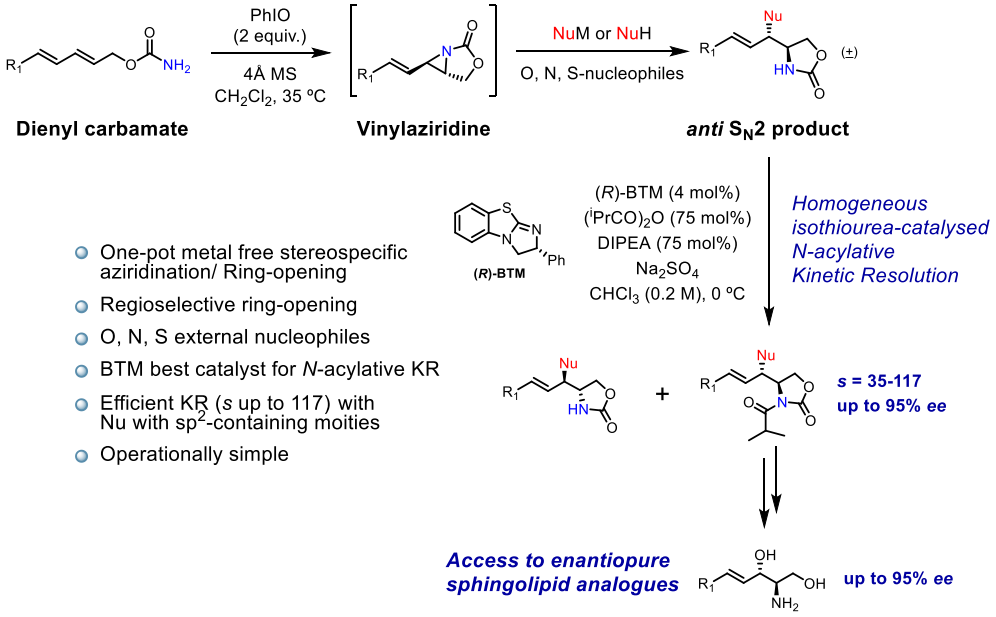

Scheme 4.2 General scheme of the sequential aziridination/ring-opening of dienyl carbamates with O, N and S-nucleophiles.

The use of fluorine as the nucleophile for this sequential transformation was considered as a metal-free methodology to obtain β-fluoroamines with hypervalent iodine reagents.

4.1.2. Use of Hypervalent Iodine Reagents towards the Aminofluorination of Dienyl Carbamates

Hypervalent iodine reagents (HIR) are compounds that contain iodine in a high oxidation state, bound to several ligands, thereby imparting a markedly electrophilic character to the iodine. In these species, the iodine has more than 8 electrons in its valence shell and is therefore categorized as hypervalent. Their environmentally benign character along with mild reaction conditions make these reagents interesting alternatives to transition metal catalysts.

Iodine atoms with +3 oxidation state (λ^3-Iodanes) display a pseudo trigonal bipyramidal geometry. In the case of trivalent iodine derivatives with general formula RIL_2, since carbon is less electronegative than heteroatoms, the alkyllic substituent is placed in the equatorial position along with iodine lone pairs, whereas heteroatomic ligands are linked to the central atom by the apical positions (Figure **4.1**). The linear L–I–L bond is known as "hypervalent bond" and its highly polarised nature is responsible for the characteristic electrophilic reactivity of hypervalent iodine reagents.

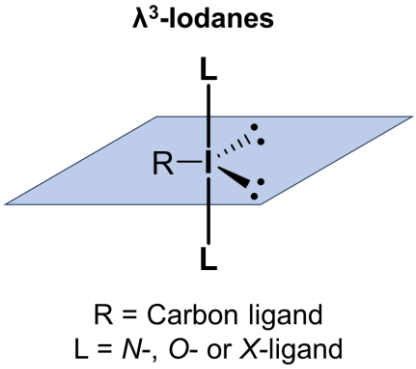

Figure 4.1. General trigonal bipyramidal geometry of RIL_2-type λ^3-Iodanes.

Although HIR have extensive reactivity, they generally act as oxidizing agents.[12] Usually, some of the ligands are labile groups, such as acetates or chlorides, and can be substituted by a number of substrates, like olefins.[13] Among the λ³-Iodanes, phenyliodine(III) diacetate (PIDA) is often used because it is a bench-stable and very cheap HIR. In addition, the acetate ligands are easily exchangeable and relatively inert.[14] Another relevant hypervalent iodine reagent is iodosobenzene (PhIO). PhIO presents a polymeric structure with [PhIO] as the monomeric motif. Although it is less stable than PIDA, it is usually more reactive. Besides, it is easy to prepare from PIDA (Scheme **4.3**) and it does not release acetate anions in the media.

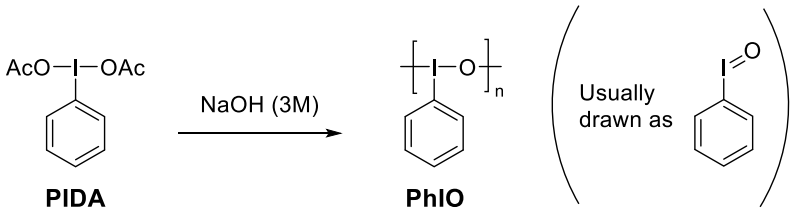

Scheme 4.3 Synthesis of PhIO from PIDA.

4.1.2.1. Direct Vicinal Difunctionalization of Alkenes

Olefins are excellent substrates for 1,2-difunctionalization due to their general accessibility and the precise stereoselectivity control facilitated by their substituents.[15] Hypervalent iodine reagents are a very useful tool for the 1,2-functionalization of alkenes, usually carried away with λ³-iodanes. Some mechanistic aspects of iodine(III)-mediated alkene derivatisation are depicted in Scheme **4.4**. Iodonium species **4.2** is originated from the coordination of electron deficient hypervalent iodine

[12] a) Yoshimura, A.; Zhdankin, V. V. *Chem. Rev.* **2016**, *116*, 3328–3435; b) Zhdankin, V. V.; Stang, P. J. *Chem. Rev.* **2008**, *108*, 5299–5358.
[13] a) R. M. Romero, T. H. Wöste, K. Muñiz, *Chem. Asian J.* **2014**, *9*, 972–983; b) Fujita, M. *Tetrahedron Lett.* **2017**, *58*, 4409–4419.
[14] Varala, R.; Seema, V.; Dubasi, N. *ACS Omega* **2020**, *5*, 918–925.
[15] Ahmad R.; Huang, D.; Liu, F.; Wang, Y. *J. Saud. Chem. Soc.* **2021**, *25*, 101260.

atom to the π-orbital of the double bond in olefin **4.1**. Dissociation of a ligand from iodine centre enhances its electrophilic character, favouring the generation of cyclic iodonium **4.2,** which is subsequently opened by external nucleophiles or released ligands to furnish iodane intermediate **4.3**. *Syn*- or *anti*-difunctionalised products **4.4** and **4.6** respectively resulted from either intermolecular S_N2 replacement of hypervalent iodine moiety or intramolecular nucleophilic displacement followed by ring-opening pathway, respectively. For aryl substituted alkenes, 1,2-migration of phenyl via intermediate formation of phenonium ion **4.7** may lead to rearranged product **4.8**.

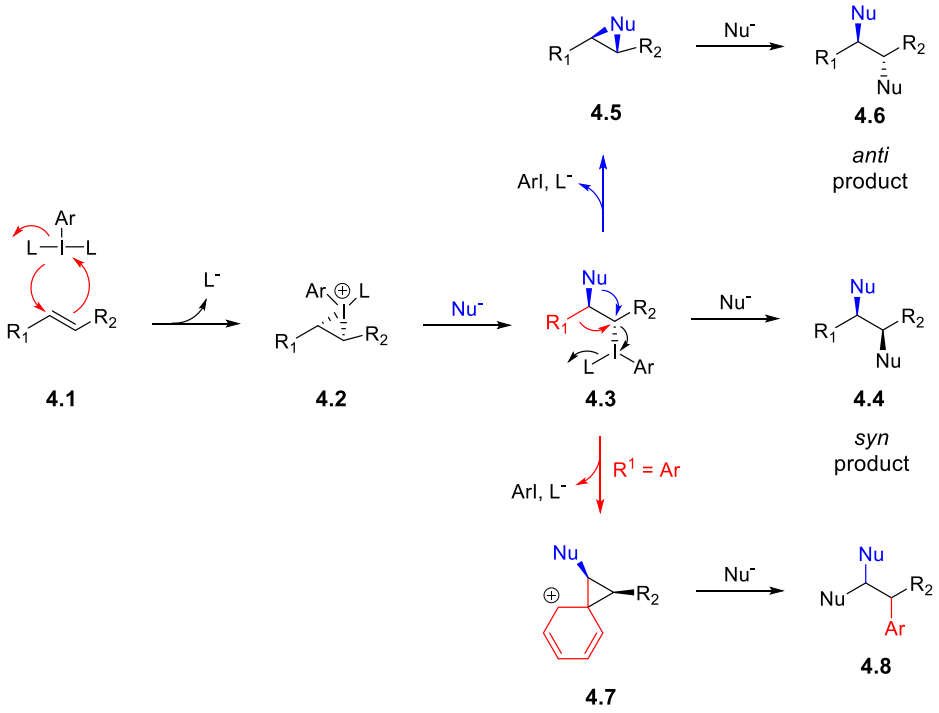

Scheme 4.4 Mechanistic pathways of iodine(III)-mediated alkene functionalisation.

Hypervalent I(III) reagents have been widely used in the difluorination of alkenes leading to 1,1- or 1,2-difluoroalcanes.[16] Generally, for the 1,2-difluorination, the mechanistic pathway is very similar to the general mechanism depicted in Scheme **4.4**, although in some cases it is proposed that Ar-IF_2 is formed in the reaction mixture as a key intermediate,[17] which acts both as the oxidizing agent and the fluorine source.

In 1998, Hara and co-workers reported the use of hypervalent iodine *p*-iodotoluene difluoride (TolIF_2) for the vicinal difluorination of terminal alkenes.[18]

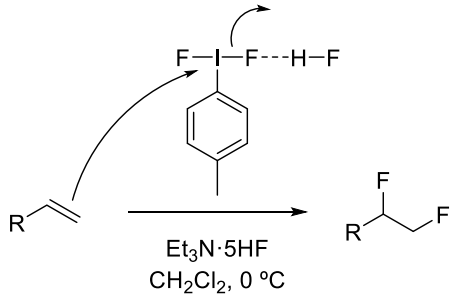

Scheme 4.5 Difluorination of terminal alkenes with TolIF_2.

In this reaction, auxiliary $Et_3N{\cdot}5HF$ is necessary to activate the iodine. Structural F-I-F can be destabilized by hydrogen bonding from HF, therefore activating the iodine and making it susceptible to nucleophilic attack from the olefin. Also, it might act as a secondary fluorine source. The difluorinated products were obtained with moderate yields (50-65%).

[16] a) Banik, S. M.; Medley, J. W.; Jacobsen, E. N. *J. Am. Chem. Soc.* **2016**, *138*, 5000-5003; b) Molnár, I. G.; Gilmour, R. *J. Am. Chem. Soc.* **2016**, *138*, 5004-5007.
[17] Kitamura, T.; Yoshida, S.; Mizuno, S.; Miyake, A.; Oyamada, J. *J. Org. Chem.* **2018**, *83*, 14853−14860.
[18] Hara, S.; Nakahigashi, J.; Ishi-I, K.; Sawaguchi, M.; Sakai, H.; Fukuhara, T.; Yoneda, N. *Synlett* **1998**, 495.

A catalytic version of this reaction was developed in 2016 by Jacobsen *et. al*[19] and Gilmour *et al.*[20] independently. Since a secondary fluorine source was needed to activate the iodane, they envisioned that formation of aryliodane difluoride could be carried out in a *one pot* reaction using catalytic amounts of a I(I) precursor and an auxiliar oxidant reagent in the presence of a fluorine source (Scheme **4.6**).

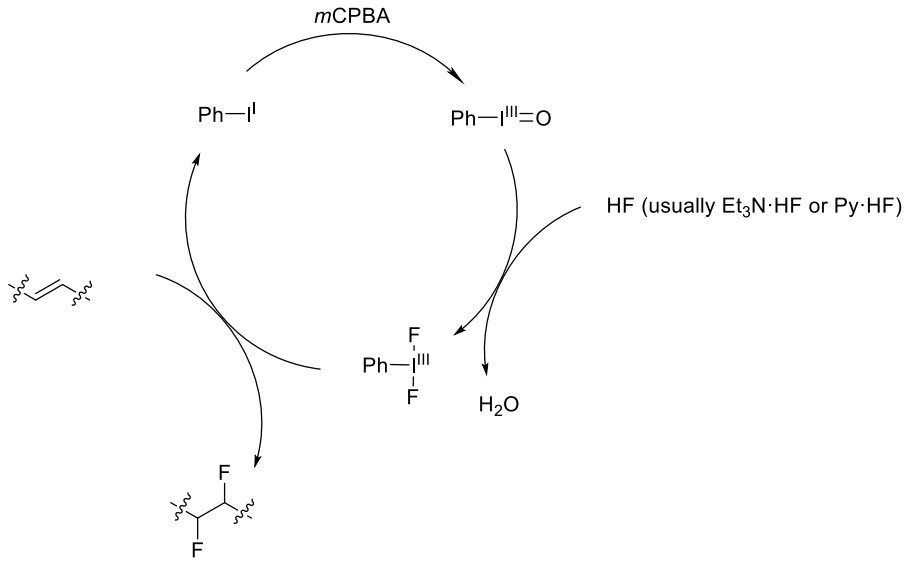

Scheme 4.6 Catalytic system for the *in situ* formation of $ArIF_2$ as the difluorination agent.

The reaction works in good to excellent yield with a wide array of activated and unactivated alkenes (Scheme **4.7**). The substrate shown in the scheme was used in Gilmour's paper for optimisation, but a large scope was performed containing long alkyl chains functionalised with esters, amides, olefins, sulfones, ethers and phenol ethers. An asymmetric version of this transformation was further developed by Jacobsen in the same paper using a chiral iodine(I) with excellent stereoselectivity.

[19] Banik, S.; Medley, J. W.; Jacobsen, E. M. *J. Am. Chem. Soc.* **2016**, *138*, 5000–5003.
[20] Molnár, I. G.; Gilmour, R. *J. Am. Chem. Soc.* **2016**, *138*, 5004–5007.

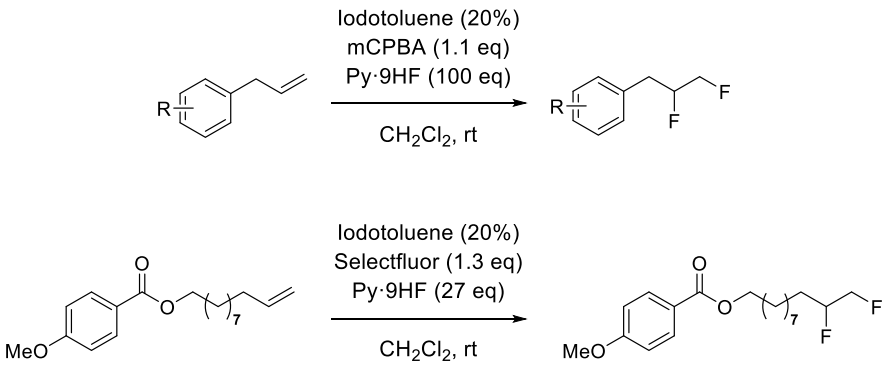

Scheme 4.7 Catalytic aminofluorination with HIR as proposed by Jacobsen (top) and Gilmour (bottom).

In similar fashion to the difluorination, the aminofluorination of alkenes is also performed using hypervalent iodine reagents. The intramolecular aminofluorination of alkenes was described by Liu *et al.* in 2009.[21] Therein, a tandem $Pd(OAc)_2$/$PhI(OPiv)_2$ acts as the oxidant agent, using AgF as the fluorine source. The system furnished β-fluorotosylpiperidines (Scheme **4.8**). Interestingly, the same transformation was tested using $PhIF_2$ instead of $PhI(OPiv)_2$/AgF and no conversion was observed.

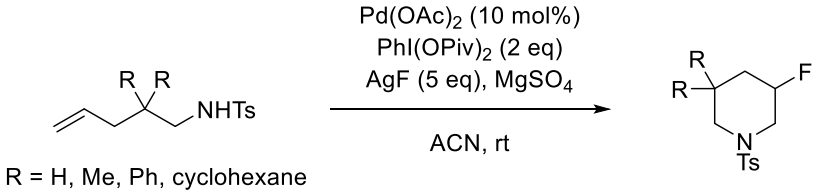

Scheme 4.8 Pd-catalysed intramolecular aminofluorination of tosylamides with HIR.

Jacobsen *et al.* developed a highly enantio- and diastereoselective *syn* aminofluorination of cinnamyl tosylamides. β-Fluoroaziridines were obtained by treating the tosylamides with a chiral I(I) catalyst, *m*CPBA and

[21] Wu, T.; Yin, G.; Liu, G. *J. Am. Chem. Soc.* **2009**, *131*, 16354–16355.

Py·HF.[22] Presumably, this reaction occurs through the electrophilic addition of iodine to the alkene, which generates a C(sp_3)-I(III) intermediate in *anti* disposition with respect to fluorine. Intramolecular nucleophilic substitution (S_N2) by the nitrogen in the tosylamide provides the corresponding *syn* β-fluoroaziridines.

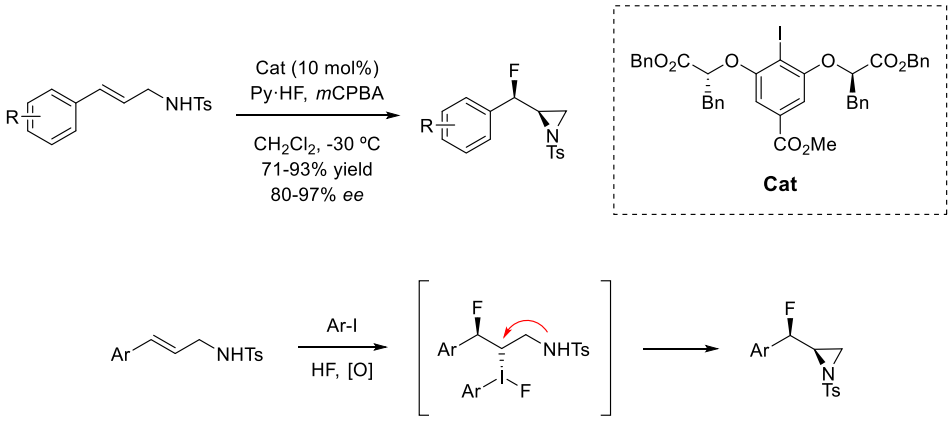

Scheme 4.9 Catalytic iodine-mediated aminofluorination of cinnamyl tosylamides and proposed mechanism overview.

This chemistry has been explored for the intramolecular aminofluorination of alkenes containing electrophilic nitrogen, mostly sulfonamides, with promising results even in catalytic and asymmetric versions. However, the metal-free aminofluorination of carbamates or less electrophilic nitrogen is yet to be explored.

Apart from the direct F,N-functionalization of alkenes, the aminofluorination of alkenes is also described via nitrene addition to the alkene. In this variation, the HIR oxidizes the nitrogen source to form a nitrene equivalent that is rapidly added to the alkene.

[22] Mennie, K. M.; Banik, S. M.; Reichert, E. C.; Jacobsen, E. N. *J. Am. Chem. Soc.* **2018**, *140*, 4797−4802.

4.1.2.2. Formation of Nitrene Sources for Aziridination

Nitrenes are neutral monovalent species with six electrons in their valence shell, and therefore are very electron-deficient species. This gives nitrenes a very electrophilic behaviour.[23] The highly reactive nature and poor selectivity of nitrenes hampered a widespread application in organic synthesis for C-N bond formation.[24] Nitrene species can be stabilised by transition metals like Fe, Cu or Ru, in conjunction with HIR as metallonitrene complexes, leading to efficient methodologies for olefin aziridination.[25]

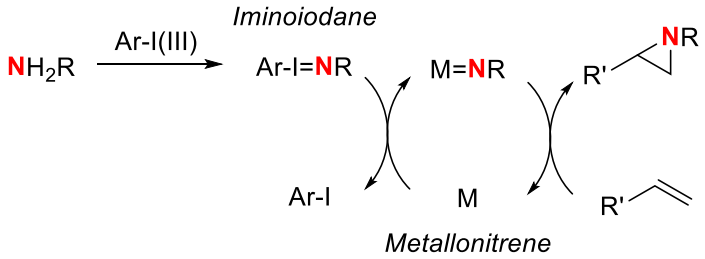

Scheme 4.10 General mechanism for the iodine-mediated aziridination of alkenes through metallonitrene addition.

Iminoiodanes, or iminoiodinanes, are a class of hypervalent iodine compounds that effectively transfer nitrogen into a metal centre (Scheme **4.10**). Moreover, metallonitrenes can also be synthesised upon treatment of amine derivatives with oxidant HIR such as PhIO or PIDA, formally generating the iminoiodane *in situ*. The inability of producing reliable iminoiodanes due to their difficulty in preparation and overall low stability makes the *in situ* generation of iminoiodanes a great tool for nitrene transfer reactions.[26]

[23] a) Dequirez, G.; Pons, V.; Dauban, P. *Angew. Chem. Int. Ed.* **2012**, *51*, 7384–7395; b) *Chem. Commun.* **2017**, *53*, 493–508.
[24] Macara, J.; Caldeira, C.; Poeira, D. L. Marques, M. *Eur. J. Org. Chem.* **2023**, e202300109.
[25] Degennaro, L.; Trinchera, P.; Luisi, R. *Chem. Rev.* **2014**, *114*, 7881–7929.
[26] a) Dauban, P.; Dodd, R. H. *Synlett* **2003**, 1571–1586; b) Dauban, P.; Dodd, R. H. *Org. Lett.* **2000**, *2*, 2327–2329; c) Espino, C. G.; Du Bois, J. *Angew. Chem. Int. Ed.* **2001**, *40*, 598–600.

The aminofluorination of carbamate hydroxylamines was studied by Lu *et al.* using Fe(II) catalysis and $Et_3N{\cdot}HF$ as the fluorinating agent (Scheme **4.11**).[27] The formation of iron-metallonitrene **4.9** was hypothesised, followed by a radical cycloaddition and fluorination, to furnish the *anti*-β-fluorooxazolidinone in moderate to good yield and complete diastereoselectivity. Convergence in selectivity from both the *cis* and the *trans* starting carbamates led to the postulation of radical intermediate **4.10**.

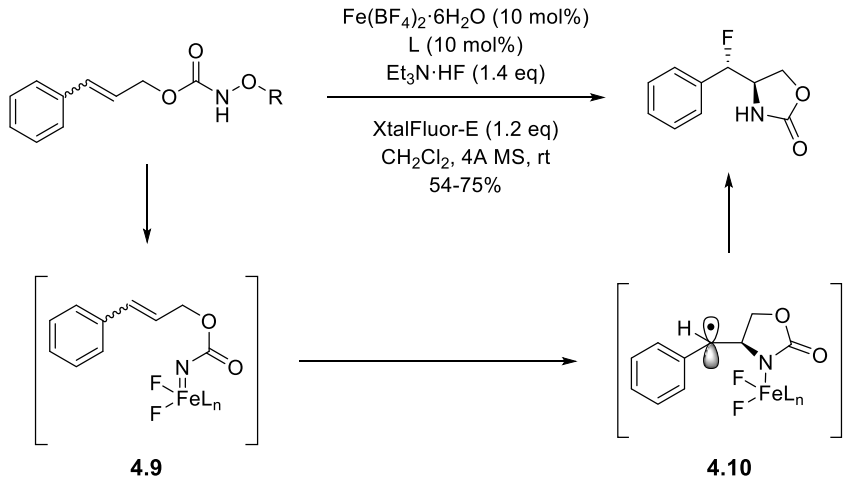

Scheme 4.11 Stereoselective Fe-catalysed aminofluorination of carbamoyl hydroxylamines.

Shibata *et al.* reported a metal-free intramolecular aminofluorination of ketones and tosylamides catalysed by a iodine(III) reagent generated *in situ* from iodotoluene, Py·HF and *m*CPBA (Scheme **4.12**, a).[28] The enantioselective synthesis of piperidines was accomplished with chiral I(III) reagents derived from **Cat** under similar conditions (Scheme **4.12**, b).

[27] Lu, D.; Liu, G.; Zhu, C.; Yuan, B.; Xu, H. *Org. Lett.* **2014**, *16*, 2912–2915.
[28] Suzuki, S.; Kamo, T.; Fukushi, K.; Hiramatsu, T.; Tokunaga, E.; Dohi, T.; Kita, Y.; Shibata, N. *Chem. Sci.* **2014**, *5*, 2754-2760.

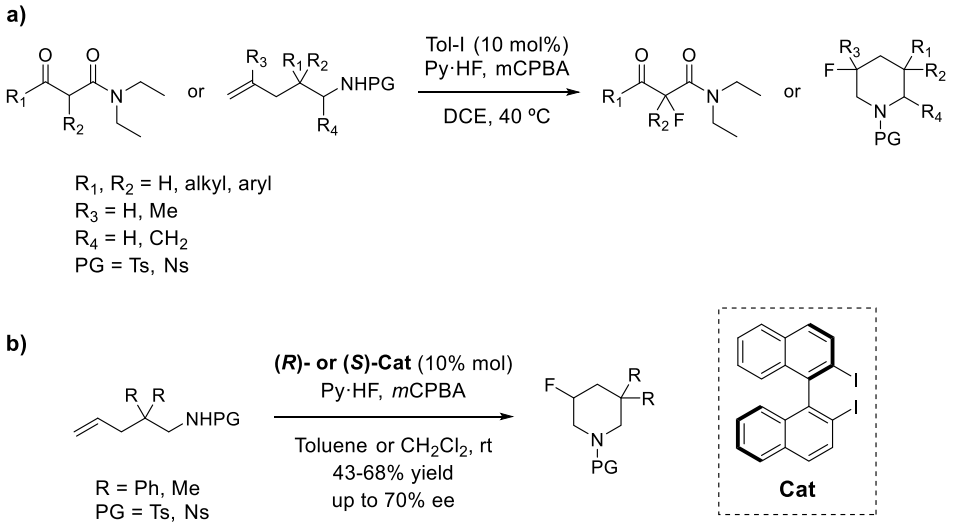

Scheme 4.12 Catalytic metal-free aminofluorination. Symmetric (a) and asymmetric version (b).

In the the intramolecular iodine-mediated aminofluorination of alkenes via nitrene transfer addition the nitrogen replaces one of the ligands of the iodane to form aminoiodonium ion **4.12**, which is added intramolecularly to the alkene to generate aziridinium **4.13** (Scheme **4.13**). This intermediate is opened by fluorine coming from either the original F^- source or the iodane yielding *β*-fluoroamine **4.14**.

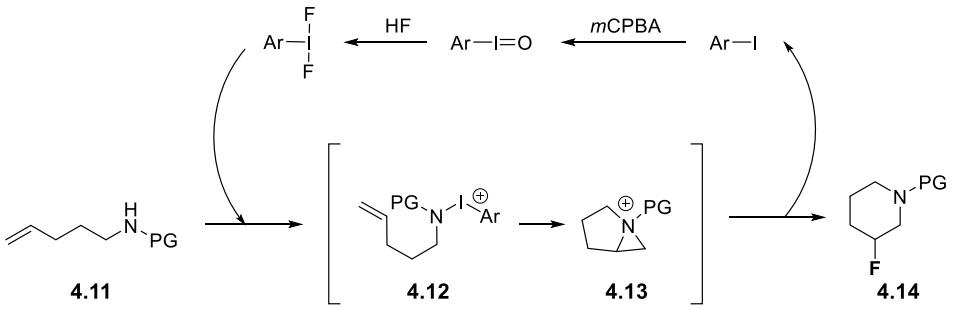

Scheme 4.13 General mechanism for the intramolecular iodine-mediated aminofluorination of alkenes via nitrene transfer addition.

Nevado *et al.* studied the aminofluorination of alkenyl tosylamides using gold catalysis chemistry.[29] In one of the experiments, Xilene-IF_2 was used without metal assistance, and *β*-fluoroamine **4.16** was obtained in 93% (Scheme **4.14**).[30] This marks the first intramolecular, metal-free regioselective aminofluorination of unactivated alkenes with $ArIF_2$-type reagents.

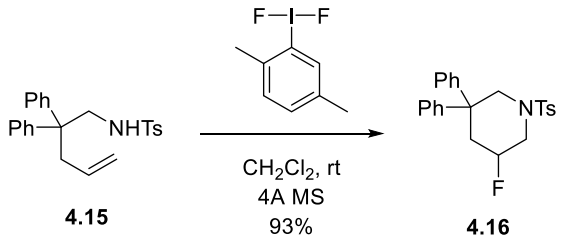

Scheme 4.14 Metal-free intramolecular aminofluorination of tosylamides with $ArIF_2$.

Mechanism experiments with deuterium-labelled alkenes showed complete stereoselectivity for the *anti* configuration between the fluorine and the nitrogen. With this result, together with some other mechanism tests, the oxidation of the tosylamide by the HIR, in the form of an aminoiodane, was proposed instead of the addition of the iodane to the double bond (Scheme **4.15**).

[29] a) Zou, Y.; Garayalde, D.; Wang, Q.; Nevado, C.; Goeke, A. *Angew. Chem. Int. Ed.* **2008**, *47*, 10110; b) Huang, X.; de Haro, T.; Nevado, C. *Chem. Eur. J.* **2009**, *15*, 5904.
[30] Kong, W.; Feige, P.; de Haro, T.; Nevado, C. *Angew. Chem. Int. Ed.* **2013**, *52*, 2469 –2473.

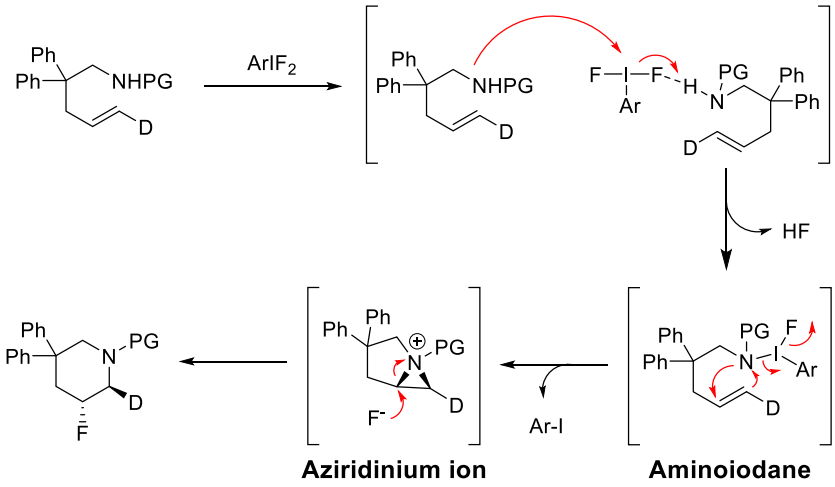

Scheme 4.15 Proposed mechanism for the metal-free intramolecular aminofluorination with $ArIF_2$.

The relevance of the acidity of the tosylamide was remarked, as the iodine(III) reagent needs H-bonding activation to react. Tosylamide activates $ArIF_2$, and a second tosylamide molecule is added to the iodine (Scheme **4.15**). The aminoiodane undergoes nitrene addition to the double bond to generate an aziridinium ion, which is ring-opened by nucleophilic attack of fluoride. Fluoride attacks the most-substituted carbon from the opposite face of the aziridinium.

Alternatively to the one-step aminofluorination of alkenes (Scheme **4.4**), oxidative single-atom difunctionalization of alkenes can give aziridines, epoxides or cyclopropanes as the final product.[31] Specifically, aziridination goes through formal nitrene addition to the double bond from an iminoiodane, which can be generated *in situ* or preformed outside. As mentioned before (Scheme **4.1**), the generated aziridine can be opened with fluorine to obtain a β-fluoroamine.

[31] Shetgaonkar, S.; Singh, F. V. *Arkivoc* **2020**, *4*, 0-0.

Aziridines are the smallest class of N-containing saturated heterocycles.[32] They are part of many important synthetic targets such as biologically active natural products,[33] pharmaceutical drugs,[34] chiral auxiliaries or catalysts ligands.[35]

The first studies in which the formation of an aziridine using HIR appeared in 1984, in the presence of an olefinic substrate using iminoiodane PhI=NTs and Fe or Mn catalysts[36] In 2005, Che and coworkers used a metal-free ArI(I)/*m*CPBA catalytic system to mediate the aziridination of activated alkenes.[37] Afterwards, many research groups have reported efficient and mild processes to obtain nitrene-mediated aziridines. The use of reagents like PhIO or PIDA are a staple in these transformations, granting excellent results with all types of alkenes.[38] Asymmetric aziridination procedures are well-known using quiral iodines.[39]

The intramolecular version of alkene aziridination using alkenyl amine derivatives has also been studied as a way to obtain N-containing

[32] a) Padwa, A. In *Comprehensive Heterocyclic Chemistry III*; Katrizky, A. R.; Ramsden, C. A.; Scriven, A. F. W.; Taylor, R. J. K.; Eds.; Elsevier: New York, USA, **2008**; Chap. *1*, pp. 1–104; b) *Aziridines and Epoxides in Organic Synthesis*; Yudin, A. K.; Ed.; Wiley-VCH: Weinheim, Germany, **2006**; c) Sabir, S.; Kumar, G.; Jat, J. L. *Asian J. Org. Chem.* **2017**, *6*, 782–793; d) Jarzyński, S.; Leśniak, S. *Chem. Heterocycl. Compd.* **2016**, *52*, 353–355; e) Degennaro, L.; Trinchera, P.; Luisi, R. *Chem. Rev.* **2014**, *114*, 7881–7929; f) Pellissier, H. *Adv. Synth. Catal.* **2014**, *356*, 1899–1935; g) Pellissier, H. *Tetrahedron* **2010**, *66*, 1509–1555; h) Singh, G. S.; D'hooghe, M.; De Kimpe, N. *Chem. Rev.* **2007**, *107*, 2080–2135.

[33] a) Ismail, F. M. D.; Levitsky, D. O.; Dembitsky, V. M. *Eur. J. Med. Chem.* **2009**, *44*, 3373–3387; b) Botuha, C.; Chemla, F.; Ferreira, F.; Pérez-Luna, A. In *Heterocycles in Natural Product Synthesis*; Majumdar, K. C.; Chattopadhyay, S. K.; Eds.; Wiley-VCH: Weinheim, Germany, **2011**; Part I, pp. 3–39.

[34] a) Singh, G. S. *Mini-Reviews in Med. Chem.* **2016**, *16*, 892–904; b) Fürmeier, S.; Metzger, J. O. *Eur. J. Org. Chem.* **2003**, 649–659.

[35] McCoull, W.; Davis, F. A. *Synthesis* **2000**, 1347–1365.

[36] Mansuy, D.; Mahy, J.; Dureault, A.; Bedi, G.; Battioni, P. *J. Am. Chem. Soc. Commun*. **1984**, *17*, 1161-1163.

[37] Li, J.; Hong Chan, P.W.; Che, C. *Org. Lett.* **2005**, *7*, 5801-5804.

[38] a) Evans, D. A.; Faul, M. M.; Bilodeau, M. T. *J. Org. Chem.* **1991**, *56*, 6744–6746; b) Krasnova, L. B.; Hili, R. M.; Chernoloz, O. V.; Yudin, A. K. *Arkivoc* **2004**, *2005*, 26–38; c) Watson, I. D. G.; Yu, L.; Yudin, A. K. *Acc. Chem. Res.* **2006**, *39*, 194-206.

[39] a) Degennaro, L.; Trinchera, P.; Luisi, R. *Chem. Rev.* **2014**, *114*, 7881–7929; b) Macara, J.; Caldeira, C.; Poeira, D. L. Marques, M. *Eur. J. Org. Chem.* **2023**, e202300109.

cycles.[40] Dienes can benefit from the intramolecular aziridination process, as sometimes regiocontrol is difficult to achieve. Substrates like dienyl carbamates are able to undergo aziridination exclusively to the double bond closer to the nitrogen. Our group described the oxyamination of dienyl carbamates as a synthetic approach for the preparation of *β*-aminoalcohol moieties.[11] Although the first aziridination assays were conducted in the presence of Rh(II) precursors, metal-free reaction using PhIO was able to aziridinate the double bond closer to the carbamate moiety regioselectively in excellent yield. Moreover, the resulting vinylaziridine proved more stable under the metal-free conditions. In the presence of $Rh(OAc)_2$, the obtained aziridine was immediately opened by one of the acetate ligands released during the transformation. Instead, metal-free conditions with PhIO yielded only the aziridine. The reaction was described to work via iminoiodane-mediated nitrene transfer.

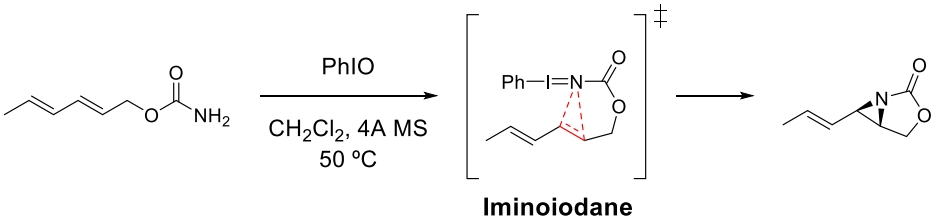

Scheme 4.16 General scheme of the aziridination of dienyl carbamates with PhIO.

The resulting bicyclic aziridine can be easily opened by many O-, S- and N-based nucleophiles via standard S_N2 pathway yielding an α-substituted oxazolidinone with *anti* configuration.

Inspired by these results, and observing the relevance of fluorine, and β-fluoroamines specifically, in medicinal chemistry, the ring-opening of these aziridines with fluoride as the nucleophile was considered.

[40] a) Hayashi, S. Yorimitsu, H.; Oshima, K. *Angew. Chem. Int. Ed.* **2009**, *48*, 7224 –7226; b) Dauban, P.; Dodd, R. H. *Org. Lett.* **2000**, *2*, 15, 2327-2329; c) Deng, H.; Wang, J.; Xu, Z.; Zhou, C.; Che, C. *Synthesis* **2011**, *18*, 2959–2967.

4.1.3. Aziridine Ring-Opening with Fluorine

Aziridine reactivity is driven by their highly strained ring structure (they present 60º bond angles instead of the commonly observed 109.5º for sp^3 hybridised atoms). This, combined with the electron-withdrawing nature of the nitrogen atom, makes aziridines prone to ring-opening reactions via C-N cleavage.[41] Thus, aziridines are versatile building blocks in organic synthesis as precursors of vicinal amines, amino-alcohols, amino acids, amino-sugars and various other valuable scaffolds.[42]

As mentioned before, the ring-opening of an aziridine with fluorine is possibly the most convenient route to access β-fluoroamines.[10] The use of HF as the nucleophilic fluorine source is ideal because it is generally cheap, available and requires mild conditions.[43] However, anhydrous HF (AHF) is an extremely hazardous chemical due to its low boiling point (19.5ºC) and high toxicity. Attempts at replacing HF with fluorine salts have been relatively unsuccessful because of the low solubility of these salts in organic solvents, and also due to the lower nucleophilicity of the fluoride ion in this form.

4.1.3.1. Complexes B·HF

HF reactivity can be controlled using complexes of the form B·HF, where B is usually an organic base or another form of H-bond accepting organic compound.[44] Organic bases make for good complexing agents because they form stable liquid solutions with HF. These complexes are liquid because the main bonding force is H-bonding, instead of Bronsted-

[41] a) Lu, P. *Tetrahedron* **2010**, *66*, 2549–2560; b) Stanković, S.; D'hooghe, M.; Catak, S.; Eum, H.; Waroquier, M.;Van Speybroeck, V.; De Kimpe, N.; Ha, H. J. *Chem. Soc. Rev.* **2012**, *41*, 643–665;

[42] a) Darses, B.; Rodrigues, R.; Neuville, L.; Mazurais, M.; Dauban, P. *Chem. Commun.* **2017**, *53*, 493–508; b) Dodd, R. H. *Molecules* **2000**, *5*, 293–298.

[43] Jeong, J. U.; Tao, R.; Sagasser, I.; Henniges, H.; Sharpless, K. B. *J. Am. Chem. Soc.* **1998**, *120*, 6844–6845.

[44] a) Hirschmann, R. F.; Miller, R.; Wood, J.; Jones, R. E. *J. Am. Soc. Chem.* **1956**, *78*, 19, 4956–4959; b) Liang, S.; Hammond, G. B.; Xu, B. *Chem. Eur. J.* **2017**, *23*, 17850–17861; c) Remete, A. M.; Kiss, L. *Eur. J. Org. Chem.* **2019**, 5574–5602.

type acid-base interactions. It was demonstrated that varying the nature of the Lewis base and the stoichiometric amount of HF, a different range of properties can be achieved.[45] The most used complexes are Py·HF (also called Olah's reagent[46]), Et_3N·HF and, more recently, DMPU·HF.

Nitrogenated bases like triethylamine and pyridine can alter the outcome of a fluorination reaction. One the one hand, they may interfere with the reactions by reducing the acidity of reaction system. On the other hand, they could strongly complex with many transition-metal catalysts and hamper their catalytic activity. Hammond and Xu, in search of an HF complexing agent, contemplated multiple organic molecules with strong H-bond acceptor attributes and low basicity. Finally, they proposed DMPU as an ideal complexing agent for HF.[47]

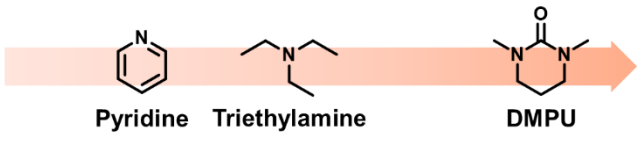

	Pyridine	Triethylamine	DMPU
H-bond Acceptor Capacity (pK_{BHX})	1.86	1.98	2.82
Basicity (pK_{BH+})	10.7	5.2	< 0

Figure 4.2. Comparison of properties of triethylamine, pyridine and DMPU as candidate complexing agents for HF.

DMPU is inexpensive and readily available. More important, DMPU is a better hydrogen-bond acceptor than pyridine and Et_3N and at same time is much less basic (Figure **4.2**) based on the pK_{BHX}[48] and pK_{BH+} parameters. Thus, the DMPU·HF complex should have higher acidity than

[45] Yoneda, N. *Tetrahedron* **1991**, *47*, 5329-5365.
[46] Olah, G. A.; Welch, J. T.; Vankar, Y. D.; Nojima, M.; Kerekes, I.; Olah, J. A. *J. Org. Chem.* **1979**, *44*, 3872–3881.
[47] Okoromoba, O. E.; Han, J.; Hammond, G. B.; Xu, B. *J. Am. Chem. Soc.* **2014**, *136*, 14381-14384.
[48] Laurence, C.; Brameld, K. A.; Graton, J.; Questel, J.; Renault, E. *J. Med. Chem.* **2009**, *52*, 14, 4073–4086.

the Py·HF and Et_3N·HF complexes. Also, DMPU is weakly coordinating to most metal catalysts, so it is unlikely to interfere strongly with most transition-metal catalysts. Finally, DMPU is a very weak nucleophile, so it will not compete with HF in nucleophilic reactions.

4.1.3.2. Aziridine Ring-Opening with B·HF Complexes

The aperture of aziridines with fluorine has been traditionally achieved with Py·HF.[49] Et_3N·HF was reported in 2014 as an aziridine ring-opening reagent as a milder HF complex.[50] The ring-opening of aziridines can lead to different isomers depending on the nucleophile and the aziridine. Stereoselectivity control has proven specially challenging when using HF complexes. Regarding regioselectivity, fluoride usually attacks the least substituted position of the aziridine as in traditional S_N2. When vicinal aryl fragments are present, they stabilize a carbocation, enhancing the electrophilicity of this benzylic position. This carbocation redirects the incoming fluorine to the more substituted position.[51]

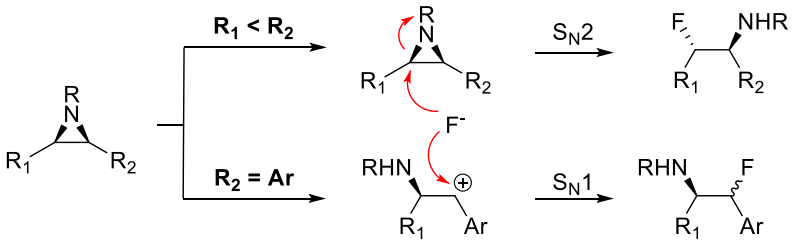

Scheme 4.17 Rationale for the obtained selectivity with Py·HF and Et_3N·HF in the ring-opening of aziridines.

[49] a) Hamatani, T.; Matsubara, S.; Matsuda, H.; Schlosser, M. *Tetrahedron* **1988**, *44*, 2875–2881; b) McNally, A.; Haffemayer, B.; Collins, B. S. L.; Gaunt, M. J. *Nature* **2014**, *510*, 129–133; c) Molnár, I. G.; Tanzer, E. M.; Daniliuc, C.;Gilmour, R. *Chem. Eur. J.* **2014**, *20*, 794–800; d) Nappi, M.; He, C.; Whitehurst, W. G.; Chappell, B. G. N.; Gaunt, M. J. *Angew. Chem. Int. Ed.* **2018**, *57*, 3178–3182.

[50] Park, H.; Yoon, D. H.; Ha, H. J.; Son, S. I.; Lee, W. K. *Bull. Korean Chem. Soc.* **2014**, *35*, 699–700.

[51] Li, J.; Huang, W.; Chen, J.; He, L.; Cheng, X.; Li, G. *Angew. Chem. Int. Ed.* **2018**, *57*, 5695–5698.

Okoromoba *et al.* studied the ring-opening of tosylaziridines with DMPU·HF. Diastereoselectivities obtained with this reagent shows more S_N1 character and improved yield with all aziridines compared to other B·HF reagents. When the reaction was performed with an enantiopure aziridine, the resulting fluoroamine was obtained with complete retention of configuration. This result rules out the formation of a carbocation as an intermediate species. Instead, the most plausible intermediate is depicted below.

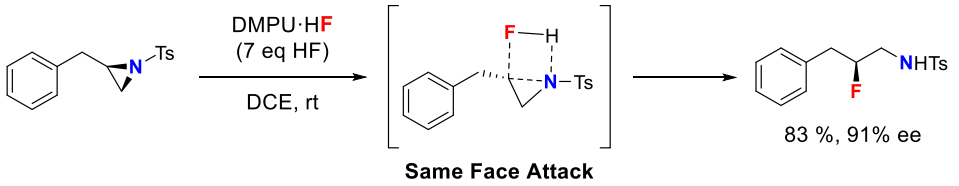

Scheme 4.18 Proposed mechanism for the ring-opening of tosylaziridines with DMPU·HF through H-bond mediated *syn* fluoride delivery.

The described mechanism contains the activation of the aziridine via protonation, followed by same-face attack of the fluoride. The activation step is in agreement with the poorer results of Et_3N·HF and Py·HF, as they are more basic reagents and are not able to protonate the aziridine.

4.2. Objectives

The ultimate aim of the project related to this chapter is to give access to a facile synthesis of β-fluoroamine scaffolds towards the preparation of fluorinated sphingosine analogues. The envisioned route entails the use of dienyl carbamates as the starting substrates, which can be transformed to β-fluorooxazolidinones via intramolecular aminofluorination upon oxidation with a I(III) reagent and fluorination with an external source of fluorine.

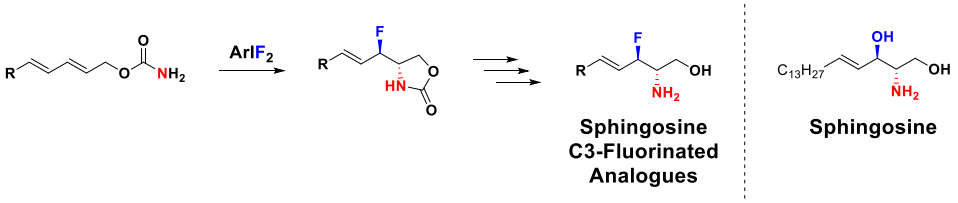

Scheme 4.19 Synthesis of sphingosine analogues fluorinated at C3 starting from a dienyl carbamate.

To this purpose, the feasibility of the reaction will be first explored using model allyl substrates. The principal objective of this chapter is to gain insight in the mechanism of the aminofluorination of allyl carbamates using hypervalent iodine reagents. Three different strategies have been envisioned for this transformation (Scheme **4.20**):

1. Tandem aminofluorination of allyl carbamates using **TolIF$_2$**, an easy-access tandem oxidation and fluorination reagent.
2. Tandem aminofluorination of allyl carbamates using *in situ* prepared ArIF$_2$ from an **Ar-I(III)**-type precursor and a **fluorine source**.
3. Sequential aminofluorination: I(III)-mediated intramolecular aziridination of allyl carbamates followed by **ring-opening of** the corresponding **aziridines with B·HF complexes**. The aziridination step has already been studied in our group[11], so the ring-opening step with fluorine will be the main focus of the strategy.

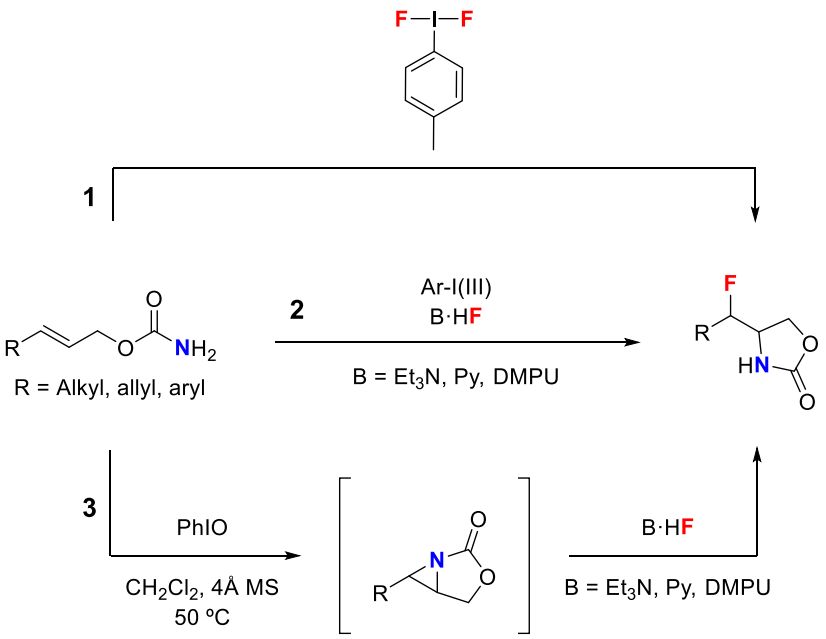

Scheme 4.20 General scheme of the three selected strategies for the aminofluorination of allyl carbamates.

The scope and the stereoselectivity of the reactions will be explored (Scheme **4.21**). In order to achieve this goal, several aspects will be studied:

- Optimisation of the reaction conditions with a model cinnamyl carbamate.
- Detection of possible intermediates by NMR spectroscopy.
- Effect of the substitution of the nitrogen in the carbamate group (R') in the interaction between the hypervalent iodine and the carbamate nitrogen.
- Substitution in the aromatic ring (R) of cinnamyl carbamates to assess the effect of the electronic density of the double bond in the transformation.
- Effect of the *cis/trans* configuration of the double bond on the final selectivity outcome of the reaction.

- Use of allyl carbamates bearing alkyl groups to test the role of a secondary electronic unit in the allyl carbamate in the interaction between $TolIF_2$ and the carbamate.

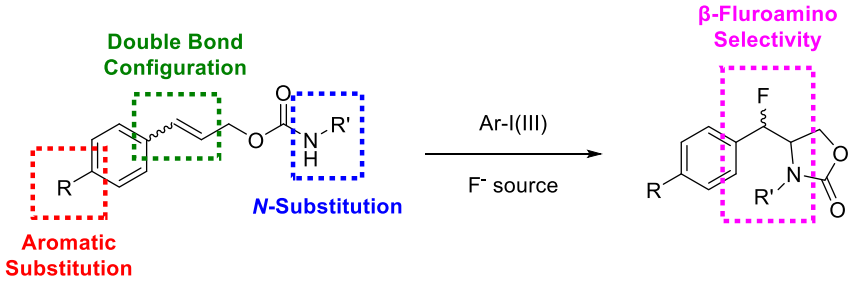

Scheme 4.21 General scheme of the aminofluorination of cinnamyl carbamate. In boxes, the main parameters studied in this chapter.

Finally, the best aminofluorination conditions will be applied to dienyl carbamates as a first step towards the access to C-3 fluorinated sphingosine analogues.

4.3. Results and Discussion

As mentioned in the objectives, the main goal of this chapter is to explore the aminofluorination of dienyl carbamates. The structure of a dienyl carbamate allows for the regioselective aziridination at the proximal alkene to give a vinyl β-F-oxazolidinone product. However, a weak nucleophile like fluorine is expected to give regioselectivity issues due to possible conjugate addition to the second alkene.

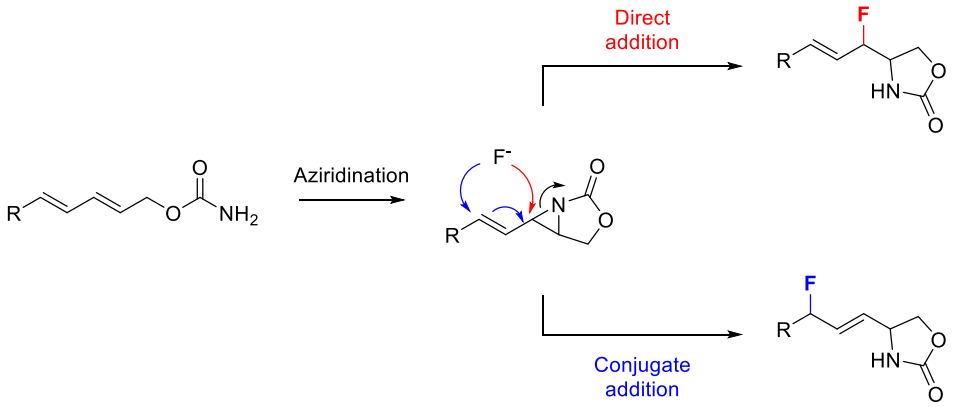

Scheme 4.22 Regioselectivity issues arising from the use of dienyl carbamates.

To circumvent this problem, cinnamyl carbamates were identified as simple model substrates of the more complex dienyl carbamates for the optimization of the reaction conditions, as the aryl group.

4.3.1. Synthesis of cinnamyl carbamates

To the purpose of studying the scope and stereoselectivity of the aminofluorination of allyl carbamates, a library of substrates was envisioned as starting materials.

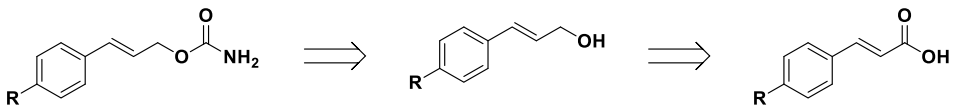

Scheme 4.23 Retrosynthetic analysis of the preparation of cinnamyl acids.

Cinnamyl carbamates can be prepared from the corresponding cinnamyl alcohols, which in turn can be reduced from the commercially available cinnamic acids (Scheme **4.23**).[52,53]

4.3.1.1. Preparation of Cinnamyl Alcohols

The reduction of carboxylic acids with methyl chloroformate goes through the formation of a transient acyl carbonate that facilitates the subsequent regioselective reduction using $NaBH_4$/MeOH. Despite obtaining small amounts of the saturated alcohol, cinnamyl alcohols **4.17**-**4.22** were obtained in 40-80% yield as white solids.

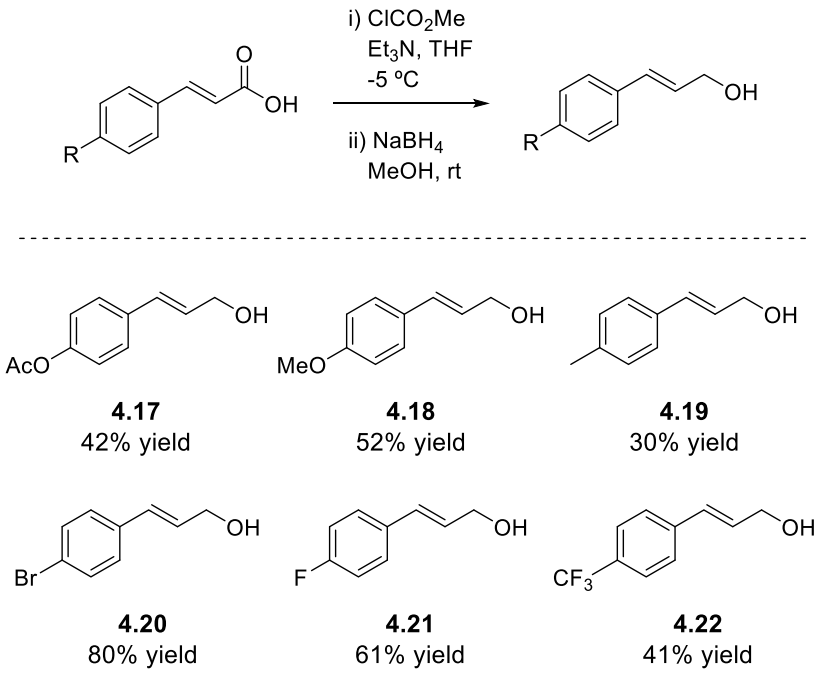

Scheme 4.24 Structure and yield of the cinnamyl alcohols prepared with this procedure.

Ciano-substituted cinnamyl alcohol **4.25** was not eligible for this synthesis since the reduction with sodium borohydride reduces the nitrile

[52] Krätzschmar, F.; Kabel, M.; Delony, D.; Breder, A. *Chem. Eur. J.* **2015**, *21*, 7030-7034.
[53] Espino, C. G.; Du Bois, J. *Angew. Chem. Int. Ed.* **2001**, *40*, 598-600.

group first. Fortunately, the preparation of *p*-cyanocinnamyl alcohol was already reported in the literature through another procedure.[54]

Thus, Sonogashira coupling between *p*-cyanoiodobenzene **4.23** and propargyl alcohol furnished the conjugated phenyl propargyl alcohol **4.25** in good yield (Scheme **4.25**).[54a] However, the partial reduction of the triple bond to the *trans* double bond using $LiAlH_4$ did not lead to the desired product, despite the authors reporting this transformation in excellent yield. Instead, the only obtained alcohol contained a formyl group in the *para* position, arising from partial reduction of the nitrile group and subsequent hydrolysis of the imine.

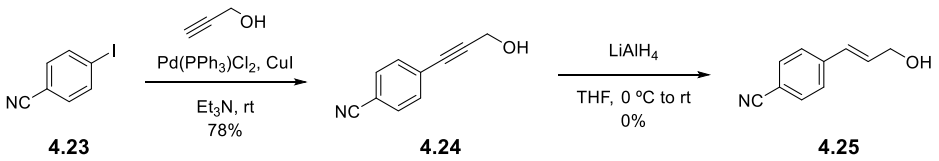

Scheme 4.25 Synthetic route for the first strategy towards the ciano-substituted cinnamyl alcohol.

An alternative approach for the synthesis of **4.25** consisted in the construction of the double bond through an olefination reaction.[54b] First, a Wittig reaction with commercially available *p*-cyanobenzaldehyde **4.26** and (formylmethylene)triphenylphosphorane yielded the *trans* aldehyde **4.27** with complete stereoselectivity. This reaction is reported at 120 ºC under microwave irradiation, but after 24 h at room temperature the reaction proceeded with excellent yield without microwave assistance. Aldehyde **4.27** was then reduced to primary alcohol **4.25** via Luche reduction with sodium borohydride. Cerium chloride heptahydrate directs the 1,2-regioselective reduction of α,β-unsaturated ketones and aldehydes to primary allyl alcohols, which serves our system well.[55]

[54] a) Bin Xu, B.; Gartman, J. A.; Tambar, U. K. *Tetrahedron* **2017**, *73*, 4150-4159; b) Craig, D.; Slavov, N. K. *Chem. Com.* **2008**, 6054–6056.
[55] Louche, J. L. *J. Am. Chem. Soc.* **1978**, *100*, 7, 2226–2227.

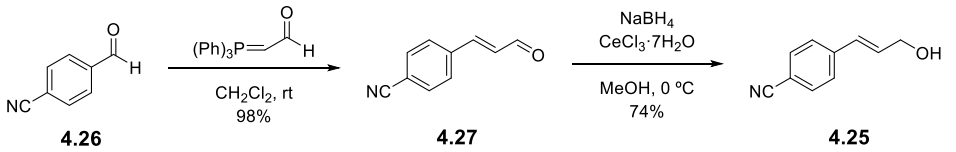

Scheme 4.26 Synthetic route for the preparation of *p*-CN-substituted cinnamyl alcohol **4.25**.

The preparation of *cis* cinnamyl alcohol **4.30** proceeded by a *one-pot* Pt-catalysed protosilylation/deprotection starting from the commercially available phenyl propargyl alcohol **4.28** (Scheme **4.27**).

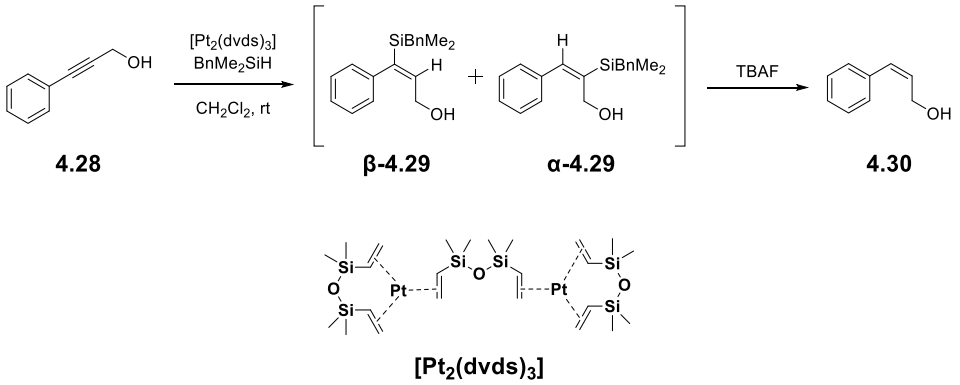

Scheme 4.27 Synthetic route for the preparation of *cis*-phenyl allyl alcohol.

Platinum catalysis ensures that addition of Si and H to the triple bond takes place on the same face, leading to the desired *cis* configuration (Scheme **4.28**). Regioisomers **α-4.29** and **β-4.29** are formed, but when they are treated with TBAF they both converge into alcohol **4.30**. Platinum(0)-1,3-divinyl-1,1,3,3-tetramethyldisiloxane ($[Pt_2(dvds)_3]$), also known as Karstedt's catalyst, is described to work better than the traditional platinum(II) chloride ($PtCl_2$) for the protosilylation of alkynes featuring a propargyl alcohol.[56] The formation of HCl as a subproduct of the protosilylation with $PtCl_2$ leads to formation of multiple subproducts resulting in a major decrease in yield and complex purification. HCl

[56] Rooke, D. A.; Ferreira, E. M. *Angew. Chem. Int. Ed.* **2012**, *51*, 3225–3230.

formation may also be circumvented by protecting the alcohol, although in synthetic processes it is usually preferred to avoid extra steps and use $[Pt_2(dvds)_3]$.

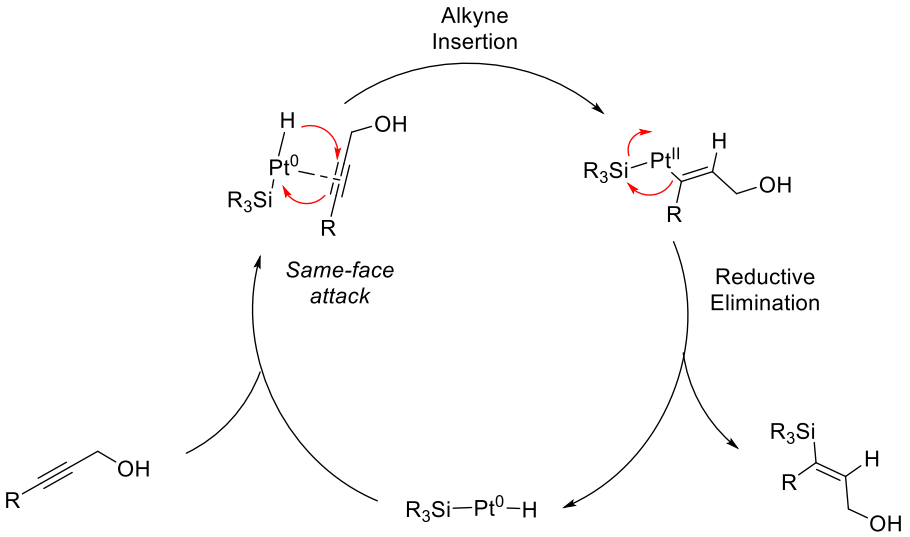

Scheme 4.28 Mechanism of the protosililation of propargyl alcohols to silyl *cis*-allyl alcohols.

All cinnamyl alcohols were submitted to carbamoylation to obtain the respective carbamates, which will serve as the model substrates for this thesis.

4.3.1.2. Carbamoylation of Cinnamyl Alcohols to Carbamates

Alcohols are easily converted to simple carbamates with a two-step process (Scheme **4.29**). The same procedure was applied to all the alcohols prepared in the last section.

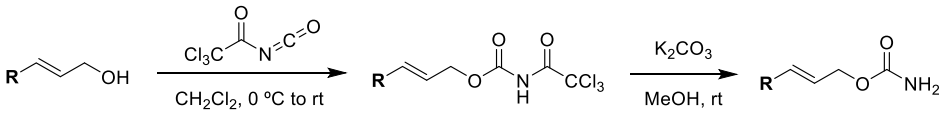

Scheme 4.29 General procedure for the carbamoylation and methanolysis of cinnamyl alcohols to carbamates.

Carbamoylation takes place by slow addition of trichloroacetyl isocyanate (TAI) to a solution of the corresponding alcohol in dry CH_2Cl_2 to render an imido carboxylate intermediate that is subsequently submitted to methanolysis.[53,57] The final carbamate is purified by column chromatography and recrystallized by slow diffusion of pentane into a quasi-saturated solution of carbamate in THF, obtaining white solids in 60-90% yield. Non-cinnamyl carbamates were also prepared using this procedure with similar results.

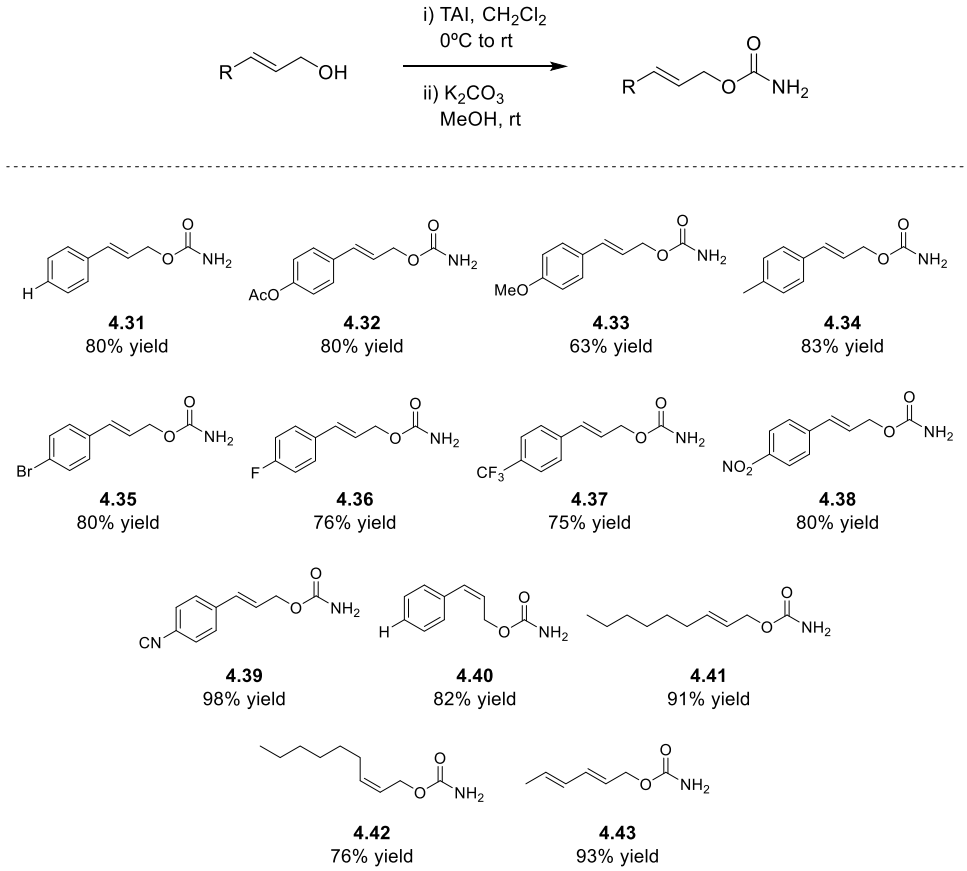

Scheme 4.30 Structure and yield of the carbamates prepared via carbamoylation and methanolysis.

[57] Kočovský, P. *Tetrahedron Letters*, **1986**, *27*, 5521–5524.

The carbamate is apparently pure by ^{1}H and ^{13}C-NMR after column chromatography. However, in the first tests performed in our group involving PhIO-mediated aziridination, non-recrystallized substrates led to non-reproducible results leading to variable but often significant amounts of a chlorinated byproduct, possibly arising from a chlorine-containing impurity non-detectable by NMR. Therefore, recrystallisation of carbamates is a crucial step in their purification.

4.3.1.3. Carbamoylation of Cinnamyl Alcohols to N-substituted Carbamates

Carbamates protected with tosyl (Ts) and benzyl (Bn) groups were prepared in order to study the effect of the acidity and the substitution of the nitrogen in the carbamate group towards aminofluorination (Scheme **4.31**). The procedure is very similar to the carbamoylation to obtain simple carbamates. In this case, tosyl or benzyl isocyanate are used instead of TAI, rendering the protected carbamate directly without methanolysis.

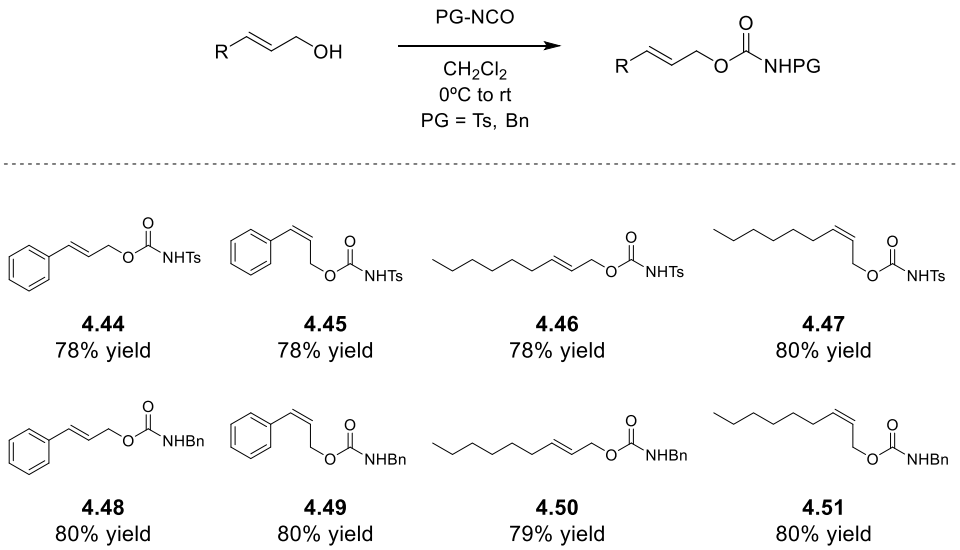

Scheme 4.31 Structure and yield of the protected carbamates prepared via carbamoylation and methanolysis procedure.

4.3.2. Strategy #1: One-pot Aminofluorination of Allyl Carbamates with TolIF$_2$

The aminofluorination of olefins is a very interesting strategy for the preparation of scaffolds containing neighbouring N and F moieties. In this line, allylic carbamates can be relevant substrates for the intramolecular aminofluorination, leading to 1-amino-2-fluoro-3-oxy fragments. As explained in the introduction, aminofluorination of olefins using hypervalent iodine can be carried out in different ways.

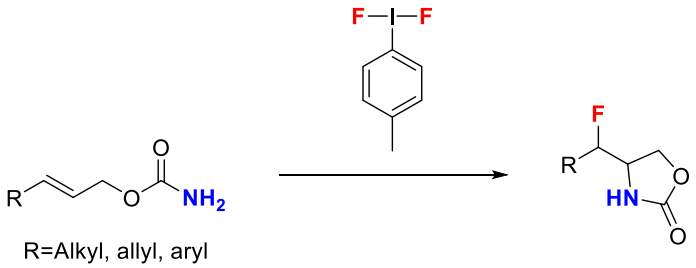

Scheme 4.32 *One-pot* aminofluorination of allyl carbamates with TolIF$_2$.

The route presented here is focused on the use of TolIF$_2$ for the one-step aminofluorination of allyl carbamates to furnish β-F-oxazolidinones in a straightforward manner (Scheme **4.32**). TolIF$_2$ is a relatively stable compound that can be prepared, purified and isolated with great purity as a yellowish solid. Because it is air and photo sensible, it must be stored in the freezer at -32 ºC, in the dark and under Ar atmosphere. It can be kept for several months without sensible decomposition.

TolIF$_2$ was prepared following a procedure described by Murphy and Tao.[58] This procedure allows for the synthesis of pure TolIF$_2$ in the multigram scale, which can be stored in the freezer under argon atmosphere without decomposing.

[58] Tao, J.; Murphy, G. K. *Synthesis*, **2019**, *51*, 3055-3057.

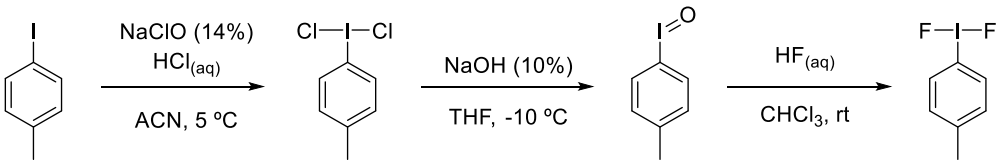

Scheme 4.33 Synthesis of TolIF$_2$ according to the procedure of Murphy and Tao.

The method consists of a three-step synthesis (Scheme **4.33**). The first step is the chlorination of 1-iodo-4-methylbenzene (TolI) using sodium hypochlorite and hydrochloric acid, generating chlorine gas *in situ*. Chlorine oxidizes TolI into the hypervalent dichloroiodotoluene (TolICl$_2$). Subsequently, TolICl$_2$ is filtered and hydrolyzed with sodium hydroxide to obtain polymeric iodosotoluene.

Finally, the solid iodane crude is filtered again and fluorinated with aqueous HF to produce TolIF$_2$, which is separated from the aqueous phase with chloroform and subsequently precipitated with hexane. After partial evaporation of the solvent with air current, the product is decanted and obtained pure as a pale-yellow solid (purity may fluctuate but it is always >95%). 65% overall yield was obtained consistently with no purification between steps. The solid is collected in polyethylene (PE) tubes, sealed with a septum under Ar atmosphere, covered with aluminium foil, and stored in the freeze (-32 ºC).

Alternatively, to avoid the preparation and potentially troublesome storage of pure TolIF$_2$, it can be freshly prepared and added to the reaction mixture without isolating/purifying it.

TolI can be oxidized in *one-pot* with Selectfluor and fluorinated with Et$_3$N·HF, obtaining TolIF$_2$.[59,60,61] The product is extracted from the reaction with a mixture of hexane/CHCl$_3$ 3:1 and transferred to another

[59] Sarie, J. C.; Thiehoff, C.; Mudd, R. J.; Daniliuc, C. G.; Kehr, G.; Gilmour, R. *J. Org. Chem.* **2017**, *82*, 11792-11796.
[60] Molnár, I. G.; Gilmour, R. *J. Am. Chem. Soc.* **2016**, *138*, 5004−5007.
[61] Meyer, S.; Häfliger, J.; Schäfer, M.; Molloy, J. J.; Daniliuc, C. G.; Gilmour, R. *Angew. Chem. Int. Ed.* **2021**, *60*, 6430–6434.

Schlenk, where the solvent is evaporated under high vacuum (Figure **4.3**). TolIF$_2$ is obtained as an off-white solid. When obtained in this way, TolIF$_2$ is usually transferred in solution and added to the reaction mixture. From this point, TolIF$_2$ obtained in this manner will be referred to as "[TolIF$_2$]" to easily differentiate it from proper isolated "TolIF$_2$".

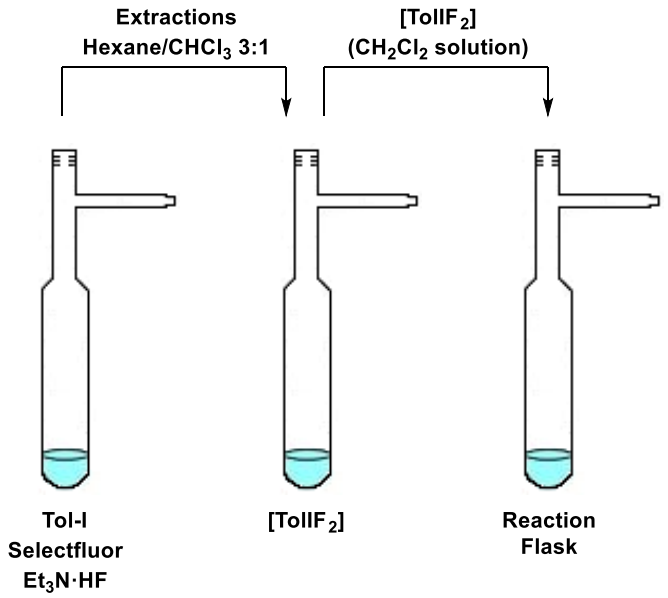

Figure 4.3. Procedure of the preparation and usage of [TolIF$_2$].

For this thesis, both TolIF$_2$ and [TolIF$_2$] are considered for the aminofluorination of allyl carbamates. The most effective method will be chosen for the rest of the study.

The formation of [TolIF$_2$] is described to proceed in 80% conversion using Et$_3$N·HF after 22 h.[59] The rest is TolI, which means that [TolIF$_2$] can be used without further purification. The use of more powerful HF sources like Py·HF or DMPU·HF might improve this result, so the reaction was also tested with the two complexes. Unfortunately, DMPU·HF yielded 58% conversion to TolIF$_2$ and Py·HF a mere 17% conversion. These values are quite approximate because the resolution of the NMR spectra was low due

to the presence of solids in the mixture, but enough to see a difference between the three complexes.

The formation of $TolIF_2$ was tested using 3.5 and 10 equiv. of HF and using Et_3N and DMPU as complexing agents for HF. Py·HF was discarded because in the first test it showed substantially lower conversion rate than the other two complexes. DMPU·HF and Et_3N·HF were expected to function in a similar manner. Reaction was followed by ^1H and ^{19}F-NMR. This reaction was studied by Gilmour *et al.* with Et_3N·HF as the F source.[59] They speculated that the reaction proceeds through an intermediate complex between the reduced product arising from Selectfluor (**4.52**) and monofluorinated iodonium (III) toluene (**4.53**) during the oxidation of TolI.

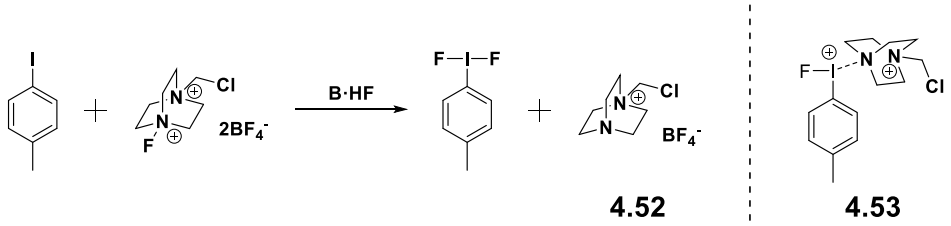

Scheme 4.34 Structure of the possible species detected during NMR studies of the formation of $TolIF_2$ in Gilmour experiments: The reduced subproduct of Selectfluor (**4.52**) and the hypothesised intermediate (**4.53**).

Reaction with Et_3N·HF (3.5 equiv. of HF) yielded $TolIF_2$ in 81% conversion (Figure **4.4**, bottom). Intermediate complex **4.53** signals were observed. In fact, as the reaction advanced, the signals corresponding to **4.52** (Figure **4.4**, spectrum **1**, top) slowly shifted downfield until after 24h conversion plateaued, and the signals stabilised to look very similar to those of **4.53** (Figure **4.4**, spectrum **6**, top).

However, ^{19}F-NMR showed only $TolIF_2$ and BF_4^{2-} peaks. These results contradict the possible formation of **4.53**. Given that the two multiplets around 3.5 ppm are observed even in the latest spectra, that $TolIF_2$ formation is very high and that there are no other signals detected in the ^{19}F-NMR spectra, the shifting signals would not seem to correspond to any

species containing fluorine or any aryl iodine(III) species. Indeed, they could correspond to a species similar to **4.52**. When using 11 equiv of HF, spectra are comparable, but conversion to $TolIF_2$ increases to 94%.

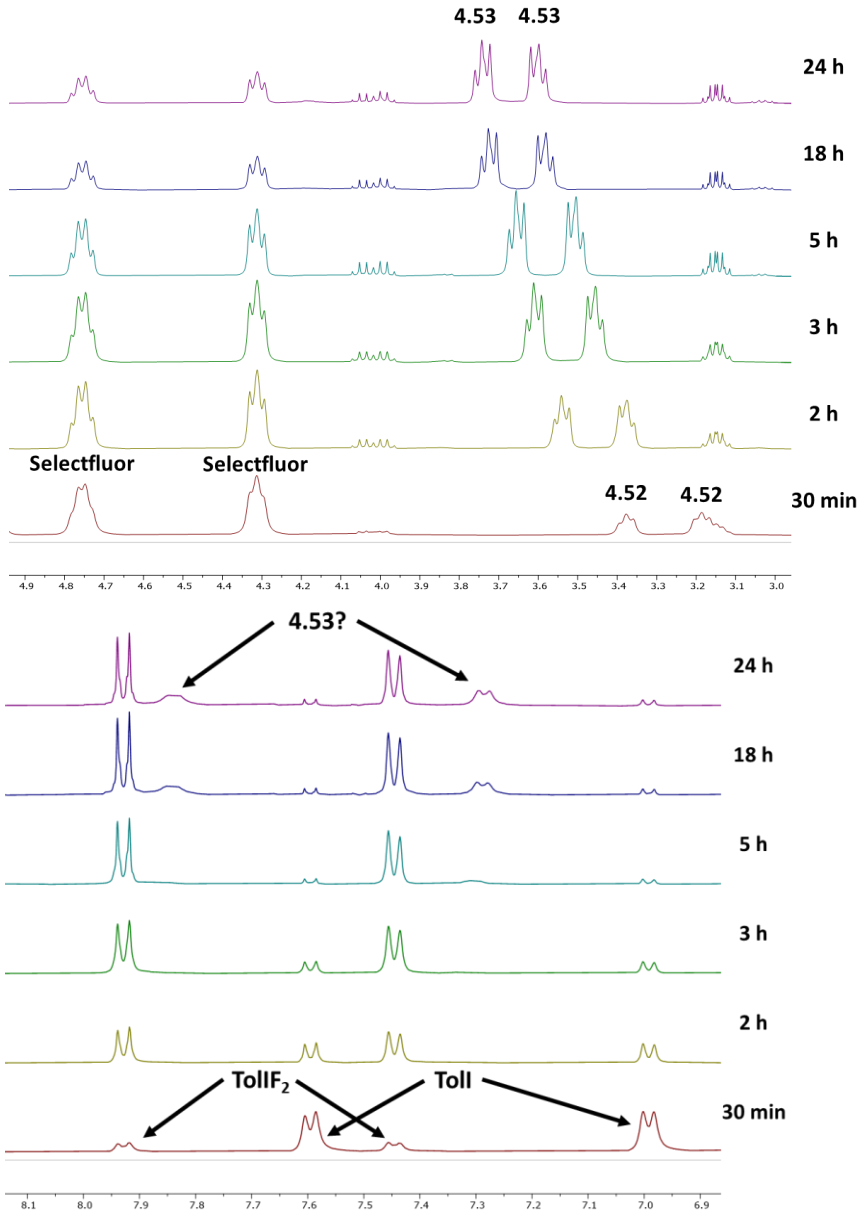

Figure 4.4. ^{1}H-NMR study of the formation of $TolIF_2$ with Selectfluor and $Et_3N{\cdot}HF$ (3.5 eq HF). Ampliations of the apliphatic (top) and the aromatic (bottom) zones.

The slight increase in chemical shift can be produced by the increasing concentration of H^+ in the medium as fluorine is incorporated to TolI, giving rise to the formation of an ammonium ion species like **4.54**.

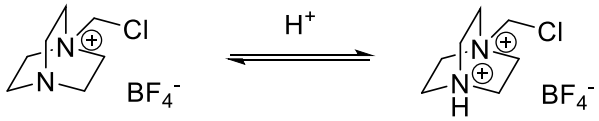

4.52 **4.54**

Scheme 4.35 Structure of the reduced byproduct of Selectfluor (**4.52**) and its protonated ammonium ion (**4.54**).

DMPU·HF experiments with 3.5 equiv of HF showed the undescribed intermediate from the beginning. Like in the Et_3N·HF experiment, signals go downfield as reaction advances, but with higher shifts. This time, suspicious signals appear in the aromatic area, which could indicate **4.53** (Figure **4.5**). Nonetheless, species **4.52** was never observed. Stronger interactions are expected with DMPU·HF because of the more acidic nature of the complex, so deshielded signals make sense conveying the formation of protonated species **4.54**. $TolIF_2$ was observed in low conversion during the first 4 h of the experiment together with **4.53**. After leaving the reaction overnight, $TolIF_2$ was no longer detectable and only signals of **4.53** were observed in the aromatic region. ^{19}F-NMR showed a big peak of $TolIF_2$ in the first measure, which slowly decreased as the reaction progressed. Indeed, the $TolIF_2$ signal was much weaker after being left overnight.

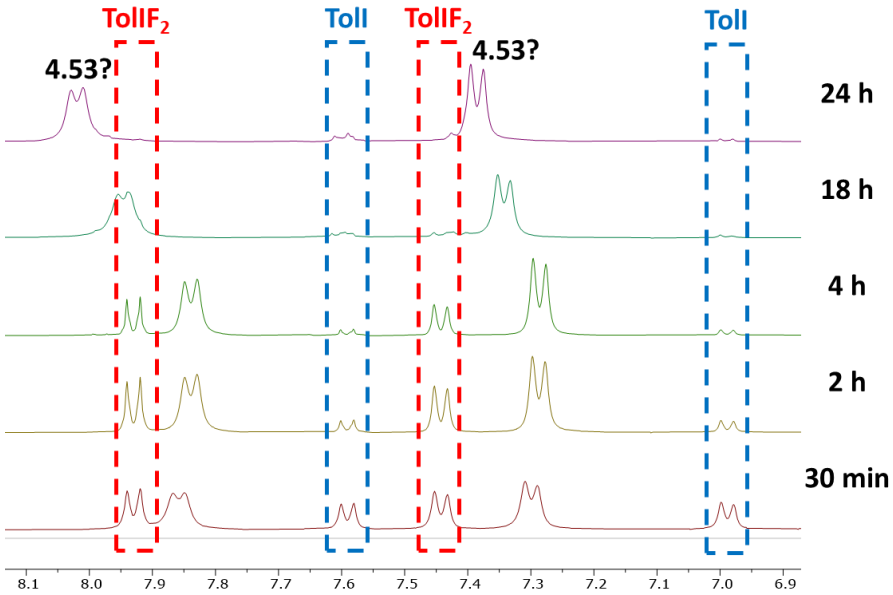

Figure 4.5. ^{1}H-NMR study of TolIF$_2$ formation with Selectfluor and DMPU·HF (3.5 equiv HF).

In contrast to Et$_3$N·HF, the equivalents of the reagent showed an impact on the reaction evolution. When 11 equiv were used, the very last shifts achieved with 3.5 equiv were observed from the first measure (Figure **4.5**, Top) and at all times. Therefore, intermediate **4.53** seems to form when an excess of HF is present. No TolIF$_2$ is observed at any point with 11 equiv of HF. Given these results, Et$_3$N·HF complex was identified as the preferred fluorine source for the preparation of [TolIF$_2$].

4.3.2.1. Method comparison: TolIF$_2$ vs. [TolIF$_2$]

Both methods are expected to yield the desired product with high and very similar purity. Nevertheless, each method has its advantages and drawbacks, and the better method must be decided prior to aminofluorination studies. They were tested for the aminofluorination of cinnamyl carbamate **4.31**. In both cases, a Schlenk with activated 4Å MS, dry CH_2Cl_2 and carbamate was prepared, and the TolIF$_2$ was added to the

mixture. Therefore, any disparity in the outcome of the reaction might be then solely attributed to the iodane.

Table 4.1. Comparison of the two proposed methodologies for the formation of $TolIF_2$ towards the aminofluorination of allyl carbamates using cinnamyl carbamate as model substrate.

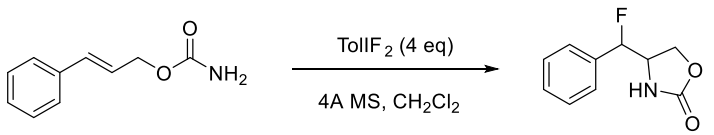

4.31 **4.55**

Entry	Method[a]	T (ºC)	Time	Yield (%)[b]	dr (*anti*/*syn*)[c]
1	$TolIF_2$	50	22 h	63	14:86
2	$[TolIF_2]$[d]	50	6 h	65	27:73

[a]Typical conditions: $TolIF_2$ = **4.31** (0.29 mmol, 50.0 mg), $TolIF_2$ (4 equiv), 4Å MS (100 mg, 1g/mmol of carbamate), CH_2Cl_2 (2.5 mL, 0.04 M). [b]Isolated yield. [c]Calculated by ^{19}F-NMR. [d] [TolIF2] = i) TolI (5 equiv, 92 mg), Selectfluor (18 equiv, 560 mg), $Et_3N{\cdot}HF$ (11 equiv of HF, 0.3 mL), ACN (11 mL); ii) **4.31** (1 equiv, 17.5 mg), CH_2Cl_2 (2.3 mL, 0.04 M), 4Å MS (100 mg, 1g/mmol of carbamate).

Surprisingly, both procedures yielded slightly distinct outcomes. Complete conversion of the starting carbamate was observed in both cases, and the yield of F-oxazolidinone **4.55** was similar. $[TolIF_2]$ achieved full conversion after six hours, while $TolIF_2$ required a longer reaction time (22h). Moreover, both reactions furnished F-oxazolidinone **4.55** as *anti*/*syn* diasteromeric mixtures, with preferential formation of the *syn* isomer. The reaction using pure $TolIF_2$ resulted more stereoselective than the $[TolIF_2]$ reaction. The *syn* selectivity was somewhat unexpected because ring-opening of imislar vinyl aziridines in our group with O, N and S-based nucleophiles showed complete *anti* selectivity.

Seeing the difference between both experiments, we sought to identify any differences between the two forms of $TolIF_2$. Isolated $TolIF_2$ is well characterised and there is no major impurity detectable by NMR. Therefore, the extracted $[TolIF_2]$ was analysed by NMR to check for any

sub-products. A small residue of TolI was observed (<5%). A second pair of signals in the same region appears in a similar amount slightly downfield, reminiscent of **4.53** (Figure **4.4**). Although this species is present in small amounts, it could be sufficient to affect the results of the aminofluorination.

A similar experiment was carried out by Shreeve et al.[62] to test the difference in reactivity of $TolIF_2$ and [$TolIF_2$] using 1,1-diphenylethene as a model substrate. $TolIF_2$ gave a difluorination rearranged product, but [$TolIF_2$] yielded a rearranged ketone as the major product. This outcome led to speculation that residual traces of Selectfluor might have caused the formation of the ketone rather than the intended difluorination product.

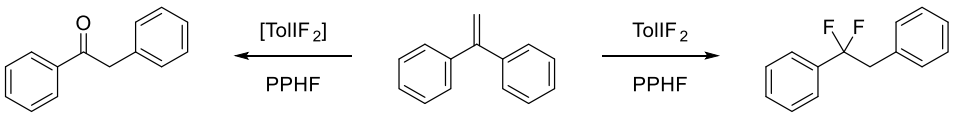

Scheme 4.36 Experiments to assess the difference in reactivity of $TolIF_2$ depending on the preparation method with 1,1-diphenylethene.

Despite the results of the aminofluorination being more similar than those of 1,1-diphenylethene, it is plausible that the small amount of unknown subproduct affects the outcome of the reaction.

With all the information in hand, it was decided that using isolated difluoroiodotoluene was the better way to carry out the reaction, despite the longer reaction time. The preparation of freshly obtained [$TolIF_2$] rendered the experiments more unpractical and difficult to reproduce.

[62] Ye, C.; Twamley, B.; Shreeve, J. M. *Org. Lett.* **2005**, *18*, 7, 3962

4.3.2.2. Optimization of the Reaction Conditions

Cinnamyl carbamate **4.31** was chosen as the model substrate for the aminofluorination of allyl carbamates. Therefore, a scope of reaction conditions was performed with this substrate to achieve the best conditions before carrying on to other substrates.

Table 4.2. Optimisation experiments for the aminofluorination of cinnamyl carbamate with $TolIF_2$.

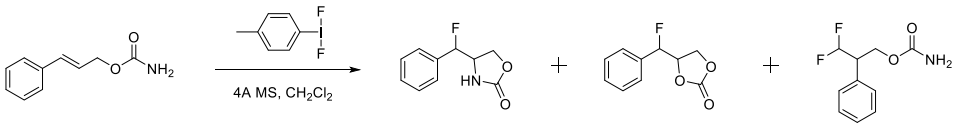

4.31 **4.55** **4.56** **4.57**

Entry	$TolIF_2$ eq$^-$	Additive	HF eq	Conc[a] (M)	T (°C)	Time	Yield (%)[b]		
							4.55[c]	4.56	4.57
1	2	-	0	0.1	rt	5d	-	-	-
2	2	-	0	0.1	50	40h	45 (55:45)	2	-
3	2	-	0	0.04	50	48h	42 (16:84)	-	-
4	4	-	0	0.1	rt	5d	-	-	-
5	4	-	0	0.1	50	40h	38 (45:55)	6	-
6	4	-	0	0.04	50	22h	67 (14:86)	-	-
7	4	-	0	0.04	80	8h	62 (8:92)	-	-
8	**4**	**-**	**0**	**0.04**	**100**	**6h**	**64 (3:97)**	**-**	**-**
9[d]	4	-	0	0.04	100	5h	53 (53:47)	-	-
10	2	DMPU·HF	10	0.1	rt	4d	-	11	5
11	4	DMPU·HF	50	0.1	50	5d	-	-	-
12	4	Py·HF	10	0.04	50	6d	8 (17:83)	-	-

Typical conditions: **4.31** (0.29 mmol, 50.0 mg), 4Å MS (100 mg, 1g/mmol of carbamate), CH_2Cl_2 (2.5 mL, 0.1 M or 6 mL, 0.04 M). [a]Carbamate concentration. [b]Isolated yield. [c]In parenthesis: *anti*:*syn* ratio, calculated by ^{19}F-NMR. [d]Without MS.

Dichloromethane was used as the solvent in all cases because aminofluorination reactions usually work better in halogenated solvents and, more specifically, in dichloromethane.[11,63] This preliminary study is intended to help in understanding the effect of each variable in the system and, ultimately, to provide valuable insight into the reaction mechanism.

Cinnamyl carbamate did not react with $TolIF_2$ at room temperature (Table **4.2**, entries **1**, **4**). When the reaction was heated up at 50 ºC, F-oxazolidinone **4.55** was observed as a diastereomeric mixture of *anti*/*syn* isomers (Table **4.2**, entries **2**, **5**, **6**, **7**, **8**). Interestingly, increasing temperature did not affect the yield, but it had some impact on the *syn* selectivity, which gradually increased up to 97:3 at 100 ºC (Table **4.2**, entries **6**, **7**, **8**).

The number of equivalents of $TolIF_2$ was also explored. The reaction was first tested using 2 equivalents following Nevado's procedure.[30] Doubling the amount of $TolIF_2$ at low concentration (0.04 M) resulted in a 20% increase in yield (Table **4.2**, entries **3** vs **6**), without affecting selectivity. This fact might be attributed to the thermal stability of $TolIF_2$, which is typically used at room temperature or lower. However, the low reactivity of our substrates requires heating, which can cause the $TolIF_2$ to decompose, therefore increasing the amount of the iodine(III) reagent necessary to transform the carbamate.

The use of lower concentrations (0,04 M) compared with the initial conditions (0,1 M) did not affect the reaction time or the yield but had a significant impact in the diastereoselectivity towards the *syn* F-oxazolidione (Table **4.2**, entries **2** vs **3**, **5** vs **6**).

An attempt was made to improve the reaction yield by adding HF to the reaction mixture (Table **4.2**, entries **10**-**12**). The addition of HF, in the form of a B·HF complex, is envisioned to have a dual impact: increasing

[63] a) Cui, J.; Jia, Q.; Feng, R.; Liu, S.; He, T.; Zhang, C. *Org. Let.* **2014**, *16*, 1442-1445; b) Li, Z.; Song, L.; Li, C. *J. Am. Chem. Soc.* **2013**, *135*, 4640.

the number of fluorine equivalents and increasing the acidity of the media, which could presumably activate $TolIF_2$ via H-bonding. However, the addition of DMPU·HF resulted in the formation of several sub-products, mainly **4.56** and **4.57**, albeit in small amounts. F-oxazolidinone **4.55** was obtained in very low yield using Py·HF after a very long reaction time. Nevertheless, it is worth noting that HF was able to activate the carbamate at room temperature.

The addition of the acidic DMPU·HF complex to the reaction mixture result in extensive protonation of the carbamate group, preventing it to react with the hypervalent iodine reagent. This would lead $TolIF_2$ to react with the alkene moiety in an analogous way to that described by Jacobsen (Scheme **4.9**), leading to a fluoro-iodonium intermediate.

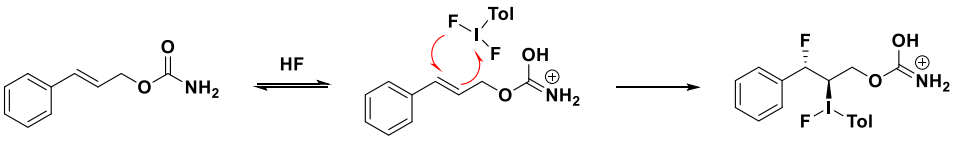

Scheme 4.37 Speculative formation of the fluoro iodane intermediate after the protonation of the carbamate moiety with DMPU·HF.

From such an intermediate, two reaction pathways are conceivable. These pathways explain the formation of the two obtained subproducts:

1) Intramolecular S_N2-type iodonium displacement by the protonated carbamate moiety, with the hydroxyl group becoming the most nucleophilic site (Scheme **4.38**). Ring-closing process on oxygen would therefore lead to the formation of a dioxolanimine, which would furnish dioxolanone **4.56** by hydrolysis during the work-up process. The product was obtained as a single diastereomer, which agrees with the proposed process. The S_N2-like substitution of the iodane would lead to only one isomer with the *syn* configuration. The *syn* configuration was attributed to **4.56** by analogy with *syn*-F-oxazolidinone **4.55**. Species **4.56** is formed through a hydroxyl group that is very deactivated by resonance with the imine, which explains the low yield.

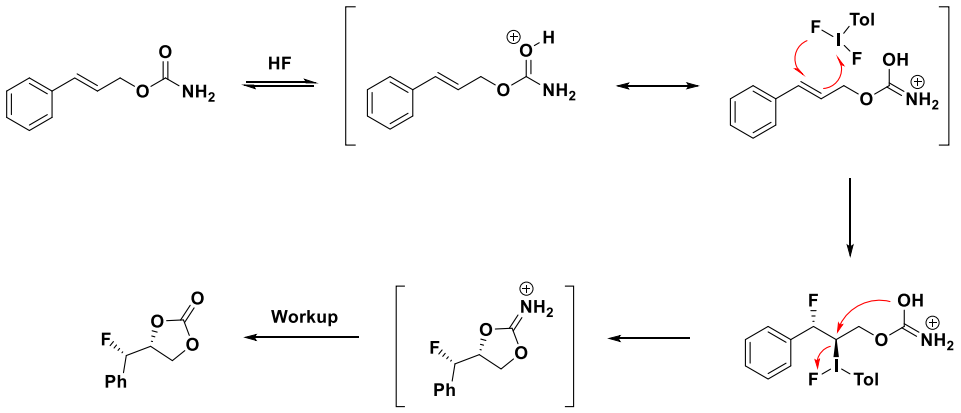

Scheme 4.38 Proposed mechanism for the formation of **4.56**.

2) Migration of the phenyl group to the internal carbon of the double bond (Scheme **4.39**). This kind of rearrangement leading to α-difluoromethyl-β-phenyl fragments has been described with allyl ketones and alcohols.[17] This rearrangement was also observed by Jacobsen *et al.* in their aminofluorination experiments with tosylaziridines bearing an aromatic ring without EWG.[16,64]

The formation of these products was explained through the displacement of the iodane by the electron-rich aromatic ring leading to a phenonium ion intermediate, from which fluoride nucleophilic attack would produce migration of the aromatic moiety to the central atom. The fact that this rearrangement happens only with substrates with non-EWG substituents in the aromatic ring points out to the implication of the phenonium ion. Withdrawal of electronic charge from the aromatic ring would discourage the formation of a positive charge in the ring during the aryl migration.

[64] Banik, S. M.; Medley, J. W.; Jacobsen, E. N. *Science* **2016**, *353*, 51.

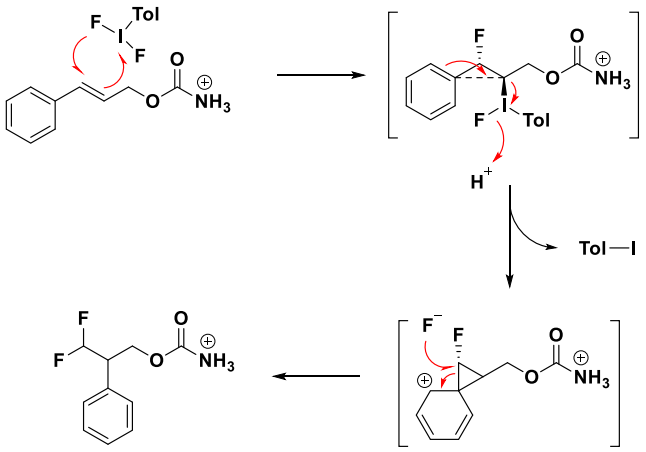

Scheme 4.39 Proposed mechanism for the formation of **4.57**.

Finally, the need for molecular sieves in the reaction mixture was addressed. In principle, no water is released during the reaction, so no MS or other dehydration agent would be required. However, performing the same reaction without molecular sieves resulted in a major change in selectivity, with a diastereomeric ratio very close to 1:1 (Table **4.2**, entry **9**). There is a possibility that molecular sieves could act as a HF scavenger agent, or even react with it leading to some sort of MS decomposition.[65] To prove this hypothesis, HF content was estimated from a mixture of 4Å MS and $Et_3N{\cdot}HF$ or DMPU·HF in CH_2Cl_2 in the same proportion than in the aminofluorination experiments: a decrease of more than 99% of the HF signal in the ^{19}F-NMR spectrum was observed during the experiments, and considerable heating and gas release were observed, indicating the decomposition of the MS rather than just trapping HF. This result would lead us to the idea that the presence of molecular sieves would act as a HF scavenger, thus preventing large concentrations of HF in the reaction mixture.

[65] MS incompatible with hydrofluoric acid (https://www.alfa.com/en/catalog/A11535/)

To sum up, the aminofluorination of cinnamyl carbamate was explored by varying several variables, achieving moderately good yield of β-fluorooxazolidinone, where the *syn* isomer was the major isomer. The chosen reaction conditions for the remaining carbamates are outlined in Table **4.2**, entry **8**. These conditions will be used in upcoming experiments.

4.3.3. One-pot Aminofluorination: Mechanistic Study

The reactivity of $TolIF_2$ has been widely studied with different types of substrates. It functions very well introducing fluorine atoms to alkenes.[18],[66] Since it is a hypervalent iodine reagent, its high reactivity with double bonds has been exploited to carry out fluorination accompanied by a second intramolecular addition, such as cyclisations, oxyfluorinations and, of course, aminofluorinations. Despite the numerous reactions described with $ArIF_2$-like reagents, or any methodology involving the formation of such, its mechanism remains unclear. From the conclusions extracted from the literature, it becomes clear that $TolIF_2$ is not a chemoselective reagent, and mechanisms are quite substrate-dependant.[67] The proposals that have been postulated for the alkene aminofluorination can be generally divided in two groups, depending on the relative reactivity of the double bond and the participating nitrogenated function. The hypervalent iodine may interact first with either group, leading to a different mechanism.

In the first scenario, the hypervalent iodine reagent is supposed to add to the double bond, in a mechanism very similar to that of a regular difluorination of an alkene: iodine (III) adds to the double bond to form a fluoroiodonium intermediate (Scheme **4.40**). Subsequent substitution of the iodinonium moiety by the nitrogen in the carbamate moiety would render the fluoro-oxazolidione.

[66] Kohlhepp , S: V.; Gulder, T. *Chem. Soc. Rev.* **2016**, *45*, 6270-6288.
[67] Kong, W.; Merino, E.; Nevado, C. *Chimia* **2014**, *68*, 430.

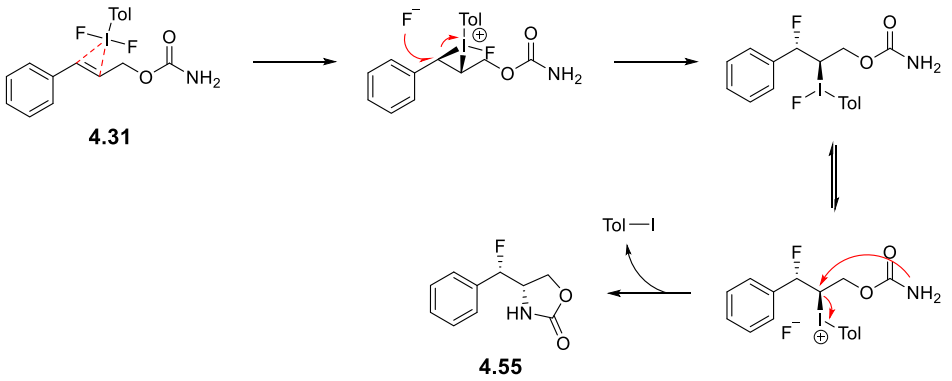

Scheme 4.40 Hypothetic mechanism for the aminofluorination of cinnamyl carbamate with $TolIF_2$ through the interaction with the double bond instead of the carbamate.

Additionally, substitution of the iodonoium moiety by the electron-rich arene could lead to the rearranged 1,2-difluoro-2-arene product **4.57** (Scheme **4.39**). This last pathway has been described by Jacobsen[22] when using cinnamyl substrates carrying non EWG. This would lead to the idea that, if this was the operating pathway in our cinnamyl carbamates, we should expect reasonable amounts of the 1,1-dilfluoro-2-arene rearrangement product altogether with fluoro-oxazolidinone, which is not observed.

On the other hand, the nitrogen could be oxidized by $TolIF_2$ to an iminoiodane intermediate, which would then act as a nitrene equivalent. Nitrenes are very reactive electrophilic species that are rapidly added to double bonds. That would lead to the formation of a bicyclic aziridine, which is finally opened with fluorine.

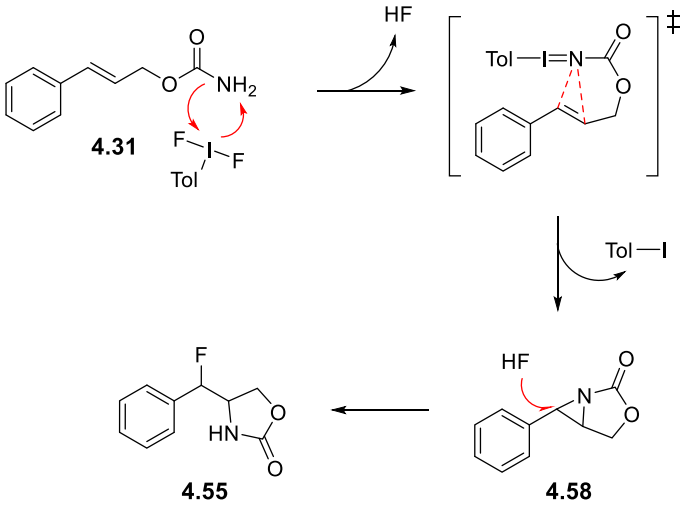

Scheme 4.41 Hypothetic mechanism for the aminofluorination of cinnamyl carbamate with $TolIF_2$ given it oxidizes the nitrogen in the carbamate group.

$TolIF_2$ can alternatively undergo simple ligand exchange with the carbamate group and form an aminoiodane, which can undergo addition ot the proximal alkene to form an aziridinium intermediate, releasing iodine(I) in the form of TolI. Like in the iminoiodane pathway, the intermediate is ring-opened with fluorine.

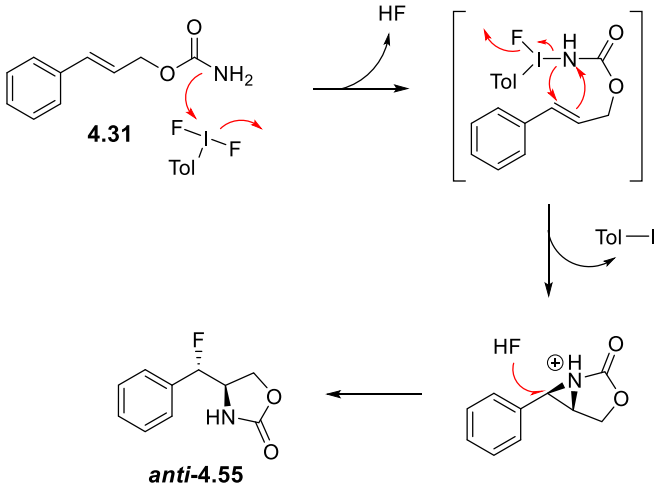

Scheme 4.42 Hypothetic mechanism for the aminofluorination of cinnamyl carbamate with $TolIF_2$ given it oxidizes the nitrogen in the carbamate group.

Nevado et al. proposed this last mechanism variation for the aminofluorination of tosylamides.[30] They emphasized the relevance of the acidity of the nitrogen, since it acts also as an activator of the iodane via H-bonding with the fluorine (Scheme **4.15**). Carbamates are usually less acidic than tosylamides, so this could be a major factor in discerning the mechanism of the transformation.

As mentioned before, the preference of iodine for either the double bond or the nitrogen is strongly dependant on the substrate. Chemoselectivity, or lack-thereof, can easily be salvaged by addition order in an intermolecular chemical reaction, but this is not possible in the aminofluorination of allyl carbamates since it is an intramolecular reaction. An extended effort will be made to understand the mechanism of the transformation.

Considering the existing literature on aminofluorination and $TolIF_2$ reactivity in general, and the experiments explained in the optimization of the reaction with cinnamyl carbamate (Table **4.2**), an initial mechanism hypothesis can be drawn. Aminofluorination of similar substrates tend to point towards an aziridine/aziridinium intermediate rather than an addition of iodine(III) to the double bond, which is more common in difluorinations. The lack of subproduct **4.57** also supports this hypothesis. Therefore, the mechanism displayed in Scheme **4.42** will serve as the initial proposal. This route has two big challenges that need to be discussed: the formation of the aziridine intermediate, and the rationale for the diastereomeric mixtures obtained in the aminofluorination of cinnamyl carbamate.

The most straightforward way to demonstrate that a chemical reaction proceeds through a specific intermediate species, is having experimental proof that such species is formed during the reaction. Aziridine **4.58** is a described compound and should be detected by proton NMR spectroscopy.

4.3.3.1. ^{1}H-NMR Studies for the Detection of the Aziridine Intermediate

The reaction between cinnamyl carbamate and TolIF$_2$ was tracked for three hours at 80ºC in an NMR pressure tube to identify aziridine formation.

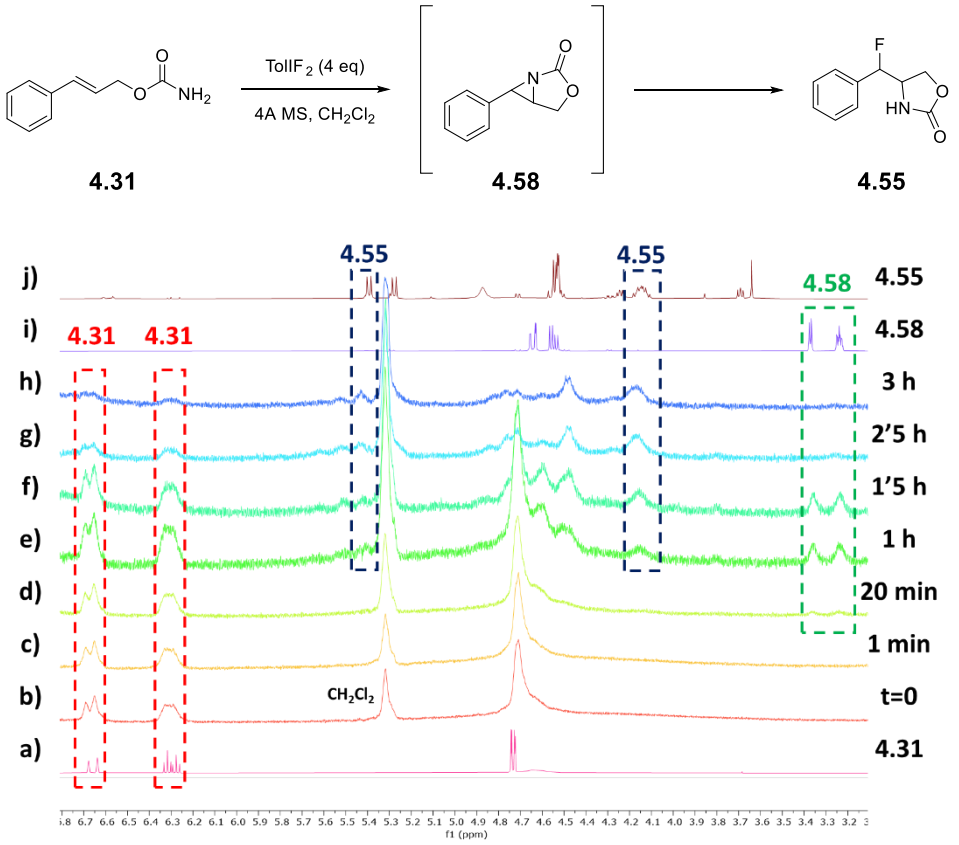

Scheme 4.43 Stack of ^{1}H-NMR spectra of the monitoring of the reaction of carbamate **4.31** with TolIF$_2$. a) Spectrum of the starting cinnamyl carbamate. b-h) Spectra of the fluoroamination reaction over 3 h. i) Spectrum of the isolated aziridine. j) Spectrum of the final F-oxazolidinone (*syn* isomer).

Scheme **4.43** shows the ^{1}H NMR spectra recorded at different reaction times (b-h) of a fluoroamination assay of **4.31** with TolIF$_2$, compared with those of cinnamyl carbamate (a), isolated aziridine **4.58** (i) and final fluoro-oxazolidinone **4.55** (j).

Despite the low resolution of the spectra, due to the low boiling point of dichloromethane and the scattered molecular sieves throughout the NMR tube, the formation of **4.58** during the reaction is clear. Signals at the more upfield area of spectra e) and f) clearly correspond to the aziridine. Moreover, these spectra show all three species (cinnamyl carbamate, aziridine and F-oxazolidinone) coexisting, perhaps suggesting a slower aziridination step compared to the subsequent ring-opening.

To support this idea, the same kinetic experiment was carried out with *p*-substituted cinnamyl carbamates, one with an EWG (NO_2^-) and one with an EDG (MeO^-) (Figure **4.6**). If the aziridination process is the rate-determining step, an electron-rich olefin should react faster than an electron-poor one since the double bond is more nucleophilic. Therefore, MeO-substituted carbamate should react much faster than NO_2-substituted carbamate.

As seen in the spectra, the NO_2 experiment show carbamate and aziridine signals throughout the experiment (Figure **4.6**, top). Instead, aziridine is not observed in the MeO experiment (Figure **4.6**, bottom). This would be in agreement with the statement above: reaction from MeO-substituted substrate would proceed through a short-lived aziridine intermediate, undetectable by NMR, whose ring-opening process should be electronically favoured by the presence of the MeO-group.

This experiment supports the hypothesis that the aminofluorination of allyl carbamates proceeds through the formation of the postulated bicyclic aziridine intermediate **4.58**.

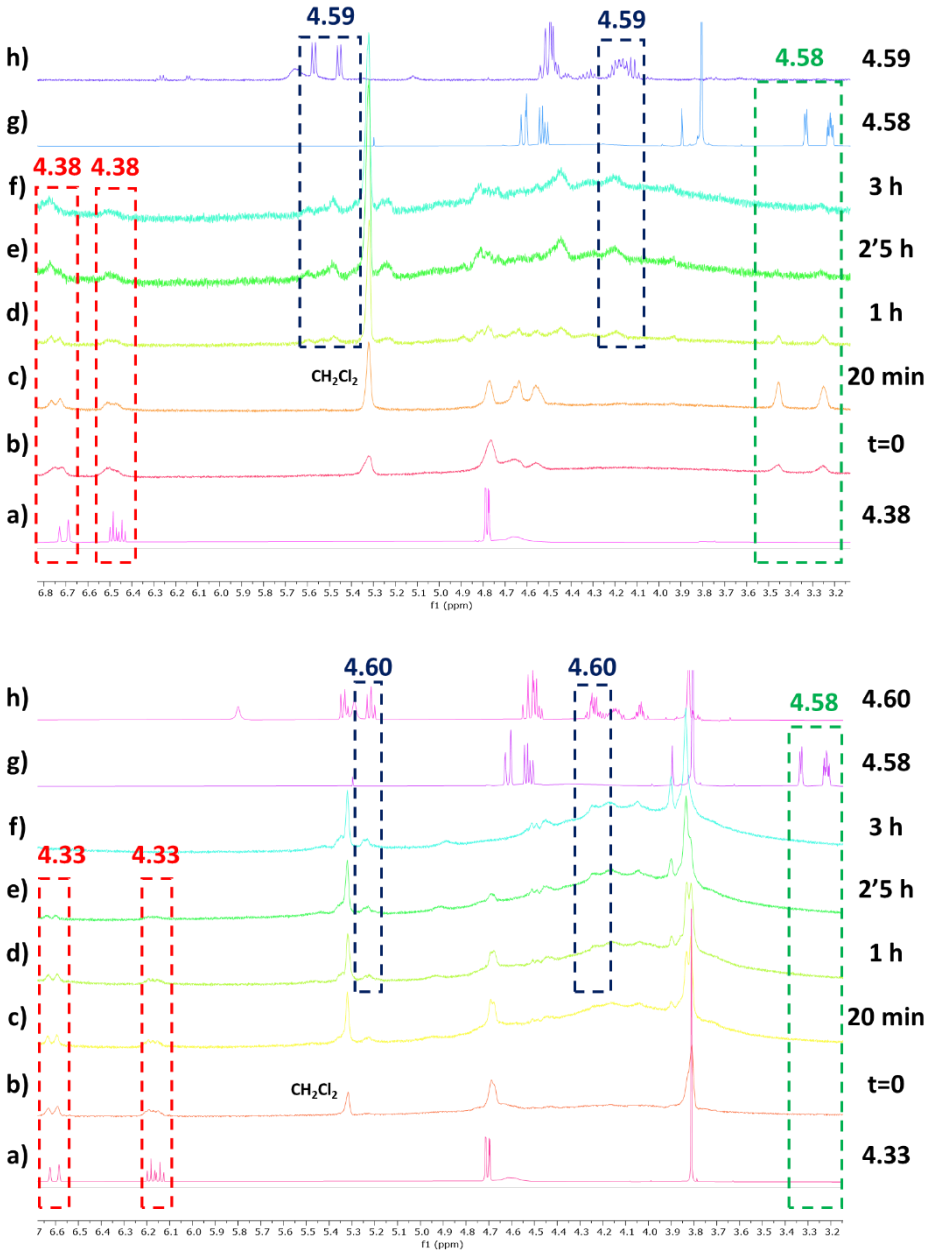

Figure 4.6. Stack of ^{1}H-NMR spectra of the monitoring of the reaction of *p*-NO_2-substituted carbamate **4.38** (top) and *p*-MeO-substituted carbamate **4.33** (bottom) with TolIF$_2$. a) Spectrum of the starting cinnamyl carbamate. b-h) Spectra of the fluoroamination reaction over 3 h. i) Spectrum of the isolated aziridine. j) Spectrum of the final F-oxazolidinone (*syn* isomer).

4.3.3.2. Effect of the Substitution on the Nitrogen of the Carbamate

The nature of the interaction between the hypervalent iodine and the nitrogen in the carbamate was explored. While some literature points to an aminoiodane as the typical nitrene source for aziridination, recent findings within our research group suggest that aziridination of allyl carbamates with PhIO likely proceeds through an iminoiodane intermediate.[11] Aminofluorination has been widely studied with tosylamides, which are more electron-deficient nitrogen functionalities than carbamates, so an aminoiodinane might be electrophilic enough to react in those cases. Furthermore, the presence of an acidic H at the tosylamide might facilitate the activation of TolIF$_2$ for N oxidation through hydrogen bonding (Scheme **4.15**).

To gain insight into the nature of the nitrene source, two experiments were then set up utilizing *N*-substituted carbamates bearing either tosyl or benzyl groups. Blocking one of the nitrogen positions negates the formation of the iminoiodane, making the aminoiodane the only alternative route. The presence of a tosyl group in the carbamate substrate would significantly increase the acidity of the NH moiety and favour the activation of TolIF$_2$ towards the formation of the hypothetical aminoiodane, in line with Nevado's experiments.[30] Conversely, the *N*-benzyl carbamate, containing a non-acidic proton, is not expected to be competent in the aziridination reaction.

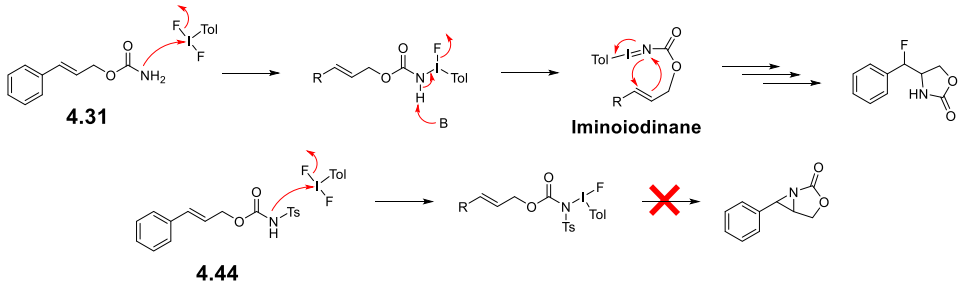

Scheme 4.44 Mechanistic discussion of the impossibility of an iminoiodane intermediate using N-monosubstituted carbamates as substrates.

None of the *N*-substituted carbamates yielded the desired F-oxazolidinones under standard conditions. N-Bn-carbamate remained unaltered for over a week and N-Ts-carbamate gave a very complex mixture of subproducts, most likely due to decomposition with temperature over time. None of them gave any signal in the ^{19}F-NMR.

Table 4.3. Results of the aminofluorination of N-monosubstituted cinnamyl carbamates with Ts and Bn.

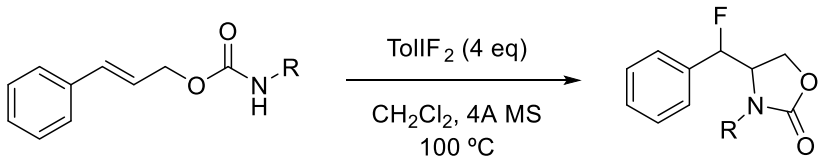

4.44 R=Ts
4.48 R=Bn

R	Time	Yield (%)[a]	dr (*anti*/*syn*)[b]
H	6 h	64	40:60
Ts	4 d	CM[c]	-
Bn	> 1 week	-	-

Typical conditions: Carbamate (0.29 mmol, 50.0 mg), TolIF$_2$ (4 eq), 4Å MS (100 mg, 1g/mmol of carbamate), CH_2Cl_2 (2.5 mL, 0.04 M). [a]Isolated yield. [b]Calculated by ^{19}F-NMR. [c]CM = Complex Mixture.

The negative results obtained with *N*-substituted cinnamyl carbamates compared with the unsubstituted one would suggest that an aminoidane is not a competent intermediate in the aziridination of these carbamate substrates, and that fluoroamination of unsubstituted carbamates might be driven by the formation of an iminoiodane. Consistent evidence of the mechanism of the formation of the aziridine is reported herein.

4.3.3.3. Effect of the Double Bond Configuration

In order to gain insight on the origin of the diastereoselectivity, the aminofluorination with $TolIF_2$ was also tested with *cis* cinnamyl carbamate **4.40**. This experiment is intended to shed some light on whether the two *cis* and *trans* carbamates will provide converging selectivity results or, on the contrary, will furnish distinct diastereoselectivity outcomes. The former would suggest a common carbocation-like intermediate, whereas differing selectivity would suggest stereospecific processes.

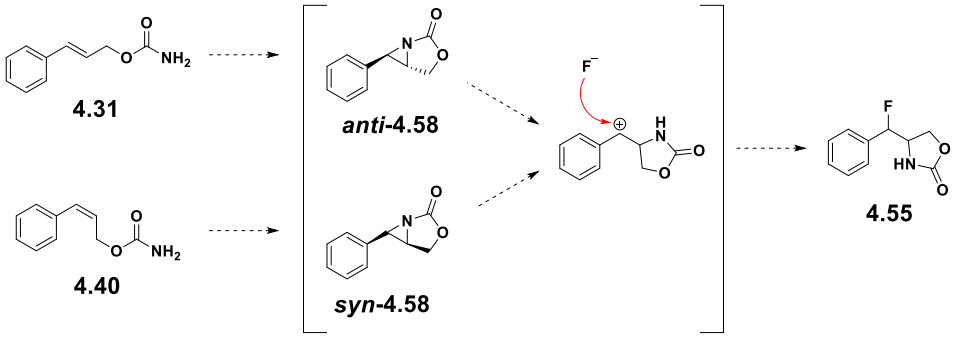

Scheme 4.45 Expected outcome of the aminofluorination through a carbocation intermediate with the *trans* and *cis* isomers.

Unfortunately, when **4.40** was submitted to the standard fluoroamination conditions, the outcome was quite different. The reaction was left to react for over one week and the starting carbamate did not convert completely (~70% conversion). Furthermore, the F-oxazolidinone was obtained in a low 21% overall as an equimolar mixture of *anti*/*syn* isomers.

Table 4.4. Results of the aminofluorination of the *trans* and *cis* cinammyl carbamates.

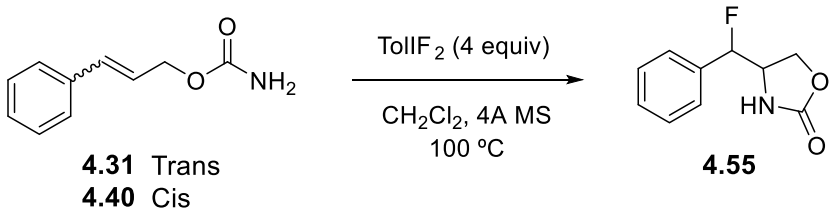

4.31 Trans
4.40 Cis

4.55

	Time	Yield[a]	dr (*anti*/*syn*)[b]
Trans	6 h	60	40:60
Cis	>1 week	21	55:45

Reaction conditions: Carbamate (1 equiv, 0.1 mmol), $TolIF_2$ (4 equiv), 4Å MS (100 mg, 1 g/mmol of carbamate), CH_2Cl_2 (2.5 mL, 0.04 M), 100 ºC. [a]Isolated yield. [b]Calculated by ^{19}F-NMR.

Recent studies in our group regarding the aziridination of 2-cis-4-trans-dienyl carbamates showed that the reaction proceeds more sluggishly than those from 2-trans-4-trans isomers.[11] Additionally, DFT calculations of the aziridination of the *trans trans* dienyl carbamate carried out by Maseras *et al* showed important π-stacking interaction between the aromatic part of the hypervalent iodine (in the form of an iminoiodane) and the distal alkene of the carbamate. Despite calculations for the *cis* isomer non-existing, it is possible that these interactions could be weaker in the *cis* configuration, rendering the aziridination process unviable/very unfavourable.

Starting from the iminoiodane, the first step is a conformational rearrangement from **1t** to **2t** via rotation around the C-O bond. Interestingly, there are two conformations of the TS: **TS 2t-3t** and **TS 2t-3t'**. The most stable **TS 2t-3t** (Figure **4.7**, bottom-left) has a close interaction between the phenyl group of the iminoiodane and the distal double bond of the substrate, while the least stable **TS 2t-3t'** (Figure **4.7**, bottom-right) has the phenyl group pointing away from the double bond.

The disposition of both groups in the *cis* scenario may be one that minimizes these key interactions.

Translating this to our system, it could be feasible to think that the *cis* carbamate may not be suited for establishing π-stacking interactions between the aromatic moiety of the iodine unit and the alkene at the transition state, making the process kinetically more unfavoured.

Nonetheless, knowing that the aziridination step is troublesome, drawing conclusions about the result of the ensuing ring-opening stage is problematic.

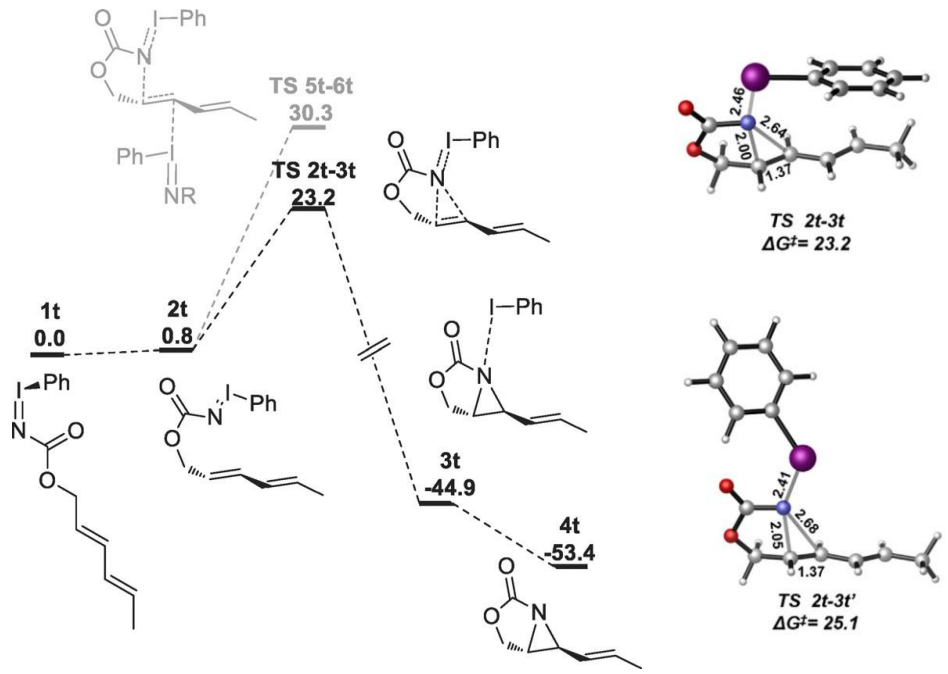

Figure 4.7. Free energy profiles (kcal/mol) for the aziridination of (2E,4E)-hexa-2,4-dien-1-yl carbamate with PhIO. Structures for the key transition states at the bottom.

4.3.3.4. Effect of the Secondary Electronic Unit in the Allyl Carbamate

The selectivity outcome of fluoroamination reactions starting from cinnamyl carbamates could be determined by the formation of a carbocation-like intermediate at the benzylic position. To gain insight on this issue, fluoroamination reaction was explored in simple allylic carbamate **4.41**, containing an aliphatic chain at the distal carbon of the doble bound.

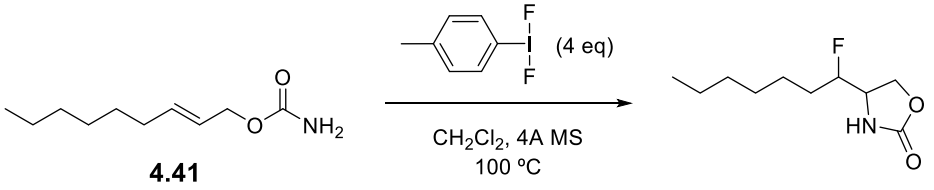

Scheme 4.46 Aminofluorination experiment with an alkyl carbamate to test the importance of a conjugated donating group.

When carbamate **4.41** was submitted to the standard fluoroamination conditions with $TolIF_2$, no conversion was observed after a week. This experiment confirms that an electron-donating secondary unit is not only highly influential, but actually mandatory for the aminofluorination with $ArIF_2$ to take place.

4.3.3.5. Application of the Aminofluorination Conditions to Dienyl Carbamates

As stated in the general objectives, this methodology is being developed as a way to access C3-fluorinated sphingosine analogues in a facile manner. The starting point to achieve such analogues would be a dienyl carbamate.

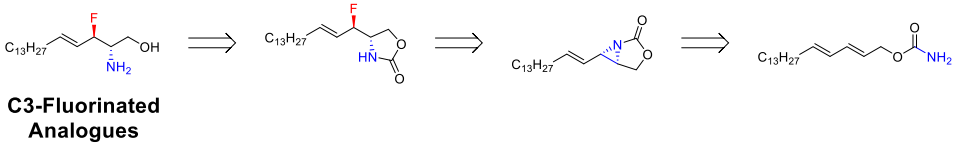

C3-Fluorinated Analogues

Scheme 4.47 Dienyl carbamates as primary source of C3-fluorinated sphingosine analogues.

To this end, the aminofluorination of dienyl carbamate **4.43** was explored. Previous studies in our group on aziridination/ring-opening process of dienyl carbamates showed that S_N2-like ring-opening of the vinyl aziridine intermediate by some heteroatomic nucleophiles could be accompanied by S_N2' sub-products, resulting from conjugated attack at the vinyl moiety. Furthermore, it was established that the more acidic the nucleophile was, the more important the S_N2' attack was.

Direct addition of fluorine to the aziridine yields the vinyl F-oxazolidinone **4.61**. Instead, conjugated attack to the vicinal alkene and further electron mobilization leads to the formation of **4.62**.

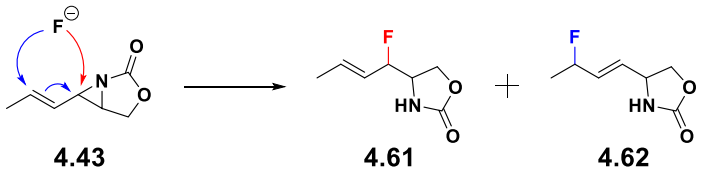

4.43 **4.61** **4.62**

Scheme 4.48 Possible regioisomers for the ring-opening of intermediate allyl aziridine **4.45** with fluorine.

Carbamate **4.43** was submitted to the standard aminofluorination conditions with $TolIF_2$. Compounds **4.61** and **4.62** were observed as *anti*/*syn* mixtures, to a total of 4 different species (Table **4.5**, entry **1**). The ring-opening diastereomers of **4.61** were easily assigned by analogy of the peaks observed in the ^{1}H-NMR for cinnamyl-derived F-oxazolidinones with high confidence. Conjugate addition diastereomers of **4.62** were also easily identified by ^{1}H- and ^{19}F-NMR, but the *anti* and *syn* configurations were not distinguished.

Direct and conjugated addition products **4.61** and **4.62** were obtained in a 60:40 proportion, with the desired product as the predominant. **4.61** was obtained as an 80:20 *anti*/*syn* mixture, very similar to that of cinnamyl carbamate (86:14, Table **4.2**, entry **6**).

Table 4.5. Results of the aminofluorination of carbamate **4.43**. Standard conditions and temperature study.

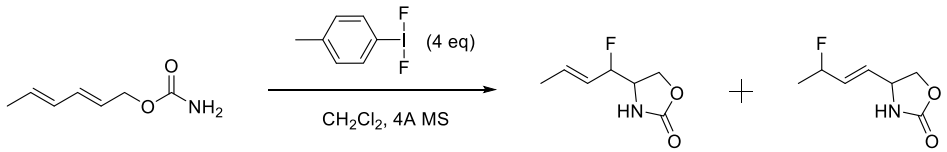

4.43 **4.61** **4.62**

Entry	T (ºC)	Time (h)	Yield 4.61 (%)[a]	dr 4.61 (*anti*/*syn*)[b]	Yield 4.62 (%)[a]
1	100	5	27	20:80	20
2	50	18	26	16:84	21
3	rt	72	33	16:84	11
4	0	120	37	3:97	7
5	-30	>1 week	-	-	-
6[c]	100	96	31 (Conv 80%)	55:45	7

Reaction conditions: Carbamate (1 eq, 0.1 mmol), TolIF$_2$ (4 eq), 4Å MS (100 mg, 1 g/mmol of carbamate), CH_2Cl_2 (2.5 mL, 0.04 M). [a]Isolated yield. [b]Calculated by ^{19}F-NMR. [c]Addition of $Et_3N{\cdot}HF$ (10 equiv HF).

In order to improve the regioselectivity towards **4.61**, some optimization was carried out.

Dichloromethane works very well as the solvent: non-polar aprotic solvents favour direct addition because they reduce solvation, enhancing fluorine nucleophilicity. Greater nucleophilicity leads to more irreversible addition reactions, resulting in kinetic control of the competition between direct and conjugate addition. Consequently, the faster 1,2-product predominates. In conclusion, no solvent screening was deemed necessary.

Temperature is another key factor in controlling regioselectivity. If the gap in activation energy of both substrates is substantial, discrimination can occur. Colder conditions favour kinetic control, thereby making the 1,2-product the primary outcome as the temperature decreases. In fact, lowering the temperature gradually increased the yield of **4.61** (Table **4.5**, entries **1-4**). Overall yield is maintained at around 45% in all experiments, yet regioselectivity greatly improves. Unfortunately, reaction did not yield any result at -30 ºC, indicating that the minimum temperature threshold has been reached.

It was envisioned that increasing the concentration of nucleophile could tilt the equilibrium towards the more accessible **4.61**. To this purpose, 10 equiv of HF were added to the reaction in the form of $Et_3N{\cdot}HF$. As expected, enhanced regioselectivity was obtained. However, the reaction lasted a lot more than without any additive and overall yield timidly decreased.

As stands, these are not convenient results, and more optimisation is required to be able to apply this methodology. Selectivity ratios are good, but yield must be sensibly improved.

4.3.3.6. Effect of the Substitution in the Aromatic Ring

Using cinnamyl carbamates as model compounds provides a convenient way to study the electronic behaviour of the process. Introducing diverse functional groups onto the *para* position of the neighbouring aromatic ring induces notable electronic changes in the carbamate's double bond, potentially influencing the reaction outcome. This collection of compounds will offer valuable insight into the nature, scope and diastereoselectivity of the reaction.

To this end, different *p*-substituted carbamates were submitted to the standard aminofluorination conditions. Table **4.6** shows the yield and the selectivity outcomes. The substituents are sorted by Sigma-Hammett parameter σ^+, a numerical representation of the electronic density

introduced by a *para*-substituent.[68] Therefore, the first substituent is the most electron-donating group (EDG), while the last is the most withdrawing (EWG). This parameter and its implications will be further explored in upcoming sections of the thesis.

All carbamates yielded the desired F-oxazolidinones with different degree of diastereoselectivity. Also notably, the preferred isomer was the *syn* isomer in all the experiments. A clear trend is observed in the results: greater electron-withdrawing effects correlate with extended reaction times, reduced yields, and more selectivity towards the *syn* isomer. AcO and CN-substituted carbamates present a lower yield than expected because of partial decomposition, arguably due to the formation of hydrofluoric acid during the reaction .

These results are consistent with the stabilisation of a carbocation in the benzylic position by more EDG, where the attack of the fluoride happens. Instead, EWG destabilise the hypothetic carbocation and fits better with an S_N2-like mechanism. However, the *anti* configuration should be expected from an S_N2 pathway.

To sum up, the mechanism of the aminofluorination of cinnamyl carbamates with $TolIF_2$ presents a significant sensitivity to electronic changes. An equilibrium is stablished between two pivotal factors that account for the selectivity of the reaction: the density of charge in the benzylic position and the interactions between the aziridine and HF.

[68] Hansch, C.; Leo, A.; Taft, W. *Chem. Rev.* **1991**, *91*, 165-195.

Table 4.6. Scope of *p*-substituted Cinnamyl Carbamates with TolIF$_2$. Results are conveyed in a double-bar graph for ease of interpretation.

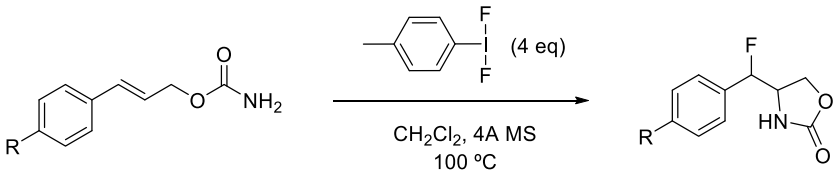

4.31 R=H
4.32 R=AcO
4.33 R=MeO
4.34 R=Me
4.35 R=Br
4.36 R=F
4.37 R=CF_3
4.38 R=NO_2
4.39 R=CN

4.55 R=H
4.63 R=AcO
4.60 R=MeO
4.64 R=Me
4.65 R=Br
4.66 R=F
4.67 R=CF_3
4.59 R=NO_2
4.68 R=CN

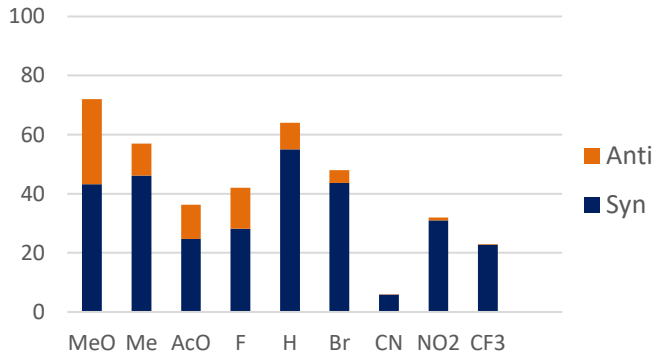

R	Time (h)	Yield (%)[a]	dr (anti/*syn*)[b]
MeO	3	72	40:60
Me	3	57	19:81
AcO	3	33	35:65
F	21	42	33:67
H	22	64	3:97
Br	20	48	9:91
CN	30	6	2:98
NO_2	72	32	3:97
CF_3	96	23	1:99

Reaction conditions: Carbamate (1 equiv, 0.1 mmol), TolIF$_2$ (4 equiv), 4Å MS (100 mg, 1 g/mmol of carbamate), CH_2Cl_2 (2.5 mL, 0.04 M), 100 ºC. [a]Isolated yield. [b]Calculated by ^{19}F-NMR.

4.3.4. Strategy #2: One-pot Aminofluorination of Allyl Carbamates with *In situ*-generated TolIF$_2$ from I(III) precursors and HF

Reaction between a hypervalent iodine reagents such as PhIO and a fluorinating agent such as Py·HF has been widely used as a practical alternative to the use of $PhIF_2$ for the difluorination of alkenes.[69] A further refinement of this approach consists in the use of a catalytic amount of PhI, which is oxidized *in-situ* to PhIO with mCPBA, and fluorinated with HF to hypothetically render $PhIF_2$, which finally reacts with the alkene. PhI is released as a by-product and can be oxidised again by mCPBA.[70]

Since PhIO is frequently used in the laboratory, PhIO will be used as a model I(III) reagent for the *in-situ* generation of PhIF2 by reaction with B·HF complexes. In this approach, these two reagents are mixed for 15 minutes and the alkene substrate is added to the reaction mixture.

The procedure was tested with Et_3N, Py and DMPU as complexing agents for HF. Et_3N·HF turned out to be very little reactive under these conditions (Table **4.7**, entry **1**). DMPU·HF yielded exclusively **4.56** and **4.57** (Table **4.7**, entries **5**, **6**). In contrast, Py·HF resulted the most reactive, providing a moderate amount of F-oxazolidinone (Table **4.7**, entry **3**).

[69] a) Banik, S. M.; Medley, J. W.; Jacobsen, E. N. *J. Am. Chem. Soc.* **2016**, *138*, 5000–5003; b) Zhou, B.; Haj, M. K.; Jacobsen, E. N.; Houk, K. N.; Xue, X. *J. Am. Chem. Soc.* **2018**, *140*, 45, 15206–15218; c) Feng, S.; Yang, S.; Tu, F.; Lin, P.; Huang, L.; Wang, H.; Huang, Z.; Li, Q. *J. Org. Chem.* **2021**, *86*, 9, 6800–6812.

[70] Kitamura, T.; Yoshida, K.; Mizuno, S.; Miyake, A.; Oyamada, J. *J. Org. Chem.* **2018**, *83*, 14853−14860.

Table 4.7. Aminofluorination of cinnamyl carbamate via *in situ* generation of $PhIF_2$ with PhIO and B·HF complexes.

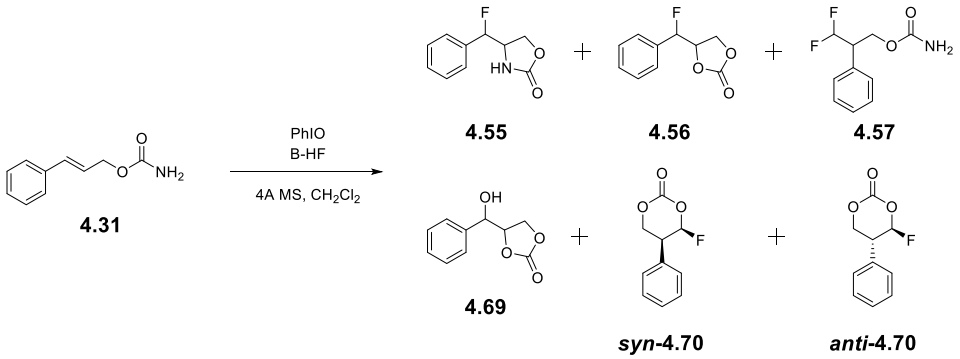

	Reagent	T (ºC)	Time (h)	Yield (%)[a]					
				4.55	**4.56**	**4.57**	**4.69**	***s*-4.70**	***a*-4.70**
1	Et_3N·HF	-45 to rt	>1 week	16[b]	-	-	17	-	-
2[d,e]	Et_3N·HF	Reflux	>1 week	-	-	-	-	-	-
3	Py·HF	-45 to rt	4h	36 (37:63)[c]	41	<5	-	-	-
4[d,e]	Py·HF	Reflux	16h	-	26	-	-	39	25
5	DMPU·HF	-45 to rt	24h	-	34	10	-	-	-
6	DMPU·HF	Reflux	5h	-	24	21	-	-	-
7[e]	DMPU·HF	Reflux	4h	-	56	16	-	-	-
8[d,e]	DMPU·HF	Reflux	16h	-	23	-	-	53	24

Reaction conditions: Cinnamyl carbamate (0.3 mmol), PhIO (1.4 equiv), CH_2Cl_2 (0.1 M), B·HF (20 equiv HF). [a]Isolated yield. [b]*Syn* isomer, calculated by ^{19}F-NMR. [c]dr (*anti*/*syn*), calculated by ^{19}F-NMR. [d]Evaporation of HF for 15 min before the addition of the carbamate. [e]PhIO (2 equiv).

Notably, products **4.56** and **4.57**, which were already observed in low amount during the optimization experiments for the aminofluorination with $TolIF_2$ (Table **4.2**), were obtained in larger quantity in most experiments. Following the argumentation laid in the optimisation process, the presence of large excess of HF might protonate the carbamate, preventing the formation of the iminoiodane and favouring hydroxyfluorination. After workup, product **4.56** is obtained (Scheme **4.49**, path A). Rearranged carbamate **4.57** is also a derivate of the blockade of the nitrogen (Scheme **4.49**, path B). Therefore, a higher amount of HF is likely to give a higher proportion of these byproducts.

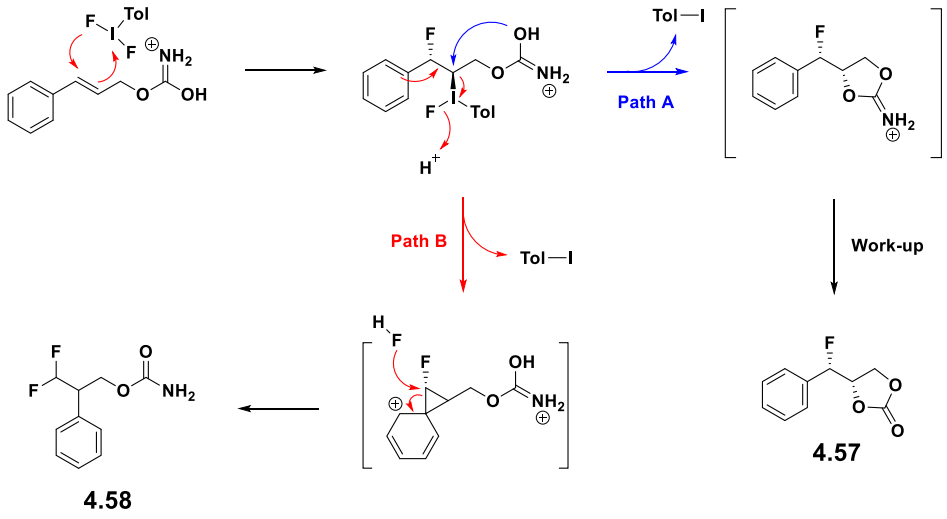

Scheme 4.49 Reaction pathways for the formation of **4.56** (Path A) and **4.57** (Path B).

It appears that Py·HF strikes a subtle balance in terms of HF power: sufficiently accessible for reaction, yet not acidic enough to protonate the carbamate. Nonetheless, due to the substantial formation of subproducts, the challenges in separation, and the resulting low yields, this procedure proved unfeasible for aminofluorination.

In order to minimize the amount of HF in the reaction mixture, PhIO and B·HF complex were mixed prior to the addition of the carbamate and, after TolIF$_2$ was completely formed, the remaining HF was evaporated. Interestingly, Et$_3$N·HF yielded no reaction (Table **4.7**, entry **2**). However, Py·HF and DMPU·HF showed similar reactivity (Table **4.7**, entries **4**, **8**). No F-oxazolidinone were observed. Dioxolanone **4.56** was obtained and, to our surprise, 1,3-dioxanones ***syn*-4.70** and ***anti*-70** were also obtained in good amount.

These products are obtained through the same phenonium migration that yields carbamate **4.57**, but with the hydroxyl group of the protonated carbamate opening the phenonium instead of an external fluorine atom. This is coherent with a lower HF concentration in the mixture.

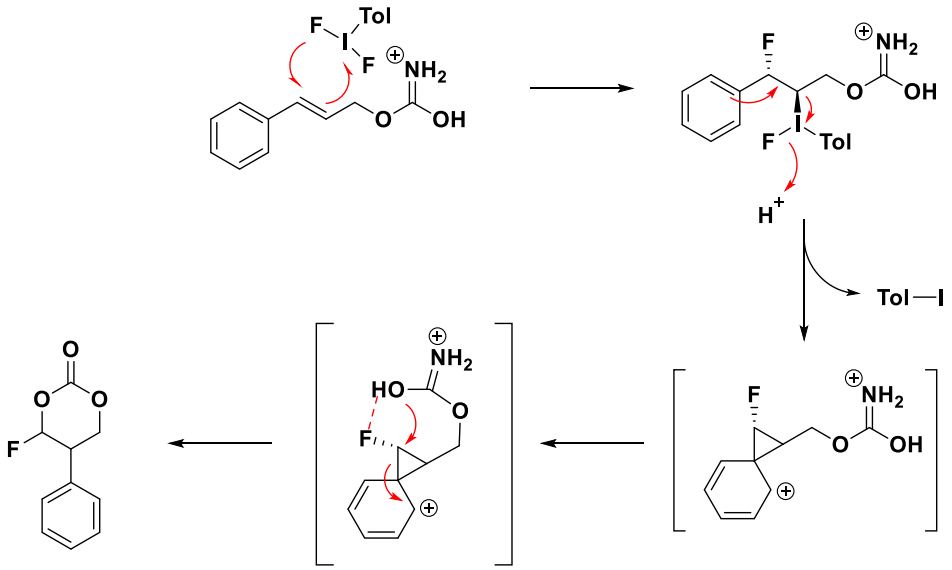

Scheme 4.50 Proposed mechanism for the formation of **4.70**.

The reactions were entirely regioselective towards the more electrophilic centre next to the fluorine atom. Stereoselectively, the *syn* isomer is found in more proportion than the *anti*, perhaps due to H-bond assistance from the neighbouring fluorine.

Considering the unexpected results, the reaction mixture was studied by NMR spectroscopy after the evaporation of HF. This was done to confirm the absence of residual HF in the medium prior to carbamate addition, and also to investigate the potential presence of any other intermediates that could contribute to this reactivity.

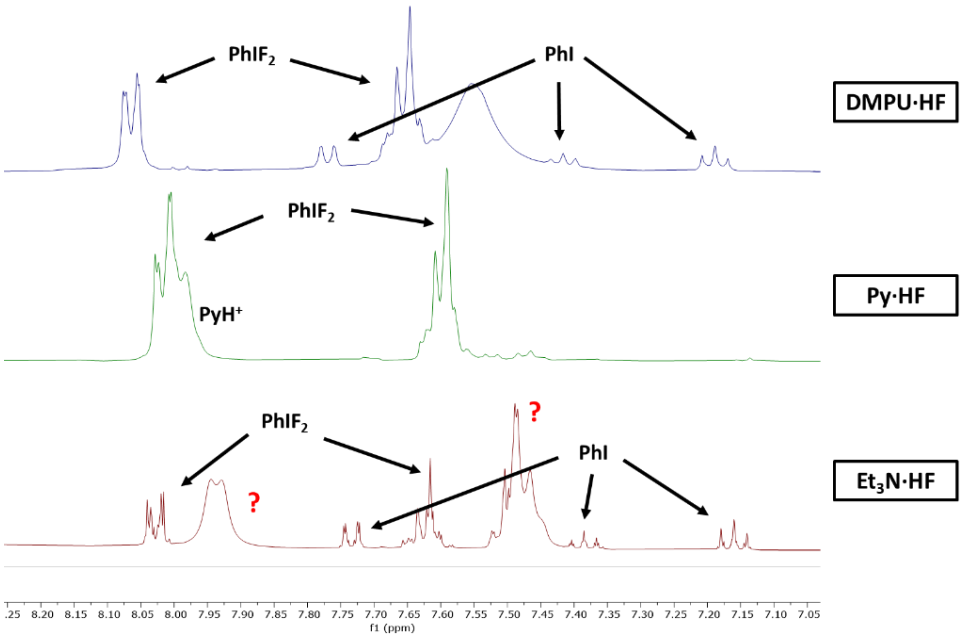

Figure 4.8. ^{1}H-NMR comparison of the remaining residue after the evaporation of HF in the PhIO/B·HF mixture. Spectra shown for DMPU·HF, Py·HF and Et_3N·HF.

$PhIF_2$ is the major product in the DMPU·HF and Py·HF experiments. PhI is also observed, which is the degradation subproduct of $PhIF_2$. Absence of other considerable signals rises confusion given the obtained results in the aminofluorination experiments. Et_3N·HF spectrum shows an unidentified pair of signals which might be causing interference in the reaction. $PhIF_2$ and a substantial amount of PhI are also observed.

In addition, ^{19}F-NMR confirms the presence of HF in the media (broad singlet around -160 ppm), in all three experiments. Longer evaporation times did not lower the amount of HF substantially either.

Despite the discouraging results, a trial was conducted to generate $ArIF_2$ through catalytic oxidation of PhI to PhIO. After three days, minimal conversion of the carbamate was observed, and no signals appeared in the ^{19}F-NMR spectrum.

Experiments aiming for the aminofluorination of cinnamyl carbamate generating the $ArIF_2$ in situ did not grant the expected results. However, this approach provided instrumental insights into the system's reactivity. Moreover, multiple subproducts have been identified and mechanisms explaining their formation have been satisfactorily formulated.

4.3.5. Strategy #3: Aminofluorination of Allyl Carbamates through Sequential I(III)-promoted Aziridination/Ring-opening with Fluoride Reagents

Based on the work done in our group by Giménez-Nueno *et al.*[11] related to the two-step I(III)-mediated aziridination of dienyl carbamates ring-opening with different O-, N- and S-heteroatomic nucleophiles to afford anti-heteroaromatic functionalized oxazolidinones, the analogous ring-opening of bicyclic aziridine **4.58** by a nucleophilic fluorine source was also explored as an alternative process for the construction of the β-fluoroamine scaffold.

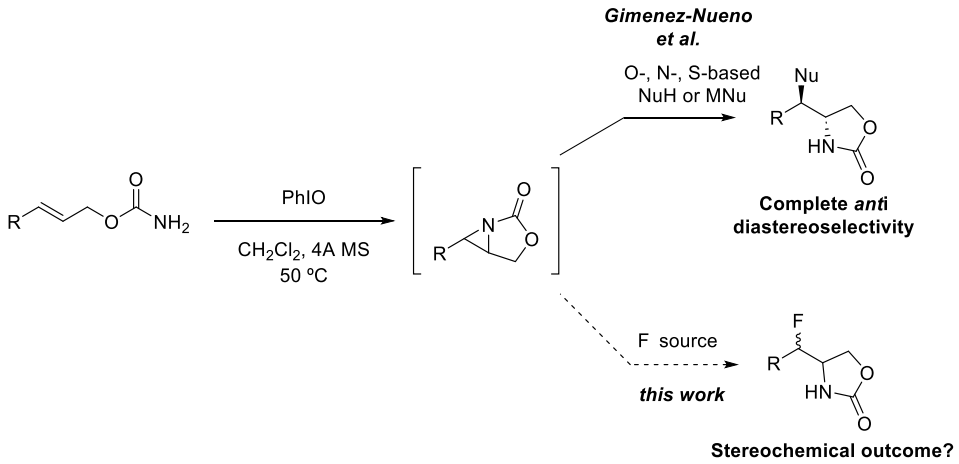

Scheme 4.51 General scheme for the sequential aminofluorination of allyl carbamates.

In this regard, a two-step procedure is proposed as an alternative to the one-pot aminofluorination of allyl carbamates exposed in the previous sections. As described before, the first step consists in the I(III-promoted aziridination of the allylic carbamate to obtain a bicyclic aziridine. Now, we sought to implement this protocol by exploring the ring-opening of the aziridine intermediate **4.58** with different nucleophilic fluorine sources in order to afford fluoro-oxaxolidinones, with special focus on the stereoselectivity control of the process.

Since the aziridination methodology has already been developed, the ring-opening of the corresponding aziridines will be the central part of the study.

4.3.5.1. I(III)-promoted Aziridination of Cinnamyl Carbamate

The aziridination of allyl carbamates has been an important field in our research group, specially focused on the metal-free intramolecular aziridination of dienyl carbamates. Hypervalent iodine reagents such as PhIO or $PhI(OAc)_2$ interact with the carbamate group to generate an iminoiodane intermediate. This nitrene equivalent then undergoes intramolecular cycloaddition with the alkene, forming a bicyclic *trans*-aziridine in a stereospecific way.

Cinnamyl carbamate was used as a model substrate to explore the sequential aminofluorination, as this would allow us to compare the results obtained with those of the one-pot process. Thus, cinnamyl carbamate was subjected to the standard aziridination conditions with PhIO. As expected, the exclusive formation of **4.58** was observed after 4 h with full conversion of the carbamate. The aziridine proved stable under the reaction conditions.

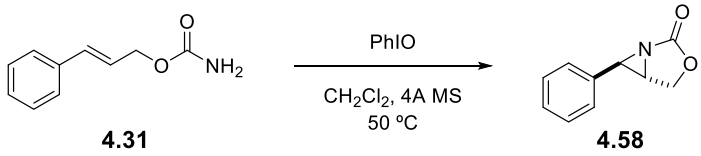

4.31 **4.58**

Scheme 4.52 Standard conditions for the aziridination of allyl carbamates applied to cinnamyl carbamate.

The aziridine was not isolated but directly submitted in the reaction mixture to ring-opening with fluoride sources. For all further experiments, complete conversion to the aziridine was assumed, as long as complete conversion of the starting carbamate is observed by TLC.

4.3.5.2. Fluorine Source Scope and Optimization of the Reaction Conditions

The ring opening of the cinnamyl carbamate-derived aziridine **4.58** was explored with a series of nucleophilic fluorine-containing reagents, namely TBAF, TMAF, KF, CsF. Additionally, acidic reagents in the form of B·HF complexes, such as Et_3N·HF, Py·HF and DMPU·HF, were also employed to assess the necessity of nitrogen activation with acid (via protonation or H-bonding) for the ring-opening reaction.[71] Finally, some optimization was performed to find the best conditions for the future experiments employing this methodology.

The use of basic nucleophiles such as TBAF or TMAF did not produce any conversion of the aziridine intermediate into the expected F-oxazolidinones (Table **4.8**, entries **13**, **14**). No reaction was observed either with the use of KF together with 18-crown-ether to increase the nucleophilicity of the fluoride (Table **4.8**, entry **15**). The use of ethylene-glycol or hydroxylic solvents had been described as a good strategy for the activation of fluoride from salts such as KF or CsF, through hydrogen-bonding.[72] In our hand, reaction with either KF in ethylene glycol or CsF in t-BuOH showed disappointed results promoting very low conversion of the aziridine into the corresponding F-oxazolidinone, which, judged by NMR was attributed exclusively to the syn-diastereomer (Table **4.8**, entries **16**, **17**). All experiments using acidic B·HF complexes resulted more competent, yielding diastereomeric *anti*/*syn* mixtures of F-oxazolidinones (Table **4.8**, entries **1**-**12**). As expected, DMPU·HF granted the biggest yield of the three HF complexes, with a noticeable improvement in yield over the other two reagents (Table **4.8**, entries **2**, **7**, **9**).

---

[71] a) Lee, J.W.; Yan, H.; Jang, H.B.; Kim, H.K.; Park, S.W.; Lee, S.; Chi, D.Y. *Angew. Chem. Int. Ed*. **2009**, *48*, 7683-7686; b) Kim, D.W.; Lim, S.T.; Sohn, M.; Katzenellenbogen, J.A.; Chi, D.Y. *J. Org. Chem*. **2008**, *73*, 957-962.

[72] a) Kim, D.W.; Song, C.E.; Chi, D.Y. *J. Am. Chem. Soc*. **2002**, *124*, 10278-10279; b) Kim, D.W.; Lim, S.T.; Sohn, M.; Katzenellenbogen, J.A.; Chi, D.Y. *J. Org. Chem*. **2008**, *73*, 957-962; c) Lee, J.W.; Yan, H.; Jang, H.B.; Kim, H.K.; Park, S.W.; Lee, S.; Chi, D.Y. *Angew. Chem. Int. Ed*. **2009**, *48*, 7683-7686.

Table 4.8. Table of the optimization of phenyl aziridine ring-opening with different fluorine sources.

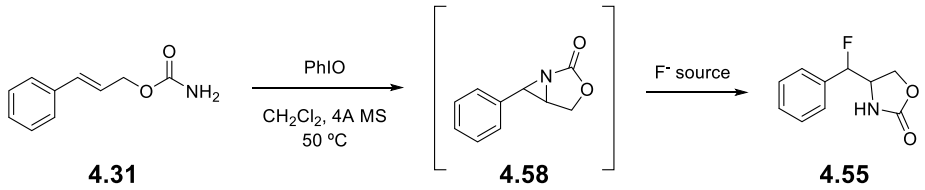

Entry	F⁻ source	F⁻ eq	Temp (ºC)	Yield (%)[a]	dr (anti/*syn*)[b]
1	$Et_3N{\cdot}HF$	26	-45	47	15:85
2	$Et_3N{\cdot}HF$	26	rt	40	15:85
3	$Et_3N{\cdot}HF$	7	rt	12	13:87
4[c]	$Et_3N{\cdot}HF$	26	rt	66	30:70
5[c,d]	**$Et_3N{\cdot}HF$**	**26**	**rt**	**77**	**32:68**
6	Py·HF	26	-45	26	75:25
7	Py·HF	26	rt	43	74:26
8	DMPU·HF	26	-45	52	74:26
9	DMPU·HF	26	rt	58	71:29
10	DMPU·HF	7	rt	55	71:29
11[c]	DMPU·HF	26	rt	69	76:24
12[c,d]	**DMPU·HF**	**26**	**rt**	**76**	**77:23**
13	TBAF	1.2	rt	-	-
14	TMAF	1.2	rt	-	-
15[e]	KF	2.5	rt	-	-
16[f]	KF	5	100	19	>1:99
17[g]	CsF	5	80	17	>1:99

Reaction conditions: Cinnamyl carbamate (0.1 mmol, 17.5 mg), PhIO (2 equiv, 44 mg), MS (100 mg, 1g/mmol of carbamate), CH_2Cl_2 (2.5 mL, 0.04 M). [a]Isolated yield. [b]Calculated by ^{19}F-NMR. [c]Filtration of the aziridine. [d]In propylene tube. [e]2,5 equiv of 18-crown-3 ether. [f]Triethylene glycol as solvent. [g] ^{t}BuOH as solvent.

Initial ring-opening assay with excess $Et_3N{\cdot}HF$ (26 equiv HF) at low temperature (-45 ºC) rendered 47% isolated yield of F-oxazolinone **4.55** as an 15:85 *anti*/*syn* mixture (Table **4.8**, entry **1**). Working at room temperature resulted in almost virtually the same results in terms of yield or selectivity (Table **4.8**, entry **2**) whereas the use of moderate excess of HF was detrimental for the reaction affording significantly lower yield (12%) (Table **4.8**, entry **15**). Likewise, the ring-process with Py·HF and DMPU·HF were also optimized. At low temperature (-45 ºC), reaction with Py·HF rendered **4.55** in comparatively lower yield (26%) but interestingly, with complementary 75:25 *anti*/*syn* stereoselectivity (Table **4.8**, entry **6**), in line with the reaction with DMPU·HF, which led to a 74:26 *anti*/*syn* selectivity but in higher 52% yield (Table **4.8**, entry **8**). Analogous reactions with Py·HF and DMPU·HF at room temperature resulted in slightly higher yields (43% and 58%, respectively) with almost no change in stereoselectivity (Table **4.8**, entries **7**, **9**). Results provided by Py·HF and DMPU·HF were quite similar in terms of stereoselectivity, with notably lower yields for Py·HF. Therefore, Py·HF was discarded as a fluorine reagent.

Revising the experimental procedure, it was envisioned that the remaining PhIO and/or MS could be somehow affecting the fate of the HF-promoted ring-opening process. Hence, the solids remaining after the aziridination step were filtered off. The ring-opening step was then carried out using the corresponding clear solution of aziridine in CH_2Cl_2 by addition of $Et_3N{\cdot}HF$ (26 equiv HF) at room temperature to afford F-oxazolidinone **4.55** in higher yield (66%) showcasing slightly diminished *syn* selectivity (30:70 *anti*/*syn* mixture, Table **4.8**, entry **4**). Analogously, when DMPU·HF was used after the filtration of the solids, F-oxazolidinone **4.55** was obtained following the same trend: higher yield (69%) and reduced *syn* selectivity (76:24 *anti*/*syn* mixture, Table **4.8**, entry **11**).

Following this line of thought, glassware could also be withdrawing HF from the system. Hence, a final refinement was implemented, comprising the separation of solids through filtration and the addition of

the aziridine solution into a polypropylene tube under inert conditions. This procedure yielded the desired F-oxazolidinones in good yield without sensible change in selectivity (Table **4.8**, entries **5**, **12**).

The increase in the *anti* isomer and in the yield observed with the removal of solids suggests that molecular sieves or/and PhIO are not innocent actors in the fate of the ring-opening step. This increase in the *anti* isomer could be explained in two ways: a) increase of HF excess in the absence of molecular sieves, known to capture/degrade HF or b) absence of PhIO, which could hypothetically form $PhIF_2$ in the reaction mixture, favouring the formation of the *syn* isomer (in line with the previous results described with $TolIF_2$). In the same direction, use of polypropylene tube would also result in the increase in HF causing an increase in the *anti* isomer).

All in all, convenient methods to obtain fluoro-oxazolidinones with complementary diastereoselectvity and good yield have been developed. These conditions will be used in upcoming experiments.

4.3.6. Sequential Aminofluorination: Mechanistic Study

As already carried out in the one-pot fluoroamination reaction with $TolIF_2$, we wanted to gain insight into the parameters that govern the sequential aminofluorination, in this case with special focus in the ring-opening using DMPU·HF and Et_3N·HF as fluorine sources. The rationale for the parameters to explore has already been detailed in Section **4.3.2.** Notably, substitution in the nitrogen and in the para position of the aromatic ring of the carbamate, configuration of the double bond and effect of the removal of the aromatic ring.

Additionally, the complementary stereochemical results obtained by the ring-opening of bicyclic aziridine **4.58** with Et_3N·HF and DMPU·HF (Table **4.8**) made clear the importance of the fluorinating complex in this reaction: In this regard, DFT calculations will help us understand the behaviour of HF as a nucleophilic agent and will grant valuable information about the process.

4.3.6.1. Effect of the Substitution in the Nitrogen of the Carbamate

Before diving into the ring-opening, the aziridination step was tested with *N*-substituted carbamates. Based on the aminoflorination of alkenyl sulphonamides described by Nevado[30] (Scheme **4.15**), the PhIO mediated aziridination of *N*-Ts-substituted carbamates was investigated. On one hand, the presence of an acidic proton might favour the activation of the I(III) reagent and, on the other hand, it could generate an analogous aminoiodane intermediate, instead of an iminoiodane, that could serve as a nitrene source for aziridination (Scheme **4.15**). In addition, the formation of an aziridinium intermediate would also favour ring-opening without the need for further activation. *N*-Bn-carbamates were also tested as a blank assay, as their acidity is similar to unsubstituted carbamates.

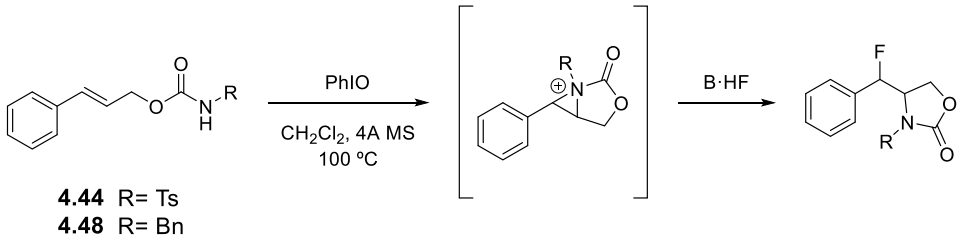

Scheme 4.53 Sequential aminofluorination of *N*-substituted cinnamyl carbamates.

However, PhIO-mediated aziridination of **4.44** and **4.48** did not afford any product and unaltered starting materials were recovered. This would suggest that the aminoiodane is not formed in the process. Since Ts-substituted carbamates are more acidic than tosylamides, it becomes apparent that acidity of the proton involved in the activation of the iodine is not the sole factor for the nitrene transfer effectiveness. The nitrogen attacking the iodine is probably not nucleophilic enough with two electron-withdrawing groups next to it. The iminoiodane intermediate appears necessary.

4.3.6.2. Effect of the Double Bond Configuration

The effect of the configuration of the alkene on the diastereoselectivity of the sequential process was explored for comparative purposes with the one-pot method. Therefore, the sequential aminofluorination of *cis*-cinnamyl carbamates was tested with either DMPU·HF or Et_3N·HF under standard conditions.

As expected from the results with $TolIF_2$, the *cis* alkene proved reluctant to the aziridination conditions. After a week, low conversion and low yield in aziridine were observed by TLC. Despite that, DMPU·HF and Et_3N·HF were tested for the ring-opening.

Table 4.9. Results of the aminofluorination of the *trans* and *cis* cinnamyl carbamates with DMPU·HF and Et_3N·HF.

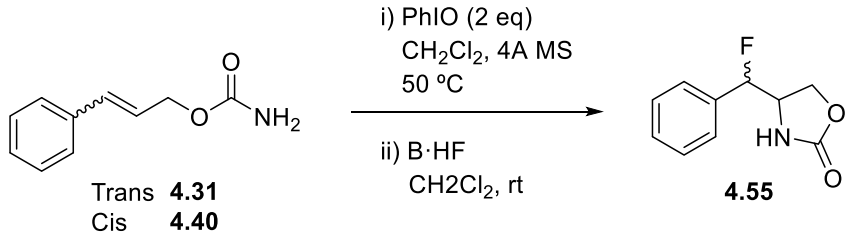

Trans **4.31**
Cis **4.40**

4.55

Entry	Config	F^- source	Yield (%)[a]	dr (anti/*syn*)[b]
1	Trans	DMPU·HF	76	77:23
2	Trans	Et_3N·HF	77	32:68
3	Cis	DMPU·HF	15	46:54
4	Cis	Et_3N·HF	18	75:25

Reaction conditions: Cinnamyl carbamate (0.1 mmol, 17.5 mg), PhIO (2 eq, 44 mg), MS (100 mg, 1 g/mmol of carbamate), CH_2Cl_2 (2.5 mL, 0.04 M), B·HF (25 equiv HF). [a]Isolated yield. [b]Calculated by ^{19}F-NMR.

The outcomes of the aminofluorination are somewhat unreliable due to the limited conversion in the aziridination step. However, there's no basis to assume that the small amount of aziridine produced does not react with HF. The possible big difference is that a very large excess of HF is introduced. Nonetheless, there are observable differences between experiments. For Et_3N·HF, a reversal on the diastereoselectivity if observed compared to that of the trans carbamate (Table **4.9**, entry **4** vs **2**). For DMPU·HF, the difference is less noticeable but still a change in the major isomer is observed (Table **4.9**, entry **3** with **1**).

4.3.6.3. Application of the Sequential Aminofluorination Conditions to Dienyl Carbamates

As stated in the general objectives, this methodology was explored en route to the development of C3-fluorinated sphingosine analogues. The starting point to achieve such analogues would be a dienyl carbamate.

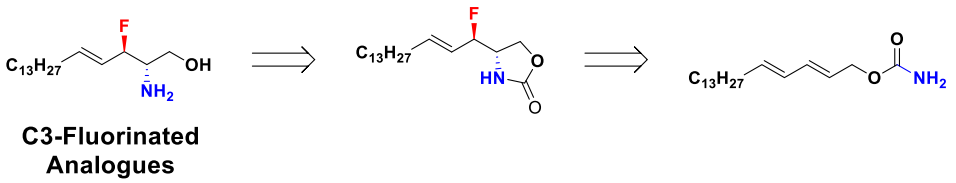

Scheme 4.54 Dienyl carbamates as primary source of C3-fluorinated sphingosine analogues.

To this end, the aminofluorination of simple methyl dienyl carbamate **4.43** as a simple dienyl carbamate was explored. Ring-opening of vinyl aziridines may present regioselective issue giving S_N2 and/or SN2' products..

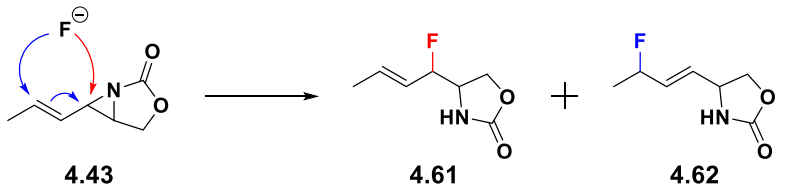

Scheme 4.55 Possible regioisomers for the ring-opening of allyl aziridine with fluorine.

Standard sequential aminofluorination conditions were tested with carbamate **4.43** with both DMPU·HF and Et_3N·HF. As already reported, aziridination proceeded readily at at 50 ªC to give full conversion to the vinyl aziridine Results of the subsequent ring-opening step with either DMPU·HF or Et_3N·HF are displayed in Table **4.10**.

Table 4.10. Results of the sequential aminofluorination of carbamate **4.43** with DMPU·HF and Et_3N·HF.

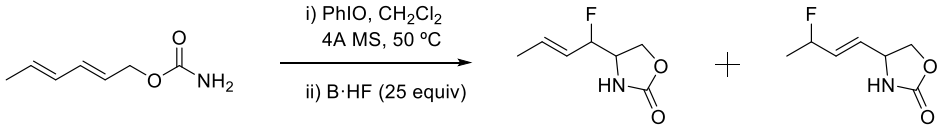

4.43 **4.61** **4.62**

Entry	F^- Source	T (ºC)	Yield 4.61 (%)[a]	dr 4.61 (*anti*/*syn*)[b]	Yield 4.62 (%)[a]	dr 4.62 (*anti*/*syn*)[b]
1	Et_3N·HF	rt	9	48:52	9	53:47
2	DMPU·HF	rt	15	65:35	13	51:49
3	DMPU·HF	0	17	75:25	10	51:49

Reaction conditions: i) Cinnamyl carbamate (0.1 mmol, 17.5 mg), PhIO (2 eq, 44 mg), MS (100 mg, 1 g/mmol of carbamate), CH_2Cl_2 (2.5 mL, 0.04 M), ii) B·HF (25 equiv HF). [a]Isolated yield. [b]Calculated by ^{19}F-NMR.

Experiments at room temperature with both HF complexes yielded equimolar mixtures of regiosiomeric products **4.61** and **4.62** arising from S_N2 and S_N2' processes, respectively, in poor yield (Table **4.10**, entries **1**, **2**). DMPU·HF afforded a marginally higher overall yield on the fluorinated products, which is coherent with the rest of the experiments. Taking into account the substantial impact of temperature in the selectivity observed towards **4.61** with $TolIF_2$, (Table **4.5**, entry **4**), the ring-opening of vinyl aziridine **4.58** with DMPU·HF was explored at 0 ºC. A slight increase in yield towards the formation of **4.61** to the detriment of **4.62** was observed at the low temperature (Table **4.10**, entry **3**). However, due to the minimal difference in yields and the generally low yields, drawing any significant conclusion is unwarranted.

Indeed, these preliminary results turned out quite underwhelming. Nonetheless, the sequential aminofluorination of dienyl carbamates still

has room for further optimization, although it unfortunately had to be discontinued due to time constraints.

4.3.6.4. Effect of the Substitution in the Aromatic Ring

Introducing EDG and EWG to the *para* position of the aromatic ring of cinnamyl carbamate would allow us to assess the sensitivity of the ring-opening to electronic changes. EDG are expected to stabilize a carbocation-like species along the process, while EWG should lead to a more covalent aziridine.

p-Substituted cinnamyl carbamates were subjected to standard sequential aziridination conditions with either $Et_3N{\cdot}HF$ and DMPU·HF. The table below shows the yield and the selectivity outcomes. The substituents are sorted by Sigma-Hammett parameter σ^+, a numerical representation of the electronic density introduced by a para substituent.[73] Therefore, the first substituent is the most electron-donating group (EDG), while the last is the most withdrawing (EWG).

Ring-opening of *p*-substituted phenyl aziridines with DMPU·HF yielded mixtures of *anti*/*syn* F-oxazolidinones in all cases (Table **4.11**). The results show a consistent trend: more EDG produce better yield and are more selective towards the *anti* isomer. Indeed, during the optimization phase starting from parent cinnamyl carbamate it was already observed that DMPU·HF favoured the *anti* isomer. All the tested carbamates yielded the *anti* isomer as the major isomer, despite more EWG showing eroded selectivity. Therefore, EWG comparatively favour the formation of the *syn* isomer, although it might have little influence in the selectivity.

[73] Hansch, C.; Leo, A.; Taft, W. *Chem. Rev.* **1991**, *91*, 165-195.

Table 4.11. Scope of *p*-substituted Cinnamyl Carbamates, aziridination + ring-opening with DMPU·HF. Results are conveyed in a double-bar graph for ease of interpretation.

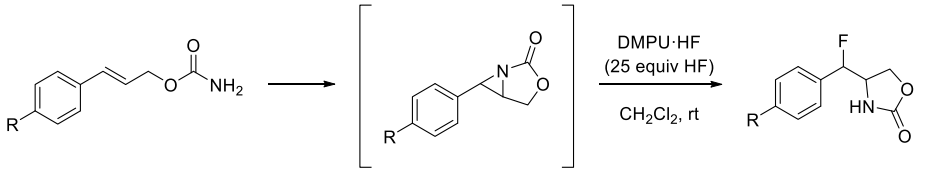

4.31 R=H **4.32** R=AcO **4.33** R=MeO **4.34** R=Me **4.35** R=Br **4.36** R=F **4.37** R=CF_3 **4.38** R=NO_2 **4.39** R=CN

4.55 R=H **4.63** R=AcO **4.60** R=MeO **4.64** R=Me **4.65** R=Br **4.66** R=F **4.67** R=CF_3 **4.60** R=NO_2 **4.68** R=CN

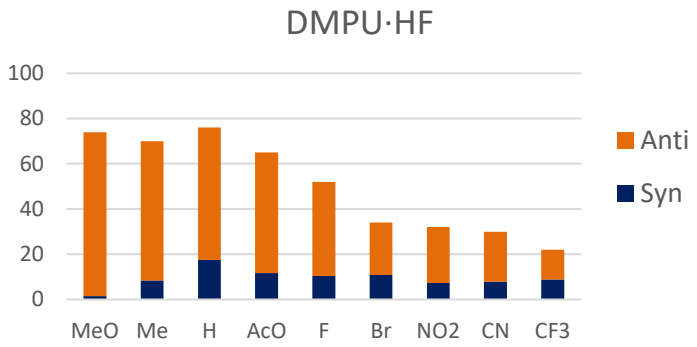

Entry	R	Yield (%)[a]	dr (*anti*/*syn*)[b]
1	MeO	74	98:2
2	Me	70	88:12
3	H	76	77:23
4	AcO	65	82:18
5	F	52	80:20
6	Br	34	68:32
7	NO_2	32	77:23
8	CN	30	74:26
9	CF_3	22	60:40

Reaction conditions: Cinnamyl carbamate (0.1 mmol, 17.5 mg), PhIO (2 equiv, 44 mg), MS (100 mg, 1g/mmol of carbamate), CH_2Cl_2 (2.5 mL, 0.04 M), DMPU·HF (25 equiv HF). [a]Isolated yield. [b]Calculated by ^{19}F-NMR.

Additionally, aziridines arising from reaction of carbamates **4.31-4.39** with PhIO were also submitted to ring-opening using $Et_3N{\cdot}HF$ as the fluorinating agent under the same reaction conditions. All of them yielded mixtures of F-oxazolidinones as well (Table **4.12**).

$Et_3N{\cdot}HF$ shows more disparity compared to DMPU·HF or $TolIF_2$. Nevertheless, decrease in yield and a preference for the *syn* isomer in EWGs are still apparent. Interestingly, a broad range of selectivity is observed with $Et_3N{\cdot}HF$, ranging from an 85:15 mixture in favour of the *anti* isomer for the MeO-derivative **4.33** to almost quantitatively *syn* isomer for CF_3-analogue **4.37**. This points out to DMPU·HF as a more powerful reagent able to produce *anti*-selectivity regardless of the substrate. The role of $Et_3N{\cdot}HF$ is less preponderant and is therefore more substrate-dependant.

Table 4.12. Scope of *p*-substituted cinnamyl carbamates, aziridination + ring-opening with $Et_3N{\cdot}HF$. Results are conveyed in a double-bar graph for ease of interpretation.

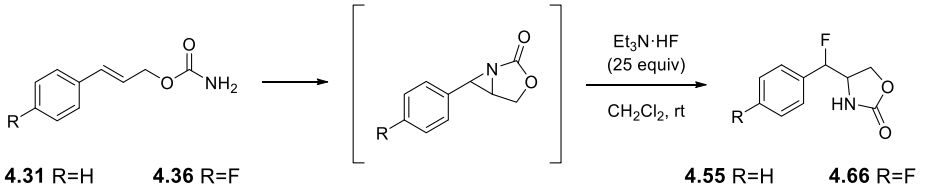

4.31 R=H **4.32** R=AcO **4.33** R=MeO **4.34** R=Me **4.35** R=Br **4.36** R=F **4.37** R=CF_3 **4.38** R=NO_2 **4.39** R=CN

4.55 R=H **4.63** R=AcO **4.60** R=MeO **4.64** R=Me **4.65** R=Br **4.66** R=F **4.67** R=CF_3 **4.59** R=NO_2 **4.68** R=CN

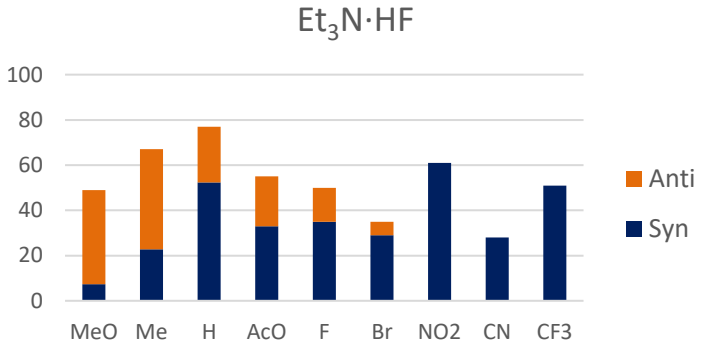

Entry	Z	Yield (%)[a]	dr (*anti*/*syn*)[b]
1	MeO	49	85:15
2	Me	67	66:34
3	H	77	32:68
4	AcO	55	40:60
5	F	50	30:70
6	Br	35	17:83
7	NO_2	61	1:99
8	CN	28	1:99
9	CF_3	51	1:99

Reaction conditions: Cinnamyl carbamate (0.1 mmol, 17.5 mg), PhIO (2 equiv, 44 mg), MS (100 mg, 1 g/mmol of carbamate), CH_2Cl_2 (2.5 mL, 0.04 M), $Et_3N{\cdot}HF$ (25 equiv HF). [a]Isolated yield. [b]Calculated by ^{19}F-NMR.

Looking at the experimental results, the role of electronics in the system becomes clear. Electronic density on aziridine favours *anti* isomer and enhances yield, as expected for a nucleophilic addition.

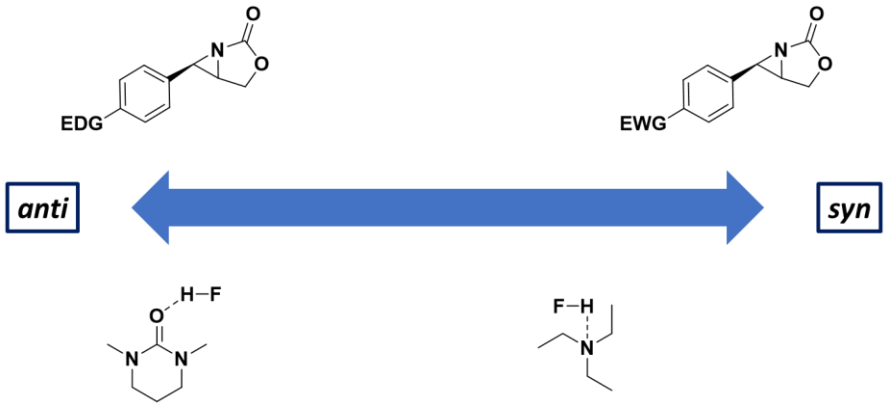

Scheme 4.56 Summarized selectivity trend of the *p*-substituted aziridines with DMPU·HF and Et_3N.

Regarding the fluorination reagent, the selectivity strongly varies using DMPU·HF or Et_3N·HF. The most crucial difference in properties between the two complexes is the acidity, so this probably plays a determining role in the process. It is observed that acidic environment promotes *anti* selectivity.

4.3.7. Hammett Plots

Substantial divergence in results using both fluorinating agents suggest different pathways for each B·HF complex. In order to have more information about the electronics of the system, Hammett plot experiments were set up.

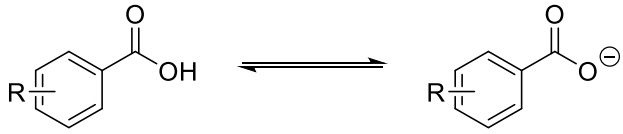

Scheme 4.57 General scheme for the ionization of benzoic acid, the system studied by Hammett to tabulate parameter σ

Hammett studied the variation of reactivity for the ionization of benzoic acid with the substitution in the *para* and *meta* positions of the aryl moiety (Scheme **4.57**).[74] He stablished a direct relationship between reaction rate and equilibrium constant, determining that an alteration of the equilibrium by substituting the *para* position of benzoic acid led to a consistent change in reaction rate following this equation:

$$\log\left(\frac{K}{Ko}\right) = \sigma\rho$$

K = Equilibrium constant
K_o = Equilibrium constant with H-substituent
ρ = Reaction constant
σ = Sigma-Hammett parameter

Scheme 4.58 Hammett equation for the relationship between *p*-substitution and reaction rate.

Subsequent investigations proved that this equation coincided also with similar systems bearing aromatic moieties close to the reaction site.[75] Therefore, this equation can reliably assess the sensibility of a reaction to

[74] Hammett, L. P. *J. Am. Chem. Soc.* **1937**, *59*, 96-103.
[75] a) Roberts, J. D.; Morelan, W. T. *J. Am. Chem. Soc.* **1953**, *75*, 9, 2167–2173. b) Taft, R. W.; Lewis, I. C. *J. Am. Chem. Soc.* **1958**, *80*, 10, 2436–2443.

electronic change in systems analogous to the ionization of benzoic acid and gain valuable insight in the mechanism of a reaction.

The Sigma-Hammett parameter (σ) is an experimental constant that depends on the substituent in the *para* position. It describes the amount of electronic density in the reaction site. It was arbitrarily assigned a value of 0 for H (K_o), and values for the other substituents are calculated experimentally. A wide library of σ for many functional groups has been built over the years.[73] EWG have positive σ values and EDG have negative σ values. A $\sigma>0$ implies $K>K_o$ (ρ will always be positive, so ρσ sign is dependent only on σ), meaning that the *p*-substituent displaces the equilibrium to product formation so reaction rate increases. In the ionization of benzoic acid, EWG stabilize the negative charge generated in the carboxylate, which displaces the equilibrium to product formation, increasing the reaction rate. On the other hand, EDG destabilize the product, lowering the reaction rate. Therefore, the bigger the σ, the more electron-withdrawing power.

The rho reaction constant (ρ) is a variable that depends on the reaction and on experimental conditions. Plotting the logarithm of the relation between the equilibrium constant of the Z-substituted and unsubstituted substrates *versus* σ for different *p*-substituted substrates, ρ is calculated as the slope of the obtained function (Scheme **4.59**). The sign and magnitude of this parameter, together with the general shape of the regression, gives information about the sensitivity of the reaction to changes in the *para* position (electronic variation). An absolute greater value correlates to a system more sensible to electronic changes. The sign of ρ shows the charge in the rate-determining step of the transformation. A positive slope means that negative charge is building up in the TS, while a negative slope indicates positive charge formation.

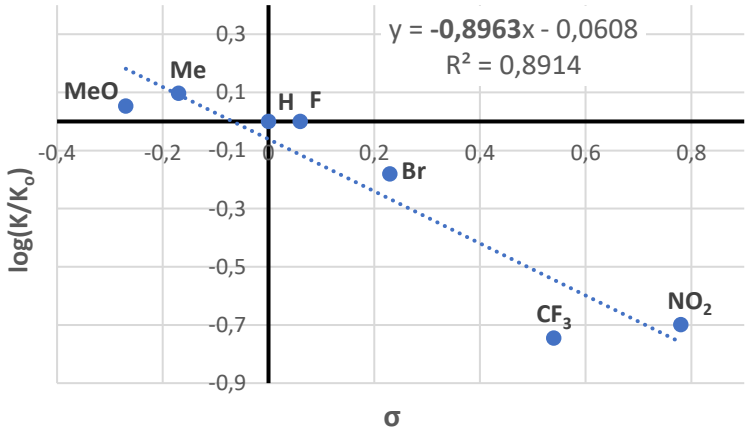

Scheme 4.59 Example of a lineal regression with different *p*-substituents. The value of the slope determines the electronic features of the reaction.

Equilibrium constants K and K_o depend on the concentration of the reagent, their reaction order magnitudes, temperature, molar activities and many other experimental factors. In order to simplify the equation and salvage the variables that are tricky to manipulate, a standard procedure was developed.

Hammett experiments are competition experiments, where both the unsubstituted and the *p*-substituted substrates are mixed together and submitted to the reaction conditions. This facilitates a couple of things: first, this allows to substitute concentration values by integration values in the NMR spectra. Second, this ensures that both reactions are being carried out under the same conditions (*k* [constant including all non-substrate-dependent variables] and concentration of the other reagents can be mathematically cancelled (Scheme **4.60**). Moreover, the reactions are forced to be of first order in the substrate by adding a large excess of the other reagents (a=1, Scheme **4.60**). Finally, the experiment is measured in a very short reaction time. This way, variation of the excess reagent is negligible and thus can be cancelled in the equation. In other words, concentration of reagents other than the study subjects are considered

constant. With these conditions stablished, the final equation can be written:

$$log\left(\frac{K}{Ko}\right) = log\left(\frac{\cancel{k}\cdot[A]^{\cancel{a}}\cdot\cancel{[B]^{b}\cdot\ldots}}{\cancel{k}\cdot[Ao]^{\cancel{a}}\cdot\cancel{[B]^{b}\cdot\ldots}}\right) = log\left(\frac{[A]}{[Ao]}\right) =$$

$$\boldsymbol{log\left(\frac{I(A)}{I(A)o}\right) = \sigma\rho}$$

Scheme 4.60 Simplification of the Hammett equation for the experimental measure of parameter *ρ*. A = p-substituted substrate. a = Reaction order of A. B = reagent in excess. b = Reaction order of B. I = integration in the NMR spectrum.

The ring-opening of phenyl aziridines is an ideal candidate for a Hammett plot. The reaction site is adjacent to an aromatic group, and B·HF is used in large excess. One difference that may cause divergence is the resonance effect of the substituents. In the deprotonation of benzoic acid, resonance in the aromatic group plays little to no role as the carboxylic group is not connected, but the reaction site in the ring-opening of the tested aziridines is in a benzylic position, which could be affected by resonance effects. Other σ parameter libraries were built using systems with resonance effect, called σ^+ and σ^-. These constants work identical to σ but consider both inductive and resonance effects. For the system in hand, σ^+ is *a priori* the most suitable parameter to use since resonance forms generate positive charge in the reactive position. σ^+ values were calculated from the solvolysis of tertiary benzyl chloride since the benzylic position allows for electron delocalisation around the ring.

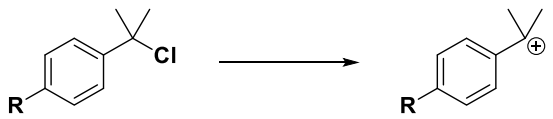

Scheme 4.61 General scheme for the model studied to tabulate σ^+ corresponding to the solvolysis of tertiary benzylic chlorides.

When the lineal regression has a good coefficient of determination (R^2) it is generally considered that the full series follows the same reaction mechanism. On the other hand, when multiple mechanisms are involved with different *p*-substituents, disparity is observed in the Hammett plot. For example, the system portraited in Scheme **4.62** was studied with a Hammett plot where σ^+ was plotted *vs.* the logarithm of the ratio of the two products (log K_{az}/K_s).[76] The study features the following experiment: substitution reaction of secondary benzylic substrates containing good leaving groups with azide as a nucleophile. Hammet competition experiments were performed using differently substituted substrates using azide or solvent as compering nucleophiles.

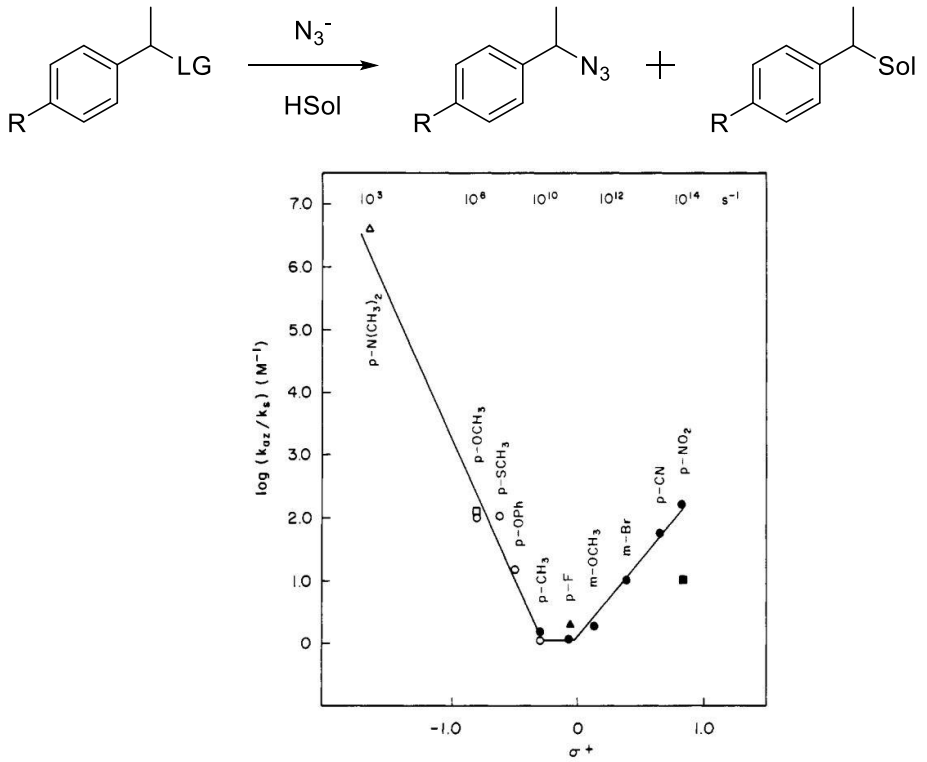

Scheme 4.62 Example of a non-linear Hammett plot, indicating a change in the mechanism.

[76] Richard, J. P; Jencks, W. P. *J. Am. Chem. Soc.* **1982**, *104*, 4689-4691.

Looking at the graphic, there is an evident break. Substituents in the negative σ^+ zone (EDG) give more azide product, near-zero σ^+ substituents give a valley of similar amount of both products and, finally, positive σ^+ (EWG) start to yield azide product again. The presence of two limbs was described to be due to a switch in the reaction mechanism from S_N1 to S_N2 that occurs as the carbocation intermediate stability decreases. The negative slope in the negative σ^+ zone indicates an accumulation of positive charge in the transition state, which coincides with a carbocation formation (S_N1). As the carbocation is destabilized, the ratio decreases. In the positive area, the slope changes to a positive sign, meaning that negative charge is building up, as happens in the S_N2 mechanism. This TS is stabilised by EWG so as σ^+ increases the ratio of azide product also rapidly increases.

In our systems, two series of competition experiments were set between unsubstituted aziridine and each of the *p*-substituted aziridines using DMPU·HF or Et_3N·HF, respectively. The reaction outcome was monitored by ^{19}F-NMR spectroscopy. The products are a pair of *anti*/*syn*-F-oxazolidinones for each aziridine, for a total of 4 signals in the spectra. As the Hammett equation studies only reaction rate, not selectivity, both diastereomeric signals were added up. With the results, log (I/Io) *vs*. σ and σ^+ were represented as a function (Figure **4.9**).

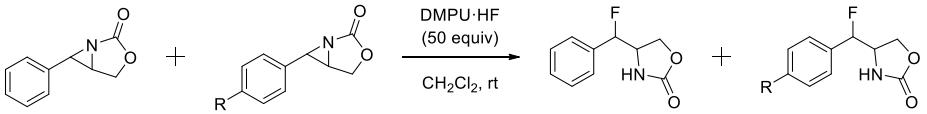

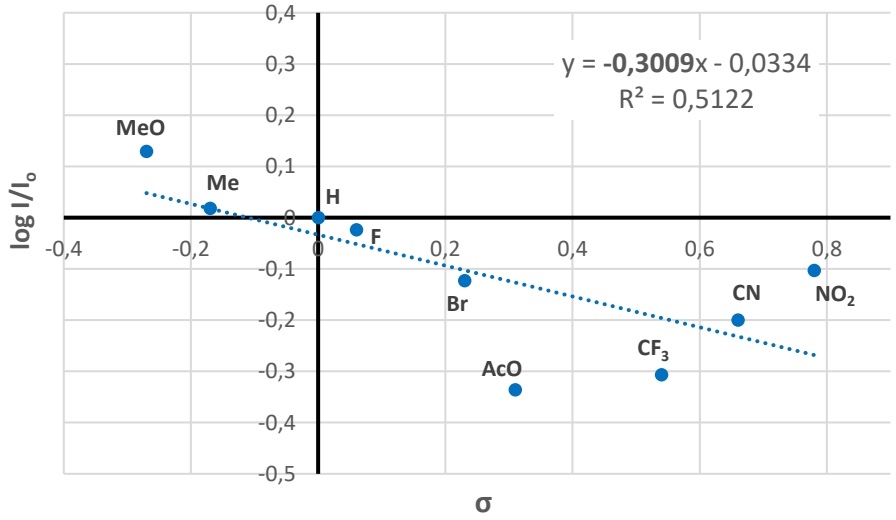

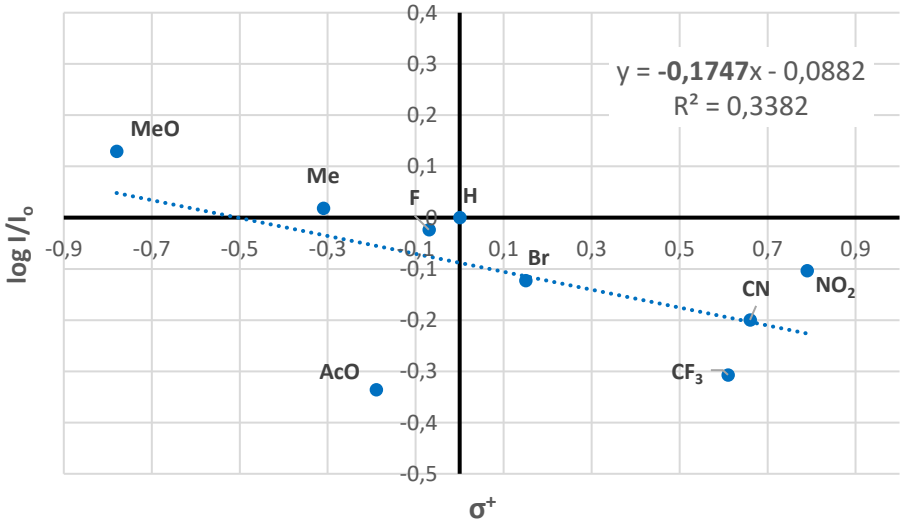

Figure 4.9. Hammett plot of the ring-opening of aziridines with DMPU·HF using the σ (Top) and σ⁺ (Bottom) parameter.

Hammett plot of the ring-opening of bicyclic aziridines using DMPU·HF (50 equiv HF) showed a non-linear correlation. At first glance, the plot appears to fit more accurately into a V-shaped reactivity-selectivity curve for these reactions. The more EDG plot a good downwards regression, denotating positive charge accumulation in the TS. However, between AcO and CF_3, there is a clear inflection point, and the plot continues upwards. This indicates a switch to a negative charge in the TS as more EWG remove charge from the system. With this information, the graph was split into two separate regions: aziridines bearing more EDG (referred from now on as "EDG") and aziridines bearing more EWG (referred as "EWG"). Two linear regression plots were drawn (Figure **4.10**).

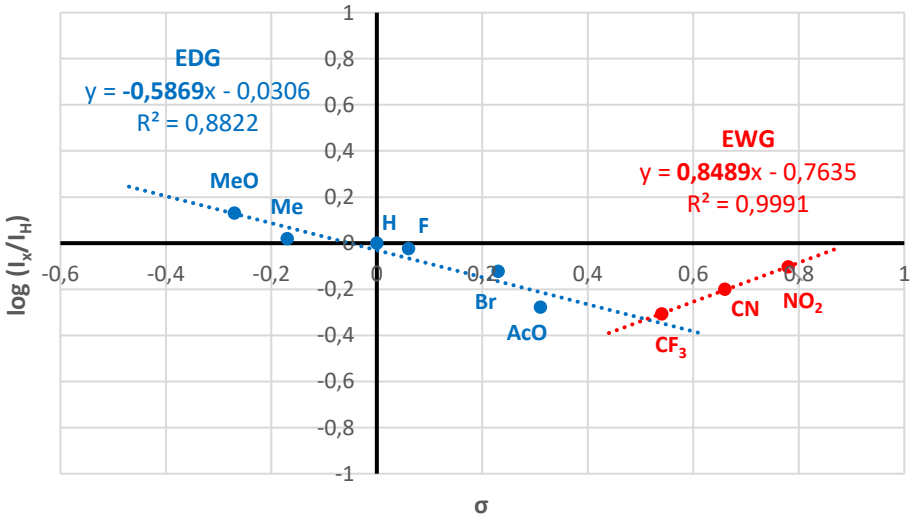

Figure 4.10. Hammett plots of the ring-opening of aziridines with DMPU·HF divided by the inflexion point.

To our delight, construction of two separate Hammet plots within each class of groups showed better correlation. This fact would lead us to a scenario where the mechanism operating for electron-poor substrates is different from that of electron-rich substrates. The slopes of the separate Hammett plots, with small absolute values ($\rho<1$), would suggest that no significant charge is being developed in any of the two possible transition

states, although EWG correlation shows a slightly larger absolute value, closer to 1.

The negative ρ sign in EDG suggests that positive charge is being developed at that transition state. Conversely, EWG show a positive slope, indicating that negative charge is building up in the transition state. It is also worth mentioning that the best correlations were observed using σ parameter, which implies low participation of the resonance effect in the TS of either part (See Annex for the other parameters' graphs).

Notably, when using σ^+, the data point corresponding to the p-OAc substituted substrate **4.32** seems to lie outside the linear regression (Figure **4.9**, bottom). This could be explained by the acidic medium provided by DMPU·HF, which is expected to protonate the acetate moiety, substantially increasing its withdrawing power by induction. Unfortunately, σ or σ^+ values for the $AcOH^+$ group are not available. Given its high electron-withdrawing character, it is reasonable to assume that it might be higher than that of AcO or H, and therefore a better alignment with the linear correlation function would be expected.

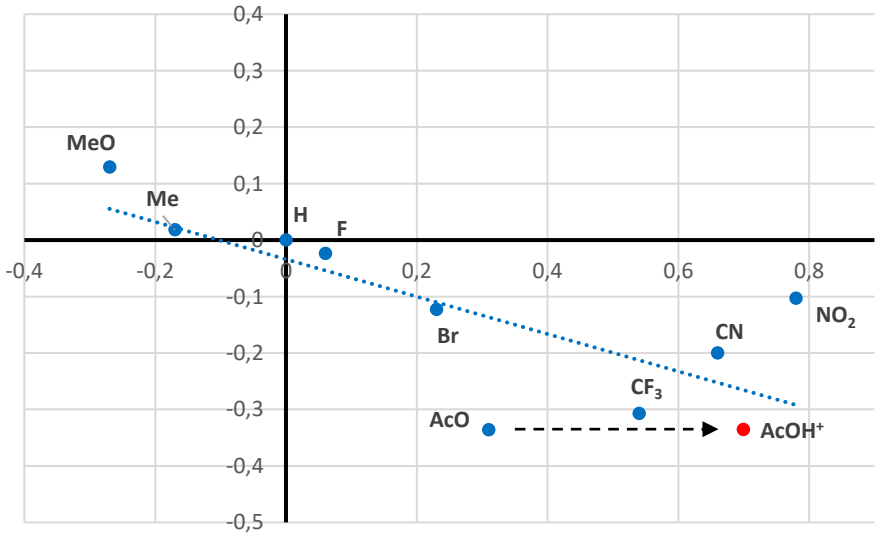

Figure 4.11. Speculative simulation of the shift of the AcO data point in the Hammett plot upon protonation ($AcOH^+$) in the reaction mixture.

Likewise, the same procedure was applied for the competitive experiments using $Et_3N{\cdot}HF$ as the fluorinating agent.

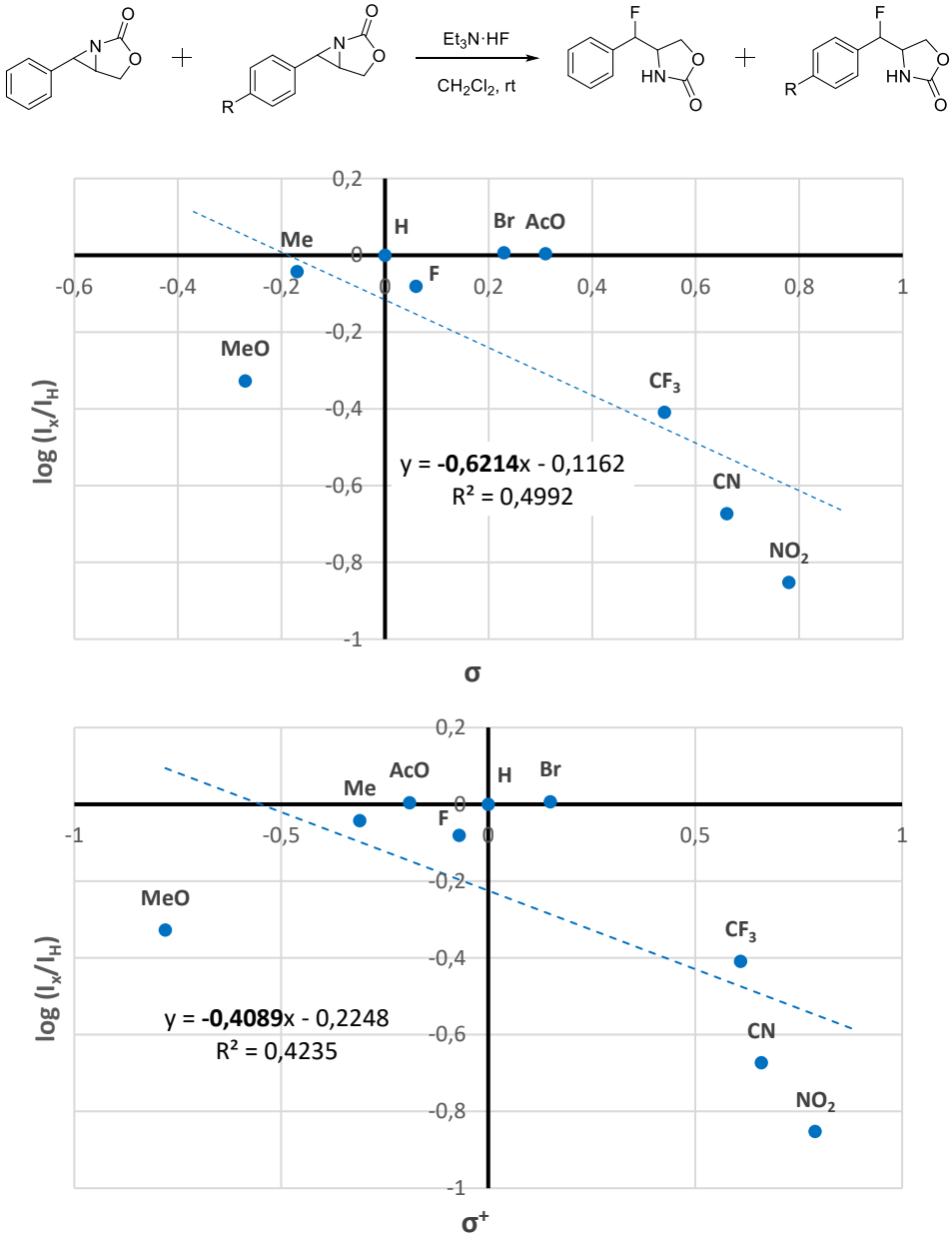

Figure 4.12. Hammett plot of the ring-opening of aziridines with $Et_3N{\cdot}HF$ using the σ (Top) and σ^+ (Bottom) parameter.

Surprisingly, $Et_3N{\cdot}HF$ plots display an inverted V-shape plot compared to the DMPU·HF graphics (Figure **4.9**). In fact, the inflection point is located in a similar spot, near the AcO point. This shows that the ring-opening with $Et_3N{\cdot}HF$ also features two distinct mechanisms depending on the electronics of the substrate. Since there is no linear correlation for the whole series, the two groups separated by the inflexion point are again plotted separately.

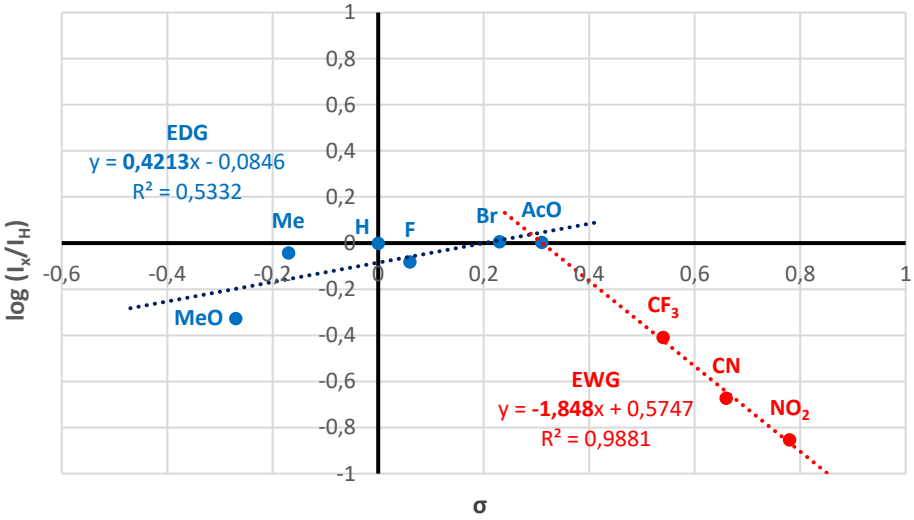

Figure 4.13. Hammett plots of the ring-opening of aziridines with $Et_3N{\cdot}HF$ divided by the inflexion point.

Data points from EWG showed good correlation, inferring one mechanism for all points. The absolute value of the slope is considerable (1.8), being larger than 1, thus inferring that some positive charge must be built up in the transition state. Instead, EDG correlation is unacceptable. The high dispersity might point towards competing mechanisms.

The Hammett plots confirm that the ring-opening step of the sequential aminofluorination presents two different mechanisms depending on the electronic structure of the substrate and on the fluorinating reagent.

4.3.8. DFT Calculations

Hammett plots confirmed the existence of two mechanisms in the ring-opening of aziridines. Nonetheless, the origin for the diastereoselectivity remains unknown. For this reason, DFT calculations were performed in collaboration with Maseras *et al*.

Since the different mechanisms are dependent on the electronic structure of the substrate, two aziridines with extremely opposite electronic nature were chosen for the study: MeO- and NO_2-p-substituted aziridines. For the sake of simplification, the ring-opening was modelled with HF as the fluorinating agent. These results might provide satisfactory insight in the structure of the feasible transition states of the sequential aminofluorination with DMPU·HF and Et_3N·HF, and perhaps also about the one-pot aminofluorination with $TolIF_2$. The aim of this study was to:

1. Identify the fluorinating agent in the direct aminofluorination with either $TolIF_2$ itself or HF generated in the reaction mixture after the aziridination step, to assess whether modelling with HF is valid for the system.

2. Explain the origin of the *syn* and *anti* selectivity. Hammett plots, together with the ring-opening experiments, might point towards separate mechanisms for the two isomers.

3. Provide a reason for the dependence of the selectivity on the nature of the Z substituent in the aromatic ring. In general, electron-poor carbamates display higher *syn* diastereoselectivities compared to the electron-rich analogues. The electron-donating capacity of the aromatic ring might influence both the electrophilicity of the benzylic position and the basicity of the nitrogen in the aziridine, two factors that might result crucial for the selectivity of the process.

4.3.8.1. Nature of the Fluorination Agent: TolIF$_2$ vs. HF

The study first sought to assess the feasibility of possible routes leading to the *anti* or *syn*-fluorinated products, by calculating the free energy barriers for different transition states arising from reaction of the *p*-NO_2 substituted carbamate.

The first issue the DFT sought to address was gaining insight into the nature of the actual fluorinating reagent in the one-pot TolIF$_2$-promoted aminofluorination process. Hydrogen fluoride is assumed to be released during the reaction, but whether HF or TolIF$_2$ is the actual fluorinating source for the ring-opening of the aziridine intermediate is not clear. If some form of HF is the main fluorinating agent, direct parallels could be drawn with the ring-opening processes conducted with DMPU·HF or Et_3N·HF.

To shed some light in the matter, DFT calculations were performed for the ring-opening of the aziridine intermediate with both HF and TolIF$_2$ as the molecule bearing the delivered fluorine (Figure **4.14**). *p*-NO_2-Substituted aziridine was used as the model substrate for the sake of comparison in later sections.

Analysing the energy barriers of all the proposed TS, it became clear that the participation of the I(III) reagent in the ring-opening step is quite demanding. The TS involving TolIF$_2$ (**TSI**) presents a high energy barrier (48.4 kcal/mol), even larger than those calculated for the transition states involving monomeric HF leading to either diastereomer (***anti*-TS1** 42.2 kcal/mol, ***syn*-TS1** 39.8 kcal/mol). Furthermore, other proposed TS structures involving iodine as a secondary activation agent also displayed higher barriers that ***anti*-TS1** and ***syn*-TS1** (See Annex, Figure **S3**), which may rule out any participation of iodine in the ring-opening step.

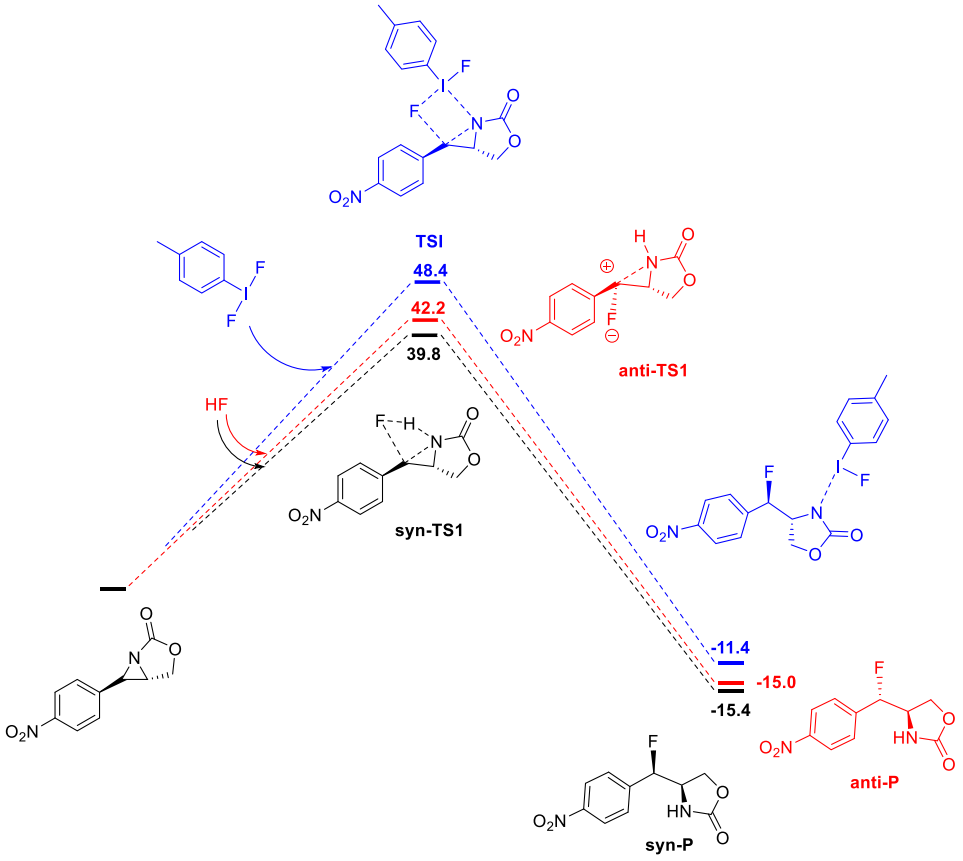

Figure 4.14. Free energy profiles (kcal/mol) for the formation of the *syn* and *anti* products derived from the NO_2-*p*-substituted aziridine with FF and TolIF$_2$.

Nevertheless, the high energy barriers obtained for transition states involving the participation of a single HF molecule made us assume that the process is unfavourable under the experimental conditions. Other possible routes envisaging the ring-opening process by hydrogen-bonding-assistance with the participation of hydrogen fluoride networks were also considered (Figure **S2** in the Annex). The number of HF molecules and the interaction position were assessed. Most of them also showed high energy barriers except for transition states **syn-TS3** and **anti-TS3** leading to either the *syn*- or the *anti*-fluoro oxazolidinones, which were calculated to be 26.8 kcal/mol and 29.1 kcal/mol, respectively (Figure **4.15**). These energy barriers could be considered in agreement with a

feasible process under the reaction conditions, and furthermore, could explain the obtained diastereoselectivity.

In conclusion, it can be assumed that HF acts as the main fluorinating agent in all three methods, as a network of HF molecules linked by H-bonding. With that, modelling of the ring-opening of aziridines with HF should adjust to the three systems.

4.3.8.2. Origin of the anti/syn Selectivity

As explained before, NO_2- and MeO-p-substituted aziridines were modelled with HF for the obtention of *syn* and *anti*-F-oxazolidinones. DFT calculations are showed in Figure **4.15** and Figure **4.16** respectively. The calculations show that *syn* isomer should be obtained as the major isomer in all cases. Energy barrier difference between the *syn* and *anti* TS is 2.3 kcal/mol for NO_2, enough to observe complete *syn* selectivity, and 1.1 kcal/mol for MeO, which could lead to *anti*/*syn* mixtures with *syn* as the major isomer. Experimental results of the aminofluorination with $TolIF_2$ and the sequential aminofluorination with $PhIO/Et_3N{\cdot}HF$ seem to fit with the proposed TS (Table **4.6**, Table **4.12**). Instead, DMPU·HF shows the opposite selectivity (Table **4.11**). It is possible that enhanced acidity would stabilize the intermediate **anti-I2/3** and therefore lower the overall energy of the pathway, thus giving more *anti* product.

Calculations with both substrates propose similar pathways for *syn* and *anti* isomers:

1. The *anti* product is obtained through a high energy *N*-protonated aziridinium intermediate (***anti*-I2/3**). *Anti*-fluoride delivery is then assisted via H-bonding with the H1-protons of the aziridine.

2. The *syn* product is obtained through a non-protonated intermediate (***syn*-I2/3**). *Syn* fluoride delivery is assisted via H-bonding of a trimeric HF cluster to the aziridine nitrogen as the hydrogen acceptor.

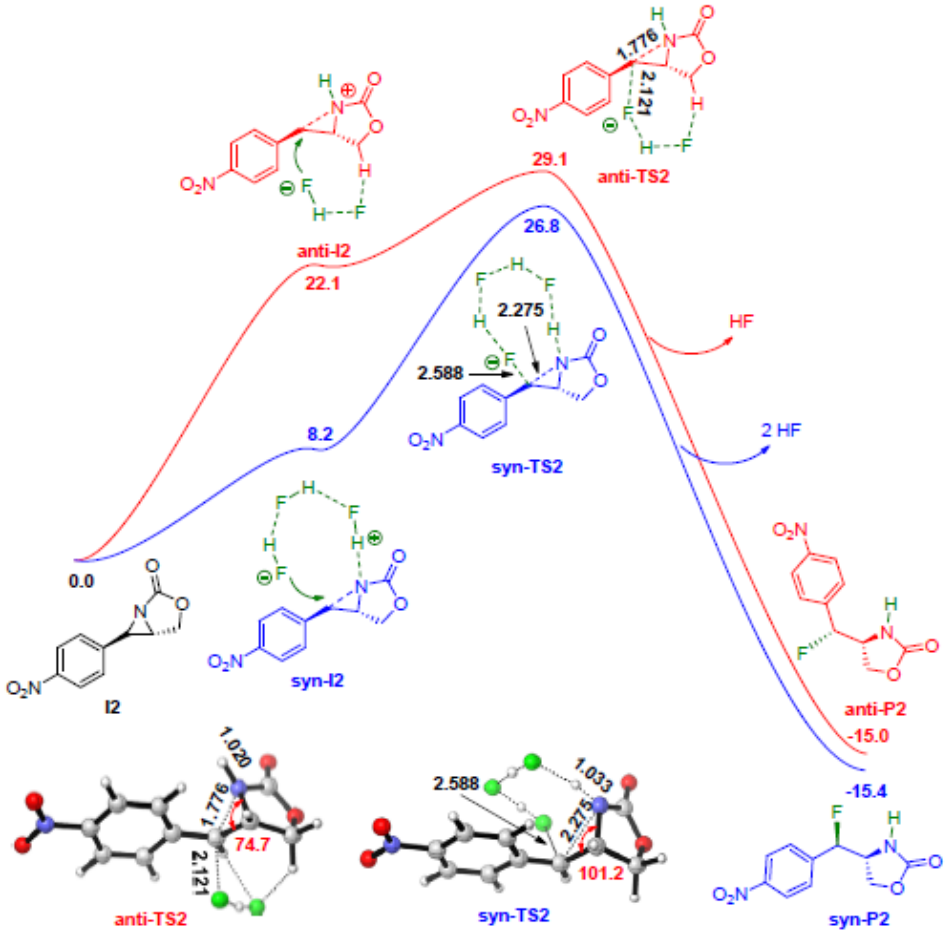

Figure 4.15. Free energy profiles (kcal/mol) for the formation of the *syn* and *anti* products derived from the NO_2-*p*-substituted aziridine. Structures for the key transition states at the bottom.

Initial protonation of the aziridine seems to be the decisive factor for the selectivity of the reaction. Protonation of the aziridine appears to prevent the H-bonding interactions between HF and the aziridine necessary for *syn* nucleophilic attack. Instead, backside S_N2-like ring-opening takes place.

Henceforth, if the protonation is a determining event, the prevalence of the protonated intermediate ***anti*-I2/3** would be expected to depend on the acidity of the medium. Thus, higher *anti* selectivity should be expected for DMPU·HF, the most acidic reagent, and higher *syn* selectivity for the least acidic $TolIF_2$. $Et_3N{\cdot}HF$ has intermediate acidity, so a mixture of both should be expected. This fits the experimental results obtained with the three reagents. Regarding the influence of the substituent, EDG are also expected to favour protonation and therefore yield more *anti* isomer, which also matches the results.

Examination of the structures of the transition states may provide additional information on the operating pathways. In the *anti*-pathway, proceeding through protonated intermediate ***anti*-I2**, the C-N bond and C-F lengths in ***anti*-TS2** (Figure **4.15**) are 1.766 Å and 2.121 Å, respectively, and more interesting, the C-C-N angle is 74.7º, a value that does not significantly differs from the angle of an aziridine, which would be in agreement with a tight S_N2-like transition state. However, this is not the case of the *syn*-pathway, proceeding through the hydrogen-bonding assisted intermediate ***syn*-I2** leading to the ***syn*-TS2** transition state, where both C-F and C-N bonds are longer (2.588 and 2.275 Å, respectively) and the C-C-N angle is significantly wider (101.2º). This can be due to the necessary steric relaxation that the transition state must undergo to make *syn* nucleophilic attack possible.

A priori, *syn*-fluoride delivery in ***syn*-TS2** would be expected to sacrifice more energy than that from the *anti*-face, because there is an electronic preference at the central carbon for *anti* processes. Nonetheless, the ***syn*-TS2** structure for the *syn* attack benefits from a substantial stabilization due to the favourable hydrogen-bonding interaction to the unprotonated nitrogen in ***syn*-TS2**.

Analysis of structural parameters in the transition states arising from the *p*-MeO-substituted carbamate **4.35** led to similar insights although with some differences (Figure **4.16**). If we compare bond

distances and the C-C-N angle in the aziridine for ***syn*-TS3** and ***anti*-TS3**, both the C-N and C-F bond lengths are longer in ***syn*-TS3** (C-N=2.062 Å and C-F= 2.896 Å in ***syn*-TS3** *vs.* C-N=2.479 Å and C-F= 1.894 Å in ***anti*-TS3**). Likewise, the C-C-N angle value for the ***syn*-TS3** is slightly wider than that observed for ***anti*-TS3** (89.3° and 80.7°, respectively) although here the difference is much less noticeable, with values that are intermediate to those observed for the *p*-NO_2 derivative (74.7° and 101.2° respectively).

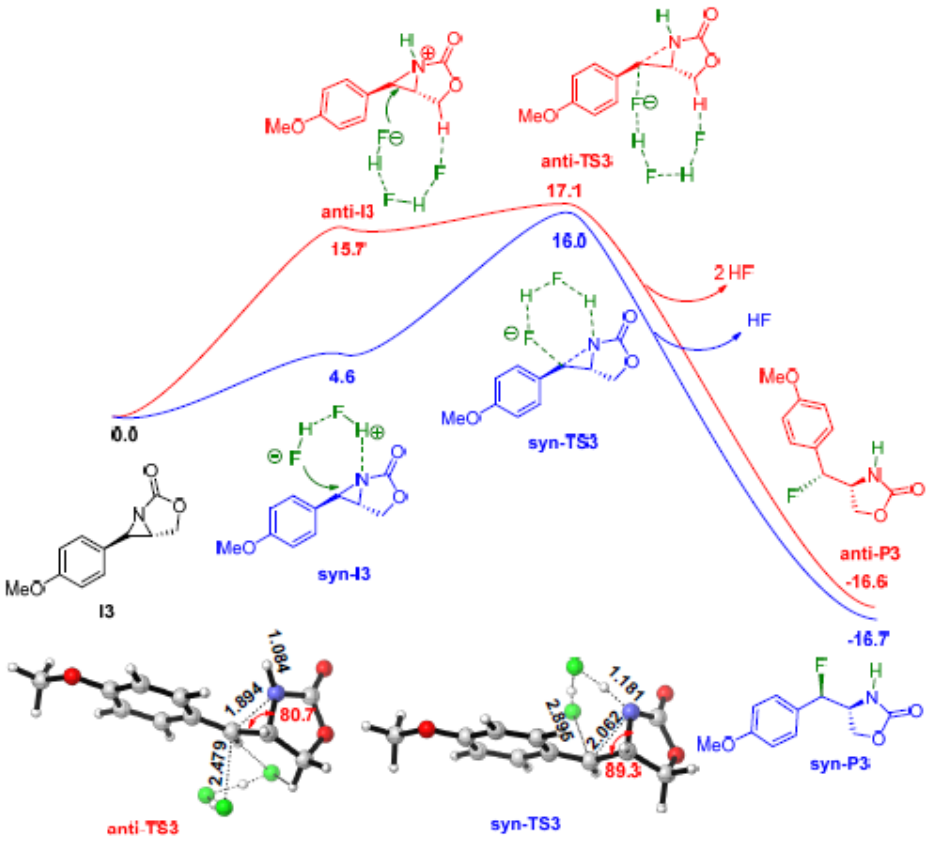

Figure 4.16. Free energy profiles (kcal/mol) for the formation of the *syn* and *anti* products derived from the MeO-*p*-substituted aziridine. Structures for the key transition states at the bottom.

Again, *syn* ring-opening would be expected to require more energy which, however, may be in part compensated by the stabilisation provided by hydrogen bonding interactions of the aziridine intermediate with the HF network. The calculated difference of 1.1 kcal/mol in favour of the ***syn*-TS3** could well explain the moderate *syn*-selectivity (40:60 *anti*/*syn*) observed in the one-pot aminofluorination of compound **4.33** with $TolIF_2$. However, the moderate *anti*-selectivity and the high *anti*-selectivity observed in the analogous ring-openings of *p*-MeO substituted aziridine coming from **4.33** with either $Et_3N{\cdot}HF$ or DMPU·HF do not correlate with the energy barriers obtained.

4.3.8.3. Dependence of Selectivity on the Nature of the Substitution of the Aromatic Ring

The intermediates and transition states proposed for the *p*-NO_2 and *p*-MeO substituted substrates show stabilization of the system when multiple HF molecules intervene in the ring-opening process (Figure **4.17**). The hydrogen bonding network most likely helps to share the charge among the HF and stabilize the system. The main structural difference between the two substrates is the number of HF molecules participating in the TS.

Further structural analysis of bond distances and angles may shed some light in the different selectivity of EWG and EDG-substrates. For ease of comprehension, the values are displayed in Figure **4.17**. In the case of the *p*-NO_2 substituted aziridine, the preferred ***syn*-TS2** displays longer bond distances (especially C-N) and wider-angle values, consistent with a more carbocation-like character in the non-protonated syn-TS. In contrast, ***anti*-TS2** appears to be a tighter TS. ***syn*-TS2** having more carbocation contribution than ***anti*-TS2** results counterintuitive, as protonation would generally lead to an elongated C-N bond, granting a bigger carbocation-like nature. This is also a hint that electronic issues are transmitted along the sigma skeleton, rather than involving π-electrons. With the MeO substrate, ***syn*-TS3** and ***anti*-TS3** differ less in their C-N distances/angles

and appear to correspond to an intermediate situation with the two TS of NO_2 derivatives.

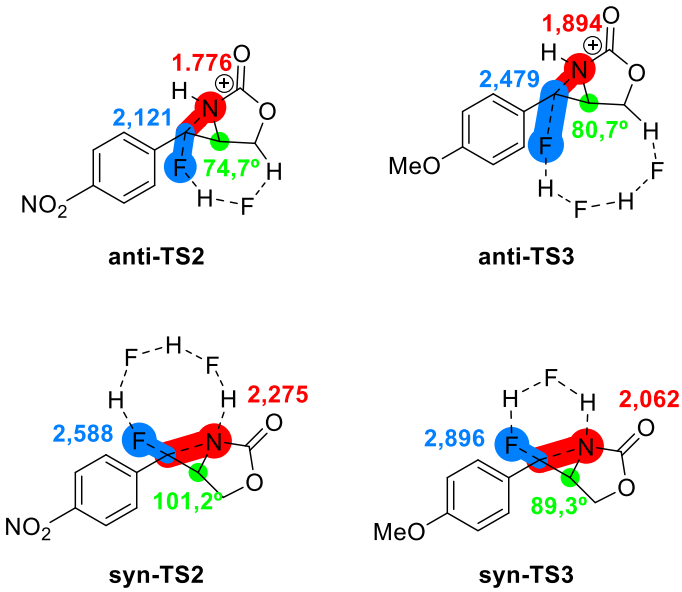

Figure 4.17. Relevant bond distances and angles of the proposed TS by DFT calculations of the ring-opening of MeO- and NO_2-substituted aziridines with HF.

As a final remark, DFT calculations were a very useful tool because they were able to draw specific pathways that explain the formation of *syn* and *anti-* products.

4.3.9. General Discussion

With the fragmented insights gathered from the experimental data, Hammet plots and DFT calculations, we sought to put all the pieces together to gain an overall overview of the aminofluorination mechanism.

Table 4.13. Compilation of the experimental results of the aminofluorination using the three studied fluorinating reagents.

	TolIF$_2$		**Et$_3$N·HF**		**DMPU·HF**	
R	**Yield (%)**	**dr (anti/syn)**	**Yield (%)**	**dr (anti:/syn)**	**Yield (%)**	**dr (anti/syn)**
MeO	72	40:60	49	85:15	74	98:2
Me	57	19:81	67	66:34	70	88:12
AcO	33	35:65	55	40:60	65	82:18
F	42	33:67	50	30:70	52	80:20
H	64	3:97	77	32:68	76	77:23
Br	48	9:91	35	17:83	34	68:32
NO$_2$	6	2:98	61	*syn*	32	77:23
CN	32	3:97	28	*syn*	30	74:26
CF$_3$	23	1:99	51	*syn*	22	60:40

Analyzing the diastereoselectivity outcomes obtained from the three reagents, the following trends can be observed:

- TolIF$_2$ renders F-oxazolidinone with overall *syn* diastereoselectivites (good for EDG and complete for EWG)
- NEt$_3$·HF ranges between moderate *anti* diastereoselectivities for EDG to complete syn diastereoselectivities for EWG
- DMPU·HF provides *anti*-diastereoselectivities, practically complete for EDG and moderately good for EWG

This leads to a scenario with two extreme situations ($TolIF_2$ and DMPU·HF) leading to *syn*- or *anti*-selectivities, respectively, that correspond to the least and the most acidic conditions. For Et_3N·HF, less acidic than DMPU·HF, the situation is intermediate. Moreover, the selectivity outcome is also tuned by the electronic properties of the *p*-substituent on the substrate. Thus, both reagents and substituents have influence in the selectivity of the process, as summarized below, especially significant for Et_3N·HF.

Table 4.14. Diastereoselectivity trend observed in the three aminofluorination methods.

	$TolIF_2$	**Et_3N·HF**	**DMPU·HF**
EDG	More syn	More anti	**Only anti**
EWG	**Only syn**	**Only syn**	More anti

DFT calculations propose the *syn* pathway as the lower energy mechanism. This fits the results of the one-pot aminofluorination with $TolIF_2$, but does not match with many of the sequential experiments performed with Et_3N·HF and any of the experiments with DMPU·HF. The influence of the complexing agents (DMPU and Et_3N) was not parametrized in the calculations and may play a part in the selectivity of the process.

The protonation of the aziridine nitrogen appears to be a decisive event for the chosen pathway. Protonation leads to *anti* formation, while non-protonated aziridine turns to syn selectivity, assisted by H-bonding from the aziridine nitrogen. DMPU·HF is a very acidic reagent, so it is safe to assume that in such acidic conditions aziridines would be extensively protonated, regardless of their electronic properties. This fact would then direct the stereoselectivity through the *anti* pathway, thus leading to high *anti* stereoselectivities. On the other hand, $TolIF_2$ is not acidic enough to protonate the aziridine in a significant amount, and an important *syn* selectivity is observed.

In an intermediate situation between DMPU·HF and $TolIF_2$, Et_3N·HF would give an intermediate selectivity. In this scenario, the substitution in the *para* position of the aryl moiety has a more relevant role in the diastereomeric outcome of the reaction. Electron-rich aziridines would be mainly protonated whereas less basic aziridines bearing electron-donating substituents would not be protonated, thus directing the ring-opening through the hydrogen-bonding assisted *syn* mechanism.

The existence of different operating mechanisms depending on the reagent and/or the substrate is also observed in the Hammet plots performed for the ring-opening of aziridines with DMPU·HF and Et_3N·HF.

DMPU·HF provided a shallow concave upwards deviation of the Hammet plot with slopes that displayed low magnitudes, suggesting low sensitivity to substituent effects. Each limb of the inflexion point shows good correlation, indicating different pathways for EDG- and EWG-aziridines. The low magnitudes of the slopes would indicate that the ring-opening is a quasi-concerted process with low charge accumulation in the reaction centre. EDG show a small negative slope (-0.4), pointing to small positive charge generation, and EWG show a slightly higher positive slope (+0.8) inferring some electronic density accumulation. These values could be associated with a tighter S_N2-like TS for EDG (Figure **4.17**, anti-TS2) or a looser S_N2-like TS for EWG (Figure **4.17**, anti-TS3).

Hammet plots obtained for the ring-opening reactions with Et_3N·HF provided two linear relationships with a concave downwards deviation of the Hammet plot, in contrast to DMPU·HF. The plots have two slopes of opposite sign (+0.4 for EDG groups and -1.8 for EWG). The magnitudes of the slopes suggest that substituent effects are negligible for EDG groups and slightly more noticeable for EWG. This piece of evidence would be consistent with the argument that a less acidic reagent such as Et_3N·HF would be able to protonate the aziridines bearing EDG to generate ***anti*-I3** and ***anti*-TS3**, but protonation will not be that extensive with the less basic aziridines bearing EWG and so the *syn* mechanism

through ***syn*-TS3** may then trigger. Moreover, the bad correlation of the $Et_3N{\cdot}HF$ plot with EDG (R^2=0,52) might suggest competing *anti* and *syn* mechanisms due to the lower acidity of $Et_3N{\cdot}HF$. For the ring-opening from aziridinium intermediates (through ***anti*-TS3**), the small magnitude of the slope suggests very low sensitivity to substituent effects, and would denote a concerted mechanism, as already seen for DMPU. The alternative *syn* pathway observed with aziridines bearing EWG could be rationalised proceeding through hydrogen-bonding assisted ***syn*-TS2**, which presents a longer C-N bond distance and a wider C-C-N angle (101.2º), reminiscent of a carbocation-like species where accumulation of positive charge takes place. This would explain the higher magnitude obtained for EWG (-1.8).

In conclusion, diastereoselectivity seems to be controlled by extensive or negligible protonation of the aziridine, which is mainly determined by the acidity of the reagent. The medium acidic $Et_3N{\cdot}HF$ has a less determinant role and thus the diastereoselectivity outcome of the reaction is ultimately modulated by substituent effects.

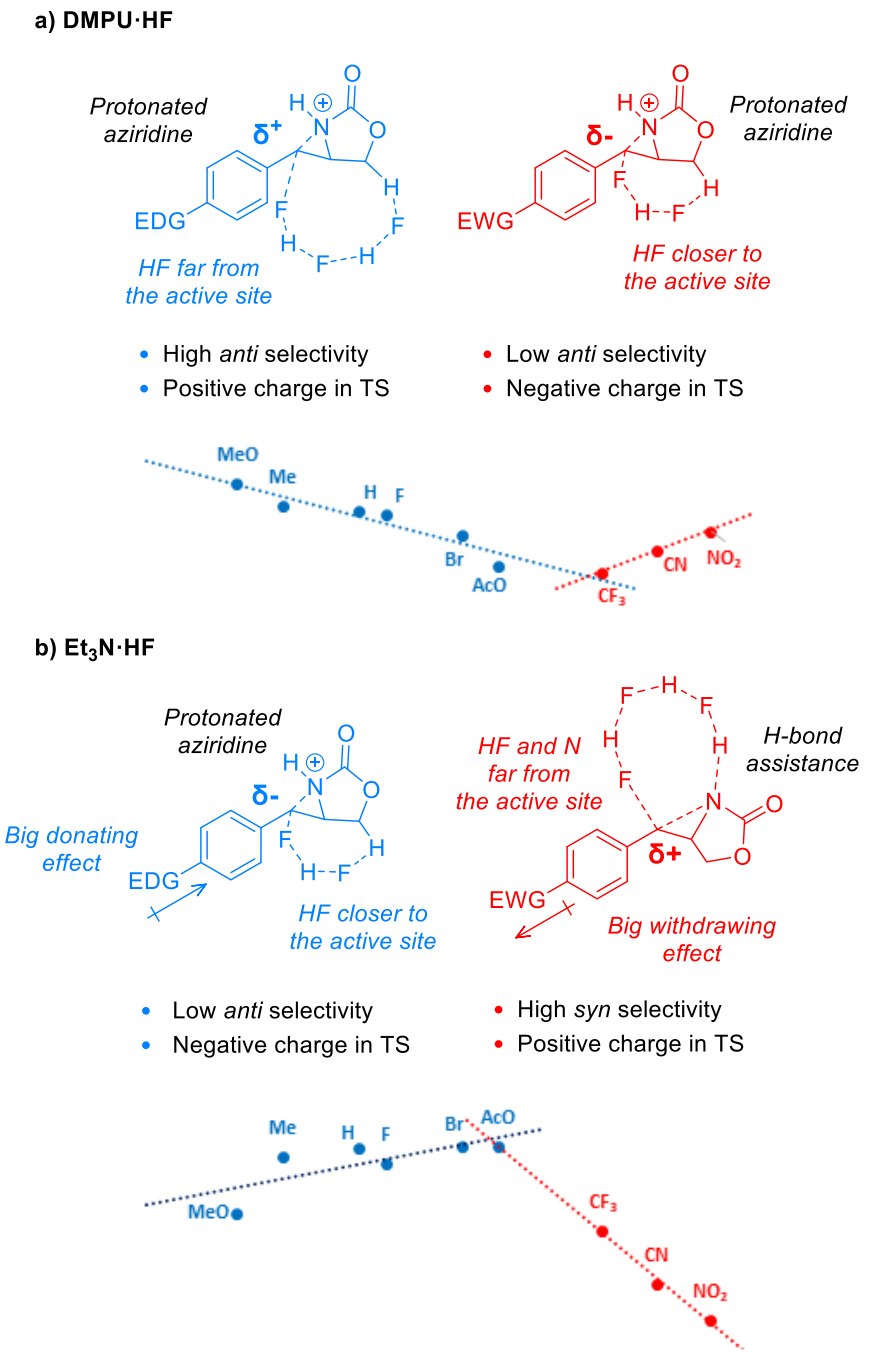

Figure 4.18. General scheme for the rationale of the p-substituted cinnamyl carbamate sequential aminofluorination with DMPU·HF (a) and Et_3N·HF (b)

To sum up the mechanistic study of the ring-opening of aziridines with fluorine reagents, the main points of the study are summarised below:

- The ring-opening with fluorine yields diastereomeric mixtures of *anti*/*syn* isomers with most substrates. This phenomenon was not observed with the same substrates using O, N or S-based nucleophiles.[11]

- Using $TolIF_2$ or $Et_3N{\cdot}HF$ as the fluorination agent leads to *syn* as the major isomer in most substrates. Instead, DMPU·HF yielded mostly the *anti* isomer. The acidity of the reagent heavily influences the selectivity of the transformation.

- Aziridines bearing electron-donating substituents led to more *anti* formation, while withdrawal furnished more *syn*. In line with the last point, more EDG increase the basicity of the aziridine.

- Hammett competitive studies of the ring-opening reaction with either DMPU·HF or $Et_3N{\cdot}HF$ led to deviations of the Hammet linear relationship suggesting that two competitive mechanisms are involved in the ring-opening, one more predominant for EDG-aziridines and the other becoming relevant for EWG.

- Different pathways were proposed using DFT compatible with the experimetrnal results. *Anti* isomer is formed via protonation of the aziridine followed by backside S_N2 fluorine nucleophilic ring-opening assited by hydrogen bonding to H1 in the substrate. H-bond assisted *syn* delivery of fluorine to an unprotonated nitrogen leads to the *syn* isomer.

After analysing all the obtained data, a deep understanding of the mechanisms of the reaction has been achieved.

4.4. Conclusions

Three different strategies for the aminofluorination of allyl carbamates have been studied. This transformation may lead to β-fluoroamine fragments, which are very relevant in medicinal chemistry. The main aim of this chapter is the elucidation of the mechanism of the transformations, as well as the exploration of its scope and stereoselectivity.

The first approach was the direct aminofluorination with $TolIF_2$. Experimental and/or computational evidence has been provided for the entirety of the process, and a final mechanism proposal has been stated. The summarized conclusions are as follows:

- $TolIF_2$-mediated aminofluorination of cinnamyl carbamate at 100 ºC yielded the targeted F-oxazolidinone in moderate yield (67%) as a 14:86 mixture of *anti*/*syn* diastereomers,. The transformation requires temperature.

- The first interaction between the carbamate and the hypervalent iodine is through to lead to the formation of an iminoiodane, which serves as the nitrene precursor for the next step. Formation of an aminoiodane and direct functionalisation of the double bond have been dismissed experimentally.

- Nitrene transfer from iodine to the double bond yields an aziridine intermediate. This species has been detected by NMR and can be isolated in the laboratory. This is in agreement with previous studies in our group.

- One-pot aminofluorination of cinnamyl carbamates bearing electron-donating substituent in the *p*-position of the aryl moiety led to the fluorooxazolidinone in higher *anti* selecitivities whereas almost complete syn diastereoselectivity was observed for electron-poor

substrates. Formal carbocation/radical intermediates are not involved in the process.

- The fluorinating agent in the ring-opening step was determined to be HF, generated during the formation of the iminoiodane, by means of DFT modelling.

- Exclusion of molecular sieves in the aminofluorination reaction with $TolIF_2$ led to decreased the syn diastereoselectivity, which could be explained by an increase of acidic conditions.

With all this evidence, a final scheme of the proposed mechanism is presented:

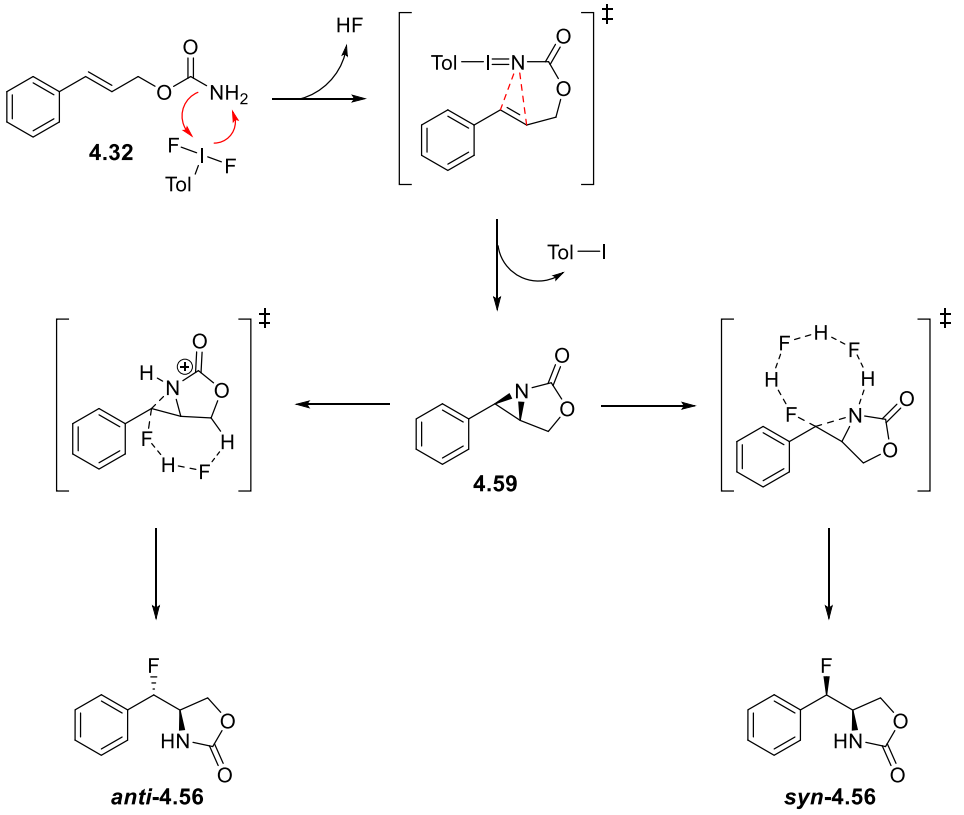

Figure 4.19. Proposed mechanism for the aminofluorination of cinnamyl carbamates with $TolIF_2$.

The second aminofluorination approach, featuring the *in situ* generation of $ArIF_2$ using PhIO as an Ar-I(III) reagent, and B·HF complexes, was also studied. The presence of excess HF in the reaction mixture turned out to be problematic. Free HF protonates the carbamate, preventing the formation of the iminoiodane and diverting the reactivity of the carbamate through the direct I(III) functionalisation of the alkene.

The final approach, the sequential aziridination + ring-opening with fluorination reagents, furnished good procedures for the diastereoselective formation of *syn* and *anti* fluoro-oxazolidinones. The ring-opening has been explored with several F^- sources, with a special interest in DMPU·HF and Et_3N·HF. The summarized conclusions are as follows:

- The aziridination procedure developed in our group can be extended to cinnamyl and many *p*-substituted analogue carbamates.

- Carbamates with substituted nitrogen do not undergo aziridination. This result agrees with the original hypothesis. The formation of the iminoiodane intermediate is not possible with substituted carbamates.

- DMPU·HF yields the desired *anti*-F-oxazolidinone with good yield and diastereoselectivity. Et_3N·HF complex delivers the *syn* isomer with also good yield and selectivity. An acidic fluorine source is necessary to open the aziridines in a satisfactory manner.

- EDGs in the *para* position of the aromatic ring favour the *anti* isomer whereas EWG show more *syn* selectivity and lower yields.

- Hammett plots reveal a shift in mechanism between electron-poor and electron-rich aziridines. Plots for DMPU·HF and Et_3N·HF as the fluorinating agent show inverse curve.

- DFT calculations on the ring-opening step from the aziridine to the F-oxazolidinone product identified two feasible pathways leading to each of the diastereoisomers, unveiling the importance of HF clusters and the assistance of hydrogen bonding interactions. The protonation of the aziridine is a crucial event.

Expansion of the scope to dienyl carbamates as the first step towards C3-fluorinated sphingosine analogues resulted challenging due to low conversion and regioselectivity problems with the conjugated addition to the intermediate vinylaziridine. More optimisation is required.

4.5. Experimental section

4.5.1. General considerations

All solvents were dried with activated 3Å molecular sieves (3Å MS). Proton (^{1}H-NMR), carbon (^{13}C-NMR) and fluorine (^{19}F-NMR) nuclear magnetic resonance spectra were recorded on a 400 MHz Varian VNMR-S400 NMR instrument at 25°C in $CDCl_3$. All chemical shifts are quoted on the δ scale in ppm using the residual solvent as internal standard (^{1}H-NMR: CDCl3=7.26ppm) and ^{13}C-NMR: $CDCl_3$=77.16ppm). Coupling constant (J) are reported in Hz with the following splitting abbreviations: s = singlet, d = doublet, t = triplet, q = quartet, m = multiplet, bs = broad singlet. Infrared (IR) spectra were recorded on a JASCO FTIR-680 plus Fourier Transform Infrared Spectrophotometer, wavenumbers (ṽ) in cm^{-1}. ESI MS were run on an Agilent®1200 Series HPLC-TOF instrument. Thin layer chromatography (TLC) was carried out on 0.25 mm E. Merck® aluminium backed sheets coated with 60 F_{254} silica gel. Visualization of the silica plates was achieved using a UV lamp (λ_{max} = 254 nm) and *p*-anisaldehyde stain. Flash column chromatography was carried out using silica gel 60 A CC (230–400 mesh). Mobile phases are reported in relative composition (*e.g.,* 1:1 hexane/EtOAc v/v). All reactions using anhydrous conditions were performed using dry apparatus under argon atmosphere. Activation of molecular sieves was performed in a flame-dried apparatus under high vacuum (<5 mbar) with a heat gun. Brine refers to a saturated solution of sodium chloride. Anhydrous sodium sulphate (Na_2SO_4) and anhydrous magnesium sulphate ($MgSO_4$) were indifferently used as drying agents after reaction work-up.

4.5.2. General Procedures

4.5.2.1. General Procedure for the Reduction of Cinnamic Acids to Cinnamyl Alcohols[77]

Cinnamic acid (9.0 mmol) was dissolved in dry THF (12 mL) in a Schlenk tube and the solution was cooled at -5ºC. Triethylamine (9 mmol, 1.3 mL) was then added to the solution and the reaction was stirred for 1 h. Methyl chloroformate (13.5 mmol, 1 mL) was added to the solution and the reaction was stirred for 1 more hour. Sodium borohydride (33.9 mmol, 1.3 g) was added, and the reaction was stirred for 30 minutes. Finally, methanol (4 mL) was added dropwise. The reaction mixture was stirred at room temperature until complete conversion. Saturated aqueous NH_4Cl (16 mL) was added to quench the reaction and the aqueous phase was extracted with dichloromethane (3x20 mL). The combined organic extracts were dried over anhydrous Na_2SO_4 and concentrated under reduced pressure. The crude was purified by flash chromatography using hexane/AcOEt mixture to give the final product.

4.5.2.2. General Procedure for the Carbamoylation of Allyl Alcohols to Carbamates[78]

Trichloroacetyl isocyanate (TAI) (10.5 mmol, 1.0 mL) was added dropwise to a stirred solution of the corresponding alcohol (7.05 mmol) in dry dichloromethane (15 mL) at 0°C. The mixture was left to stir at room temperature until TLC showed complete consumption of the starting alcohol. Then, a 20 mol% solution of K_2CO_3 in MeOH (3 mL/mmol alcohol) was added and the mixture was stirred at room temperature for 3 hours. After solvent evaporation, the residue was dissolved in a 1:1 mixture of Et_2O and brine. The aqueous phase was extracted with Et_2O, and the combined organic extracts were dried over $MgSO_4$ and concentrated under reduced pressure. The crude was purified by column chromatography

[77] Krätzschmar, F.; Kabel, M.; Delony, D.; Breder, A. *Chem. Eur. J.* **2015**, *21*, 7030-7034
[78] Agirre, M.; Henrion, S.; Rivilla, I.; Miranda, J. I.; Cossío, F. P.; Carboni, B.; Villalgordo, J. M.; Carreaux, F. *J. Org. Chem.* **2018**, *83*, 14861−14881

using mixtures of Hexane/EtOAc and recrystallized by slow diffusion of pentane into a solution of the carbamate in THF.

4.5.2.3. General Procedure for the Carbamoylation of Allyl Alcohols to N-substituted Carbamates[78]

The corresponding alcohol (1 mmol) was dissolved in dry dichloromethane followed by the dropwise addition of benzyl or tosyl isocyanate (1.5 mmol). The reaction was stirred until TLC showed complete consumption of the starting material. The crude was treated with saturated NH_4Cl solution, and the aqueous phase was extracted with Et_2O. The combined organic extracts were dried over $MgSO_4$ and concentrated under reduced pressure. The crude was purified by silica chromatography using mixtures of Hexane/EtOAc. and recrystallized by slow diffusion of pentane into a solution of the carbamate in THF.

4.5.2.4. General Procedure for the Sequential Aziridination + Ring-Opening of Allyl Carbamates

To a flame-dried Schlenk charged with activated 4Å MS (1 g/mmol carbamate), dry CH_2Cl_2 (2.5 mL), carbamate (0.1 mmol) and PhIO (0.2 mmol, 44 mg) were added. The mixture was stirred at 50ºC until complete consumption of carbamate followed by TLC. Afterwards, the mixture containing the aziridine was filtered through a syringe filter into a polypropylene tube under argon atmosphere. Either DMPU·HF or Et_3N·HF (26 equiv HF) was then added at 0ºC, and the reaction mixture was stirred at room temperature until complete consumption of aziridine, followed by TLC. The solution was quenched with $NaHCO_3$, and the aqueous phase was extracted with CH_2Cl_2. The organic phases were dried over with anhydrous $MgSO_4$, filtered and evaporated under reduced pressure. The resulting crude was purified by flash chromatography using hexane/AcOEt mixtures to obtain the F-oxazolidinone product as a mixture of *syn/anti* diastereomers. When necessary for identification purposes, a sample of the diastereomeric mixture was separated by flash chromatography using

toluene/THF or hexane/AcOEt mixtures to obtain pure fractions of each isomer.

4.5.2.5. General Procedure for the One-pot Aminofluorination of Allyl Carbamates with pure Difluoro(*p*-tolyl)-λ³-iodane (pure TolIF₂)

$TolIF_2$ (1.16 mmol, 297 mg), carbamate (0.29 mmol) and dry CH_2Cl_2 (3 mL) were added to a flame-dried Schlenk charged with activated 4Å MS (1 g/mmol carbamate). The Schlenk was protected from the light with aluminium foil and heated up to 100ºC. The mixture was stirred until complete consumption of the carbamate followed by TLC. The mixture was filtered through a pad of celite, washed with CH_2Cl_2 and the solvent was removed under reduced pressure. The resulting crude was purified by flash chromatography using hexane/AcOEt mixtures.

4.5.2.6. General Procedure for the Aminofluorination of Allyl Carbamates with Freshly Preformed Difluoro(*p*-tolyl)-λ³-iodane ([$TolIF_2$])[59]

$Et_3N{\cdot}HF$ (7 equiv HF) was added to a flame-dried Schlenk containing a solution of 4-iodotoluene (0.45 mmol, 98 mg) and Selectfluor (1.62 mmol, 574 mg) in dry CH_3CN (11 mL). The reaction mixture was protected from the light with aluminium foil and stirred for 22h at room temperature. Solvent was removed under inert conditions and reduced pressure. $TolIF_2$ was extracted from the residue left in the Schlenk using a dry mixture of hexane/$CHCl_3$ 3:1, with the aid of sonication. The extraction was repeated 3 times. The extracts were transferred to another Schlenk and concentrated under inert conditions and reduced pressure. The resulting $TolIF_2$ was dissolved in dry CH_2Cl_2 (2.3 mL) and transferred to a flame-dried Schlenk with carbamate (0.09 mmol, 1 eq) and preactivated 4Å MS (1 g/mmol carbamate). The reaction mixture was heated to 50ºC and stirred until complete consumption of carbamate, followed by TLC. The mixture was filtered through a pad of celite, washed with CH_2Cl_2 and concentrated under reduced pressure. The resulting crude was purified by flash chromatography using hexane/AcOEt mixtures.

4.5.2.7. General Procedure for the Aminofluorination with *in-situ* Generated TolIF$_2$

DMPU·HF or Et_3N·HF (20 equiv HF), PhIO (0.58 mmol, 128 mg) and dry CH_2Cl_2 (0.2 mL) were added to a Schlenk. The mixture was stirred for 15 minutes at room temperature, and a solution of carbamate (0.29 mmol) in dry CH_2Cl_2 (0.8 mL) was added. The reaction mixture was stirred at 50ºC until complete consumption of carbamate, followed by TLC. The mixture was quenched with $NaHCO_3$, and the aqueous phase was extracted with CH_2Cl_2. The organic phases were dried over anhydrous $MgSO_4$, filtered and evaporated under reduced pressure. The resulting crude was purified by flash chromatography using hexane/AcOEt mixtures.

4.5.2.8. General Procedure for the Hammett Plot Competitive Experiments

To a flame-dried Schlenk charged with activated 4Å M.S. (1 g/mmol carbamate) dry CH_2Cl_2 (1 mL), carbamates (0.04 mmol each) and PhIO (0.16 mmol, 36 mg) were added. The mixture was stirred at 50ºC overnight. Completion of the aziridination of both carbamates was ensured by ^{1}H-NMR (aziridine signals must integrate 1:1). Afterwards, the mixture containing the aziridine was filtered through a syringe filter into a polypropylene tube under argon atmosphere. Either DMPU·HF or Et_3N·HF (50 equiv HF) were added to the Schlenk at rt and Schlenk was shaken to ensure homogeneity. A 0.7 mL aliquot was taken immediately from the reaction mixture, filtered through a syringe filter, and added to an NMR tube under Ar. The sample was immediately measured by ^{19}F-NMR.

4.5.3. Compound Characterization Data

Preparation of iodosylbenzene (PhIO)

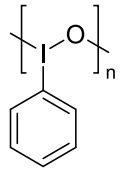

A sodium hydroxide solution (3M, 20 mL) was added over a 10-minute period to finely ground (diacetoxyiodo)benzene (12.4 mmol, 4.0 g) in a beaker under vigorous stirring. The reaction mixture was left at room temperature until completion (about 45 min). Then, H_2O (15 mL) was added and the crude, solid PhIO, was filtered off on a Büchner funnel. The wet solid was returned to the beaker, triturated with H_2O (25 mL), collected again on a Büchner funnel, washed with water and dried overnight under vacuum. Final purification was done by triturating the dried solid with chloroform (10 mL) in a beaker, separating it by filtration and drying under vacuum to afford 2.0 g (75% yield) of iodosylbenzene as a pale-yellow powder.

Preparation of *p*-difluoroiodotoluene ($TolIF_2$)[58]

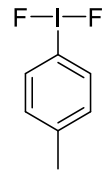

Iodotoluene (10.9 g, 50.0 mmol 1 eq) and MeCN (100 mL) were added to a 1 L round-bottom flask and the mixture was stirred to give a colourless solution. The flask was then cooled in a 5°C ice-water bath and 14% aq. NaOCl (150 mL, 4.2 eq) were added. The flask was then equipped with a 125 mL pressure-equilibrating addition funnel charged with concentrated HCl (100 mL, 24.8 eq). The reaction mixture was stirred vigorously and HCl was then added dropwise over 30 minutes. After the addition was complete, the reaction mixture was stirred for an additional

30 minutes. The mixture was filtered off and washed with water (3×200 mL) and hexane (3×50 mL). The wet filter cake was immediately transferred into a 300 mL round-bottomed flask, using THF (100 mL) to assist with the transfer. The flask was cooled to <–10°C in an ice-acetone bath and equipped with a 125 mL pressure-equilibrating addition funnel charged with 3M NaOH (50 mL, 3 eq). NaOH was added to the flask dropwise over 5 minutes, and then stirred for an additional 30 min, yielding an off-white solid suspended in a colourless solution. CH_2Cl_2 (100 mL) was added to the reaction flask, and the resulting suspension was stirred for an additional 2 min and filtered. The off-white filter cake was washed with water (5 × 30 mL) and CH_2Cl_2 (3×30 mL), which resulted in a pale-yellow paste. The wet filter cake was transferred to a 250 mL Teflon beaker and charged with chloroform (80 mL). The reaction vessel was cooled to 0°C in an ice-water bath and six portions of concentrated HF (6×2.5 mL, 6×1.4 eq) were continuously added dropwise using a 3 mL polypropylene graduated pipette. The mixture was then stirred for 30 minutes, after which the solid was no longer visible and the reaction mixture consisted of two colourless phases. The reaction vessel was then removed from the cooling bath and the top layer of the biphasic mixture was removed by using a 3 mL polypropylene pipette. Ensuring complete removal of all the aqueous droplets was critical to the success of this reaction. The beaker was then placed in a 40°C water bath and stirred while being concentrated to approximately 25% of its original volume by using a gentle stream of argon. Crystallization of the crude *p*-difluoroiodotoluene was induced by slowly adding hexanes (100 mL) at 40°C over 1 minute. The resulting mixture was concentrated to approximately 25% of its original volume with a gentle stream of argon. The resulting slurry was cooled to 0°C and decanted, ensuring that the white solid adhering to the side of the Teflon beaker was quickly scraped down into the bulk solid by using a metal spatula. (If desired, a polypropylene funnel equipped with filter paper can be used to collect any lost p-difluoroiodotoluene during decantation). This bulk solid was washed twice with hexanes (50 mL), decanting between

washes. The resulting white solid was transferred to a Teflon vial, placed into a 40°C water bath, and the excess hexanes was evaporated by concentration under a gentle stream of argon. The vial containing the solid was dried under vacuum to give a white powder (35.5 mmol, 71% yield).

^{1}H-NMR ($CDCl_3$, 400 MHz, δ in ppm): 7.83 (d, 2H, $^{3}J_{HH}$=6.2 Hz), 7.39 (d, 2H, $^{3}J_{HH}$=6.6 Hz), 2.47 (s, 3H); **^{13}C-NMR** ($CDCl_3$, 100.6 MHz, δ in ppm): 142.5, 132.4, 130.4 (t, $^{3}J_{CF}$=3.2 Hz), 121.0 (t, $^{2}J_{CF}$=11.2 Hz), 21.8; **^{19}F-NMR** ($CDCl_3$, 377 MHz, δ in ppm): -176.9; **HR ESI-TOF MS** $[M+H]^+$ calc for $C_7H_5IF_2$: 256.9639, found = 256.9644. Characterisation data corresponds to the data reported in the literature.[58]

(*E*)-3-(4-acetoxyphenyl)prop)-2-en-1-ol (4.17)

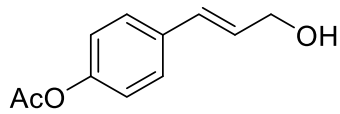

The title compound was prepared following the general reduction of cinnamic acids starting from commercially available *p*-acetoxycinnamic acid (1600 mg, 7.76 mmol). The crude was purified by column chromatography using a mobile phase of CH_2Cl_2/AcOEt (60:40) to give **4.17** as a yellowish solid (626 mg, 3.26 mmol, 42% yield).

^{1}H-NMR (400 MHz, $CDCl_3$, δ in ppm): 7.36 (d, J=8.6 Hz, 2H, H_{ar}), 7.03 (d, J=8.6 Hz, 2H, H_{ar}), 6.57 (d, J=15.9 Hz, 1H, H_3), 6.29 (dt, J=15.9, 5.4 Hz, 1H, H_2), 4.28 (d, J=5.4 Hz, 2H, H_1), 2.29 (s, 3H, CH_3CO), 2.00 (bs, 1H, H_{OH}). **^{13}C-NMR** (100 MHz, $CDCl_3$, δ in ppm): 169.7 (CH_3CO), 150.1 (C_{ar}), 134.6 (C_{ar}), 130.0 (C_3), 128.9 (C_2), 127.5 (C_{ar}), 121.8 (C_{ar}), 63.6 (C_1), 21.2 (CH_3CO). **HR ESI-TOF MS** $[M+Na]^+$ calc for $C_{11}H_{12}O_3Na$: 215.0679, found = 215.0680. Characterisation data corresponds to the data reported in the literature.[79]

[79] Paraskar, A. S.; Sudalai, A. *Tetrahedron*, **2006**, *62*, 5756 -5762.

(*E*)-3-(4-methoxyphenyl)prop)-2-en-1-ol (4.18)

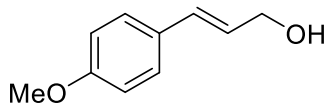

The title compound was prepared following the general reduction of cinnamic acids starting from commercially available *p*-methoxycinnamic acid (713 mg, 4.00 mmol). The crude was purified by chromatography column using a mobile phase of hexane/AcOEt (70:30) to give **4.18** as a white solid (342 mg, 2.08 mmol, 52% yield).

^{1}H-NMR (400 MHz, $CDCl_3$, δ in ppm): 7.31 (d, J=8.7 Hz, 2H, H_{ar}), 6.85 (d, J=8.7 Hz, 2H, H_{ar}), 6.54 (d, J=15.9 Hz, 1H, H_3), 6.23 (dt, J=15.9, 5.9 Hz, 1H, H_2), 4.28 (dd, J=5.9, 1.2 Hz, 2H, H_1), 3.80 (s, 3H, CH_3O), 1.82 (bs, 1H, H_{OH}). **^{13}C-NMR** (100 MHz, $CDCl_3$, δ in ppm): 159.4 (C_{ar}), 131.0 (C_3), 129.5 (C_{ar}), 127.8 (C_{ar}), 126.4 (C_2), 114.1 (C_{ar}), 64.0 (C_1), 55.4 (CH_3O). **HR ESI-TOF MS** for $[M_+]$ $C_{10}H_{12}O_{2+}$ (m/z): 168.0837 found: 164.0837. Characterisation data corresponds to the data reported in the literature.[80]

(*E*)-3-(p-tolyl)prop)-2-en-1-ol (4.19)

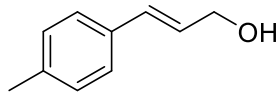

The title compound was prepared following the general reduction of cinnamic acids starting from commercially available *p*-methylcinnamic acid (600 mg, 3.70 mmol). The crude was purified by chromatography column using a mobile phase of hexane/AcOEt (80:20) to give **4.19** as a white solid (291 mg, 1.96 mmol, 53% yield).

^{1}H-NMR (400 MHz, $CDCl_3$, δ in ppm): 7.27 (d, J=8.1 Hz, 2H, H_{ar}), 7.18 – 7.09 (d, J=8.1 Hz, 2H, H_{ar}), 6.56 (d, J=15.9 Hz, 1H, H_3), 6.30 (dt, J=15.9, 5.8 Hz, 1H, H_2), 4.28 (d, J=5.8 Hz, 2H, H_1), 2.33 (s, 3H, CH_3), 1.95 (bs, 1H, H_{OH}). **^{13}C-NMR** (100 MHz, $CDCl_3$, δ in ppm): 137.6 (C_{ar}), 134.0 (C_{ar}), 131.2 (C_3),

[80] Peng, D.; Zhang, M.; Huang, Z. *Chem. Eur. J.* **2015**, *21*, 14737-14741.

129.4 (C_{ar}), 127.6 (C_2), 126.5 (C_{ar}), 63.8 (C_1), 21.3 (CH_3). **HR ESI-TOF MS** for [M_+] $C_{10}H_{12}O_+$ (m/z): 148.0888; found: 148.0886. Characterisation data corresponds to the data reported in the literature.[81]

(*E*)-3-(4-bromophenyl)prop)-2-en-1-ol (4.20)

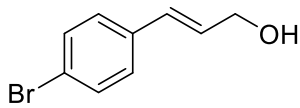

The title compound was prepared following the general reduction of cinnamic acids starting from commercially available *p*-bromocinnamic acid (454 mg, 2.00 mmol). The crude was purified by chromatography column using a mobile phase of hexane/AcOEt (70:30) to give **4.20** as a white solid (341 mg, 1.60 mmol, 80% yield).

^{1}H-NMR (400 MHz, $CDCl_3$, δ in ppm): 7.42 (d, J=8.5 Hz, 2H, H_{ar}), 7.22 (d, J=8.5 Hz, 2H, H_{ar}), 6.54 (d, J=15.9 Hz, 1H, H_3), 6.33 (dt, J=15.9, 5.1 Hz, 1H, H_2), 4.22 (d, J=5.1Hz, 2H, H_1), 1.96 (bs, 1H, H_{OH}). **^{13}C-NMR** (100 MHz, $CDCl_3$, δ in ppm): 135.7 (C_{ar}), 131.8 (C_3), 129.8 (C_{ar}), 129.4 (C_{ar}), 128.1 (C_2), 121.5 (C_{ar}), 63.5 (C_1). **HR ESI-TOF MS** for [M-H$_-$] $C_9H_9BrO^-$ (m/z): 211.9837 found: 211.9838. Characterisation data corresponds to the data reported in the literature.[81]

(*E*)-3-(4-fluorophenyl)prop)-2-en-1-ol (4.21)

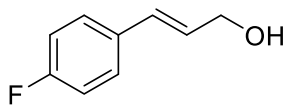

The title compound was prepared following the general reduction of cinnamic acids starting from commercially available *p*-fluorocinnamic acid (693 mg, 4.17 mmol). The crude was purified by chromatography column using a mobile phase of hexane/AcOEt (60:40) to give **4.21** as a white solid (387 mg, 2.54 mmol, 61% yield).

[81] Knežević, A.; Landek, G.; Dokli, I.; Vinković, V. *Tetrahedron Asymmetry*, **2011**, *22*, 936-941.

^{1}H-NMR (400 MHz, $CDCl_3$, δ in ppm): 7.33 (dd, J=8.7, 5.5 Hz, 2H, H_{ar}), 7.00 (t, J=8.7 Hz, 2H, H_{ar}), 6.57 (d, J=15.9 Hz, 1H, H_3), 6.41 – 6.21 (dt, J=15.9, 5.7, 1H, H_2), 4.30 (d, J=5.7 Hz, 2H, H_1), 1.92 (bs, 1H, H_{OH}). **^{13}C-NMR** (100 MHz, $CDCl_3$, δ in ppm): 162.5 (d, J=246.8 Hz, C_{ar}), 133.0 (d, J=3.1 Hz, C_{ar}), 130.0 (C_2), 128.4 (d, J=2.2 Hz, C_3), 128.1 (d, J=8.0 Hz, C_{ar}), 115.6 (d, J=21.7 Hz, C_{ar}), 63.64 (C_1). **^{19}F-NMR** (377 MHz, $CDCl_3$, δ in ppm): -114.4. **HR ESI-TOF MS** for [M_+] $C_9H_9FO_+$ (m/z): 152.0637 found: 152.0635. Characterisation data corresponds to the data reported in the literature.[82]

(*E*)-3-(4-(trifluoromethyl)phenyl)prop)-2-en-1-ol (4.22)

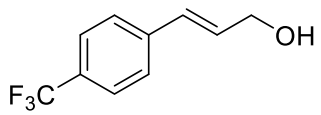

The title compound was prepared following the general reduction of cinnamic acids starting from commercially available *p*-(trifluoromethyl)cinnamic acid (550 mg, 2.55 mmol). The crude was purified by chromatography column using a mobile phase of hexane/AcOEt (70:30) to give **4.22** as a white solid (211 mg, 1.04 mmol, 41% yield).

^{1}H-NMR (400 MHz, $CDCl_3$, δ in ppm): 7.56 (d, J=8.3 Hz, 2H, H_{ar}), 7.45 (d, J=8.3 Hz, 2H, H_{ar}), 6.65 (d, J=16.0 Hz, 1H, H_3), 6.44 (dt, J=16.0, 5.3 Hz, 1H, H_2), 4.36 (dd, J=5.3, 1.3 Hz, 2H, H_1), 1.94 (bs, 1H, H_{OH}). **^{13}C-NMR** (100 MHz, $CDCl_3$, δ in ppm): 140.3 (d, J=1.2 Hz, C_{ar}), 131.4 (C_3) 129.6 (d, J=32.7 Hz, C_{ar}), 129.1 (C_2), 126.7 (C_{ar}), 125.7 (q, J=3.8 Hz, C_{ar}), 124.9 (q, J=270.5 Hz, CF_3), 63.4 (C_1). **^{19}F-NMR** (377 MHz, $CDCl_3$, δ in ppm): -62.5. **HR ESI-TOF MS** for [M-H_-] $C_{10}H_8F_3O_-$ (m/z): 201.0527; found: 201.0537. Characterisation data corresponds to the data reported in the literature.[83]

[82] Spoehrle, S. S. M.; West, T. H.; Taylor, J. E.; Slawin, A. M. Z.; Smith, A. D. *J. Am. Chem. Soc.* **2017**, *139*, 11895-11902.
[83] Noquet, P. A.; Corbu, A.; Meerpoel, L.; Stansfield, I.; Berthelot, D.; Angibaud, P.; Cossy, J. *Eur. J. Org. Chem.* **2017**, 3343-3354.

(*E*)-3-(4-cyanophenyl)prop)-2-en-1-ol (4.25)

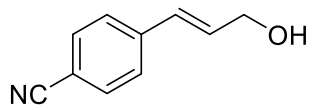

$CeCl_3 \cdot 7H_20$ (370 mg, 1.50 mmol, 1.5 eq) was added to a solution of *p*-cyanocinnamyl aldehyde (157 mg, 1.00 mmol) in dry MeOH (13 mL) and the mixture is stirred at rt until the cerium is completely dissolved. Afterwards, the solution is cooled to 0ºC and $NaBH_4$ is added in portions. The reaction mixture is stirred at 0ºC for 30 minutes. The reaction was quenched with 10% aqueous NaOH. The mixture was filtrated to remove $Ce(OH)_3$, extracted with CH_2Cl_2, washed with brine and dried over anhydrous $NaSO_4$. The solution was concentrated under reduced pressure. The crude was purified by chromatography column using a mobile phase of hexane/AcOEt (60:40) to give **4.25** as a white solid (118 mg, 0.74 mmol, 74% yield).

^{1}H-NMR (400 MHz, $CDCl_3$, δ in ppm): 7.61 (d, J=8.1 Hz, 2H, H_{ar}), 7.46 (d, J=8.3 Hz, 2H, H_{ar}), 6.66 (d, J=16.0 Hz, 1H, H_3), 6.49 (dt, J=16.0, 5.2, 1H, H_2), 4.39 (td, J=5.6, 1.7, 2H, H_1), 1.55 (bs, 1H, H_{OH}). **^{13}C-NMR** (100 MHz, $CDCl_3$, δ in ppm): 141.2 (C_{Ar}), 132.6 (C_3), 132.4 (C_{Ar}), 128.7 (C_2), 126.9 (C_{Ar}), 118.9 (CN), 110.7 (C_{Ar}), 63.1 (C_1). **HR ESI-TOF MS** for $[M+NH_{4+}]$ $C_{10}H_{13}N_3O_2$ (m/z): 177.1028, found: 177.1033. Characterisation data corresponds to the data reported in the literature.[54b]

(*E*)-3-(phenyl)allyl carbamate (4.31)

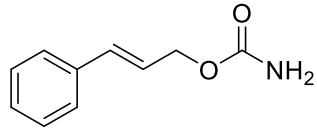

The title compound was prepared following the general carbamoylation of cinnamyl alcohols starting from commercially available cinnamyl alcohol (1055 mg, 7.90 mmol) and TAI (0.6 mL, 8.30 mmol). The crude was purified by chromatography column using a mobile phase of hexane/AcOEt (60:40). Recrystallization by slow diffusion of pentane in a

solution of carbamate in THF rendered **4.31** as a white solid (1162 mg, 6.56 mmol, 83% yield).

M. p. 120-126 °C. **IR (neat):** 3409, 3328, 3264, 3055, 1679, 1626, 1602, 1409, 1341, 1115, 1048, 969 cm^{-1}. **^{1}H-NMR** (400 MHz, $CDCl_3$, δ in ppm): 7.40-7.37 (m, 2H, H_{ar}), 7.34-7.30 (m, 2H, H_{ar}), 7.28-7.24 (m, 1H, H_{ar}), 6.65 (d, J=15.9 Hz, 1H, H_3), 6.29 (dt, J=15.9, 6.4 Hz, 1H, H_2), 4.99 (bs, 2H, H_{NH}), 4.73 (dd, J=6.4, 1.3 Hz, 2H, H_1). **^{13}C-NMR** (100 MHz, $CDCl_3$, δ in ppm): 157.0 (OC(O)NH2), 136.3 (C_{ar}), 133.9 (C_3), 128.7 (C_{ar}), 128.1 (C_{ar}), 126.7 (C_{ar}), 123.6 (C_2), 65.7 (C_1). **HR ESI-TOF MS** for $[M+Na]^+$ $C_{10}H_{11}NNaO_2$ (m/z): 200.0682, found: 200.0680.

(*E*)-4-(3-(carbamoyloxy)prop-1-en-1-yl)phenyl acetate (4.32)

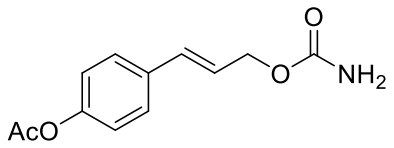

The title compound was prepared following the general carbamoylation of cinnamyl alcohols starting from alcohol **4.17** (1 g, 5.20 mmol) and TAI (651 μL, 5.46 mmol). The crude was purified by chromatography column using a mobile phase of hexane/AcOEt (60:40). Recrystallization by slow diffusion of pentane in a solution of carbamate in THF rendered **4.32** as a white solid (1028 mg, 4.37 mmol, 80% yield).

M. p. 138-139 °C. **IR (neat):** 3419, 3335, 3255, 3210, 2966, 2364, 1754, 1683, 1617, 1508, 1350, 1214, 1062 cm-1. **^{1}H-NMR** (400 MHz, $CDCl_3$, δ in ppm): 7.42 – 7.37 (m, 2H), 7.07 – 7.03 (m, 2H), 6.63 (d, J=15.9 Hz, 1H), 6.25 (dt, J=15.9, 6.4 Hz, 1H), 4.72 (dd, J=6.3, 1.4 Hz, 2H), 2.30 (s, 2H). **^{13}C-NMR** (100 MHz, $CDCl_3$, δ in ppm): 169.6 (CH_3CO), 156.6 ($OCONH_2$), 150.5 (C_{ar}), 134.2 (C_{ar}), 133.0 (C_3), 127.7 (C_2), 124.0 (C_{ar}), 121.9 (C_{ar}), 65.7 (C_1), 21.3 (CH_3CO). **ESI-TOF MS** for $[M+Na_+]$ $C_{12}H_{13}NNaO_{3+}$ (m/z): 242.0788; found: 242.0735.

(*E*)-3-(4-methoxyphenyl)allyl) carbamate (4.33)

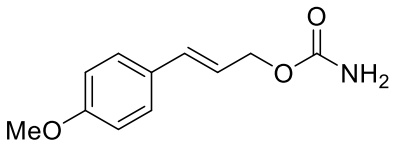

The title compound was prepared following the general carbamoylation of cinnamyl alcohols starting from alcohol **4.18** (446 mg, 2.71 mmol) and TAI (203 µL, 2.84 mmol). The crude was purified by chromatography column using a mobile phase of hexane/AcOEt (60:40). Recrystallization by slow diffusion of pentane in a solution of carbamate in THF rendered **4.33** as a white solid (354 mg, 1.71 mmol, 63% yield).

M. p. 110-118 °C. **IR (neat):** 3429, 3332, 3270, 3205, 2954, 2832, 2359, 1683, 1511, 1352, 1251 cm^{-1}. **^{1}H-NMR** (400 MHz, CD_2Cl_2, δ in ppm): 7.34 (d, J=8.7 Hz, 2H, H_{ar}), 6.86 (d, J=8.7 Hz, 2H, H_{ar}), 6.59 (d, J=15.9 Hz, 1H, H_3), 6.16 (dt, J=15.9, 6.4 Hz, 1H, H_2), 4.79 (bs, 2H, H_{NH}), 4.66 (dd, J=6.4, 1.1 Hz, 2H, H_2), 3.79 (s, 3H, $C\underline{H_3}O$). **^{13}C-NMR** (100 MHz, CD_2Cl_2, δ in ppm): 160.1 ($OC(O)NH_2$), 157.1 (C_{ar}), 133.7 (C_3), 129.5 (C_{ar}), 128.3 (C_{ar}), 122.1 (C_2), 114.5 (C_{ar}), 66.2 (C_1), 55.8 (CH_3O). **ESI-TOF MS** $[M+Na^+]$ $C_{11}H_{13}NNaO_{3+}$ (m/z): 230.0788; found: 230.0791.

(*E*)-3-(*p*-tolyl)allyl carbamate (4.34)

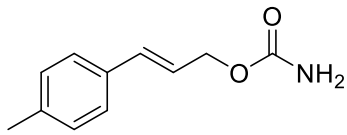

The title compound was prepared following the general carbamoylation of cinnamyl alcohols starting from alcohol **4.19** (433 mg, 2.90 mmol) and TAI (218 µL, 3.04 mmol). The crude was purified by chromatography column using a mobile phase of hexane/AcOEt (60:40). Recrystallization by slow diffusion of pentane in a solution of carbamate in THF rendered **4.34** as a white solid (260 mg, 2.41 mmol, 83% yield).

^{1}H-NMR (400 MHz, CD_2Cl_2, δ in ppm): 7.29 (d, J=8.1 Hz, 2H, H_{ar}), 7.16 (d, J=8.1 Hz, 2H, H_{ar}), 6.61 (d, J=15.9 Hz, 1H, H_3), 6.25 (dt, J=15.9, 6.3 Hz, 1H, H_2), 4.72 (dd, J=6.4, 1.3 Hz, 2H, H_1), 4.61 (bs, 2H,, H_{NH}), 2.33 (s, 3H, CH_3). **^{13}C-NMR** (100 MHz, CD_2Cl_2, δ in ppm): 157.0 ($OC(O)NH_2$), 138.5 (C_{ar}), 134.0 (C_{ar}), 133.8 (C_3), 129.7 (C_{ar}), 126.9 (C_{ar}), 123.2 (C_2), 66.0 (C_1), 21.4 (CH_3). **ESI-TOF MS** for [M+Na$^+$] $C_{11}H_{13}NNaO_{2+}$ (m/z): 214.0838; found: 214.0839. Characterisation data corresponds to the data reported in the literature.[40c]

(*E*)-3-(4-bromophenyl)allyl carbamate (4.35)

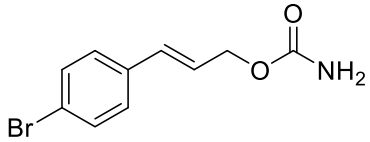

The title compound was prepared following the general carbamoylation of cinnamyl alcohols starting from alcohol **4.20** (561 mg, 2.63 mmol) and TAI (197 µL, 2.76 mmol). The crude was purified by chromatography column using a mobile phase of hexane/AcOEt (60:40). Recrystallization by slow diffusion of pentane in a solution of carbamate in THF rendered **4.35** as a white solid (539 mg, 2.10 mmol, 80% yield).

^{1}H-NMR (400 MHz, CD_2Cl_2, δ in ppm): 7.46 (d, J=8.5 Hz, 2H, H_{ar}), 7.28 (d, J=8.5 Hz, 2H, H_{ar}), 6.59 (d, J=16.0 Hz, 1H, H_3), 6.30 (dt, J=16.0, 6.1 Hz, 1H, H_2), 4.88 – 4.54 (m, 4H, H_1, H_{NH}). **^{13}C-NMR** (100 MHz, CD_2Cl_2, δ in ppm): 156.9 ($OC(O)NH_2$), 134.0 (C_{ar}), 132.3 (C_{ar}), 132.2 (C_3), 128.6 (C_{ar}), 125.4 (C_2), 122.2 (C_{ar}), 65.7 (C_1). **ESI-TOF MS** for [M+Na$^+$] $C_{10}H_{10}BrNNaO_{2+}$ (m/z): 277.9787; found: 277.9789. Characterisation data corresponds to the data reported in the literature.[40c]

(*E*)-3-(4-fluorophenyl)allyl carbamate (4.36)

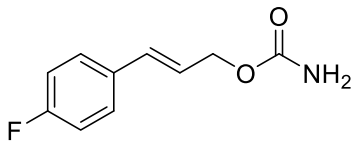

The title compound was prepared following the general carbamoylation of cinnamyl alcohols starting from alcohol **4.21** (511 mg, 3.36 mmol) and TAI (252 µL, 3.53 mmol). The crude was purified by chromatography column using a mobile phase of hexane/AcOEt (60:40). Recrystallization by slow diffusion of pentane in a solution of carbamate in THF rendered **4.36** as a white solid (498 mg, 2.55 mmol, 76% yield).

^{1}H-NMR (400 MHz, $CDCl_3$, δ in ppm): 7.46 – 7.31 (m, 2H, H_{ar}), 7.12 – 6.94 (m, 2H, H_{ar}), 6.62 (d, J=15.9 Hz, 1H, H_3), 6.23 (dtd, J=15.9, 6.2, 0.5 Hz, 1H, H_2), 4.68 (dd, J=6.2, 1.4 Hz, 2H, H_1). **^{13}C-NMR** (100 MHz, CD_2Cl_2, δ in ppm): 163.1 (d, J = 246.4 Hz, C_{ar}), 157.3 ($OC(O)NH_2$), 133.3 (d, J=3.2 Hz, C_{ar}), 132.7 (C_3) 128.8 (d, J=8.0 Hz, C_{ar}), 124.4 (d, J=2.1 Hz, C_2), 116.02 (d, J=21.7 Hz, C_{ar}), 65.9 (C_2). **^{19}F-NMR** (377 MHz, CD_2Cl_2 , δ in ppm): -112.9. **ESI-TOF MS** for $[M+Na_+]$ $C_{10}H_{10}FNNaO_{2+}$ (m/z): 218.0588; found: 218.0587. Characterisation data corresponds to the data reported in the literature. [40c]

(*E*)-3-(4-(trifluoromethyl)phenyl)allyl carbamate (4.37)

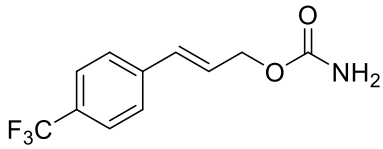

The title compound was prepared following the general carbamoylation of cinnamyl alcohols starting from alcohol **4.22** (294 mg, 1.45 mmol) and TAI (109 µL, 1.52 mmol). The crude was purified by chromatography column using a mobile phase of hexane/AcOEt (60:40).

Recrystallization by slow diffusion of pentane in a solution of carbamate in THF rendered **4.37** as a white solid (267 mg, 1.09 mmol, 75% yield).

M. p. 118-120 °C. **IR (neat):** 3443, 3327, 3268, 3197, 3038, 2966, 2359, 2327, 1740, 1686, 1321, 1065 cm^{-1}. **^{1}H-NMR** (400 MHz, $CDCl_3$, δ in ppm): 7.57 (d, J=8.2 Hz, 2H, H_{ar}), 7.48 (d, J=8.2 Hz, 2H, H_{ar}), 6.68 (d, J=16.0 Hz, 1H, H_3), 6.38 (dt, J=16.0, 6.1 Hz, 1H, H_2), 4.90 – 4.61 (m, 4H, H_1, H_{NH}). **^{13}C-NMR** (100 MHz, $CDCl_3$, δ in ppm): 156.5 ($OC(O)NH_2$), 139.9 (C_{ar}), 132.1 (C_3), 129.9 (q, J=32.2 Hz, C_{ar}), 127.0 (apparent d, J=271.9 Hz, CF_3) 126.9 (C_{ar}), 126.6 (C_2), 125.73 (q, J=4.5 Hz, C_{ar}), 65.3 (C_1). **^{19}F-NMR** (377 MHz, $CDCl_3$, δ in ppm): -62.6. **ESI-TOF MS** for [M-H$^-$] $C_{11}H_9F_3NO_2^-$ (m/z): 244.0585; found: 244.0590.

(*E*)-3-(4-nitrophenyl)allyl carbamate (4.38)

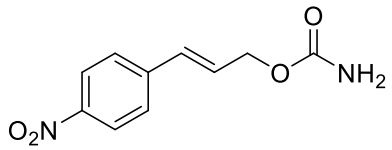

The title compound was prepared following the general carbamoylation of cinnamyl alcohols starting from commercially available 4-nitrocinnamyl alcohol (300 mg, 1.67 mmol) and TAI (125 µL, 1.75 mmol). The crude was purified by chromatography column using a mobile phase of hexane/AcOEt (60:40). Recrystallization by slow diffusion of pentane in a solution of carbamate in THF rendered **4.38** as a white solid (297 mg, 1.34 mmol, 80% yield).

^{1}H-NMR (400 MHz, $CDCl_3$, δ in ppm): 8.19 (d, J=8.8 Hz, 2H, H_{ar}), 7.52 (d, J=8.8 Hz, 2H, H_{ar}), 6.71 (d, J=16.0 Hz, 1H, H_3), 6.46 (dt, J=16.0, 5.8 Hz, 1H, H_2), 4.77 (dd, J=5.8, 1.3 Hz, 2H, H_2), 4.70 (bs, 2H, H_{NH}). **^{13}C-NMR** (100 MHz, $CDCl_3$, δ in ppm): 156.3 ($OC(O)NH_2$), 147.3 (C_{ar}), 142.8 (C_{ar}), 131.0 (C_3), 128.8 (C_2), 127.3 (C_{ar}), 124.2 (C_{ar}), 65.0 (C_1). **ESI-TOF MS** for [M-H$^-$] $C_{10}H_9N_2O_4^-$ (m/z): 221.0562; found: 221.0537. Characterisation data corresponds to the data reported in the literature.[40c]

(*E*)-3-(4-cyanophenyl)allyl carbamate (4.39)

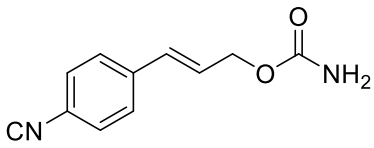

The title compound was prepared following the general carbamoylation of cinnamyl alcohols starting from alcohol **4.25** (118 mg, 0.74 mmol) and TAI (125 µL, 1.75 mmol). The crude was purified by chromatography column using a mobile phase of hexane/AcOEt (70:30 to 60:40). Recrystallization by slow diffusion of pentane in a solution of carbamate in THF rendered **4.39** as a pale-yellow solid (148 mg, 0.73 mmol, 98% yield).

M. p. 166-168 °C. **IR (neat):** 3419, 3335, 3255, 3210, 2966, 2364, 1754, 1683, 1617, 1508, 1350, 1214, 1062 cm-1. **^{1}H-NMR** (400 MHz, $CDCl_3$, δ in ppm): 7.61 (d, J=8.4 Hz, 2H, H_{ar}), 7.46 (d, J=8.3 Hz, 2H, H_{ar}), 6.65 (dt, J=16.1, 1.6 Hz, 1H, H_3), 6.41 (dt, J=16.0, 5.9 Hz, 1H, H_2), 4.76 (dd, J=6.0, 1.5 Hz, 2H, H_1), 4.68 (bs, 2H, H_{NH}). **^{13}C-NMR** (100 MHz, $CDCl_3$, δ in ppm): 156.4 ($OC(O)NH_2$), 140.90 (C_{ar}), 132.6 (C_3), 131.5 (C_{ar}), 128.0 (C_2), 127.2 (C_{ar}), 118.9 (C_{ar}), 111.4 (CN), 65.1 (C_1). **ESI-TOF MS** for $[M+Na^+]$ $C_{11}H_{10}N_2NaO_2^+$ (m/z): 212.1694; found: 212.1686.

(*Z*)-3-phenylallyl carbamate (4.40)

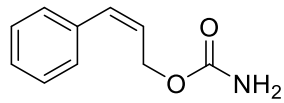

The title compound was prepared following the general carbamoylation of cinnamyl alcohols starting from alcohol **4.30** (134 mg, 1.00 mmol) and TAI (0.13 mL, 1.05 mmol). The crude was purified by chromatography column using a mobile phase of hexane/AcOEt (80:20). Recrystallization by slow diffusion of pentane in a solution of carbamate in THF rendered **4.40** as a white solid (146 mg, 0.82 mmol, 82% yield).

^{1}H-NMR (400 MHz, $CDCl_3$, δ in ppm): 7.36 – 7.09 (m, 5H, H_{ar}), 6.59 (d, J=11.8 Hz, 1H, H_3), 5.75 (dt, J=11.8, 6.5 Hz, 1H, H_2), 4.78 (dd, J=6.5, 1.7 Hz, 2H, H_1), 4.69 (s, 2H, H_{NH}). **^{13}C-NMR** (100 MHz, $CDCl_3$, δ in ppm): 156.80 (CO), 136.01 (C_{ar}), 132.71 (C_3), 128.70 (C_{ar}), 128.34 (C_{ar}), 127.47 (C_{ar}), 126.13 (C_2), 62.10 (C_1). **ESI-TOF MS** for [M+Cl-] $C_{10}H_{11}NClO_{2-}$ (m/z): 212.1694; found: 212.1686. Characterisation data corresponds to the data reported in the literature.[84]

(E)-non-2-en-1-yl tosylcarbamate (4.41)

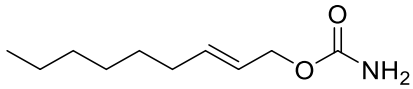

The title compound was prepared following the general carbamoylation of cinnamyl alcohols starting from commercially available *trans*-2-nonen-1-ol (142 mg, 1.00 mmol) and TAI (129 µL, 1.05 mmol). The crude was purified by chromatography column using a mobile phase of hexane/AcOEt (80:20). Recrystallization by slow diffusion of pentane in a solution of carbamate in THF rendered **4.41** as a white solid (169 mg, 0.91 mmol, 91% yield).

^{1}H-NMR (400 MHz, $CDCl_3$, δ in ppm): 5.71 (dt, J=15.0, 6.7 Hz, 1H, H_2), 5.50 (dtt, J=15.4, 6.5, 1.4 Hz, 1H, H_3), 4.52 (s, 2H, NH), 4.44 (dd, J=6.5, 0.9 Hz, 2H, H_1), 1.98 (q, J=7.2 Hz, 2H, H_4), 1.38 – 1.27 (m, 2H, H_5), 1.25 – 1.13 (m, 6H, $H_{6,7,8}$), 0.81 (t, J=6.9 Hz, 3H, H_9). **^{13}C-NMR** (100 MHz, $CDCl_3$, δ in ppm): 157.2 (CO), 136.4 (C_2), 124.0 (C_3), 65.8 (C_1), 32.2 (C_4), 31.6 (C_5), 28.81 (C_6), 28.78 (C_7), 22.5 (C_8), 14.0 (C_9). **ESI-TOF MS** for [M-H-] $C_{10}H_{19}NO_{2-}$ (m/z): 208.1308; found: 208.1299.

[84] Kamon, T.; Shigeoka, D.; Tanaka, T.; Yoshimitsu, T. *Org. Biomol. Chem.* **2012**, *10*, 12, 2363 - 2365

(*Z*)-3-non-2-en-1-yl carbamate (4.42)

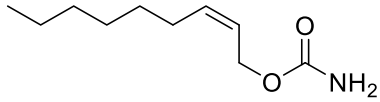

The title compound was prepared following the general carbamoylation of cinnamyl alcohols starting from commercially available *cis*-2-nonen-1-ol (1055 mg, 7.05 mmol) and TAI (1.0 mL, 8.46 mmol). The crude was purified by chromatography column using a mobile phase of hexane/AcOEt (80:20). Recrystallization by slow diffusion of pentane in a solution of carbamate in THF rendered **4.42** as a white solid (993 mg, 5.36 mmol, 76% yield).

^{1}H-NMR (400 MHz, $CDCl_3$, δ in ppm): 5.62 – 5.53 (m, 1H, H_2), 5.46 (dtt, J=10.9, 6.8, 1.4 Hz, 1H, H_3), 4.71 (s, 2H, NH), 4.55 (d, J=6.5 Hz, 2H,H_1), 2.01 (td, J=13.6, 7.0 Hz, 2H, H_4), 1.35 – 1.15 (m, 8H, $H_{5,6,7,8}$), 0.81 (t, J=6.9 Hz, 3H, H_9). **^{13}C-NMR** (100 MHz, $CDCl_3$, δ in ppm): 135.32 (C_2), 123.46 (C_3), 61.01 (C_1), 31.64 (C_5), 29.43 (C_4), 28.82 (C_7), 27.48 (C_6), 22.57 (C_8), 14.04 (C_9). **ESI-TOF MS** for [M-H-] $C_{10}H_{19}NO_2^-$ (m/z): 208.1308; found: 208.1304.

(2E,4E)-hexa-2,4-dien-1-yl carbamate (4.43)

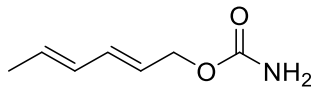

The title compound was prepared following the general carbamoylation of cinnamyl alcohols starting from commercially available (*2E,4E*)-hexa-2,4-dien-1-ol (1.1 mL, 10.00 mmol) and TAI (0.8 mL, 10.50 mmol). The crude was purified by chromatography column using a mobile phase of hexane/AcOEt (70:30). Recrystallization by slow diffusion of pentane in a solution of carbamate in THF rendered **4.43** as a white solid (1313 mg, 9.30 mmol, 93% yield).

M. p. 93-95 ºC. **IR (neat)**: 3426, 3296, 3213, 2911, 2851, 1652, 1616, 1429, 1344, 1314, 1108, 1054, 990 cm^{-1}. **^{1}H-NMR** (400 MHz, $CDCl_3$, δ in ppm): 6.24 (dd, J=15.2, 10.5 Hz, 1H, H_3), 6.04 (ddd, J=14.2, 10.5, 1.3 Hz, 1H, H_4), 5.74 (dq, J=14.2, 6.7 Hz, 1H, H_5), 5.62 (dt, J=15.2, 6.6 Hz, 1H, H_2), 4.85 (brs, 2H, NH2), 4.55 (d, J=6.6 Hz, 2H, H_1), 1.75 (dd, J=6.7, 1.3 Hz, 3H, H_6). **^{13}C-NMR** (100 MHz, CDCl3, δ in ppm): 157.0 (C=O), 134.7 (C_3), 131.3 (C_5), 130.5 (C_4), 124.1 (C_2), 65.7 (C_1), 18.3 (C_6). **HR ESI-TOF MS** for [M-H$^-$] $C_7H_{10}NO_{2-}$ (m/z): 164.0682; found: 164.0682.

(*E*)-3-phenylallyl tosylcarbamate (4.44)

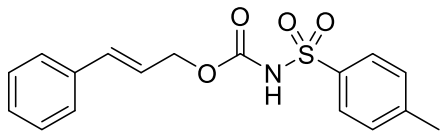

The title compound was prepared following the N-protected carbamoylation of cinnamyl alcohols starting from commercially available cinnamyl alcohol (973 mg, 7.04 mmol) and tosyl isocyanate (1.1 mL, 7.4 mmol). The crude was purified by chromatography column using a mobile phase of hexane/AcOEt (80:20). Recrystallization by slow diffusion of pentane in a solution of carbamate in THF rendered **4.44** as a white solid (1819 mg, 5.49 mmol, 78% yield).

^{1}H-NMR (400 MHz, $CDCl_3$, δ in ppm): 7.89 – 7.84 (m, 2H, H_4), 7.49 (s, 1H, H_{NH}), 7.32 – 7.24 (m, 5H, H_{ar}), 7.23 – 7.17 (m, 2H, H_5), 6.51 (dt, J=15.8, 1.2 Hz, 1H, H_3), 6.07 (dt, J=15.9, 6.6 Hz, 1H, H_2), 4.65 (dd, J=6.6, 1.2 Hz, 2H, H_1), 2.34 (s, 3H, H_{CH3}). **^{13}C-NMR** (100 MHz, $CDCl_3$, δ in ppm): 150.58 (CO), 145.08 (CS), 135.78 (C_3), 135.43 (C_{ar}), 135.25 (C_{ar}), 129.61 (C_4), 128.61 (C_5), 128.40(C_{ar}), 128.32 (C_{ar}), 126.68(C_{ar}), 121.65 (C_2) , 67.35 (C_1), 21.62 (C_{CH3}). **ESI-TOF MS** for [M-H$_+$] $C_{17}H_{16}NSO_{4-}$ (m/z): 330.0827; found: 330.0809. Characterisation data corresponds to the data reported in the literature.[78]

(*E*)-3-phenylallyl tosylcarbamate (4.45)

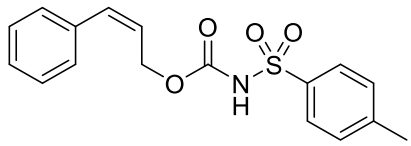

The title compound was prepared following the N-substituted carbamoylation of cinnamyl alcohols starting from alcohol **4.30** (973 mg, 7.04 mmol) and tosyl isocyanate (1.13 mL, 7.40 mmol). The crude was purified by chromatography column using a mobile phase of hexane/AcOEt (80:20). Recrystallization by slow diffusion of pentane in a solution of carbamate in THF rendered **4.45** as a white solid (1820 mg, 5.49 mmol, 78% yield).

^{1}H-NMR (400 MHz, $CDCl_3$, δ in ppm: 7.89 – 7.84 (m, 2H, H_4), 7.49 (s, 1H, H_{NH}), 7.32 – 7.24 (m, 5H, H_{ar}), 7.23 – 7.17 (m, 2H, H_5), 6.51 (dt, J=15.8, 1.2 Hz, 1H, H_3), 6.07 (dt, J=15.9, 6.6 Hz, 1H, H_2), 4.65 (dd, J=6.6, 1.2 Hz, 2H, H_1), 2.34 (s, 3H, H_{CH3}).**^{13}C-NMR** (100 MHz, $CDCl_3$, δ to ppm: 150.58 (CO), 145.08 (CS), 135.78 (C_3), 135.43 (C_{ar}), 135.25 (C_{ar}), 129.61 (C_4), 128.61 (C_5), 128.40(C_{ar}), 128.32 (C_{ar}), 126.68(C_{ar}), 121.65 (C_2) , 67.35 (C_1), 21.62 (C_{CH3}). **ESI-TOF MS** for [M-H+] $C_{17}H_{16}NSO_{4-}$ (m/z): 330.0827; found: 330.0809. Characterisation data corresponds to the data reported in the literature.[85]

(*E*)-3-phenylallyl tosylcarbamate (4.46)

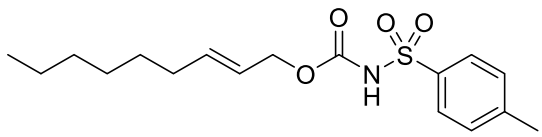

The title compound was prepared following the N-protected carbamoylation of cinnamyl alcohols starting from commercially available

[85] Beccalli, E. M.; Broggini, G.; Foschi, F.; Lo Presti, L.; Loro, C.; Oble, J.; Poli, G.; Sala, R. *Org. Lett.* **2020**, *22*, 4, 1402–1406

trans-2-nonen-1-ol (250 mg, 1.76 mmol) and tosyl isocyanate (0.32 mL, 2.10 mmol). The crude was purified by chromatography column using a mobile phase of hexane/AcOEt (90:10). Recrystallization by slow diffusion of pentane in a solution of carbamate in THF rendered **4.46** as a white solid (466 mg, 1.37 mmol, 78% yield).

^{1}H-NMR (400 MHz, $CDCl_3$, δ in ppm): 7.90 (s, 1H, NH), 7.88 – 7.83 (m, 2H, H_{10}), 7.26 (d, J=8.5 Hz, 2H, H_{11}), 5.71 – 5.60 (m, 1H, H_2), 5.37 (dt, J=15.1, 6.6 Hz, 1H, H_3), 4.43 (d, J=6.6 Hz, 2H, H_1), 2.36 (d, J=5.8 Hz, 3H, H_{12}), 1.93 (dd, J=13.9, 6.9 Hz, 2H, H_4), 1.32 – 1.10 (m, 8H, $H_{5,6,7,8}$), 0.81 (q, J=6.7 Hz, 3H, H_9). **^{13}C-NMR** (100 MHz, $CDCl_3$, δ in ppm): 150.59 (CO), 144.90 (CS), 137.97 (C_2), 129.51 (C_{10}), 128.37 (C_{11}), 122.42 (C_3), 67.60 (C_1), 32.15 (C_4), 31.61 (C_5), 28.76 (C_6), 28.66 (C_7), 22.53 (C_8), 21.62 (C_{12}), 14.04 (C_9). **ESI-TOF MS** for $[M\text{-}H_+]$ $C_{17}H_{25}NSO_{4-}$ (m/z): 338.4427; found: 338.4371. Characterisation data corresponds to the data reported in the literature.[86]

(*E*)-3-non-2-en-1-yl tosylcarbamate (4.47)

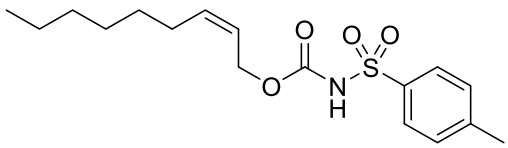

The title compound was prepared following the N-protected carbamoylation of cinnamyl alcohols starting from commercially available *cis*-2-nonen-1-ol (250 mg, 1.76 mmol) and tosyl isocyanate (0.32 mL, 2.10 mmol). The crude was purified by chromatography column using a mobile phase of hexane/AcOEt (90:10) and rendered **4.47** as a colourless oil (478 mg, 1.41 mmol, 80% yield).

IR (neat): 3239, 2956, 2926, 2856, 1746, 1598, 1443, 1343, 1186, 1156, 1089, 909, 856, 730, 661 cm^{-1}. **^{1}H-NMR** (400 MHz, $CDCl_3$, δ in ppm) δ 7.89 – 7.81 (m, 2H, H_{10}), 7.42 (d, J=23.3 Hz, 1H, NH), 7.30 – 7.24 (m, 2H, H_{11}),

[86] Bauer, J. M.; Frey, W.; Peters, R. *Eur. J.* **2016**, *22*, 16, 5767 - 5777

5.58 (dt, J=8.6, 7.6 Hz, 1H, H_2), 5.41 – 5.30 (m, 1H, H_3), 4.57 – 4.52 (m, 2H, H_1), 2.38 (s, 3H, H_{12}), 1.96 (dd, J=14.1, 6.7 Hz, 2H, H_4), 1.33 – 1.10 (m, 8H, $H_{5,6,7,8}$), 0.84 – 0.77 (m, 3H, H_9). ^{13}**C-NMR** (100 MHz, $CDCl_3$, δ in ppm): 150.76 (CO), 144.88 (CS), 136.49 (C_2), 129.50 (C_{10}), 128.36 (C_{11}), 121.95 (C_3), 62.61 (C_1), 31.59 (C_4), 29.22 (C_5), 28.76 (C_6), 27.50 (C_7), 22.60 (C_{12}), 21.64 (C_8), 14.07 (C_9). **HR ESI-TOF MS** for [M-H-] $C_{17}H_{24}NSO_{4-}$ (m/z): 362.1397; found: 362.1398.

(*E*)-3-phenylallyl benzylcarbamate (4.48)

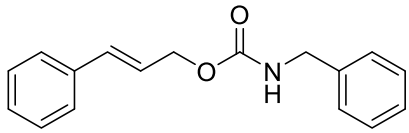

The title compound was prepared following the N-protected carbamoylation of cinnamyl alcohols starting from commercially available cinnamyl alcohol (1106 mg, 8.00 mmol) and benzyl isocyanate (1.09 ml, 8.80 mmol). The crude was purified by chromatography column using a mobile phase of hexane/AcOEt (80:20). Recrystallization by slow diffusion of pentane in a solution of carbamate in THF rendered **4.48** as a white solid (1711 mg, 6.40 mmol, 80% yield).

^{1}H-NMR (400 MHz, $CDCl_3$, δ in ppm): 7.61 – 7.18 (m, 10H, H_{ar}), 6.64 (d, J=15.9 Hz, 1H, H_3), 6.30 (dt, J=15.8, 6.3 Hz, 1H, H_2), 5.20 (s, 1H, H_{NH}), 4.77 (t, J=7.7 Hz, 2H, H_1), 4.39 (d, J=5.9 Hz, 1H, H_4). **^{13}C-NMR** (100 MHz, $CDCl_3$, δ in ppm): 156.38 (CO), 138.48 (C_{ar}), 136.32 (C_{ar}), 133.64 (C_3), 128.66 (C_{ar}), 128.58 (C_{ar}), 127.97 (C_{ar}), 127.52 (C_{ar}), 127.48 (C_{ar}), 126.60 (C_{ar}), 123.89 (C_2), 65.58 (C_1), 45.11 (C_4). **ESI-TOF MS** for [M+Na+] $C_{17}H_{17}NNaO_{2-}$ (m/z): 290.3192; found: 290.1144. Characterisation data corresponds to the data reported in the literature.[87]

[87] Matsuoka, J.; Fujimoto, Y.; Miyawaki, A.; Yamamoto, Y. *Org. Lett.* **2022**, *24*, 51, 9447 - 9451

(*E*)-3-phenylallyl benzylcarbamate (4.49)

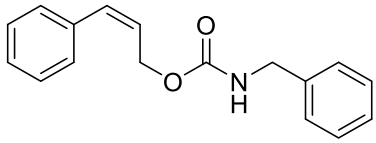

The title compound was prepared following the N-substituted carbamoylation of cinnamyl alcohols starting from alcohol **4.30** (1106 mg, 8.00 mmol) and benzyl isocyanate (1.09 ml, 8.80 mmol). The crude was purified by chromatography column using a mobile phase of hexane/AcOEt (80:20). Recrystallization by slow diffusion of pentane in a solution of carbamate in THF rendered **4.49** as a white solid (1711 mg, 6.40 mmol, 80% yield).

^{1}H-NMR (400 MHz, $CDCl_3$, δ in ppm: 7.61 – 7.18 (m, 10H, H_{ar}), 6.64 (d, J=15.9 Hz, 1H, H_3), 6.30 (dt, J=15.8, 6.3 Hz, 1H, H_2), 5.20 (s, 1H, H_{NH}), 4.77 (t, J=7.7 Hz, 2H, H_1), 4.39 (d, J=5.9 Hz, 1H, H_4). **^{13}C-NMR** (100 MHz, $CDCl_3$, δ in ppm: 156.38 (CO), 138.48 (C_{ar}), 136.32 (C_{ar}), 133.64 (C_3), 128.66 (C_{ar}), 128.58 (C_{ar}), 127.97 (C_{ar}), 127.52 (C_{ar}), 127.48 (C_{ar}), 126.60 (C_{ar}), 123.89 (C_2), 65.58 (C_1), 45.11 (C_4). **ESI-TOF MS** for [M+Na_+] $C_{17}H_{17}NNaO_{2-}$ (m/z): 290.3192; found: 290.1145. Characterisation data corresponds to the data reported in the literature.[87]

(*E*)-3-phenylallyl benzylcarbamate (4.50)

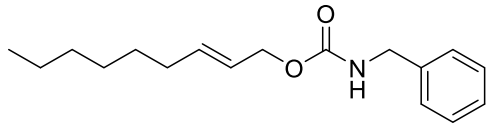

The title compound was prepared following the N-protected carbamoylation of cinnamyl alcohols starting from commercially available *trans*-2-nonen-1-ol (284 mg, 2.00 mmol) and benzyl isocyanate (260 µL, 2.10 mmol). The crude was purified by chromatography column using a mobile phase of hexane/AcOEt (90:10). Recrystallization by slow diffusion of pentane in a solution of carbamate in THF rendered **4.50** as a white solid (435 mg, 1.58 mmol, 79% yield).

M. p. 28-29 °C. **IR (neat)**: 3305, 3062, 3031, 2921, 2872, 2848, 1685, 1538, 1466, 1454, 1250, 1136, 1050, 981, 965, 747, 695, 651 cm^{-1}. **^{1}H-NMR** (400 MHz, $CDCl_3$, δ in ppm): 7.31 – 7.11 (m, 5H, H_{ar}), 5.76 – 5.58 (m, 1H, H_2), 5.47 (dt, J=13.9, 6.4 Hz, 1H, H_3), 5.08 (s, 1H, NH), 4.44 (d, J=6.3 Hz, 2H, H_1), 4.26 (d, J=5.9 Hz, 2H, H_{10}), 1.95 (dd, J=14.1, 6.9 Hz, 2H, H_4), 1.39 – 1.10 (m, 8H, $H_{5,6,7,8}$), 0.80 (t, J=6.7 Hz, 3H, H_9). **^{13}C-NMR** (100 MHz, $CDCl_3$, δ in ppm): 156.48 (CO), 136.18 (C_2), 128.58(C_{ar}), 128.56 (C_{ar}), 127.46 (C_{ar}), 127.37 (C_{ar}), 127.35 (C_{ar}), 124.29 (C_3), 65.80 (C_1), 45.02 (C_{10}), 32.24(C_4), 31.67 (C_5), 28.87 (C_6), 28.82 (C_7), 22.59 (C_8),14.08 (C_9). **HR ESI-TOF MS** for [M-H-] $C_{17}H_{24}NO_2^-$ (m/z): 298.1777; found: 298.1780.

(Z)-non-2-en-1-yl benzylcarbamate (4.51)

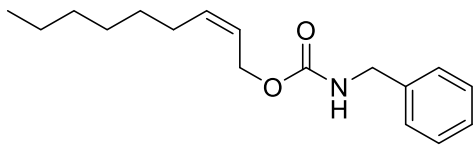

The title compound was prepared following the N-protected carbamoylation of cinnamyl alcohols starting from commercially available *cis*-2-nonen-1-ol (284 mg, 2.00 mmol) and benzyl isocyanate (260 µL, 2.10 mmol). The crude was purified by chromatography column using a mobile phase of hexane/AcOEt (80:20) and rendered **4.51** as a colourless oil (441 mg, 1.60 mmol, 80% yield).

IR (neat): 3331, 2955, 2925, 2855, 1696, 1517, 1455, 1241, 1134, 1040, 971, 734, 696 cm^{-1}. **^{1}H-NMR** (400 MHz, $CDCl_3$, δ in ppm): 7.33 – 7.10 (m, 5H, H_{ar}), 5.84 (s, 1H, NH), 5.55 (dd, J=10.8, 7.3 Hz, 1H, H_2), 5.48 (dd, J=11.7, 5.6 Hz, 1H, H_3), 4.56 (d, J=6.1 Hz, 2H, H_1), 4.23 (d, J=5.8 Hz, 2H, H_{10}), 2.04 (q, J=6.7 Hz, 2H, H_4), 1.42 – 1.14 (m, 8H, $H_{5,6,7,8}$), 0.88 (t, J=6.7 Hz, 3H, H_9). **^{13}C-NMR** (100 MHz, $CDCl_3$, δ in ppm): 156.79 (CO), 134.48 (C_2), 128.27 (C_{ar}), 127.39 (C_{ar}), 127.10 (C_{ar}), 124.21 (C_3), 60.63 (C_1), 44.93 (C_{10}), 31.71 (C_4), 29.54 (C_5), 28.86 (C_6), 27.49 (C_7), 22.69 (C_8), 14.19 (C_9). **HR ESI-TOF MS** for [M-H-] $C_{17}H_{24}NO_2^-$ (m/z): 298.1777; found: 298.1780.

-(fluoro(phenyl)methyl)oxazolidin-2-one (*anti*/*syn*-4.55)

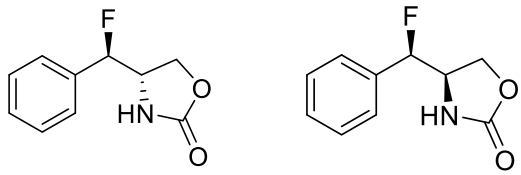

The title compounds were prepared following the general sequential aziridination + ring-opening from carbamate **4.31** (17.5 mg, 0.10 mmol) using DMPU-HF (0.6 mL, 2.60 mmol). The crude was purified by chromatography column using a mobile phase of hexane/AcOEt (60:40) to give a diastereomeric mixture 23:77 *syn*/*anti* (14.1 mg, 0.72 mmol, 72% yield). For the sake of characterization, a small sample was separated by column chromatography. Complete separation of the *syn*/*anti* diastereomers was achieved by chromatography column using a mobile phase of hexane/AcOEt (50:50).

***Anti*-4.55:** **^{1}H-NMR** (400 MHz, $CDCl_3$, δ in ppm): 7.43 (m, 3H), 7.34 (m, 2H), 5.47 (s, NH), 5.35 (dd, 1H, J^2_{H-F}=47.7Hz, J^3_{H-H}=6.7Hz), 4.30 (ddd, 1H, J^2_{H-H}=8.7Hz, J^3_{H-H}=8.4Hz, J^4_{H-F}=2.4Hz), 4.22 (m, 1H), 4.14 (dd, 1H, J^2_{H-H}=8.4Hz, J^3_{H-H}=4.0Hz); **^{13}C-NMR** (100 MHz, CDCl3, δ in ppm): 158.7, 134.5 (d, J^2_{C-F}=20.2Hz), 130.1 (d, J^4_{C-F}=2.0), 129.3, 126.4 (d, J^3_{C-F}=6.4Hz), 94.8 (d, J^1_{C-F}=177.9Hz), 65.5 (d, J^3_{C-F}=7.0Hz), 56.8 (d, J^2_{C-F}=24.0Hz); **^{19}F-NMR** ($CDCl_3$, 377 MHz, δ in ppm): -181.8 (dd, J^2_{F-H}=47.3Hz, J^3_{F-H}=13.8Hz); **HR ESI-TOF MS** for [M-H-] $C_{10}H_9FNO_2^-$ (m/z): 218.0593; found: 218.0587. Characterisation data corresponds to the data reported in the literature.[27]

***Syn*-4.55:** **^{1}H-NMR** (400 MHz, $CDCl_3$, δ in ppm): 7.43 (m, 3H), 7.34 (m, 2H), 5.15 (s, NH), 5.35 (dd, 1H, J^2_{H-F}=46.4Hz, J^3_{H-H}=6.4Hz), 4.54 (m, 2H), 4.14 (m, 1H); **^{13}C-NMR** (100 MHz, CDCl3, δ in ppm): 158.6, 135.2 (d, J^2_{C-F}=20.1Hz), 130.0 (d, J^4_{C-F}=1.7), 129.3, 126.3 (d, J^3_{C-F}=6.4Hz), 93.7 (d, J^1_{C-F}=178.5Hz), 67.1 (d, J^3_{C-F}=2.9Hz), 56.2 (d, J^2_{C-F}=32.4Hz); **^{19}F-NMR** ($CDCl_3$, 377 MHz, δ in ppm): -188.0 (dd, J^2_{F-H}=46.5Hz, J^3_{F-H}=10.1Hz); **HR ESI-TOF**

MS for [M-H-] $C_{10}H_9FNO_2^-$ (m/z): 259.0853; found: ([M+H+]): 259.0851. Characterisation data corresponds to the data reported in the literature.[27]

4-(fluoro(phenyl)methyl)-1,3-dioxolan-2-one (4.56)

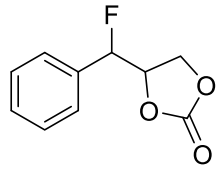

The title compound was obtained as a major byproduct following the general aminofluorination method with *in situ* generated $TolIF_2$ from carbamate **4.31** (50 mg, 0.29 mmol) using Py-HF (0.17 mL, 0.94 mmol). The crude was purified by chromatography column using a mobile phase of hexane/AcOEt 80:20 (23.3 mg, 0.12 mmol, 41% yield).

^{1}H-NMR (400 MHz, $CDCl_3$, δ in ppm): 7.44 (m, 3H), 7.39 (m, 2H), 5.53 (dd, J=45.5, 4.6 Hz, 1H), 5.00 (dddd, J=16.6, 8.5, 6.5, 4.9 Hz, 1H), 4.42 (dd, J=9.7, 8.7 Hz, 1H), 4.33 (dd, J=9.2, 6.5 Hz, 1H); **^{13}C-NMR** (100 MHz, $CDCl_3$, δ in ppm): 154.2, 133.1 (d, J=20.4 Hz), 130.0 (d, J=2.0 Hz), 129.1, 126.4 (d, J=6.5 Hz), 92.0 (d, J=181.3 Hz), 76.8, 65.1 (d, J=4.6 Hz); **^{19}F-NMR** (377 MHz, $CDCl_3$, δ in ppm): -189.4 (dd, J=45.6, 18.6 Hz); **HR ESI-TOF MS** for [M+H+] $C_{10}H_{10}FO_3^+$ (m/z): 197.0614; found: 197.0613.

3,3-Difluoro-2-phenylpropyl carbamate (4.57)

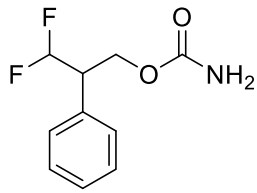

The title compound was obtained as a major byproduct following the general aminofluorination method with *in situ* generated $TolIF_2$ from carbamate **4.31** (50 mg, 0.29 mmol) using DMPU-HF (0.17 mL, 0.94 mmol). The crude was purified by chromatography column using a mobile phase of hexane/AcOEt 80:20 to 70:30 (3.2 mg, 0.02 mmol, 16% yield).

^{1}H-NMR (400 MHz, $CDCl_3$, δ in ppm): 6.03 (td, J=55.7, 3.4 Hz, 1H), 4.53 (dd, J=11.2, J=7.2 Hz, 1H), 3.45 (m, 1H); **^{13}C-NMR** (100 MHz, $CDCl_3$, δ in ppm): 156.1, 116.2 (t, J=244.0 Hz), 49.0 (t, J=20.5 Hz), 63.1 (t, J=5.7 Hz); **^{19}F-NMR** (377 MHz, $CDCl_3$, δ in ppm): -122.8 (ddd, J=282.8, 55.4, 13.4 Hz), -120.7 (ddd, J=283.5, 55.9, 17.4 Hz); **HR ESI-TOF MS** for $[M+H_+]$ $C_{10}H_{12}F_2NO_{2+}$ (m/z): 216.0836; found: 216.0845.

(*E*)-4-(1-fluorobut-2-en-1-yl)oxazolidin-2-one (4.61)

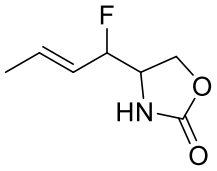

The title compound was prepared following the general aminofluorination method with $TolIF_2$ from carbamate **4.43** (14.1 mg, 0.10 mmol). The crude was purified by chromatography column using a mobile phase of Hexane/AcOEt (60:40) as an inseparable mixture of *syn*/*anti* isomers (4.1 mg, 0.03 mmol, 26% yield).

^{1}H-NMR (400 MHz, $CDCl_3$, δ in ppm): 5.99 (dq, J=18.2, 5.7 Hz, 1H), 5.50 (dddq, J=33.4, 15.2, 7.8, 1.5 Hz, 1H), 4.74 (dt, J=47.2, 7.0 Hz, 1H), 4.48 (t, J=8.8 Hz, 1H), 4.32 (dd, J=9.2, 4.6 Hz, 1H), 3.98 (m, 1H), 1.80 (dddd, J=6.7, 5.2, 3.6, 1.7 Hz, 3H). **^{13}C-NMR** (100 MHz, $CDCl_3$, δ in ppm): 159.4, 135.8 (d, J=11.5 Hz), 124.1 (d, J=19.3 Hz), 93.4 (d, J=172.0, Hz), 66.4 (d, J=4.4 Hz), 54.8 (d, J=29.4 Hz), 29.8. **^{19}F-NMR** (377 MHz, $CDCl_3$, δ in ppm): -177.77 (dtd, J=48.9, 11.8, 6.0 Hz), -181.1 (ddd, J=47.6, 10.8, 5.4 Hz); **HR ESI-TOF MS** for $[M+H_+]$ $C_7H_9FNO_{2+}$ (m/z): 177.1034; found: 177.1030.

(*E*)-4-(3-fluorobut-1-en-1-yl)oxazolidin-2-one (4.62)

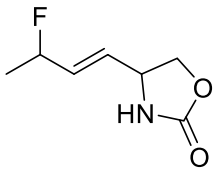

The title compound was obtained as a major byproduct following the general aminofluorination method with $TolIF_2$ from carbamate **4.43** (14.1 mg, 0.10 mmol). The crude was purified by chromatography column using a mobile phase of Hexane/AcOEt (60:40) as an inseparable mixture of *syn*/*anti* isomers in a (3.3 mg, 0.02 mmol, 21% yield).

^{1}H-NMR (400 MHz, $CDCl_3$, δ in ppm): 5.84 (ddd, J=29.5, 15.7, 5.1 Hz, 1H), 5.73 (m, 1H), 5.09 (dp, J=48.3, 6.3 Hz, 1H), 4.55 (t, J=8.5, 1H), 4.42 (m, 1H), 4.07 (dd, J = 8.6, 6.6 Hz, 1H); **^{13}C-NMR** (100 MHz, $CDCl_3$, δ in ppm): 159.4, 134.2 (d, J=19.8 Hz), 129.6 (d, J=10.6 Hz), 88.5 (d, J=168.0 Hz), 70.0 (d, J=2.1 Hz), 54.2, 21.2 (d, J=23.3 Hz). **^{19}F-NMR** (377 MHz, $CDCl_3$, δ in ppm): -170.9 (ddq, J=47.1, 24.3, 13.2 Hz). **HR ESI-TOF MS** for $[M+H_+]$ $C_7H_9FNO_{2+}$ (m/z): 158.0623; found: 158.0601.

4-(fluoro-2-oxoxazolidin-4-yl)methyl)phenyl acetate (*anti*/*syn*-4.63)

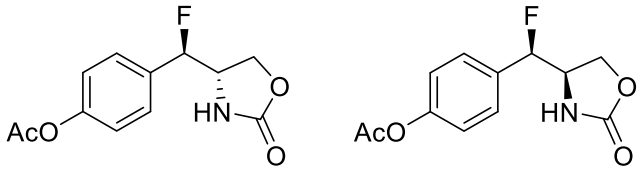

The title compounds were prepared following the general sequential aziridination + ring-opening from carbamate **4.32** (50.0 mg, 0.21 mmol) using DMPU-HF (0.15 mL, 0.46 mmol). The crude was purified by chromatography column using a mobile phase of Et_2O/AcOEt (90:10) to give a diastereomeric mixture 18:82 *syn*/*anti* (34.6 mg, 0.14 mmol, 65%). For the sake of characterization, a small sample was separated by column chromatography.

IR (neat): 3290, 2923, 2851, 2349, 1742, 1509, 1408, 1370, 1192, 911 cm^{-1}.

***Anti*-4.63:** **^{1}H-NMR** (400 MHz, $CDCl_3$, δ in ppm): 7.36 (dd, J=8.5, 1.1 Hz, 1H), 7.21 – 7.14 (m, 1H), 5.52 – 5.48 (m, 1H), 5.35 (dd, J=46.8, 6.8 Hz, 1H), 4.32 (td, J=8.4, 2.4 Hz, 3H), 4.26 – 4.12 (m, 1H), 2.32 (s, 1H). **^{13}C-NMR** (100 MHz, CDCl3, δ in ppm): 169.4, 158.9, 151.7 (d, J=2.0 Hz) 132.8 (d, J=20.2 Hz), 127.5 (d, J=6.7 Hz), 122.5, 93.1 (d, J=179.2 Hz), 66.8 (d, J=2.9 Hz), 56.3 (d, J=31.5 Hz), 21.3. **^{19}F-NMR** ($CDCl_3$, 377 MHz, δ in ppm): -181.46 (dd, J=46.3, 15.3 Hz). **HR ESI-TOF MS** for [M-H-] $C_{12}H_{11}FNO_{2-}$ (m/z): 276.0643; found: 276.2481.

***Syn*-4.63:** **^{1}H-NMR** (400 MHz, $CDCl_3$, δ in ppm): 7.37 (d, J=8.5 Hz, 2H), 7.17 (d, J=8.5 Hz, 2H), 5.52 (bs, 1H), 5.36 (dd, J=46.1, 6.8 Hz, 1H), 4.54 – 4.46 (m, 2H), 4.22 – 4.06 (m, 1H), 2.32 (s, 3H). **^{13}C-NMR** (100 MHz, CDCl3, δ in ppm): 169.4, 158.9, 151.7 (d, J=2.0 Hz) 132.8 (d, J=20.2 Hz), 127.5 (d, J=6.7 Hz), 122.5, 93.1 (d, J=179.2 Hz), 66.8 (d, J=2.9 Hz), 56.3 (d, J=31.5 Hz), 21.3. **^{19}F-NMR** ($CDCl_3$, 377 MHz, δ in ppm): -186.9 (dd, J = 46.1, 6.8 Hz **HR ESI-TOF MS** for [M-H-] $C_{12}H_{11}FNO_{2-}$ (m/z): 276.0643; found: 276.0643.

4-(fluoro(4-methoxyphenyl)methyl)oxazolidin-2-one (*anti*/*syn*-4.60)

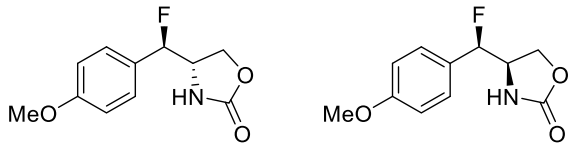

The title compounds were prepared following the general aminofluorination method with $TolIF_2$ from carbamate **4.33** (20.7 mg, 0.10 mmol). The crude was purified by chromatography column using a mobile phase of hexane/AcOEt (50:50) to give a diastereomeric mixture 60:40 *syn*/*anti* (16.2 mg, 0.07 mmol, 72%). For the sake of characterization, a small sample was separated by column chromatography.

IR (neat): 3288,2920,2850,1743,1614,1515,1246,1178,1025 cm^{-1}

***Anti*-4.60:** **^{1}H-NMR** (400 MHz, $CDCl_3$, δ in ppm): 7.49 – 7.41 (m, 2H, Har), 7.35 (m, 2H, Har), 5.80 (s, HNH), 5.35 (dd, J=46.3, 7.0 Hz, 1H, H1'), 4.23 (m, 4.28 – 4.20, 2H, H1, H1'), 4.03 (m, 4.06 – 4.01, 1H, H2); **^{13}C-NMR** (100 MHz, $CDCl_3$, δ in ppm): 160.8, 128.1 (J=5.5 Hz), 126.2 (d, J=20.6 Hz), 114.6, 94.8 (d, J=176.1 Hz), 65.4 (d, J=6.5 Hz), 56.5 (d, J=25.0 Hz). **^{19}F-NMR** (377 MHz, $CDCl_3$, δ in ppm): -173.31 (dd, J=46.4, 13.6 Hz); **HR ESI-TOF MS** for [M+Na^+]: $C_{11}H_{12}FNNaO_{2+}$ (m/z): 218.0588; found: 218.0593.

***Syn*-4.60:** **^{1}H-NMR** (400 MHz, $CDCl_3$, δ in ppm): 7.49 – 7.41 (m, 2H, Har), 7.35 (m, 2H, Har), 5.35 (dd, J=46.3, 7.0 Hz, 1H, H1'), 5.15 (bs, 1H, HNH), 4.54 – 4.50 (m, 2H, H5), 4.20 – 4.09 (m, 1H, H4). **^{13}C-NMR** (100 MHz, $CDCl_3$, δ in ppm): 158.8, 135.1 (d, J=19.7 Hz), 129.9 (d, J=1.8 Hz), 129.3, 126.3 (d, J=6.7 Hz), 93.6 (d, J=178.6 Hz), 66.9 (d, J=2.8 Hz), 56.3 (d, J=31.5 Hz). **19F-NMR** (377 MHz, $CDCl_3$, δ in ppm): -186.3 (dd, J=46.3, 10.5 Hz). **HR ESI-TOF MS** for [M+Na^+]: $C_{11}H_{12}FNNaO_{2+}$ (m/z): 218.0588; found: 218.0593.

4-(fluoro(4-methylphenyl)methyl)oxazolidin-2-one (*anti*/*syn*-4.64)

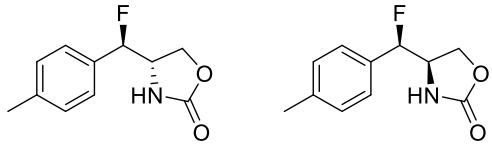

The title compounds were prepared following the general aminofluorination method with $TolIF_2$ from carbamate **4.34** (19.1 mg, 0.10 mmol). The crude was purified by chromatography column using a mobile phase of Et_2O/Hexane (80:20) to give a diastereomeric mixture 81:19 *syn*/*anti* (11.9 mg, 0.06 mmol, 57%). For the sake of characterization, a small sample was separated by column chromatography.

IR (neat): 3305, 1756, 1722, 1408, 1284, 1113, 1020, 767, 736 cm^{-1}.

***Anti*-4.64:** **^{1}H-NMR** (400 MHz, $CDCl_3$, δ in ppm): 7.25 – 7.22 (m, 4H), 5.30 (dd, J=47.1, 7.0 Hz, 1H), 4.31 – 4.15 (m, 2H), 4.16 – 4.08 (m, 1H), 2.38 (d, J=1.7 Hz, 4H). **^{13}C-NMR** (100 MHz, $CDCl_3$, δ in ppm): 166.3, 159.0, 139.7

(d, J=20.0 Hz), 131.3, 130.26, 125.9 (d, J=7.0 Hz), 92.8 (d, J=179.0 Hz), 66.2 (d, J=4.0 Hz), 56.2 (d, J=29.0 Hz). **^{19}F-NMR** (377 MHz, $CDCl_3$, δ in ppm): -179.07 (dd, J=47.1, 13.2 Hz). **HR ESI-TOF MS** for $[M+H]^+$: $C_{11}H_{13}FNO_{2+}$ (m/z): 254.0829; found: 254.0835.

***Syn*-4.34:** **^{1}H-NMR** (400 MHz, $CDCl_3$, δ in ppm): 7.24 (s, 4H), 5.28 (dd, J=46.2, 7.5 Hz, 1H), 4.60-4.49 (m, 2H), 4-18.4-08 (m, 1H), 2.38 (d, J=1.5 Hz, 3H). **^{13}C-NMR** (100 MHz, $CDCl_3$, δ in ppm): 166.25, 158.8, 139.1 (d, J=20.0 Hz), 131.5, 130.32, 126.1 (d, J=7.0 Hz), 93.6 (d, J=179.0 Hz), 65.3 (d, J=7.0 Hz), 56.5 (d, J=24.0 Hz). **^{19}F-NMR** (377 MHz, $CDCl_3$, δ in ppm): -183.47 (d, J=49.0 Hz). **HR ESI-TOF MS** for $[M+H]^+$: $C_{11}H_{13}FNO_{2+}$ (m/z): 254.0829; found: 254.0835.

4-(fluoro(4-bromophenyl)methyl)oxazolidin-2-one (*anti*/*syn*-4.65)

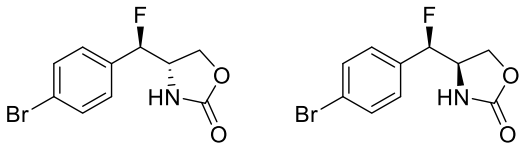

The title compounds were prepared following the general aminofluorination method with $TolIF_2$ from carbamate **4.35** (20.1 mg, 0.10 mmol). The crude was purified by chromatography column using a mobile phase of Et_2O/Hexane (80:20) to give a diastereomeric mixture 81:19 *syn*/*anti* (13.2 mg, 0.05 mmol, 48%). For the sake of characterization, a small sample was separated by column chromatography.

IR(neat):3251, 2954, 2921, 2851, 1766, 1641, 1239, 1203, 1027cm^{-1}.

***Anti*-4.65:** **^{1}H-NMR** (400 MHz, $CDCl_3$, δ in ppm): 7.34 (ddt, J=6.4, 5.1, 1.3 Hz, 2H), 7.17 – 7.09 (m, 2H), 6.00 (s, 1H), 5.34 (dd, J=46.6, 6.8 Hz, 1H), 4.34 – 4.14 (m, 2H), 4.14 – 4.06 (m, 1H)**. ^{13}C-NMR** (100 MHz, $CDCl_3$, δ in ppm): 163.59 (dd, J=249.6, 2.2 Hz), 159.00, 130.41 (dd, J=20.6, 3.3 Hz), 128.48 (dd, J=8.5, 6.1 Hz), 116.42 (d, J=21.8 Hz), 94.11 (d, J=177.9 Hz), 65.38 (d, J=6.5 Hz), 56.66 (d, J=24.6 Hz). **^{19}F-NMR** (377 MHz, $CDCl_3$, δ in ppm): -

182.3 (dd, J = 46.1, 11.5 Hz). **HR ESI-TOF MS** for [M+Na+]: $C_{10}H_9FNNaO_{2+}$ (m/z): 295.9698; found: 295.9693.

***Syn*-4.65:** **^{1}H-NMR** (400 MHz, $CDCl_3$, δ in ppm): 7.59 (d, J=8.4 Hz, 2H, H_{ar}), 7.23 (d, J=8.4 Hz, 2H, H_{ar}), 5.32 (dd, J=46.1, 7.1 Hz, 1H, H1'), 4.81 (bs, 1H, HNH), 4.64 – 4.42 (m, 2H, H5), 4.20 – 4.05 (m, 1H, H4). **^{13}C-NMR** (100 MHz, $CDCl_3$, δ in ppm): 159.0, 134.1 (d, J=20.2 Hz), 132.4, 127.8 (d, J=6.8 Hz), 124.1 (d, J=2.1 Hz), 92.97 (d, J=179.6 Hz), 66.63 (d, J=3.3 Hz), 56.14. **^{19}F-NMR** (377 MHz, $CDCl_3$, δ in ppm): -186.3 (dd, J=46.1, 11.5 Hz). **HR ESI-TOF MS** for [M+Na+]: $C_{10}H_9FNNaO_{2+}$ (m/z): 295.9698; found: 295.9693.

4-(fluoro(4-fluorophenyl)methyl)oxazolidin-2-one (*anti*/*syn*-4.66)

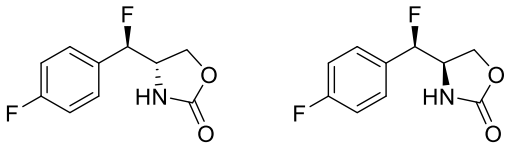

The title compounds were prepared following the general aminofluorination method with $TolIF_2$ from carbamate **4.36** (19.5 mg, 0.10 mmol). The crude was purified by chromatography column using a mobile phase of Et_2O/Hexane (80:20) to give a diastereomeric mixture 91:9 *syn*/*anti* (9.0 mg, 0.04 mmol, 42%). For the sake of characterization, a small sample was separated by column chromatography.

IR(neat): 3280, 2956, 2952, 2852, 1749, 1494, 1229, 1024, 892 cm^{-1}.

***Anti*-4.66:** **^{1}H-NMR** (400 MHz, $CDCl_3$, δ in ppm): 7.34 (ddt, J=6.4, 5.1, 1.3 Hz, 2H), 7.17 – 7.09 (m, 2H), 6.00 (s, 1H), 5.34 (dd, J=46.6, 6.8 Hz, 1H), 4.34 – 4.14 (m, 2H), 4.14 – 4.06 (m, 1H). **^{13}C-NMR** (100 MHz, $CDCl_3$, δ in ppm): 163.59 (dd, J=249.6, 2.2 Hz), 159.00, 130.41 (dd, J=20.6, 3.3 Hz), 128.48 (dd, J=8.5, 6.1 Hz), 116.42 (d, J=21.8 Hz), 94.11 (d, J=177.9 Hz), 65.38 (d, J=6.5 Hz), 56.66 (d, J=24.6 Hz). **^{19}F-NMR** (377 MHz, $CDCl_3$, δ in ppm): -

110.67 (qd, J=8.4, 4.3 Hz), -179.75 (dd, J=46.6, 13.7 Hz). **HR ESI-TOF MS** for $[M+Na]^+$: $C_{10}H_9FNNaO_{2+}$ (m/z): 236.1730; found: 236.0495.

***Syn*-4.66:** **^{1}H-NMR** (400 MHz, $CDCl_3$, δ in ppm): 7.61 – 7.57 (m, 1H), 7.25 – 7.20 (m, 1H), 5.47 (s, 1H), 5.32 (dd, J=46.8, 6.7 Hz, 0H), 4.31 (td, J=8.5, 2.3 Hz, 1H), 4.23 – 4.10 (m, 1H). **^{13}C-NMR** (100 MHz, $CDCl_3$, δ in ppm): 163.59 (dd, J=249.6, 2.2 Hz), 159.00, 130.41 (dd, J=20.6, 3.3 Hz), 128.48 (dd, J=8.5, 6.1 Hz), 116.42 (d, J=21.8 Hz), 94.11 (d, J=177.9 Hz), 65.38 (d, J=6.5 Hz), 56.66 (d, J=24.6 Hz). **^{19}F-NMR** (377 MHz, $CDCl_3$, δ in ppm): -183.35 (dd, J=46.0, 9.5 Hz). **HR ESI-TOF MS** for $[M+Na]^+$: $C_{10}H_9FNNaO_{2+}$ (m/z): 236.1730; found: 236.0495.

Syn-4-(fluoro(4-(trifluoromethyl)phenyl)methyl)oxazolidin-2-one (*syn*-4.67)

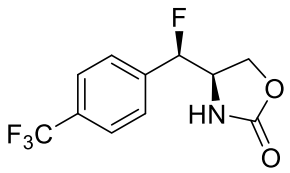

The title compound was prepared following the general aminofluorination method with $TolIF_2$ from carbamate **4.37** (24.5 mg, 0.10 mmol). The crude was purified by chromatography column using a mobile phase of Et_2O/Hexane (80:20) as a white solid (6.1 mg, 0.02 mmol, 23% yield).

M. p. 108-110 °C. **IR (neat):** 3290, 2923, 2851, 2349, 1742, 1509, 1408, 1370, 1192, 911 cm^{-1}. **^{1}H-NMR** (400 MHz, $CDCl_3$, δ in ppm): 7.72 (d, J=8.1 Hz, 2H, Har), 7.49 (d, J=81 Hz, 2H, Har), 5.44 (dd, J=46.2, 6.6 Hz, 1H, H1'), 5.16 (bs, 1H, HNH), 4.59 – 4.44 (m, 2H, H5), 4.25 – 4.05 (m, 1H, H4). **^{13}C-NMR** (100 MHz, $CDCl_3$, δ in ppm): 158.9, 138.9 (d, J=20.2 Hz), 126.4, 126.3, 126.1 (q, J=3.7 Hz), 123.7 (q, J=272.5 Hz), 92.6 (d, J=180.6 Hz), 66.2 (d, J=3.7 Hz), 56.2 (d, J=29.5 Hz). **^{19}F-NMR** (377 MHz, $CDCl_3$, δ in ppm): -62.91, -189.44 (dd, J=46.1, 10.5 Hz). **ESI-TOF MS** for $[M+Na_+]$ $C_{11}H_9F_4NO_{2-}$ (m/z): 286.0462; found: 286.0453.

Syn-4-(fluoro(4-nitrophenyl)methyl)oxazolidin-2-one (*syn*-4.59)

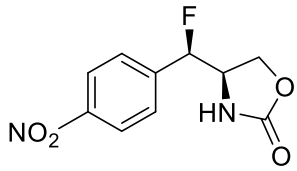

The title compound was prepared following the general aminofluorination method with $TolIF_2$ from carbamate **4.38** (22.0 mg, 0.10 mmol). The crude was purified by chromatography column using a mobile phase of Et_2O/Hexane (80:20) as a yellowish oil (7.7 mg, 0.03 mmol, 32% yield).

^{1}H-NMR (400 MHz, $CDCl_3$, δ in ppm): 5.91 (s, 1H, NH), 5.51 (dd, J=46.1, 6.4, 1H), 4.51 (dd, J=17.7, 9.3, 1H), 4.49 (dd, J=17.4, 9.4, 1H), 4.17 (m, 1H). **^{13}C-NMR** (100 MHz, $CDCl_3$, δ in ppm): 153.6, 140.1 (d, 21.0 Hz), 127.1 (d, J=7.7 Hz), 126.6, 124.2, 90.3 (d, 184.6), 65.0 (d, J=4.2 Hz), 60.8. **^{19}F-NMR** (377 MHz, $CDCl_3$, δ in ppm): -190.28 (dd, J=45.9, 11.9) **ESI-TOF MS** for [M+IsoProp+H_+] $C_{13}H_{18}FN_2O_{5-}$ (m/z): 161.0653; found: 161.0834.

4-(hydroxy(phenyl)methyl)oxazolidin-2-one (4.69)

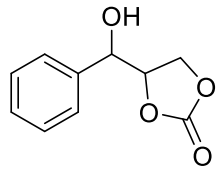

The title compound was obtained as a major byproduct following the general aminofluorination method with *in situ* generated $TolIF_2$ from carbamate **4.31** (50 mg, 0.29 mmol) using Et_3N-HF (0.3 mL, 1.90 mmol). The crude was purified by chromatography column using a mobile phase of hexane/AcOEt (70:30 to 50:50) and **4.69** was obtained as a yellowish oil (63 mg, 0.32 mmol, 17% yield).

^{1}H-NMR (400 MHz, $CDCl_3$, δ in ppm): 7.39 (m, 5H), 5.15 (dd, 1H, $^{3}J_{HH}$=3.5), 4.84 (ddd, 1H, J^{3}_{H-H}=8.4, 6.5, 3.6), 4.55 (dd, 1H, $^{2}J_{HH}$=8.5, $^{3}J_{HH}$=6.5), 4.24 (dd, 1H, $^{2}J_{HH}$=8.5, $^{3}J_{HH}$=8.5), 2.88 (d, 1H, J^{3}_{HH}=3.5); **^{13}C-NMR** (100 MHz, $CDCl_3$, δ in ppm): 155.3, 137.2, 129.1, 128.9, 126.0, 79.1, 72.0, 64.6; **HR ESI-TOF MS** for [M+Na^{+}] $C_{11}H_9F_4NNaO_{2}^{+}$ (m/z): 217.0477; found: 217.0486.

***Anti*-4-fluoro-5-phenyl-1,3-dioxan-2-one (*anti*-4.70)**

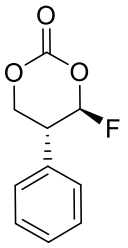

The title compound was obtained as a major byproduct following the general aminofluorination method with *in situ* generated $TolIF_2$ from carbamate **4.31** (50 mg, 0.29 mmol) using DMPU-HF (0.17 mL, 0.94 mmol), evaporating the remaining HF before the addition of the carbamate. The crude was purified by chromatography column using a mobile phase of Hexane/AcOEt 70:30 (13.7 mg, 0.07 mmol, 24% yield).

^{1}H-NMR (400 MHz, $CDCl_3$, δ in ppm): 7.38 (m, 5H), 6.10 (ddd, J=55.2, 3.8, 1.1 Hz, 1H), 4.83 (ddd, J=11.5, 4.5, 2.4 Hz, 1H), 4.60 (ddd, J=11.4, 5.4, 1.2 Hz, 1H), 3.43 (dq, J=11.3, 4.5 Hz, 1H); **^{13}C-NMR** (100 MHz, $CDCl_3$, δ in ppm): 108.6 (d, J=234.6 Hz), 67.5 (d, J=3.1 Hz), 41.4 (d, $^{2}J_{CF}$=21.1 Hz); **^{19}F-NMR** (377 MHz, $CDCl_3$, δ in ppm): -114.4 (ddd, J=55.2, 11.0, 2.4 Hz); **HR ESI-TOF MS** for [M+Na^{+}] $C_{10}H_9FNaO_{3}^{+}$ (m/z): 219.0433; found: 219.0430.

Syn-4-fluoro-5-phenyl-1,3-dioxan-2-one (*syn*-4.70)

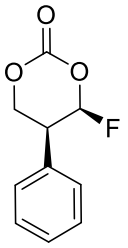

The title compound was obtained as a major byproduct following the general aminofluorination method with *in situ* generated $TolIF_2$ from carbamate **4.1** (50 mg, 0.29 mmol) using DMPU-HF (0.17 mL, 0.94 mmol), evaporating the remaining HF before the addition of the carbamate. The crude was purified by chromatography column using a mobile phase of Hexane/AcOEt 70:30 (30.2 mg, 0.15 mmol, 53% yield).

^{1}H-NMR (400 MHz, $CDCl_3$, δ in ppm): 7.38 (m, 5H), 6.01 (dt, J=55.5, 1.7 Hz, 1H), 4.91 (dd, J=12.9, 10.8 Hz, 1H), 4.53 (ddt, J=10.8, 5.8, 1.6 Hz, 1H), 3.57 (dddd, J=28.6, 12.9, 5.7, 1.8 Hz, 1H); **^{13}C-NMR** (100 MHz, $CDCl_3$, δ in ppm): 106.6 (d, J=234.7 Hz), 67.0 (d, J=6.0 Hz), 41.6 (d, $^{2}J_{CF}$= Aprox 19.5 Hz); **^{19}F-NMR** (377 MHz, $CDCl_3$, δ in ppm): -132.8 (dd, J=55.6, 28.3 Hz); **HR ESI-TOF MS** for $[M+Na^+]$ $C_{10}H_9FNaO_3^+$ (m/z): 219.0433; found: 219.0434.

UNIVERSITAT ROVIRA I VIRGILI
INSIGHTS INTO AMINOFLUORINATION STRATEGIES AND SPHINGOSINE ANALOGUE SYNTHESIS TOWARDS THE DEVELOPMENT OF SELECTIVE SPHK2 INHIBITORS
Albert Granell Fort

CHAPTER V

General Conclusions

UNIVERSITAT ROVIRA I VIRGILI
INSIGHTS INTO AMINOFLUORINATION STRATEGIES AND SPHINGOSINE ANALOGUE SYNTHESIS TOWARDS THE DEVELOPMENT OF SELECTIVE SPHK2 INHIBITORS
Albert Granell Fort

8.1. General conclusions

This thesis is a dual work with the aim to advance in the inhibition of Sphingosine Kinase 1 and 2. In Chapter 3, the guest-host interactions with two sphingosine analogues with selective inhibition activity towards SphK2 has been studied. In Chapter 4, the aminofluorination of allyl carbamates with hypervalent iodine reagents has been explored as a method to obtain β-fluoroamines that may serve for the preparation of a family of fluorinated sphingosine analogues.

Chapter 3

- Inhibitors **3.7** and **3.8** have been prepared in a 5-step synthesis starting from 1-pentadecyne as racemic mixtures. Separation of the enantiomers via chiral chromatography or by derivatization with chiral Mosher acid was not possible.

- Docking studies have been performed to predict interactions between the prepared inhibitors and SphK1. The triple bond linker shapes the lipidic tail in a way that the fit with the enzyme is less convenient and interactions are lost. This is in agreement with the loss of inhibition compared to the olefinic analogues.

- The docking poses for the separated enantiomers revealed that the (2*R*,3*S*) enantiomers are oriented away from possible key interactions in the polar head of the pocket of the enzyme. Therefore, (2*S*,3*R*) enantiomers should have more inhibition activity.

- Molecular dockings were performed also in an SphK2 homology model. In spite of the awkward positioning of the analogues with SphK1, the alkynylic linker provides a better fit in the longer lipidic pocket of Sph2. This is in agreement with **3.7** and **3.8** being selective inhibitors of SphK2.

- Cell viability assays showed no cytotoxicity of analogue **3.7** to human endothelial cells at 30 μM, which is higher than its IC50.

Chapter 4

- A library of allylic carbamates has been synthetized as substrates for the study. It contains allyl carbamates with alkyl, allyl and aryl substituents in E and Z conformation, *p*-substituted cinnamyl carbamates, N-tosyl allyl carbamates and N-benzyl allyl carbamates.

- Mixtures of F-oxazolidinones have been obtained in good to moderate yield in the aminofluorination with $TolIF_2$, as well as with the tandem aziridination + ring-opening with non-N-substituted carbamates. It has been constated that a secondary unit next to the olefine is necessary for the transformation to occur, possibly due to crucial pi stacking interactions with the aryl iodane(III).

- A mechanism has been postulated for the aminofluorination of allyl carbamates with $TolIF_2$. The reaction goes through the oxidation of the nitrogen in the carbamate group in the form of an iminoiodane, followed by formal nitrene addition to the olefin to generate a bicyclic aziridine. This aziridine is destabilized by the secondary unit and forms a pseudocarbocation-like intermediate that is attacked by a H-bond network of HF. The nature of the secondary unit dictates the cationic nature of the intermediate, with more EWG giving almost equimolar *syn/anti* diastereomeric mixtures.

- DMPU·HF and Et_3N·HF are good reagents for the ring-opening of the bicyclic aziridines obtained from allyl carbamates. DMPU·HF yields the *anti* isomer with good yield and diastereoselectivity, and Et_3N·HF complex delivers the *syn* isomer with also good yield and seleshow a more substrate-dependent *anti*:*syn* selectivity.

- The electronic density of the alkene has a big impact in the diastereomeric outcome. EWG favour the *syn* isomer, and EDG favour the *anti* isomer.

UNIVERSITAT ROVIRA I VIRGILI
INSIGHTS INTO AMINOFLUORINATION STRATEGIES AND SPHINGOSINE ANALOGUE SYNTHESIS TOWARDS THE DEVELOPMENT OF SELECTIVE SPHK2 INHIBITORS
Albert Granell Fort

UNIVERSITAT ROVIRA I VIRGILI
INSIGHTS INTO AMINOFLUORINATION STRATEGIES AND SPHINGOSINE ANALOGUE SYNTHESIS TOWARDS THE DEVELOPMENT OF SELECTIVE SPHK2 INHIBITORS
Albert Granell Fort

UNIVERSITAT ROVIRA I VIRGILI
INSIGHTS INTO AMINOFLUORINATION STRATEGIES AND SPHINGOSINE ANALOGUE SYNTHESIS TOWARDS THE DEVELOPMENT OF SELECTIVE SPHK2 INHIBITORS
Albert Granell Fort

UNIVERSITAT
ROVIRA i VIRGILI